Towards the prediction of the effect of food on orally administered medicines using preclinical in vivo models and machine learning technologies

Francesca Gavins

Thesis Submitted for the Degree of Doctor of Philosophy

Declaration

I, Francesca Katherine Hilary Gavins confirm that the work presented in this thesis is my own. Where information has been derived from other sources, I confirm that this has been indicated in the thesis.

Francesca K.H. Gavins

Signed:

Research funding

This research was funded by the Engineering and Physical Sciences Research Council (EPSRC) UK, grant number EP/L01646X/1.

Acknowledgements

A big thank you to the Central for Doctoral Training (CDT) in Advanced Therapeutics and Nanomedicines for providing training opportunities and funding (Engineering and Physical Sciences Research Council [EP/L01646X/1]). Special mentions to Prof Steve Brocchini and Prof Gareth Williams for their support and encouragement.

Thank you to my supervisors Prof Mine Orlu and Prof Abdul Basit for giving me continuous opportunities, challenging my abilities, and pushing me to become the pharmaceutical scientist and pharmacist I am today. Big highlights of my PhD were in collaboration by them: writing a news piece for Nature Biomedical Engineering and speaking at the Controlled Release Society conference.

MPharm then PhD, I have spent eight years at the UCL School of Pharmacy and believe it to be a special place, full of inspiring people. Special thanks to the Basit Research Group and my CDT cohort 2018 for the fun times, too many names to mention. Thank you especially Christine Madla for your friendship, a kind and incredible person and friend.

From a research perspective, I have met the most brilliant minds. Collaborations with the UCL School of Electrical and Electronic Engineering and Sun Yat-sen University allowed me to work with Miya, Moe, Zihao, Youssef, and Fanying, producing novel findings in biopharmaceutics and machine learning. I am forever grateful for their expertise.

Finally, and most importantly, I would like to thank my family and friends who have been there for me, throughout the challenges. Alex, forever grateful for all your support and guidance, encouraging me to work hard, and most importantly, play hard. Also, my family Joanna, Philip, Gaby, Vicky, Lily, and Charlie, this would not have been possible without you.

Having spent eight years at UCL School of Pharmacy, it is the end of era. I feel very privileged to be part of a strong community of pharmacists and pharmaceutical scientists.

Abstract

The intake of food and drinks with orally administered medicines can significantly impact the therapeutic efficacy or adverse side effects of a drug, posing barriers to effective therapeutic treatment in patient populations. There are unmet pharmaceutical and clinical needs to improve the prediction of the food effect in drug product development. This research has focused on *in vivo* and *in silico* tools that can be used in early drug development to predict the food effect. The overall aims of this research were to: explore the food-mediated changes to intestinal efflux transporter expression in rodent animal models, and leverage machine learning tools to predict the food effect.

Our understanding of the effects of the fed state on clinically relevant transporters in preclinical rodent animal models has been enhanced. P-glycoprotein (P-gp), breast cancer resistance protein (BCRP), and multidrug resistance-associated protein 2 (MRP2) expression were altered to different extents between the prandial states, sexes, and strains. A non-nutritive fibre meal increased the acute expression of intestinal P-gp, BCRP, and MRP2. Significant changes were seen in male rats, when comparing the fibre meal and the standard housing meal, but not in female rats.

The repertoire of computational tools to predict the food effect was expanded. Here, classification and regression machine learning technologies were tested to predict the food effect on large datasets of >300 drugs using key drug physicochemical properties.

In summary, this work has uncovered that the rodent animal model shows food, sex, and strain differences for the expression of key intestinal efflux transporters. Furthermore, machine learning technologies were harnessed to predict the food effect from the drug structure. While more work is needed to further understand the mechanisms of the food effect and to build more accurate machine learning tools, these findings offer insights to guide early drug development.

Impact Statement

Most oral drugs must be absorbed across the gastrointestinal (GI) tract to have their intended pharmacological actions. The co-administration of a drug with food can affect its bioavailability, relative to the fasted state, termed the food effect. If food effects are discovered for a drug product, re-formulation strategies can be explored in the laboratory, or in the clinic, patients are given strict instructions to adhere to in relation to concomitant food intake.

The Food and Drug Administration (FDA) and European Medicines Agency (EMA) regulatory bodies ask for clinical trials to investigate food effect in human subjects, requiring dosing in the fasted and fed state. To expedite the costly and lengthy drug development process, preclinical tools are used to predict the effect of food on drug bioavailability in humans. They include as mathematical modelling and *in vivo* animal models. However, food effects are complex and hard to predict, and current tools possess distinct limitations, such as the under or over-prediction of the food effect.

Animal models are used in preclinical development to assess the safety and efficacy of new chemical entities, although the most appropriate model for testing is not always known. This thesis details the characterisation of the rat animal model following food intake (fasted versus fed), in the sexes (males versus females), and between the strains (Wistar versus Sprague Dawley). A comprehensive library of the expression of P-gp, BCRP, and MRP2 is compiled, chosen as clinically relevant efflux transporters that can limit the oral absorption of a wide range of endogenous and exogenous substrates, including medicines. A deeper understanding of the effects of food on the rodent GI physiology and efflux transporter expression can lead to improved translation from animal studies to human pharmacokinetic studies.

Digital pharmaceutics tools can be used in conjugation with *in vitro* and *in vivo* testing to predict key pharmacokinetic properties, leveraging the power of data. Here, machine learning tools were developed to predict the effect of food on drugs from their physicochemical properties. Computational tools are presented here that can be used

by pharmaceutical scientists and data scientists early in drug development to screen new drugs for food effects.

Importantly, accurate preclinical and computational tools could ensure that food effect-related risks are forecast in early drug development, leading to optimised therapeutic outcomes for our patient population.

Contents

List of figures

List of tables

List of equations

Abbreviations

ABC	ATP binding cassette
ADA	AdaBoost
ADME	Absorption, distribution, metabolism, and excretion
ADMET	Absorption, distribution, metabolism, excretion, and toxicity
ANDA	Abbreviated new drug application
API	Active pharmaceutical ingredient
ANOVA	Analysis of variance
AUC	Area under the curve, total absorption
BCS	Biopharmaceutics Classification System
BCRP	Breast cancer resistance protein
BDDCS	Biopharmaceutics Drug Disposition Classification System
C_{max}	Maximum plasma concentration
CYP	Cytochrome
EECs	Enteroendocrine cells
ELISA	Enzyme linked immunoassay
EMA	European Medicines Agency
F+	Positive food effect
F-	Negative food effect
F0	No food effect
FaSSGF	Fasted state simulated gastric fluid
FaSSIF	Fasted state simulated intestinal fluid
FeSSGF	Fed state simulated gastric fluid
FeSSIF	Fed state simulated intestinal fluid
FDA	Food and Drug Administration
FP	False positive
FN	False negative
GB	Gradient Boosting
GI	Gastrointestinal
HRP	Horseradish peroxidase
ICH	International Council for Harmonisation
IND	Investigational New Drug Applicatio
IQR	Interquartile range
ITC	International Transporter Consortium
IVIVC	*In vitro – in vivo* correlation (IVIVC)

KBR	Krebs-bicarbonate Ringer's solution
kNN	K nearest neighbour
LASSO	Least absolute shrinkage and selection operator
LC-MS/MS	Liquid chromatography–mass spectrometry/mass spectrometry
LR	Logistic regression
MAE	Mean Absolute Error
MLP	Multiple layer perceptron
MMC	Migrating motor complex
MRP2	Multidrug resistance-associated protein 2
MSE	Mean squared error
NDA	New Drug Application
NBF	Nucleotide binding fold
NIH	National Institutes of Health
OOB	Out of bag
PBS	Phosphate buffered saline
PBPK	Physiologically based pharmacokinetic
PMSF	Phenylmethylsulfonyl fluoride
P-gp	Permeability-glycoprotein
RF	Random forest
PCR	Polymerase chain reaction
SLC	solute carrier
SVM/SVR	Support vector machine/support vector regression
Tmax	Time to peak drug concentration
TP	True positive
TN	True negative
XGB	Extreme gradient boosting

UCL Research Paper Declaration Form: referencing the doctoral candidate's own published work(s)

Please use this form to declare if parts of your thesis are already available in another format, e.g. if data, text, or figures:

- have been uploaded to a preprint server;
- are in submission to a peer-reviewed publication;
- have been published in a peer-reviewed publication, e.g. journal, textbook.

This form should be completed as many times as necessary. For instance, if you have seven thesis chapters, two of which containing material that has already been published, you would complete this form twice.

Chapter 1

1. For a research manuscript that has already been published (if not yet published, please skip to section 2)**:**		
a) Where was the work published? (e.g. journal name)	Advanced Drug Delivery Reviews	
b) Who published the work? (e.g. Elsevier/Oxford University Press):	Elsevier	
c) When was the work published?	15/05/2021	
d) Was the work subject to academic peer review?	Yes	
e) Have you retained the copyright for the work?	Yes	
[If no, please seek permission from the relevant publisher and check the box next to the below statement]: ☐ *I acknowledge permission of the publisher named under 1b to include in this thesis portions of the publication named as included in 1a.*		
2. For a research manuscript prepared for publication but that has not yet been published (if already published, please skip to section 3)**:**		
a) Has the manuscript been uploaded to a preprint server? (e.g. medRxiv):	Please select.	**If yes, which server?** Click or tap here to enter text.

b) Where is the work intended to be published? (e.g. names of journals that you are planning to submit to)	Click or tap here to enter text.
c) List the manuscript's authors in the intended authorship order:	Click or tap here to enter text.
d) Stage of publication	Please select.

3. For multi-authored work, please give a statement of contribution covering all authors (if single-author, please skip to section 4**):**

C.M. Madla – conceptualisation, investigation, review original draft preparation, writing review and editing, visualisation, project administration

F.K.H. Gavins – original draft preparation, writing review and editing

H.A. Merchant – review and editing

M. Orlu – review and editing, funding acquisition, supervision

S. Murdan – review and editing, funding acquisition, supervision

A.W. Basit – writing review and editing, funding acquisition, supervision

4. In which chapter(s) of your thesis can this material be found?

Chapter 1

5. e-Signatures confirming that the information above is accurate (this form should be co-signed by the supervisor/ senior author unless this is not appropriate, e.g. if the paper was a single-author work):

Candidate:	Francesca Gavins	**Date:**	16/12/2022
Supervisor/ Senior Author (where appropriate)**:**	Mine Orlu	**Date:**	16/12/2022

Chapter 2

1. For a research manuscript that has already been published (if not yet published, please skip to section 2)**:**		
a) Where was the work published? (e.g. journal name)	Click or tap here to enter text.	
b) Who published the work? (e.g. Elsevier/Oxford University Press):	Click or tap here to enter text.	
c) When was the work published?	Click or tap to enter a date.	
d) Was the work subject to academic peer review?	No	
e) Have you retained the copyright for the work?	No	
[If no, please seek permission from the relevant publisher and check the box next to the below statement]: ☐ *I acknowledge permission of the publisher named under 1b to include in this thesis portions of the publication named as included in 1a.*		
2. For a research manuscript prepared for publication but that has not yet been published (if already published, please skip to section 3)**:**		
a) Has the manuscript been uploaded to a preprint server? (e.g. medRxiv):	No	**If yes, which server?** Click or tap here to enter text.
b) Where is the work intended to be published? (e.g. names of journals that you are planning to submit to)	Biomedicine & Pharmacotherapy	
c) List the manuscript's authors in the intended authorship order:	F.K.H. Gavins, L. Dou, Y. Qin, C.M. Madla, S. Murdan, A.W. Basit, Y. Mai., M.Orlu.	
d) Stage of publication	Undergoing revision after peer review	
3. For multi-authored work, please give a statement of contribution covering all authors (if single-author, please skip to section 4**):**		

F.K.H. Gavins – conceptualisation, methodology, investigation, data curation, software, formal analysis, original draft preparation, writing review and editing, visualisation, project administration.

L. Dou – conceptualisation and methodology.

Y. Qin – investigation, data curation and data validation.

C.M. Madla – methodology and writing—review and editing.

S. Murdan – methodology, resources, and supervision.

A.W. Basit – conceptualisation, methodology, writing—review and editing, supervision, and funding acquisition.

Y. Mai – conceptualisation, methodology, investigation, data curation, data validation, formal analysis, writing review and editing.

M. Orlu – conceptualisation, methodology, writing—review and editing, supervision, and funding acquisition.

4. In which chapter(s) of your thesis can this material be found?

Chapter 2

5. e-Signatures confirming that the information above is accurate (this form should be co-signed by the supervisor/ senior author unless this is not appropriate, e.g. if the paper was a single-author work):

Candidate:	Francesca Gavins	**Date:**	30/11/2022
Supervisor/ Senior Author (where appropriate)**:**	Mine Orlu	**Date:**	30/11/2022

Chapter 3

1. For a research manuscript that has already been published (if not yet published, please skip to section 2)**:**		
a) Where was the work published? (e.g. journal name)	Pharmaceutics	
b) Who published the work? (e.g. Elsevier/Oxford University Press):	MDPI	
c) When was the work published?	26/10/2021	
d) Was the work subject to academic peer review?	Yes	
e) Have you retained the copyright for the work?	Yes	
[If no, please seek permission from the relevant publisher and check the box next to the below statement]: ☒ *I acknowledge permission of the publisher named under 1b to include in this thesis portions of the publication named as included in 1a.*		
2. For a research manuscript prepared for publication but that has not yet been published (if already published, please skip to section 3)**:**		
a) Has the manuscript been uploaded to a preprint server? (e.g. medRxiv):	Please select.	**If yes, which server?** Click or tap here to enter text.
b) **Where is the work intended to be published?** (e.g. names of journals that you are planning to submit to)	Click or tap here to enter text.	
c) List the manuscript's authors in the intended authorship order:	Click or tap here to enter text.	
d) **Stage of publication**	Please select.	
3. For multi-authored work, please give a statement of contribution covering all authors (if single-author, please skip to section 4**):**		
F.K.H. Gavins – conceptualisation, methodology, investigation, data curation, software, formal analysis, original draft preparation, writing review and editing, visualisation, project administration.		

Y. Mai – conceptualisation, methodology, investigation, data curation, data validation, formal analysis, writing review and editing.

L. Dou – conceptualisation and methodology.

J. Liu – investigation, data curation and data validation.

F. Taherali – methodology and writing—review and editing.

M.E. Alkahtani – writing—review and editing.

S. Murdan – methodology, resources, and supervision.

A.W. Basit – conceptualisation, methodology, writing—review and editing, supervision, and funding acquisition.

M. Orlu – conceptualisation, methodology, writing—review and editing, supervision, and funding acquisition.

4. In which chapter(s) of your thesis can this material be found?

Chapter 3

5. e-Signatures confirming that the information above is accurate (this form should be co-signed by the supervisor/ senior author unless this is not appropriate, e.g. if the paper was a single-author work):

Candidate:	Francesca Gavins	**Date:**	06/10/2022
Supervisor/ Senior Author (where appropriate)**:**	Mine Orlu	**Date:**	06/10/2022

Chapter 4

1. For a research manuscript that has already been published (if not yet published, please skip to section 2)**:**		
a) Where was the work published? (e.g. journal name)	International Journal of Pharmaceutics	
b) Who published the work? (e.g. Elsevier/Oxford University Press):	Elsevier	
c) When was the work published?	05/01/2022	
d) Was the work subject to academic peer review?	Yes	
e) Have you retained the copyright for the work?	Yes	
[If no, please seek permission from the relevant publisher and check the box next to the below statement]: ☐ *I acknowledge permission of the publisher named under 1b to include in this thesis portions of the publication named as included in 1a.*		
2. For a research manuscript prepared for publication but that has not yet been published (if already published, please skip to section 3)**:**		
a) Has the manuscript been uploaded to a preprint server? (e.g. medRxiv):	Please select.	**If yes, which server?** Click or tap here to enter text.
b) **Where is the work intended to be published?** (e.g. names of journals that you are planning to submit to)	Click or tap here to enter text.	
c) List the manuscript's authors in the intended authorship order:	Click or tap here to enter text.	
d) **Stage of publication**	Please select.	
3. For multi-authored work, please give a statement of contribution covering all authors (if single-author, please skip to section 4**):**		
F.K.H. Gavins – conceptualization, methodology, software, validation, formal analysis, investigation, writing – original draft, writing – review & editing, resources, data		

curation, visualization, and project administration.

Z. Fu – methodology, software, validation, formal analysis, investigation, writing – original draft, data curation, and visualization.

M. Elbadawi – conceptualization, methodology, software, validation, formal analysis, writing – review & editing, resources, visualization, and supervision.

A.W. Basit – writing review and editing, resources, funding acquisition, and supervision.

M.R.D. Rodrigues – conceptualization, methodology, validation, formal analysis, writing – review & editing, Resources, Visualization, Supervision.

M. Orlu – conceptualization, methodology, formal analysis, writing – review & editing, resources, supervision, and funding acquisition.

4. In which chapter(s) of your thesis can this material be found?

Chapter 4

5. e-Signatures confirming that the information above is accurate (this form should be co-signed by the supervisor/ senior author unless this is not appropriate, e.g. if the paper was a single-author work):

Candidate:	Francesca Gavins	**Date:**	16/12/2022
Supervisor/ Senior Author (where appropriate)**:**	Mine Orlu	**Date:**	16/12/2022

Chapter 1 : Introduction

1. Food and Oral Drug absorption

1.1 Overview

Oral drug administration is the most preferred route of administration due to patient preference and pharmaceutical manufacturing experience and capabilities [1]. Drug absorption through the intestinal tract is composed of highly complex processes and can be influenced by multiple internal physiological factors, ranging from GI motility patterns, varying pH profile, intestinal surface area, epithelial permeability, the mucus layer, and the presence of enzymes and bile salts [2,3]. Patient-specific external factors can also alter the extent of drug absorption, examples include the sex of the individual, ethnicity, disease status, pregnancy status, and importantly, diet and food intake [4-7]. Food-mediated inter- and intra-individual variability pose a greater risk for drugs with narrow therapeutic indices, multiple dosing frequencies, and non-linear kinetics [8]. Therefore, in order for the patient to receive the suitable pharmacotherapy for their indication, differences in the GI tract physiologies between the fasted and fed state should be considered.

1.2 Food effect

The intake of food induces dynamic physiological changes in the GI tract, which can have significant impacts on drug pharmacokinetics and bioavailability, relative to the fasted state, termed the food effect [9-11]. The intake of food activates gastric and pancreatic secretions and alters GI motility, that together regulate motor, secretory, and absorptive functions of the intestine [12]. In 1977, Welling published the first landmark review on the influence of food and diet on drug absorption [13]. A follow-up review by Welling in 1989 classified food-drug interactions, now referred to in the pharmaceutical field as the food effect, into five categories: (i) reduced extent of bioavailability; (ii) delayed rate of absorption; (iii) increased extent of bioavailability; (iv) accelerated rate of absorption; and (v) no effect [14]. Since then, the food effect has been further categorised into the

terms ‘positive food effect’ and ‘negative food effect’, to describe an increase or decrease in the overall extent of bioavailability, respectively [15].

Currently the only regulatory approved studies to characterize the impact of food intake on drug absorption are to conduct clinical investigations in human subjects [16]. The FDA require ‘Food-Effect Bioavailability and Fed Bioequivalence Studies’ to assess the effects of food on pharmacokinetic parameters for all investigational new drug applications (INDs), new drug applications (NDAs), and abbreviated new drug applications (ANDAs) [11]. The FDA suggests that the effects of food on pharmacokinetics should be investigated before conducting pivotal safety and efficacy trials. Unless the target population dictates specific dosing restrictions, the food effect assessment is usually conducted early in development, often as early as part of first-in-human single-ascending dose studies. In addition, the food effect assessment is sometimes repeated with the final-to-be-marketed oral formulation in a definitive food effect study to inform the final product label [17]. For generic drug products or in the post approval space, fed bioequivalence studies may be necessary if the type of formulation developed is different [18].

The drug products are usually tested using a cross-over design in the fasted and fed state. Clinical trials subjects in the fasted arm are fasted overnight for 8 hours (EMA) or 10 hours (FDA) [11,19]. The fed subjects are required to consume a high-fat (500–600 kcal of total calories derived from fat), high-caloric meal (800–1000 kcal), which consists of two slices of toast with butter, two slices of fried bacon, two eggs fried in butter, 113 g hash-brown potatoes and a 240 mL glass of whole milk, in a 30-minute window before administration of the drug product. The meal is designed to evoke the maximum physiological response, and therefore be a worst-case scenario. This level of standardisation across clinical trials is necessary as timing, caloric density and the specific effects of macronutrients can affect gastric volume [20,21]. Subjects in both experimental arms will administer the drug products with 240 mL of water and no food is allowed post-dose. The EMA also recommends different meal types, such as a moderate meal, carbohydrate-rich meal, or snacks [19].

Pharmacokinetic parameters are compared between the fasted and fed states by statistical analyses. Specifically, the peak exposure or plasma concentration (C_{max}), time to peak plasma concentration (T_{max}), and total exposure or area under the curve (AUC). A food effect is categorised if the 90% confidence intervals for the ratio of population geometric means, based on log transformed data, for either $AUC_{0-\infty}$ or Cmax fall outside of the 80-125% bioequivalence limits, relative to the fasted state [11]. As mentioned, food effect studies are tightly controlled in accordance with regulatory requirements. This level of control aims to avoid physiological variabilities, such as differences in the GI pH, fluid volume, osmolality, and motility. Importantly, the FDA bioequivalence criteria does not consider the therapeutic window and the pharmacokinetic variability of the drug. As a result, even if bioequivalence is not achieved between the fasted and fed state, if the drug shows a wide therapeutic window and a large variability, slight changes in bioavailability may not result in any clinical significance in patients, and the drug can be administered without respect to food [22].

Food intake causes significant changes in the physiological conditions of the GI tract. Therefore, the pharmacokinetic profile of a drug can be affected due to food-mediated changes to the dissolution, absorption, distribution, metabolism, and excretion of a drug, known as unspecific pharmacokinetic changes, and depend on the drug properties and formulation properties. On the other hand, specific pharmacokinetic food-drug effects are due to direct interactions. For example, the most publicised clinical interaction is the inhibition of cytochrome P450 (CYP450) by grapefruit juice and other flavonoid containing foods, that can in turn affect the bioavailability of more 85 drugs [23]. There are a number of reviews that discuss bio-enabling formulation strategies to reduce the variabilities between the fasted and fed state and mitigate against the food effect, which is out of the scope of this thesis [8,10,22].

Figure 1-1 shows the key differences in the human GI physiology between the fasted and fed states.

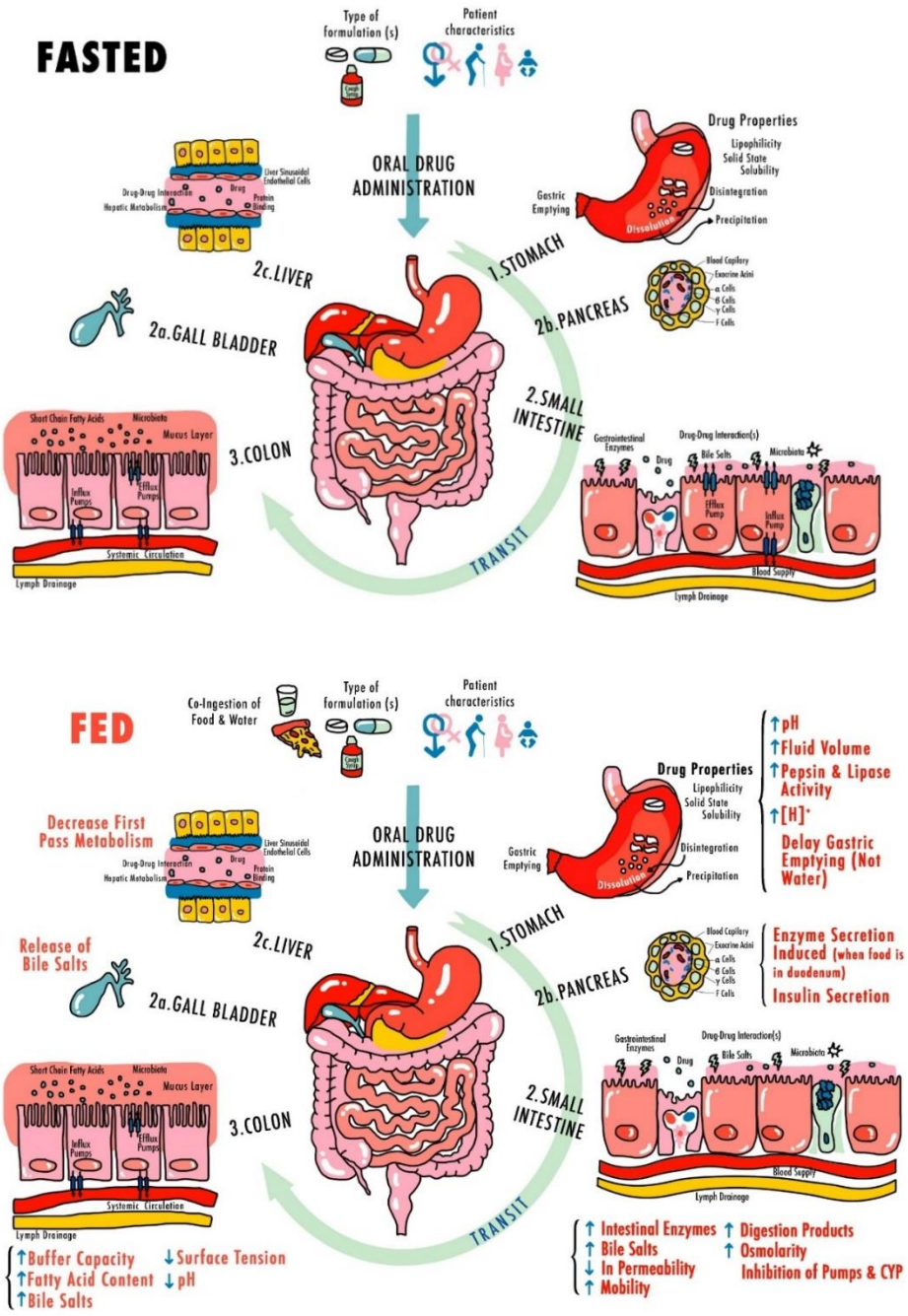

Figure 1-1 Key gastrointestinal physiological changes between the fasted and fed states [9,10,24]

1.2.1 Gastrointestinal luminal environment

In the fasted to the fed state in the stomach, the most significant changes are the increase in gastric pH, fluid volume, buffer capacity, viscosity, and the presence of dietary lipids and their products of digestion [25-28]. The increased gastric pH can alter the solubility and dissolution of ionisable drug compounds. For example, for weak acids such as cefuroxime, an increase in the AUC and C_{max} can be seen [29]. For weak bases, such as dipyridamole, a decrease in AUC and C_{max} is observed [30].

The fasting period is characterised by the inter-digestive migrating motor complex (MMC), where cyclical contractions spread through the stomach and small intestines. Following food intake, the stomach motility alters with the proximal stomach relaxing to accommodate the food, and the distal stomach mixing to digest the food. Gastric emptying is delayed, allowing for food to be broken down by the mixing and the gastric secretions. The longer residence time of the drug in the stomach can result in a lag in the time it takes for the drug product to be absorbed in the small intestine, known as a lag time (T_{lag}). There may also be an increase in T_{max} and a decrease in C_{max}. This is seen for paracetamol and is a commonly cited example [31]. For drugs where the pharmacodynamics depends on overall drug exposure rather than peak plasma levels C_{max}, delayed absorption may not be clinically relevant [32].

In the small intestine, the most the prominent changes following food intake are the increase in bile salt concentration, and the presence of the products of lipid digestion [33]. The increased presence of solubilising agents, such as bile salts, lipids, and lipid digestion products, can increase the solubilisation of poorly water-soluble drugs. Highly lipophilic drugs, such as griseofulvin, show greater absorption in the fed state due to enhanced solubilisation in the lipid matrices of foodstuff [34]. Another example of a highly lipophilic drug is alectinib, following a high-fat meal, the pharmacokinetics of alectinib showed an increased C_{max} and AUC, in relation to the fasted state [35]. The increased viscosity of the intestinal fluid due to the presence of chyme can reduce the water diffusivity and as a result, the slower penetration of the luminal fluids into the

dosage forms can increase the disintegration time. Ciprofloxacin tablets showed prolonged disintegration times, with a prolonged T_{max} and a decrease in C_{max} [36]. In the fed state, there may also be a reduction in first pass metabolism due to the increased splanchnic blood flow, reduced enteric metabolism, and increased lymphatic uptake [37-39].

Nutrient sensing enteroendocrine cells (EECs) represent less than 1% of gut epithelial cells of the human body and regulate secretion, motility, hunger, satiety, and metabolism [40,41]. When the duodenal EECs are in contact with nutrients, the duodeno-gastric negative feedback are activated, mediated by vago-vagal reflexes and hormonal signals (such as cholecystokinin [CCK]). The role of this feedback is to delay the entry of acidic, calorie-rich contents into the duodenum by controlling gastric emptying [42]. Depending on the physical consistency and particle size of the food stuff, the gastric residence time of non-digestible solids can be up to several hours [43]. The gastric transit of a non-disintegrating tablet in the fasted, pre-fed, and fed state were reported as a median (interquartile range [IQR]), showing a gastric emptying time of 37 (19-74), 39 (25-169), and 149 (119-171) minutes, respectively [44]. Postprandially, the small intestinal transit time is poorly understood, and is reported in both the pre- and postprandial state as a mean value of 3-4 h [44]. Although, there is significant inter- and intra-individual variability.

1.2.2 Transporters

Absorption of molecules through the GI tract can take place by passive diffusion (through concentration gradients), or active diffusion (by transporters). Intestinal enterocytes express numerous influx and efflux transporters, as well as CYP450 enzymes. More than 400 membrane transporters in two major superfamilies – ATP binding cassette (ABC) and solute carrier (SLC) – have been discovered in the human genome [45]. Efflux transporters are located on the apical part of the plasma membrane of polarised cells

such as the epithelia, and substrates are translocated from the basolateral to the apical side of the epithelium.

The International Transporter Consortium (ITC) and the Food and Drug Administration (FDA) recognise P-gp and BCRP as clinically relevant transporters [46,47]. In addition, the European Medicines Agency (EMA) recognises the importance of MRP2 as a key efflux transporter, with high levels of expression in barrier tissues [19,48,49]. Clinical substrates for P-gp include dabigatran etexilate, digoxin, and fexofenadine; BCRP are rosuvastatin and sulfasalazine; and MRP2 are cisplatin and vincristine [50,51], with a more comprehensive list shown in Table 1-1. These efflux transporters are responsible for pharmacokinetics, safety and efficacy of a wide range of drugs [46]. They are expressed in blood-brain barrier and epithelia of the kidney, liver, as well as in the enterocytes of the intestinal tract. At the intestinal layer, membrane transporters are implicated in the efflux of endogenous and exogenous substrates, potentially limiting absorption into systemic circulation. As shown in Table 1-1, a wide range of structurally unrelated hydrophobic substances bind to these transporters and show partial overlapping substrate specificity [52].

The overexpression of ABC transporters in cancer cells is associated with multidrug resistance, and has driven extensive mechanistic studies into the expression of these proteins [53]. To date, a total of 50 ABC transporters have been characterised in humans [54]. The most characterised ABC transporter is P-gp (molecular mass of 170 kDa), where the ‘P’ stands for permeability, and was identified in colchicine resistant Chinese hamster ovarian cells by Juliano and Ling in 1976 [55]. More than 20 years later, the related transporters MRP2 was characterised as a canalicular multi-specific organic anion transporter in hepatocytes in 1996, also known as the canalicular multi-specific organic anion transporter 1 (cMOAT) [56,57]. Later in 1998, BCRP was isolated in multidrug resistant breast cancer lines 1998 [58].

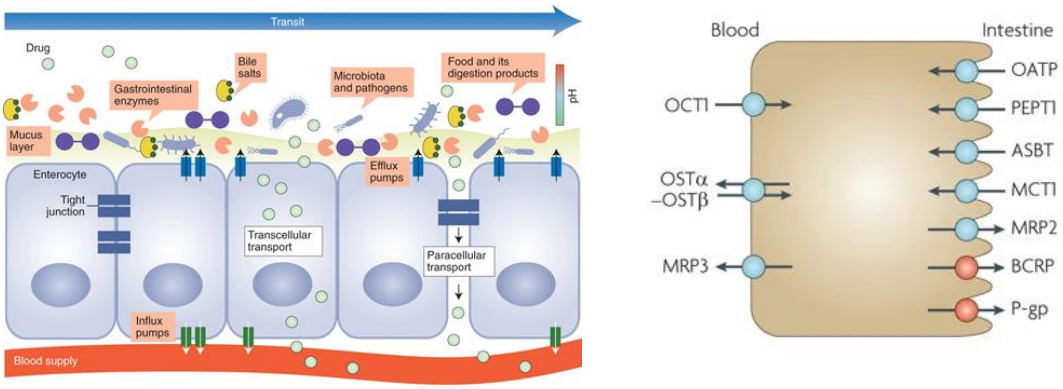

Figure 1-2 Schematic diagram of the intestinal tract and the (B) transporters in the intestinal plasma membrane. Taken from [59] and [46].

Figure 1-2 displays a schematic of the intestinal epithelia and shows the location of certain efflux pumps on the apical side of the epithelia. ABC transporters consist of two sets of hydrophobic parts that span the membrane and confer most of the specificity of the transporter, and a pair of ATP-binding domains or nucleotide-binding folds (NBF) [60]. P-gp (*abcb1*) consists of two similar halves, with 6 putative transmembrane segments, and an intracellular ATP binding site. The first extracellular loop in P-gp is heavily N-glycosylated. MRP2 has an extra N-terminal domain compared with P-gp, that is located extracellularly located. BCRP (*abcg2*) is a 'half ABC transporter' (72kDa) comprised of 655 amino acids, a single N-terminal, intracellular ATP binding site, and six transmembrane domains. BCRP may function as a homodimer. It is believed that ABC transporters use the energy released by ATP hydrolysis as their energy sources, pumping substrates against a concentration gradient [61].

There are broad substrate specificities of the P-gp, BCRP, and MRP2 transporters (Table 1-1and Table 1-2). There is also partial substrate overlap between P-gp, BCRP, and MRP2 [62].

Table 1-1 Overview of the drug substrates, inhibitors and inducers with P-gp, BCRP, and MRP2, adapted from [50,51,60,63-65]

Transporters	Drug interaction
P-gp	**Drug substrates:** cimetidine, colchicine, docetaxel, digoxin, fexofenadine, indinavir, loperamide, octreotide, paclitaxel, quinidine, ranitidine, ritonavir, saquinavir, talinolol, topotecan, vinblastine, vincristine **Drug inhibitors:** amiodarone, azithromycin (systemic), cannabidiol, carvedilol, clarithromycin, cobicistat, cyclosporine (systemic), erythromycin (systemic), itraconazole, ketoconazole (systemic), lapatinib, posaconazole, quinine, ranolazine, reserpine, ritonavir, tacrolimus, tamoxifen, ticagrelor, verapamil, zosuquidar **Drug inducers:** carbamazepine, phenytoin, rifampicin
BCRP	**Drug substrates:** abacavir, ciprofloxacin, dantrolene, daunorubicin, doxorubicin, mitoxantrone, novobiocin, prazosin, sulfasalazine, rosuvastatin, topotecan **Drug inhibitors**: elacridar, sulfasalazine
MRP2	**Drug substrates:** ampicillin, azithromycin, cefodezime, cisplatin, cyclosporine, doxorubicin, epirubicin, etoposide, indinavir, methotrexate, mitoxantrone, olmesartan, pravastatin, vinblastine, vincrisitine **Drug inhibitors:** cyclosporine, delaviridine, efavirenz, emtricitabine, pantoprazole, probenecid **Drug inducer:** rifampicin

In 2018, the ITC published a whitepaper that provided a comprehensive review of changes in transporter expression and activity associated with acute and chronic diseases, regulatory pathways, and mechanisms that may affect transporter expression and function [66]. However, no white paper has been released on the impact of food

and diet on these key efflux transporters. As highlighted, food components as well as drugs can also interact with these transporters and limit the bioavailability of several drugs by food-drug interactions at the transporter level (Table 1.2) [63]. Monoglycerides and bile salts were reported *in vitro* to have an inhibitory effect on both uptake and efflux transporters [67]. As a result, some researchers hypothesise that high-fat meals may inhibit efflux and uptake transporters [68]. Although, to-date no clinically relevant interactions involving intestinal transporter effects have been reported so far. The interaction between CYP450 and foods rich in flavonoids, such as herbs, red wine, and certain fruits, have been extensively studied [63]. However, more research is needed to uncover the clinical relevance of these interactions [63]. Transporters may be saturable, and as a result, changes in the luminal environment can have significant effects on drug bioavailability, especially in the case of non-linear pharmacokinetics for some poorly soluble drugs.

Table 1-2 Overview of the food components that can interact with P-gp, BCRP, and MRP2, adapted from [69,70]

Transporters	**Food component interaction**
P-gp	**Inhibitors:** Green tea, rosemary extract, grapefruit juice, Seville orange juice, orange extract, strawberry extract, monoglycerides, oleic acid, dietary fatty acids, sweet pepper, piperine, mint extract, apricot extract **Inducer:** St John's Wort
BCRP	**Substrates:** daidzein, genistein Inhibitor: bergamottin, hesperetin, quercetin, kaempferol, nobiletin, tangeretin
MRP2	**Substrates:** food-derived (pre-)carcinogens **Inhibitor:** Resveratrol, chrysin, glyceollins, glucose,

1.3 Sex differences

The incidence of adverse drug reactions is 50 to 75% higher in females than males [71], and 60% of all patients hospitalised for adverse drugs reactions were females [72]. A prominent sex-gap exists in pharmaceutical research, ranging from preclinical studies, clinical trials, to post-marketing surveillance, with a focus on male subjects [73]. Traditionally in biomedical research from the 1980s to 90s human and non-human females have been poorly represented in experimental design [74]. The most cited assumptions for the lack of female subjects are that the findings from males will be applicable for females, and that female hormonal cycles will complicate experimental designs, and therefore female subjects were not included [75]. In addition, the thalidomide tragedy and the risks of teratogenicity in females of child-bearing potential previously led to the exclusion of females from clinical trials in the past [76,77].

In 1993, the National Institutes of Health (NIH) Revitalization Act required the inclusion of females in NIH-funded clinical research in sufficient numbers in phase III clinical trials to allow for valid statistical analyses of potential sex differences [78]. In the same year, the FDA published a guideline for industry entitled 'Study and Evaluation of Gender Differences in the Clinical Evaluation of Drugs' calling for the evaluation of males and females in all phases of drug clinical trials, including safety, efficacy, and dose-determination studies [74]. Twenty two years later, in 2015, the NIH published further policies requiring the consideration of sex as a biological variable in experimental design, analysis, and publications [79]. Recently in 2022, the UK Medical Research Council introduced the requirement of including both sexes in experimental designs and analyses plans [80]. While there is awareness of the need for females in clinical trials, researchers designing preclinical studies often overlook the need to evaluate sex differences in animal models. If data are not stratified according to sex, it could potentially skew or obscure any sex differences in the findings [75].

The phrase 'every cell has a sex' reflects sex differences at the cellular and molecular level [81]. These sex-specific differences can alter drug pharmacokinetics, which can in

turn, can affect drug efficacy and safety. Fundamental physiological differences exist between the sexes in for example, body fat content, water volume, plasma volume, organ blood flow, and hormonal control [82]. In the GI tract, different expression of CYP450 is reported, with higher CYP3A4 expression in women, and higher CYP2D6, CYP1A2 and CYP2E1 in men [83,84]. There is an increasing number of studies reporting the sex-specific expression of several efflux transporters, that can cause differing treatment successes [85]. For example, sex differences in the bioavailability of cyclosporine A, a P-gp substrate, was reported after a fat-rich meal, where decreased bioavailability was seen in females and increased bioavailability in male humans [86]. In addition, the MRPs transporters report sex-specific expression, influenced by sex hormones [87].

Sex differences also exist for the absorption of food [73]. For instance, females can take longer to digest food and in the fed state, the secretion of acid is significantly higher in males than females [88]. These physiological parameters are not always considered in analyses and can result in differing responses to medicines [4]. There are comprehensive reviews from our research group on sex differences in GI physiological and medicines performance [73,89].

The intake of food with drugs can affect oral drug absorption between the sexes. In preclinical studies, diet can affect the weight, metabolism, hormone concentration, and immune function, and therefore the diet choice should be stated any publications or protocols [90]. Diets rich in phytoestrogens, a component in soy, which is often included in rodent diet, may have sex-specific effects on cardiac health. In male humans, it was observed that soy-based diets significantly decreased cardiac function and associated heart failure, to a lesser extent in females [91].

As mentioned, preclinical animal studies conventionally use male animals as researchers believed that females would introduce variability due to the female oestrous cycle and body fat content and increase cost and sample sizes [92]. However, the lack of female animal models in biomedical research may have ignored potential sex differences [73].

1.4 Preclinical assessment of the food effect

The conduct of preclinical studies is vital to understand the drug pharmacokinetics before clinical studies. Although, there is heterogeneity in the approaches to predict and assess the food effect across the pharmaceutical field. To complicate things further, numerous models exist as food-drug interactions can occur at many different stages of drug processing. Therefore, no optimal *in vitro* and *in silico* model exists.

In pharmaceutical drug development, new drug candidates are tested on a case-by-case basis. Figure 1-3 details how the food effect is assessed for new drug candidates.

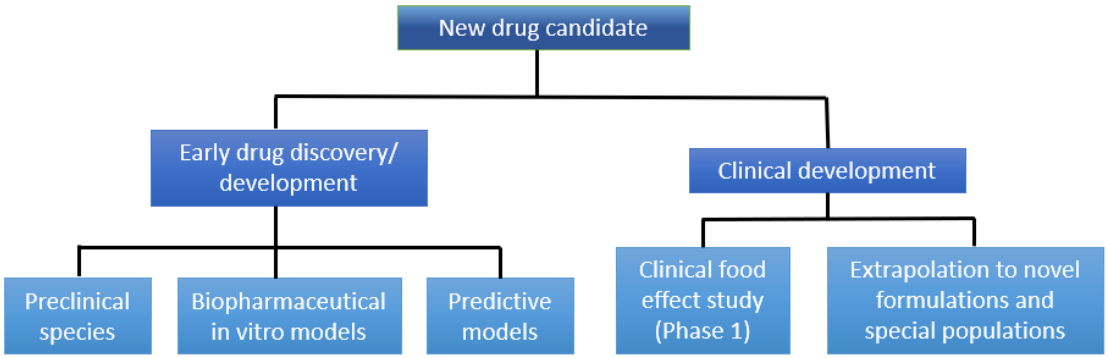

Figure 1-3 Assessment of the food effect for a new drug candidate

A number of *in vitro* biopharmaceutics models have been developed using dissolution testing with fasted or fed state biorelevant media to mimic the human GI environment under the different prandial states. Traditional dissolution media, such as simulated gastric fluid (SGF) and simulated intestinal fluid (SIF), are described in the British and international Pharmacopoeias. More recently, fasted state gastric and intestinal fluids (FaSSGF and FaSSIF) have been developed that contain physiological concentrations of natural bile salts (sodium taurocholate) and lecithin (a natural surfactant) [93-95]. The fed state versions of these media (FeSSGF and FeSSIF) are more complex in nature, containing milk or lipolysis products to appropriately simulate the influence of food

digestion. There is no universal fed state media, and the composition varies between studies. Lipolysis models have also been developed to test lipid-based formulations using FaSSIF or FeSSIF with porcine pancreatic lipase and pancreatin at 37 °C [96].

In some instances, dissolution findings in biorelevant media and/or preclinical *in vivo* models are combined with modelling to estimate the food effect [97-100]. For low solubility drugs, aspirated human intestinal fluids and biorelevant media such as FaSSIF and FeSSIF have been used for *in vivo* predictions of intestinal absorption [101]. Dissolution data from poorly soluble drugs in FaSSIF/FeSSIF showed excellent correlation with the *in vivo* behaviour in the fasted and fed state [102].

1.4.1 Animal models

Preclinical animal models are commonly used for testing novel drug products and predicting the oral dosage form performance in humans. Increasingly, researchers are subject to strict ethical requirements when designing their experiments. The principles of the 3Rs (replacement, reduction, and refinement) were developed more than 60 years ago by Russell and Burch, and guide the use of animals in research [103]. In the UK, the Animals (Scientific Procedures) Act 1986 has adopted the 3Rs. Replacement encourages the use of non-animal assays in the form of *in vitro* and *in silico* technologies to avoid the use of animals. Reduction involves using animal models but minimising the number used through optimised study designs, whilst also considering statistical power and the scientific question of the experiment. Refinement describes where techniques are used to minimise pain, suffering, distress, or lasting harm to the animal in the experiments. The studies described in this thesis used the reduction principle by minimising in the number of animals used in each experimental unit and replacement with the use of *in silico* computational models. Refinement was also used in the housing and the treatment of the animals.

While models such as Caco-2 cell-lines and rodent small intestinal perfusion models exist, these models do not take into considerations factors such as solubility,

formulation, food composition, chemical composition, fluctuations in the pH profile, motility, and blood flow. Therefore, pharmacokinetic studies in animals are usually carried out [104]. Animal models commonly used in pharmaceutical research include rats, mice, dogs, pigs, and monkeys. Although, due to distinct physiological differences, the use of animal models can lead to poor predictions of oral bioavailability. Some of the food effect studies in animal models are retrospective: if a food effect is found in the clinic, then investigational studies are performed in the animal model to understand the underlying food effect mechanism or evaluate different formulations that could mitigate the food effect [105].

Figure 1-4 shows the studies where 'food effect', and the animal models 'dog', 'pig', or 'rat' were keywords between 1990 and 2021. The dog model is the most frequently used animal model for studies into the effect of food on drug products [106]. The dog model has physiological and size advantages over other animal models and will willingly receive infrequent meals on command [107]. Paulson *et al.* characterised the pharmacokinetic profile of celecoxib in dog models using aliquots of low-, medium-, and high-fat human meal homogenates, and was compared to the results seen in humans [108]. The dog model was found to overpredict the human food effect by overpredicting the solubility enhancing effect of food [108]. In addition, there are physiological differences in gastric emptying and intestinal transit times between dogs and humans [107,109]. In recent years, the pig model is gaining popularity in food effect studies [110-114]. Importantly like in the human, pig models secrete bile in the presence of food [115]. Similarities in the GI physiologies between humans and the animal models should be identified in the literature and through experiments, the optimal model can be chosen for the experiment that is being conducted, and preclinical findings should be interpreted accordingly.

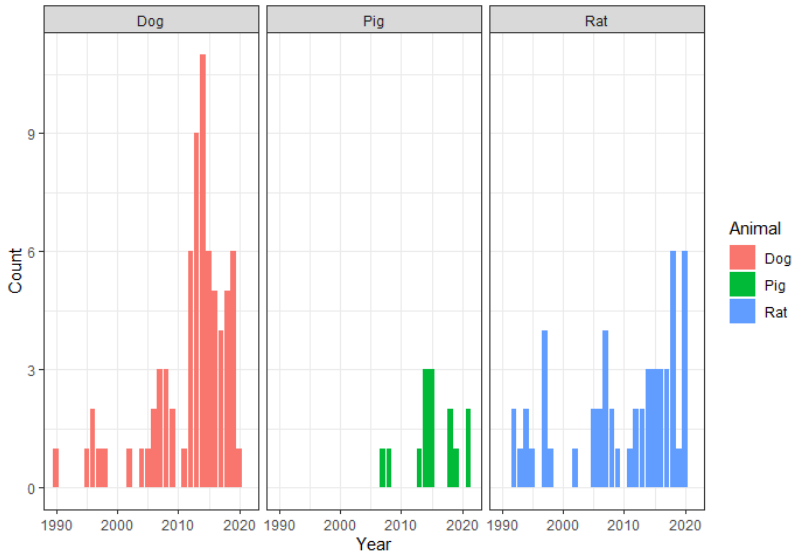

Figure 1-4 Number of studies of "food effect" AND 'dog' or 'pig' or 'rat' from 1990 to 2021 (search conducted using PubMed on 6th July 2021).

Animal biorelevant media are commercially available and based on the composition of canine GI fluids. They are used to simulate conditions in the canine GI tract and to improve the in vitro-in vivo-correlation (IVIVC). The composition of the GI fluids varies greatly between species, and to improve IVIVC the fundamental properties of common preclinical species should be understood, which then could be translated to *in vitro* models predicting the performance of drug products in rats.

In preclinical absorption, distribution, metabolism, excretion, and toxicity (ADMET) studies, two animal species are used, in one rodent and one non-rodent animal model [116]. Rats are one of the most commonly used pre-clinical animal models in oral drug development due to their low cost and ease of handling [117]. There are distinct differences as well as similarities between rodent GI physiological properties and those of humans (Figure 1-5). For example, the small intestinal transit time of 3–4 h in rats is similar to humans [118,119]. In the fasted state, the half-life of the gastric emptying time of liquids is approximately 15 to 30 minutes, which is similar to the observations in humans [118]. Furthermore, the rate of gastric emptying is controlled by the energy

content of the ingested food, comparable to humans. Furthermore, rats are cited as good predictors of human intestinal permeability with similar intestinal absorption profiles, where a correlation of >0.8 was seen for 16 compounds that were both passive and carrier mediated substrates [120].

A significant difference between the behaviours of rodents and humans is that rats are nocturnal animals. Animal studies may potentially disturb their day-night cycle, which could cause stress to the animal [118]. A higher metabolic rate is observed in rats when compared to humans [118]. Further limitations are the significantly smaller body size compared with humans, on average 17 cm in body length [117], which limits the testing of the same dosage sizes, and also there is a difference in dietary intake between the species as rats are vegetarians. Specific to the GI tract, rats have a larger relative gastric volume and 90% of the rat small intestine is the jejunum [121], the main site of absorption. In addition, rats lack a gall bladder and dilute bile is secreted continuously into the duodenum. In humans, on the other hand, the release of concentrated bile only occurs when chyme is present [121]. Therefore, the testing of lipid-based formulations in the rat is less appropriate as the continuous secretion of bile may underestimate the solubilisation capacity of the formulation [22]. Interspecies extrapolation from rats to humans requires careful consideration of these parameters.

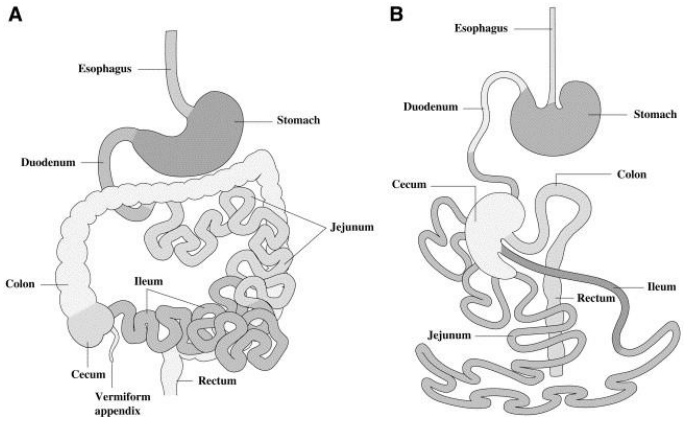

Figure 1-5 Gastrointestinal anatomy of the human (left) and rat (right) GI tract

Taken from [121]

Several studies aim to evaluate the food effect in rat animal models. Yu et al., orally administered lurasidone in male Sprague Dawley rats (n=5), where the fasted arm were fasted overnight and the fed arm was allowed free access to food [122]. A food effect was found, where the AUC and C_{max} was 1.5 times higher for the suspension in the fed state than the fasted state. Mou et al tested the potential for a food effect for Sporanox® pellets in Wistar rats (sex not disclosed, n=6) [123]. A positive food effect was found with a 44% and 18% increase in the C_{max} and AUC, respectively. A similar methodology was used, where the fasted state rats were fasted for 12 hours. In another investigation, the food effect potential for Sporanox® capsules was assessed in a fasted group (12 hour fast) and a normal housing food group in male Sprague Dawley rats (n=5). The intake of the normal food caused a 19% and 17% increase in C_{max} and AUC, relative to the fasted state. These studies show that free access to food can result in a positive food effect, and a similar methodology was used in Chapter 2. However, it is noted that the magnitude of the food effect in rats is less than the extent seen in humans [22].

1.4.2 Computational predictive tools

Biopharmaceutics processes, such as the food effect, are multifaceted, and therefore can be challenging to predict [124]. The chemical features of drug chemical entities can provide a guide for forecasting food effects, and can be used in food effect predictive models [8]. Rule of thumb such as the Biopharmaceutical Classification System (BCS) and Biopharmaceutical Drug Disposition Classification System (BDDCS) can provide simple approaches to predict the food effect [67,125,126], shown in Figure 1-6. The BCS classifies drugs based on their permeability rate and solubility, whereas the BDDCS categorises drugs based on their solubility and metabolism [127]. In general, high-fat meals do not affect the absorption of BCS/BDDCS Class I drugs, increase the extent of absorption for BCS/BDDCS Class II drugs, decrease the extent of absorption for BCS/BDDCS Class III, and there is insufficient data to show a trend for Class IV compounds [127]. These classification systems provide a straightforward reference for predicting food effect but are poorly predictive and therefore more advanced *in silico* tools need to be developed.

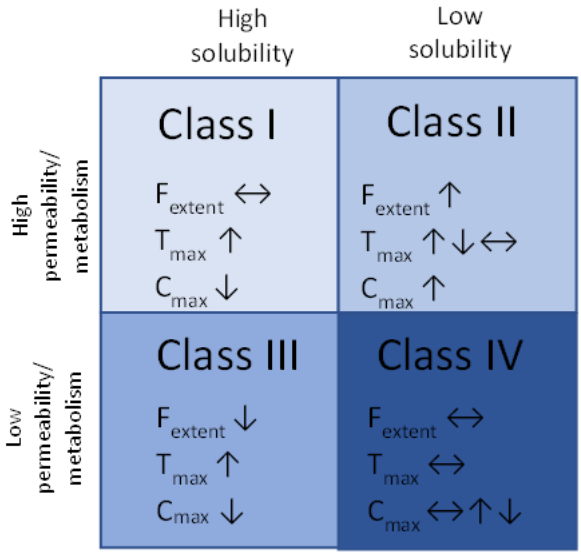

Figure 1-6 Predicted effect of high-fat meals by BCS/BDDCS class [10,67].

Over the past ten years, numerous studies have used physiologically based pharmacokinetic (PBPK) models for the prediction of the food effect for individual drugs [128,129], using the commercial software GastroPlus™ and SimCyp®. PBPK use mathematical equations to model physiological and anatomical processes. Compartments are constructed that correspond to the different organs or tissues in the body and flow rates are used [130]. Drug-related properties are inputted with human physiology-specific data to explore the mechanisms underlying the effects of food on oral absorption. The user can adjust the parameters in the software, such as the bile salt concentration in each compartment in the fasted and fed state [131]. The software simulates a drug plasma concentration-time profile in the fasted and fed state.

Emami Riedmaier et al., built and verified mechanistic PBPK models for 30 drugs compounds using controlled input data and methods of data generation [132]. A total of 8 compounds were classified with high confidence, implementing a middle-out simulation approach [133]. However, so far mostly poorly-soluble drugs have been investigated, without investigating other drug compounds [134]. In addition, usually drugs are inputted and investigated one-by-one, which is time-consuming and limits the large-scale evaluation of datasets.

The majority of the studies in the literature have used PBPK to model drugs showing positive food effects, where the key mechanisms for the positive food effect were the physiological changes that enhanced drug solubility. To-date, PBPK models are limited in their abilities to predict negative food effects [135]. Furthermore, PBPK modellers may spend a significant proportion of their time optimising the model parameters to produce the desired result. In fact, a literature search found that drug dissolution rates and precipitation times were most commonly optimised when an initial PBPK model could not accurately capture the effect of food [134]. Furthermore, *in vivo* data are typically required and at the early drug development, these data may not be available. Predictions can be successful estimated from *in vitro* or *in silico* data by applying modelling techniques at the drug discovery and early drug development stage. Follow-up PBPK

studies could then be conducted later in drug development to investigate chemical entities of interests.

1.4.2.1 Digital Pharmaceutics

Modelling and simulation approaches have become an integral part of drug discovery and now drug development [136]. The use of machine learning in drug development, however, is still in its infancy in supporting the data-driven drug discovery process. A number of studies have emerged in the pharmaceutics space for the prediction of formulation optimisation [137], molecular absorption, and oral bioavailability [138,139], which could expedite the lengthy drug development pipeline and improve the attrition rate. However, the use of machine learning techniques to predict the food effect is underdeveloped.

In the pharmacokinetics sector, artificial intelligence and machine learning have been successfully applied to predict adverse side effects [140], 2018), drug-drug and food-drug interactions [141-143], human ADME properties [144], and pharmacometrics [145]. Furthermore, machine learning applications are being explored for drugs with narrow therapeutic indices, such as tacrolimus using peak trough drug concentrations [146]. Recently, machine learning models are being developed more and more in the biopharmaceutics field, in this case to predict drug permeability across Caco-2 cells [147]. The development of machine learning models that aim to predict in vivo performance, including pharmacokinetic properties, have clear ethical and economic benefits [148].

1.4.2.2 Machine learning technologies

Machine learning, a subset of artificial intelligence, allows for pattern recognition from complex datasets, supporting complex data insight and accurate prediction making [149]. Recent advances in machine learning algorithms, faster computing hardware, and

the availability of user-friendly machine learning toolkits have improved access to machine learning tools. Machine learning models – which are typically learn using data-driven algorithms – can be used to predict a given outcome (model output) from a number of features (model inputs). Machine learning predictions can take seconds to minutes [150] in contrast to lengthy experimental methods.

Machine learning has been adopted by nearly every sector in society, from identifying tumours in magnetic resonance images to powering map-based search engines [151,152]. In the pharmaceutical industry, artificial intelligence and machine learning have been successful used in the drug discovery field [153,154], capturing headlines in the identification new drug targets [155]. Furthermore, a number of alliances have been built between traditional biopharma and new start-up artificial intelligence companies [156]. Current pharmaceutical development strongly relies on trial-and-error methods with laborious, time-consuming and costly studies [157].

1.4.2.2.1 Machine learning workflow

The machine learning process involves a series of steps that combine to form an overall pipeline (Figure 1-7). Supervised tasks contain inputs or features and labelled target outputs.

Figure 1-7 Overview of a typical machine learning pipeline.

Data acquisition

The data can be acquired either by mining data from the literature or experimentally. The data can be text, images, voice, or numerical data.

Data pre-processing

The data must be pre-processed or cleaned prior to any machine learning development. A recent evaluation found that data scientists spend up to 50 to 80% of their time on cleaning data and pre-processing [158]. Importantly, noisy data can affect the performance of machine learning algorithms. Data cleaning involves detecting inconsistencies in the data to improve the quality of the data [159]. Datasets can contain null values, outliers, irrelevant values, inconsistent values, and errors. First, exploratory data analysis can be conducted to detect any errors or inconsistencies. Then the inconsistencies can be processed by deleting the erroneous values or transforming the data. Next, the verification stage can be conducted to evaluate the effectiveness of the operations. Then, a new transformed dataset is created [160].

Feature engineering

Several techniques can be used for feature generation. Molecular inputs can be derived from computer simulations or experimental measurements. Identifying or deriving the most relevant features is known as feature engineering and is a key step for improving the performance of a machine learning model. Normalising the data can improve the training and testing performance [161].

1.4.2.2.2 Machine learning models

Supervised machine learning tasks aim to predict a numerical value or class for a specific target output. The prediction of numerical values is referred to as a regression task. On the other hand, a classification task predicts a category of an output. Machine learning differs from PBPK, molecular dynamics, and molecular docking.

Machine learning models each differ in their learning styles, vary in their assumptions about the data, the intricacies of the relationship between features and targets, and the generation processes [162]. Models also differ in their predictive abilities, interpretability, and robustness [148]. Well known software programmes, libraries, and

packages exist in Python and R. Some examples are *scikit-learn* [163], *Keras* [164], and *TensorFlow* [165]. There are linear models and non-linear models. The simplest machine learning model is linear regression which assumes that the target output can be predicted linearly from the input features. However, linear regression can be considered simplistic and has clear limitations in its modelling abilities [166]. Non-linear models can be categorised into tree-based, kernel-based, and deep learning algorithms.

1.4.2.3 Challenges to the adoption of digital pharmaceutics

The rarity of high-quality labelled data, nascent regulations, and legal concerns about sharing data are major barriers currently impeding the integration of digital pharmaceutics tools [167]. While machine learning algorithms are evolving to interpret small datasets, more data samples and larger datasets can improve the performance of machine learning algorithms [162,168]. In the pharmaceutics field, data collection by laboratory experiments can be time and resource expensive. Therefore, many studies in the biological, chemical, and pharmaceutical fields rely on data mining from the published literature [169]. Another challenge is the legal concerns as company data are not usually made publicly available due to intellectual property (IP) reasons. In academia, data may be kept private due to the competitive nature of the field. Although more and more, academics and industrialists are publishing their studies in open access publications and making their datasets available [170]. In addition, IP issues could be overcome by encryption methods, known as privacy-preserving machine learning [171]. Although, data must be unified and cleaned, which may be problematic with encrypted data.

Another barrier is the 'black-box' effect of machine learning algorithms, where the learning process is not shown by the model, and therefore it cannot be understood or interpreted by the pharmaceutical and data scientists. Some machine learning techniques, such as the decision tree-based models, allow the user to output graphical representations [172]. Recently, there has been a shift towards 'explainable' machine

learning algorithms that allows the user to understand the prediction processes [172]. One method, SHapley Additive exPlanations (SHAP), deconstructs a prediction into the sum of contributions [173]. It has the benefits of functioning with any machine learning algorithm and will give a value for how much a variable contributes to the final prediction. Other method is local interpretable model-agnostic explanations (LIME) that perturbs a data-point and looks at prediction [174]. Whilst it works with any machine learning algorithm, it can only work on individual data points. Clean high-dimensional data with consistent methodologies should be collected, and stored in open-source repositories so that lessons can be learnt from drugs that meet or fail to meet the market. As with other fields, best practices should be developed for the digital pharmaceutics field, the assumptions made emphasised, and limitations of each model highlighted.

Scope

It has been known for decades that there is fasted-fed variability in the absorption of oral medicines, however the issue still poses a significant problem in drug development. This introduction has outlined the assessment of food effects, both from a clinical perspective, the current gold standard method, and from a preclinical perspective. Traditional preclinical models were discussed, with a focus on animal models and computational models, with current limitations identified. There is a clear need for accurate preclinical tools to forecast potential food effects. The food effect must be considered in early drug development to enable the design of the most effective medicines with limited variability between the fasted and state states. The following chapters will outline current knowledge gaps in the field of oral drug absorption and the food effect, and will offer novel insights into the effect of food intake on rat animal model and showcase the development of new machine learning tools to aid the prediction of the food effect.

Thesis Objectives

This thesis can be summarised into the following aims and objectives:

Chapter 2

Aim: To map the multi-dimensional effect of food, sex, and strain on the key efflux transporters P-gp, BCRP, and MRP2 using commonly used quantification techniques: PCR and ELISA.

Objectives:

- To quantify the intestinal expression of P-gp, MRP2, and BCRP in the fasted and fed state by ELISA
- To quantify the expression of *abcb1a*, *abcg2*, and *abcc2* in the fasted and fed state by PCR
- To explore if sex differences are seen between male and female rats
- To explore if strain differences are seen between Wistar and Sprague Dawley rats
- To explore the correlation between ELISA and PCR methods

Chapter 3

Aim: To understand the effect of three feeding interventions – fasted, housing food (normal meal), and a non-nutritive substance (fibre meal) on efflux transporters (P-gp, BCRP, and MRP2)

Objectives:

- To characterise the GI luminal characteristics (pH and buffer capacity) in the stomach, small intestine, and colon following food intake
- To investigate the intestinal expression of three clinically relevant efflux transporters: P-gp, BCRP, and MRP2 under three feeding interventions
- To investigate if sex differences are seen in the expression levels

- To quantify the plasma concentration of sex hormones (testosterone and estradiol) and a gastrointestinal hormone (cholecystokinin) and assess if there is a correlation between the transporter expression and hormone concentration
- To investigate the trends in transporter expression (P-gp, BCRP, and MRP2) over time (0 to 2 h)

Chapter 4

Aim: to test if machine learning technologies can be used to predict the food effect

Part 1: to use classification tasks to predict the food effect

Objectives:

- To conduct exploratory data analysis on the dataset [175]
- To perform data cleaning on the feature set
- To use a toolkit of machine learning algorithms (random forest [RF], logistic regression [LR], support vector machine [SVM] and k-Nearest neighbour [kNN])
- To train and test machine learning tasks
- To achieve an optimal task performance for predicting how the intake of food will affect drug absorption

Part 2: to use regression tasks to predict food-mediated changes to key pharmacokinetic changes - AUC and C_{max}

Objectives:

- To conduct exploratory data analysis on the dataset [176]
- To perform data cleaning on the feature sets - RDKit, ADMET, and Morgan fingerprint (MFP) feature sets

- To use a toolkit of machine learning algorithms (AdaBoost [ADA], Gradient Boosting [GB], extreme Gradient Boosting (XGB), kNN, Least Absolute Shrinkage and Selection Operator [LASSO], RF, Multilayer Perceptron [MLP], and support vector regression [SVR])
- To train and test machine learning tasks
- To achieve an optimal task performance for predicting how the intake of food will affect drug absorption

Chapter 2 : The rat as a preclinical model in the fasted and fed state

2. 1 Introduction

2.1.1 Rats as preclinical models

A major goal of preclinical drug development is to predict drug activity in humans using models [117]. *In vitro* models, computational predictive tools, and *in vivo* animal models are harnessed for valuable early insights. In the regulatory space, the International Council for Harmonisation (ICH) requires studies using two species – a rodent and non-rodent – for small molecule new chemical entities, in line with the ICH M3 (R2) guideline [177]. In fact, rats are one of the most used pre-clinical animal models in oral drug development due to their ease of handling, low cost, and the similarities between their GI tract and those of humans [117,118,178].

2.1.2 Rat strain

The *Rattus* genus is a term for the rat species. Originally, rats are thought to have originated from parts of Asia. In Europe, *Rattus rattus* were well recognised by 1100 AD [179]. The laboratory rat can be traced back to the 18th century. English physician John Berkenhout first documented the wild brown *Rattus norvegicus* in 1769 and believed that these rats migrated to England from Norwegian ships in 1728 [180]. Over the centuries, rats were bred for sport with dogs in rat-baiting events [181]. Albino rats were often removed and kept separately for further selective breeding [182].

Brown rats were amongst the earliest mammalian species used for laboratory experiments [181]. In the early 1900s at the Wistar Institute of Philadelphia, its first scientific director Henry H. Donaldson started the first breeding programs to create specific laboratory inbred strains [183]. Scientists at the Wistar Institute are credited for developing cages, diets, breeding practices, and facilities for holding and breeding rats [183]. The Sprague Dawley rat is an outbred rat, first produced in 1925 by Robert W. Dawley from a Wistar female and a hybrid male of unknown origins in the Sprague-Dawley Animal Company, established in Madison, Wisconsin [184]. Harlan acquired the company in the 1980s and Harlan then became Envigo in 2015 [185]. Charles River then

developed a new line of Sprague Dawley rats with better microbial status by caesarean derivation [186].

Today, there are 51 known species of the *Rattus* of both albino and pigmented types. Wistar rats and Sprague Dawley rats are becoming the most used laboratory animals worldwide. Musther et al. reviewed over 122 articles in the biomedical space from 1969 to 2012 and reported that 49% of studies on oral and intravenous bioavailability used the Sprague Dawley strain [187]. Wistar rats were used in 35% of studies, and 16% used the albino rat, Long Evans, Fischer 344, and Lewis types. There are innate physiological, anatomical, and behavioural differences between the strains. For example, Sprague Dawley have long narrow heads, are calmer in nature, grow faster and show high reproductive rates. In addition, Sprague Dawley rats cost less. Wistar rats, on the other hand, have wide heads, long ears, and show higher survival rates [184,188].

2.1.3 Sex differences in rats

Published in 1993, the NIH Revitalization Act requires the inclusion of females in NIH-funded clinical research. The same year the FDA published a guideline for industry entitled 'Study and Evaluation of Gender Differences in the Clinical Evaluation of Drugs' calling for the evaluation of males and females in all phases of drug clinical trials, including safety, efficacy, and dose-determination studies [74]. Twenty two years later, in 2015 NIH published further policies requiring the consideration of sex as a biological variable in experimental design, analysis, and publications [79]. Recently in 2022, the UK Medical Research Council introduced the requirement to include both sexes in experimental design and analysis plans [80]. While there is awareness of the need for females in clinical trials, preclinical studies often overlook the need to evaluate sex differences in animal models. If results are not stratified according to sex, it could potentially skew or obscure sex differences in the findings [75].

There is a wealth of research that shows sex differences in drug and therapeutic effectiveness in humans and preclinical rat models [73]. The innate differences at the

physiological, chemical, and biological levels can lead to alterations in drug pharmacokinetic and pharmacodynamic processes. In addition, the presence of endogenous steroid hormones can contribute to these differences.

2.1.3 Efflux transporters expression

A large body of research has characterised intestinal transporters, focussing on tissue expression profiles, substrate and inhibitor profiles, and interspecies differences [64]. Most efflux transporters belong to ABC family and actively pump substrates out of cells. The overexpression of ABC transporters in cancer cells results in multidrug resistance, and this phenomenon has driven extensive mechanistic studies into the expression of these proteins [53]. To date, a total of 50 ABC transporters have been characterised in humans [54]. The most characterised ABC transporter is P-gp.

BCRP and MRP2 are also key efflux transporters, with high levels of expression in barrier tissues [65]. These transporters are found in the blood-brain barrier and epithelia of the kidney, liver, as well as in the enterocytes of the intestinal tract. At the intestinal layer, membrane transporters are apically located and efflux endogenous and exogenous substrates, limiting their absorption into the systemic circulation. Physiologically, efflux transporters protect the body from toxic substances, such as tumour necrosis factor and lipopolysaccharide in cases of injury [189]. P-gp was also reported to be involved in cholesterol trafficking [190] and lipid homeostasis [191]. BCRP is reported to transport conjugates of steroid hormones [192], and MRP2 is found to transport glutathione, glucuronide, and sulphate conjugates. A wide range of structurally unrelated hydrophobic substances bind to these transporters and show partial overlapping substrate specificity [52]. Food components as well as drugs are reported to interact with these transporters and can limit oral bioavailability by food-drug interactions at the transporter stage [63]. The bioavailability of orally administered drugs is in part dependent on the expression and activity of these transporters. Importantly, the distribution of these efflux transporters in the GI tract is heterogenous and each GI

segment (duodenum, jejunum, ileum, and colon) shows different patterns of expression [193,194]. This regional heterogeneity in the drug transporter expression may impact the absorption site of an oral drug product.

2.1.4 Quantification methods

Multiple quantification techniques are available in biomedical research. The quantification of efflux transporters along the intestinal tract can help to predict the intestinal drug absorption of substrates. As detailed in a recent White Paper, variability in protein quantification data may be due to differences in sample collection, e.g. fresh, snap-frozen, or formalin-fixed, postsurgical, or post-mortem tissue [195]. Measurement techniques introduce further variability. Biological samples use tissue lysates, membrane extracts, and biological fluids. Proteins are extracted using ionic detergents, such as sodium dodecyl sulfate (SDS), N-lauryl sarcosine, cetyltrimethyl-ammoniumbromide (CTAB), and sodium cholate

Traditional methods such as Western Blot possess several distinct disadvantages that limit their usefulness in providing accurate protein quantification data. Western Blot is a multistep process that provides protein quantification data relative to an internal reference protein. The chosen internal reference protein differs between studies in the literature, and may show variable expression along the intestinal tract. Western Blot is commonly used and is relatively simple to conduct. Although, some limitations are that it is low throughput, lack specificity, time-consuming, technically demanding, there is limited cross-comparability, and is a semi-quantitative technique. In addition, antibodies and purified standards for transporter and receptor proteins are not frequently available. Western Blot can produce erroneous results, where false-positive results are found if the antibody reacts with a non-intended protein, and on the other hand, false-negative findings can be shown if larger proteins are not given sufficient time to properly transfer to the membrane [196].

Other robust techniques exist for protein quantification such as liquid chromatography-mass spectrometry/mass spectrometry (LC-MS/MS). It is associated with high resolution and sensitivity, although can be time-consuming and costly to develop sensitive methods. LC-MS/MS sample preparation requires protein precipitation, liquid/liquid extraction, and solid-phase extraction procedures [197]. Several of these preparation techniques can take over an hour to perform, with long incubation periods in between steps. More and more, the pharmaceutical industry favours high-throughput experimentation and rapid screening [198]. The differences in LC-MS/MS methodologies (global or targeted proteomics, relative or absolute, enriched fractions/cel lysates, and label-free or label-based) has produced discrepancies in the literature [199]. Therefore, LC-MS/MS may be too slow and technically difficult to accelerate drug development timelines.

2.1.4.1 Enzyme-linked immunosorbent assay (ELISA)

Enzyme-linked immunosorbent assay (ELISA) is a 96-well plate-based assay technique that can detect and quantify soluble substances, such as proteins. ELISA is high throughput, highly selective, easy to perform, quantitative, shows less interference, and can detect target analytes within heterogenous samples. Furthermore, the experimental time of ELISA method can be at least half the time of that of LC-MS/MS [200]. There are four main types: direct ELISA, indirect ELISA, sandwich ELISA, and competitive ELISA. Sandwich ELISA was used in this thesis, and the main steps are detailed below.

1) **Coating with capture antibody** – immobilisation of the capture protein (antibody) to the wells of the plate and followed by an incubation period. A wash cycle is then performed to remove any unadsorbed capture protein from the well surface. Some ELISA kits have pre-coated well plates, such as the ELISA kits used in this work.

2) **Blocking** – block unbound sites using proteins such as bovine serum albumin or casein to prevent the target protein from adsorbing non-specifically. This increases the assay sensitivity by lowering background noise.
3) **Addition of the sample** – incubate the sample (antigen) to allow the target antigens to bind to the immobilised capture antibody. This is followed by a wash cycle to remove unbound antigen.
4) **Addition of the detection antibody label conjugate and secondary antibody** – incubate the detection antibody in the well, which will bind to a different part of the antigen than the capture antibody. This is followed by a wash cycle.
5) **Detection** – add the substrate (commonly horse radish peroxidase [HRP] and alkaline phosphatase [ALP]) and measure the output (chemiluminescence/ chromogenic/fluorescence) from an enzyme-substrate interaction or fluorophore.

2.1.4.2 PCR (polymerase chain reaction)

Real-time reverse transcription polymerase chain reaction (PCR) is the method of choice by many researchers for the quantification of mRNA expression [201]. PCR can be conducted using an automatic thermocycler that alters the temperature of the reaction to allow DNA denaturing and synthesis.

There are three major steps in the PCR thermocycler, as detailed below.

1) **Denaturation** – the heat (95°C) breaks the hydrogen bonds in the DNA and separates the DNA into single strands (called the denaturation of double stranded-DNA).
2) **Annealing** – the sample mixture is cooled to between 50 to 60°C which allows the DNA primers and DNA polymerase to bind to the individual strands of DNA (called the annealing of the primers). Nucleotides (A, T, C, G) from the added

mixture solution will pair by ionic bonds with the individual separated strands of DNA.

3) **Extension** – a new complementary strand of DNA is formed.

The temperature cycles from 95°C to 50 to 60°C. The cycle is then repeated about 35 to 40 times

The three main steps of reverse transcriptase-PCR are detailed below.

1) **Reverse transcription** - reverse transcriptase (RT)-dependent conversion of RNA into cDNA. The RNA is used as a template and oligo (dT) or random primers and reverse transcriptase are used to reverse transcription into single-stranded cDNA.
2) **Amplification** of the cDNA using polymerase chain reaction.
3) **Detection** and quantification of the resulting amplification products are compared to other nucleotides segments.

Quantitative PCR is a variation of traditional PCR that allows the analysis of the amplified DNA in real-time using fluorescent dyes. The fluorescent dyes attach to some of the nucleotide strands which allows the measurement of the specific products. The fluorescence is measured inside the tube at every cycle.

2.2 Aims

Here, this study aims to be the first to map the multi-dimensional effect of food, sex, and strain on the key efflux transporters P-gp, BCRP and MRP2 using commonly used quantification techniques: PCR and ELISA.

Objectives

- To quantify the expression of P-gp, BCRP, and MRP2 in the fasted and fed state by ELISA
- To quantify the expression of *abcb1a*, *abcg2*, and *abcc2* in the fasted and fed state by PCR
- To explore if sex differences are found between male and female rats
- To explore if strain differences are found between Wistar and Sprague Dawley rats
- To explore the correlation between ELISA and PCR methods

2.3 Materials and methods

2.3.1 Materials

Krebs-bicarbonate Ringer's solution (KBR), pH 7.4, was freshly prepared before the experiment at room temperature and was kept at 37 °C. KBR was composed of 10 mM D-glucose, 1.2 mM CaCl2, 1.2 mM MgCl2, 115 mM NaCl, 25 mM NaHCO3, 0.4 mM KH2PO4 and 2.4 mM K2HPO4 [13]. Lysis buffer was freshly prepared with 50 mM Tris, 250 mM NaCl, 5 mM ethylenediaminetetraacetic acid (EDTA), 1 mM Na3VO4, 1 mM phenylmethylsulfonyl fluoride (PMSF), 1% Nonidet P40 and protease inhibitor cocktail from Sigma in a phosphate-buffered saline (PBS) solution and stored at 4 °C. All other chemicals and kits are mentioned individually in the following methods.

2.3.2 Animals

Five male and five female Wistar and Sprague Dawley rats (healthy, 8 to 13 weeks old) respectively were used as the animal models. The rats were housed at room temperature (25°C) in a light–dark cycle of 12 h. The rats acclimatised to the animal unit for at least 7 days. On the day before the experiments, the fasted group of rats were fasted overnight and housed individually in metabolic cages until the following morning at 8 am. For the fed group of rats, no fasting took place. All animal work was conducted in accordance with the project license (8002536), approved by the Home Office under the Animals (Scientific Procedures) Act 1986 on 7 June 2012.

2.3.3 Intestinal tissue collection

Their intestines were immediately excised and stored in an ice-cold KBR solution, following sacrifice by CO2 asphyxiation. Roughly 2 cm pieces of the small intestine; duodenum (1 cm from the ligament of Treitz), jejunum (10 cm from the ligament of Treitz), ileum (1 cm from the cecum) and colon (descending) were opened along their

mesenteric border. The tissues were gently washed with KBR solution to remove the intestinal contents.

2.3.4 Initial total protein quantification

The mucosal tissues (approximately 50 mg) were cut into small pieces and homogenized in 0.5 mL RIPA lysis buffer at 30 Hz for 30 s with a TissueLyser (QIAGEN) and repeated twice at intervals of 30 s for complete homogenisation. The tissue homogenates were incubated at 4°C for 2 h, and then centrifuged at 12,000 *g* for 5 min. The total tissue protein was collected in the supernatants, and its concentration was subsequently determined with the Pierce™ BCA protein assay kit (Beyotime Biotechnology) according to the manufacturer's instructions.

2.3.5 Measurement of P-gp, BCRP, and MRP2 Protein Levels in by ELISA

ELISA kits were purchased from MEIMAN Biotech. The ELISA kits were as follows: rat P-gp ELISA Kit (MM-0604R2), rat BCRP ELISA kit (MM-0606R2), and rat MRP2 ELISA kit (MM-0607R2). To measure the P-gp, BCRP, and MRP2 transporter protein level by ELISA, ELISA kits (Meimian Biotech) were used based on the manufacturer's description; a volume of the supernatant (from Section 2.4) containing a mass of 50 µg of total protein lysate was taken.

Beta-actin was chosen as the internal control protein which was measured by ELISA Assay kit (RTDL00014, Assay Genie). Briefly, 50 µL of serially titrated standards, diluted samples and blanks were added to the standard wells of the i) P-gp; ii) BCRP; and iii) MRP2 microplates in duplicates, respectively. 100 µL of HRP-conjugate reagent was then added to each well apart from the blank wells. The plate was covered with a plate sealer membrane and incubated for 60 min at 37°C. The plate sealer was then removed, and the liquid discarded by rigorously flicking into an acceptable waste receptacle. The washing buffer solution provided in the assay kit was diluted 20-fold with distilled water.

It was then added to each well, shaken on a plate stirrer for 3 s and drained. This was repeated 5 times and wells were blotted dry using a paper towel to remove any remaining liquid. 50 µL Chromogen Solution A and 50 µL Chromogen Solution B was added to each well, covered and incubated for 15 min at 37°C. 50 µL of the Stop Solution was added to each well; a blue colour change to a yellow solution would have indicated a stop in the reaction. Upon analysis, the blank well was taken as zero. Absorbance was then measured at 450 nm in a plate reader following the addition of the Stop Solution within 15 min.

A linear calibration line was constructed using P-gp; BCRP; MRP2, and appropriately diluted in 50 mM carbonate buffer (pH 9.5). Tissue supernatants for protein transporter quantification, were also appropriately diluted to 50 mM carbonate buffer (pH 9.5). Absorbance was measured at 450 nm after the reaction and the protein and hormone expression was calculated according to the standard protein calibration curve. Protein in all unknown and standard preparations were measured as per instructions of the ELISA kit in duplicate.

2.3.6 Measurement of P-gp, BCRP, and MRP2 mRNA levels in by PCR

Following collection (as described in Sections 2.3 and 2.4), the mucosal tissues were kept in RNAlater Stabilization Solution (Thermofisher). Total RNA in each intestinal sample was isolated and purified with the PureLink RNA Mini Kit (Thermofisher), and RNA concentration was measured with a Nanodrop 2000 (Thermofisher) according to the manufacturer's instructions.

Subsequently, the quantification of the target RNA was conducted as follows: 1 mg of total RNA of each sample was reverse-transcribed using the iScript cDNA Synthesis Kit (BioRad). To quantify the level of P-gp mRNA (*abcb1*), BCRP mRNA (*abcg2*), and MRP2 mRNA (*abcc2*), PCR was performed on the 7500 Real-Time PCR System (Applied Biosystems, Thermofisher) using the method described in a study by MacLean et al [202]. Briefly, 50 µL of PCR reaction contained 25 µL of PowerUp SYBR Green PCR Master Mix

(Thermofisher), 500 nM each of forward and reverse primers, and 1 μg of cDNA. β-actin (*ACTB*) was used for normalization and amplification of 1 μg of cDNA. PCR was carried out in 96-well PCR plates (Thermofisher). The amplification program for all genes consisted of one preincubation cycle at 95 °C with a 10 min hold, followed by 45 amplification cycles with denaturation at 95 °C with a 10 s hold, an annealing temperature of 50 °C with a 10 s hold and an extension at 72 °C with a 10 s hold. Amplification was followed by a melting curve analysis which ran for one cycle with denaturation at 95 °C with a 1 s hold, annealing at 65 °C with a 15 s hold and melting at 95 °C with a 1 s hold. Distilled water was included as a negative control in each run to determine the specificity of primers and possible contaminants.

Primers (shown in Table 2-1) were designed by primer-BLAST searching with publicly available sequence information of the GeneBank of the National Center for Biotechnology Information (NCBI) and purchased from Eurofins (Eurofins Genomics, Germany).

Relative expressions of *abcb1a*, *abcg2*, and *abcc2* mRNA in different intestinal segments were calculated using 7500 software (version 2.0.6, Thermofisher). The average of the threshold cycle (Ct) values for tested genes and the internal control (β-actin, *ACTB*) was taken, and then the differences between Ct values for tested genes and internal control (ΔCt) were calculated for all of the experimental samples.

Table 2-1 Primers used for the analysis of P-gp, BCRP, and MRP2 in rat intestines by PCR

Gene		Primer (5′–3′)	Amplicon (bp)	Genebank accession
P-gp				
abcb1a	forward	CACCATCCAGAACGCAGACT	139	NM_133401
	reverse	ACATCTCGCATGGTCACAGTT		
BCRP				
abcg2	forward	GTAGGTCGGTGTGCGAGTCA	717	NM_181381
	reverse	AACCAGTTGTGGGCTCATCC		

MRP2				
abcc2	forward	GACGACGATGATGGGCTGAT	883	NM_012833
	reverse	AGGCACGGATAATGGGCAAA		
Beta-actin				
ACTB	forward	GCAGGAGTACGATGAGTCCG	74	NM_031144
	reverse	ACGCAGCTCAGTAACAGTCC		

2.3.7 Statistical Analyses

The data was tested for normality using the Shapiro-Wilk test. As this was true, significant differences among experimental groups were analysed by one-way analysis of variance (ANOVA) followed by Tukey's post hoc analysis using Python (version 3.9.0). A significance value of $p < 0.05$ was used for all tests. The correlations between the ELISA and PCR methods for protein (P-gp, BCRP, and MRP2) and mRNA (*abcb1a*, *abcg2*, and *abcc2*) expression, respectively, were assessed by the Spearman's rank coefficient method in Python.

2.3.8 Data presentation

Most of the figures were constructed as box plots consisting of a central line indicative of the median, a box indicative of the IQR, where the whiskers were 1.5 times the 25th and 75th percentile, respectively and the diamond shapes represented the outliers. No outliers were removed. Any value that was 1.5 x IQR greater than the third quartile was classified as an outlier and any value that was 1.5 x IQR less than the first quartile was also as an outlier. Correlation plots were represented as line and scatter plots. Jupyter Notebook version 6.0.3 was used with the Matplotlib package version 3.4.3 [203].

2.4 Results

2.4.1 ELISA calibration curves

Figure 0-1, and Figure 0-2, and Figure 0-3 (Appendix) report the ELISA calibration curves of P-gp, BCRP, and MRP2.

2.4.2 Intestinal P-gp and *abcb1a* quantification

2.4.2.1 Intestinal P-gp and *abcb1a* quantification in Wistar rats

Figure 2-1 shows the P-gp expression in Wistar rats, comparing the feeding states. The trend in P-gp expression in the fasted and fed states were statistically different between the sexes ($p < 0.05$). In the male rat, feeding decreased the P-gp expression in the duodenum (-32%), jejunum (-42%), ileum (-29%), and colon (-35%). On the other hand, in the female rat feeding increased the P-gp expression in the jejunum (28%), ileum (70%), and colon (140%). Intestinal regional differences were observed. The fasted male showed differences from the duodenum to the jejunum, the jejunum to the ileum, and the ileum to the colon ($p < 0.05$). Fasted female P-gp expression were comparable; except a decrease was seen from the ileum to the colon (10.22 ± 1.25 ng/mg to 8.50 ± 1.06 ng/mg, respectively).

(A)

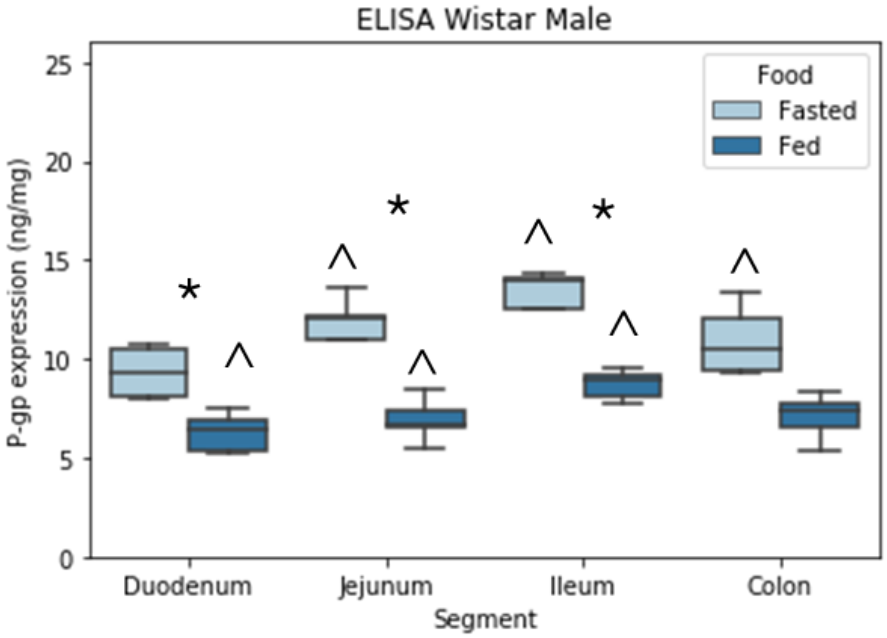

(B)

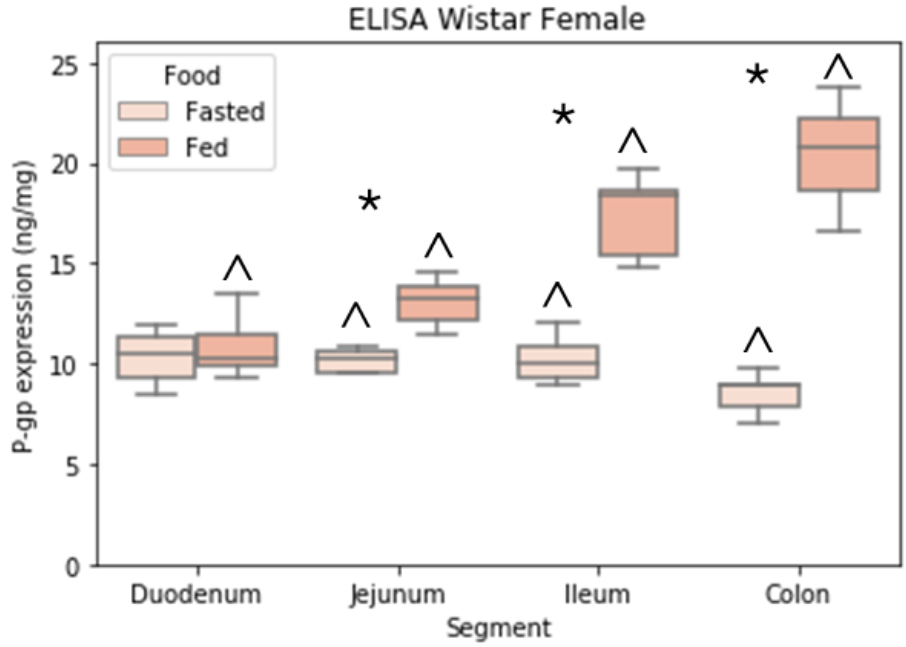

Figure 2-1 P-gp expression in fasted and fed (A) male and (B) female Wistar rats quantified by ELISA (n=5). The * symbol denotes statistical significance between the feeding state and ^ denotes a statistical significance between the sexes in an intestinal region ($p < 0.05$)

The *abcb1* PCR quantification showed similar trends to the P-gp protein quantification in the male rat – feeding decreased the *abc1a* expression by -55% in both jejunum and ileum (Figure 2-4). In contrast, the *abc1a* quantification in the female showed differing trends in the jejunum and ileum. Interestingly, differing trends were seen between the PCR and ELISA techniques in the female Wistar rat. Feeding significantly decreased *abc1a* levels in the jejunum from 7.53 ± 0.52 to 5.74 ± 0.35 and the ileum from 7.09 ± 0.64 to 6.60 ± 0.51 ng/mg. In contrast, feeding increased P-gp expression in the jejunum and ileum (Figure 2-1). Sex differences were seen in the jejunum, ileum, and colon in both prandial states.

(A)

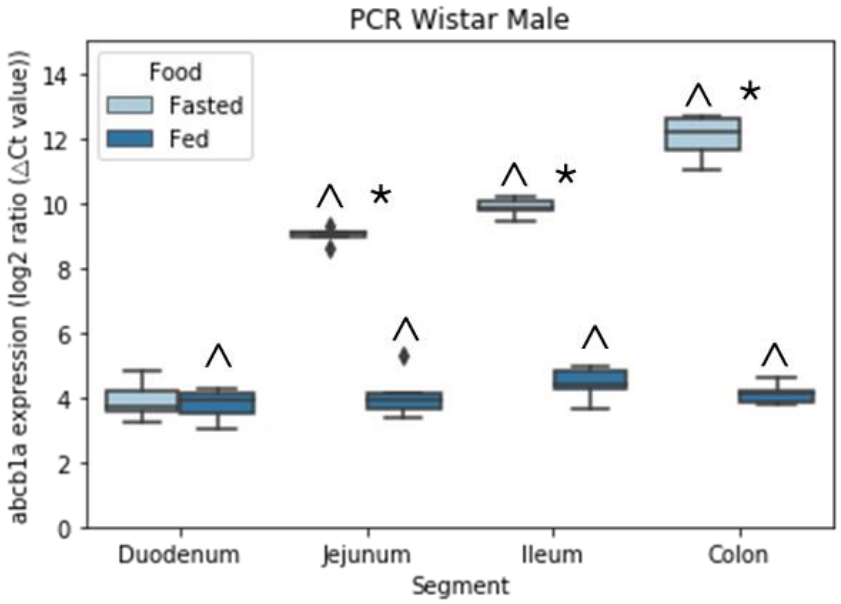

(B)

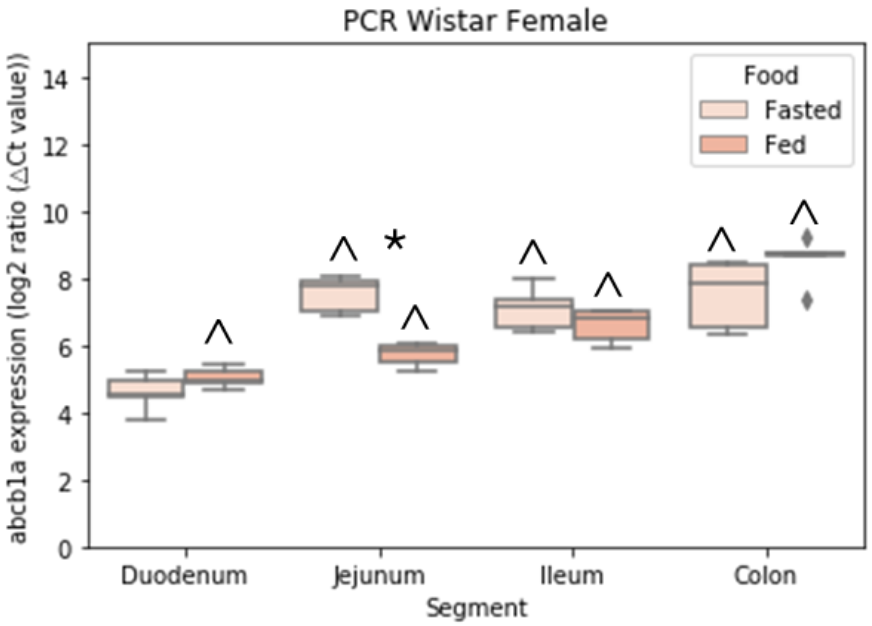

Figure 2-2 *abcb1a* expression in fasted and fed (A) male and (B) female Wistar rats quantified by PCR (n=5). The * symbol denotes statistical significance between the feeding state and ^ denotes a statistical significance between the sexes in an intestinal region ($p < 0.05$)

A moderately strong correlation (r=0.615) was seen for the Wistar rat between the ELISA protein quantification method and PCR mRNA quantification method (Figure 2-3).

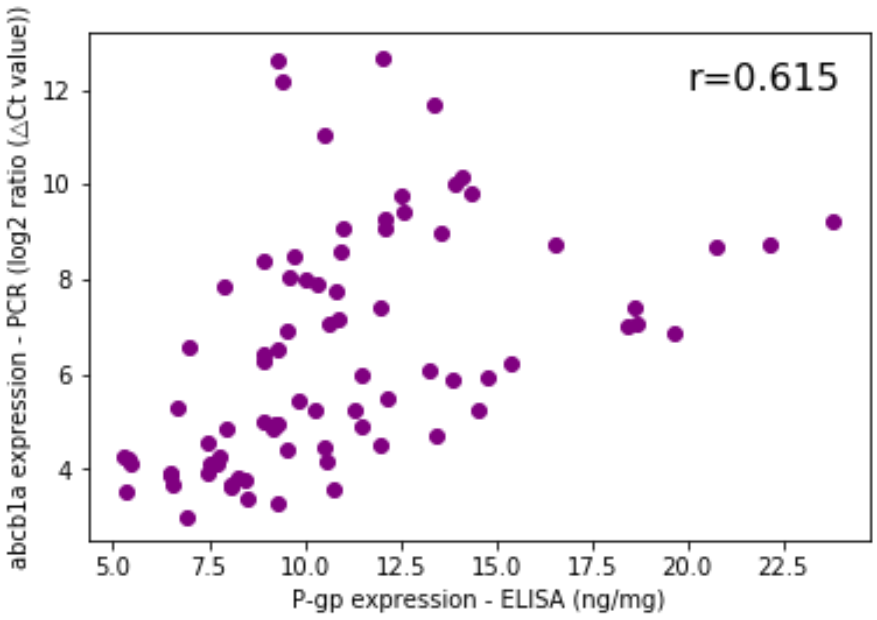

Figure 2-3 Correlation of intestinal P-gp expression quantified by ELISA and *abcb1a* expression quantified by PCR in Wistar rats

2.4.2.2 Intestinal P-gp and *abcb1a* quantification in Sprague Dawley rats

Figure 2-4 displays the P-gp expression in Sprague Dawley rats. In the intestinal tract, P-gp increased across the small intestine (from the duodenum to the ileum), then decreased in the colon. In the male rats, feeding decreased the ileal P-gp expression by 20%. In the female rat, feeding increased the colonic P-gp expression, from 11.88 ± 1.66 ng/mg to 17.24 ± 2.56 ng/mg. Sex differences were observed in the ileum in both prandial states. The fasted female ileal P-gp was 11% lower than the male ileal P-gp. On the other hand, the fed female ileal P-gp was 23% higher. The largest inter-individual variability was seen in the fed state, with the largest standard deviation of 3.61 ng/mg in the fed male jejunum.

(A)

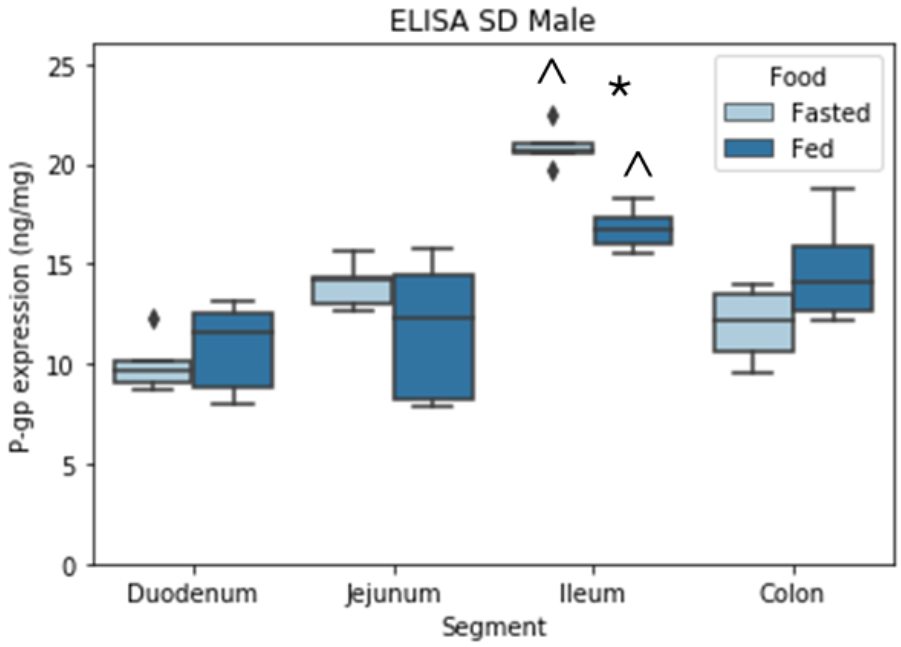

(B)

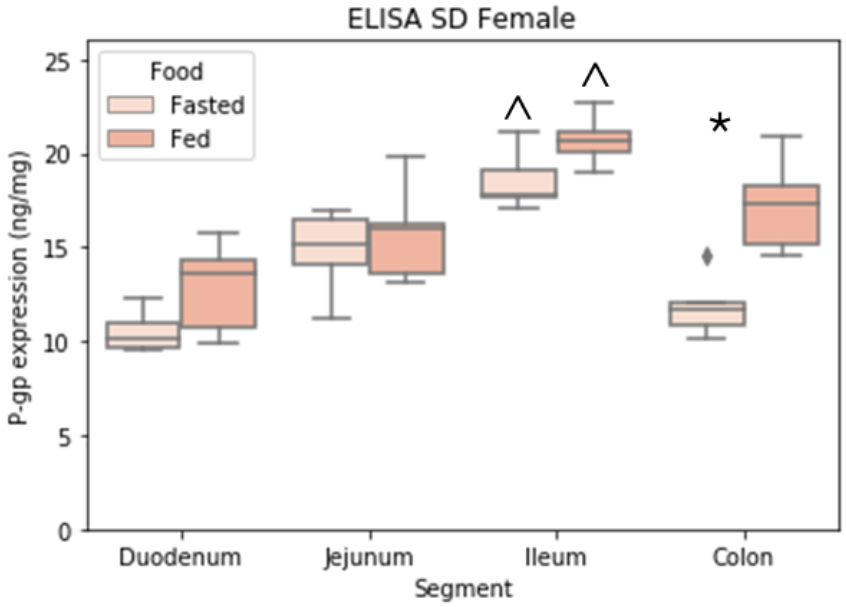

Figure 2-4 P-gp expression in fasted and fed (A) male and (B) female Sprague Dawley rats quantified by ELISA (n=5). The * symbol denotes statistical significance between the feeding state and ^ denotes a statistical significance between the sexes in an intestinal region ($p < 0.05$).

Figure 2-5 shows the *abc1a* expression in Sprague Dawley rats. Sex differences were seen in the fed state. The fed state female *abc1a* expression was 21%, 17%, and 11% higher than their male counterpart in the duodenum, jejunum, and colon, respectively. In the female Sprague Dawley rat, the feeding intervention increased *abc1a* expression by 19% and 28% in the duodenum and colon. Regional differences were seen between the jejunum and ileum.

(A)

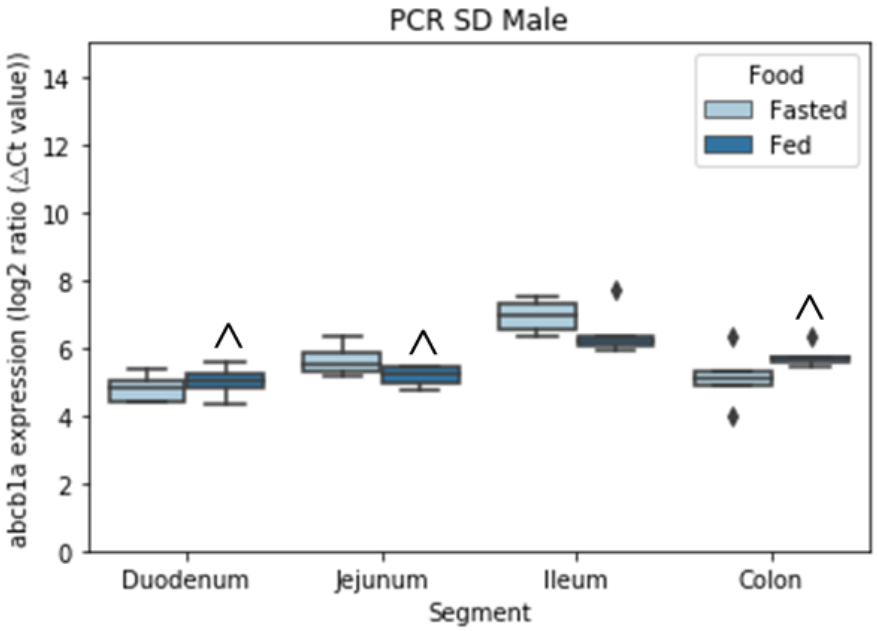

(B)

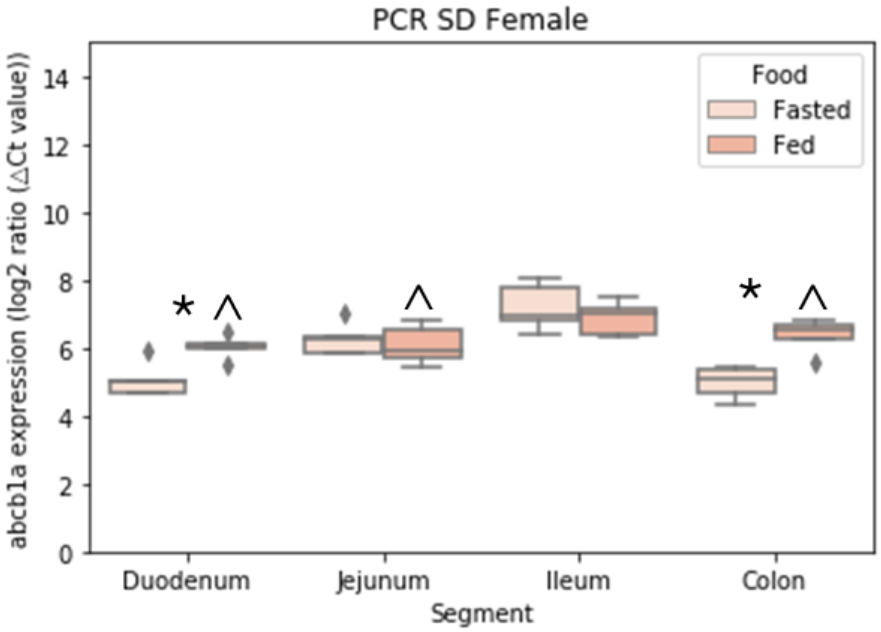

Figure 2-5 *abcb1a* expression in fasted and fed (A) male and (B) female Sprague Dawley rats quantified by PCR (n=5). The * symbol denotes statistical significance between the feeding state and ^ denotes a statistical significance between the sexes in an intestinal region ($p < 0.05$).

A moderately strong correlation (r=0.741) was seen for the Sprague Dawley rat between ELISA P-gp and PCR *abc1a* expression (Figure 2-6).

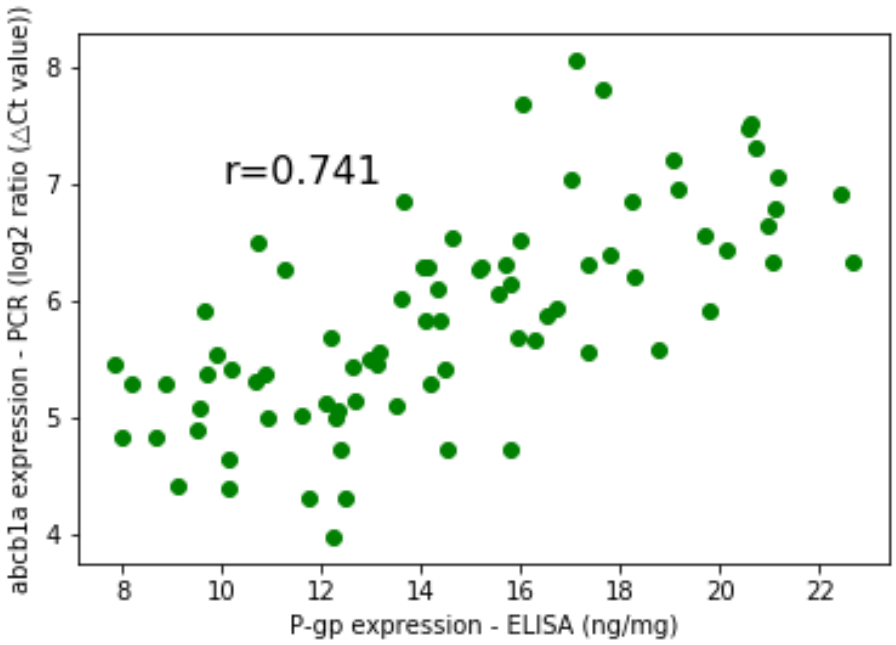

Figure 2-6 Correlation of intestinal P-gp expression quantified by ELISA and *abcb1a* expression quantified by PCR in Sprague Dawley rats

2.4.2.3 Strain Differences in Intestinal P-gp and *abcb1a* expression between Wistar and Sprague Dawley Rats

Strain differences were displayed in the P-gp protein and *abc1a* mRNA expression between the Wistar and Sprague Dawley rats ($p < 0.05$) (Figure 2-7, Figure 2-8, Figure 2-9, and Figure 2-10). To be precise in male rats, strain differences were seen in the *abc1a* expression in both prandial states, and P-gp expression in the fed state and the fasted jejunum and ileum.

In female rats, a strain difference was seen in the fasted jejunum, ileum, and colon, as well as the fed ileum with ELISA. For the mRNA levels, strain differences were observed in the jejunum and colon in both prandial states. Overall, Sprague Dawley rats showed higher P-gp and *abc1a* expression than Wistar rats by ELISA and PCR, respectively.

(A)

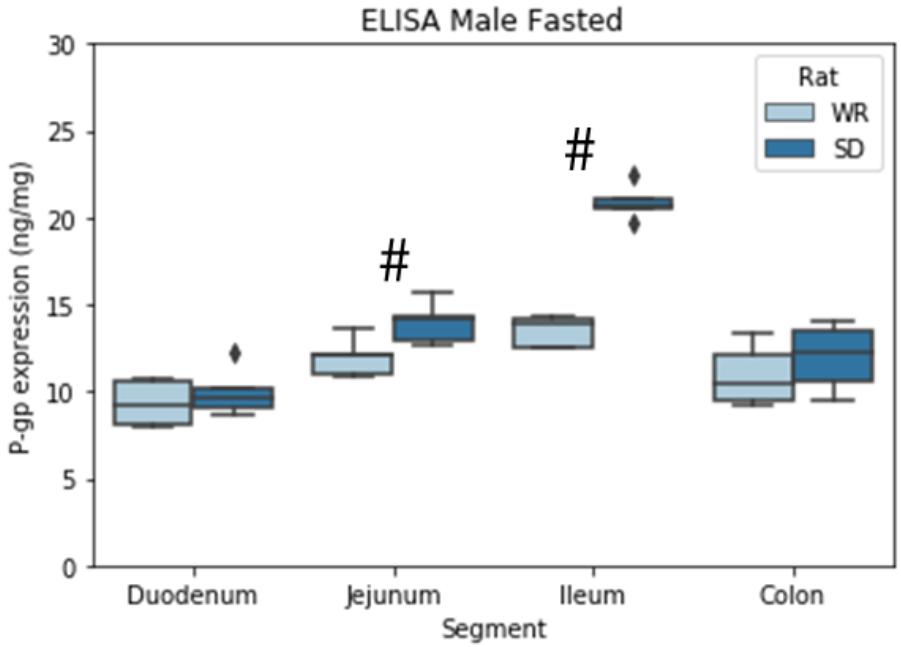

(B)

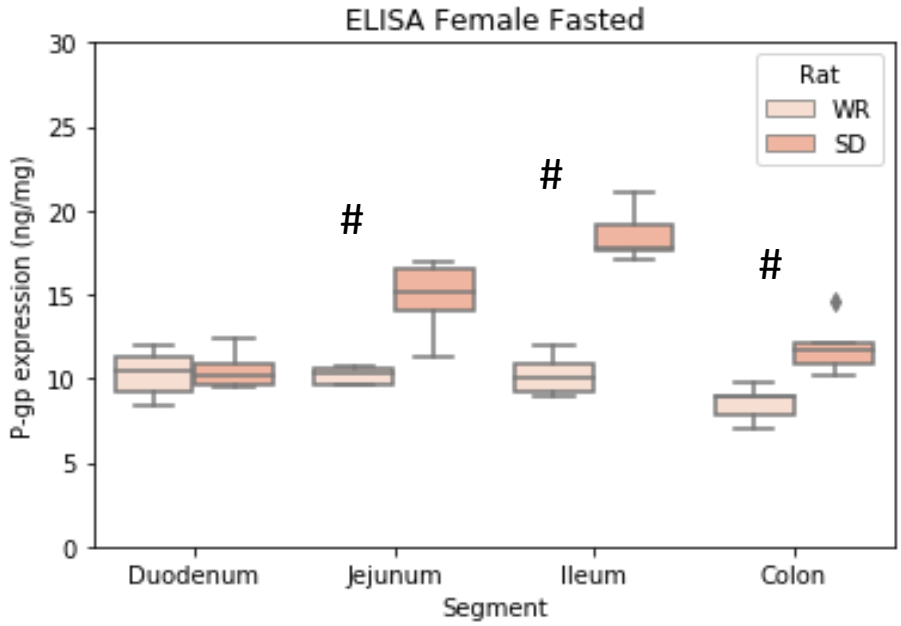

Figure 2-7 Strain differences in P-gp expression in fasted male and female Wistar and Sprague Dawley rats quantified by ELISA (n = 5). The symbol # denotes statistical significance between the two strains at an intestinal region ($p < 0.05$).

(A)

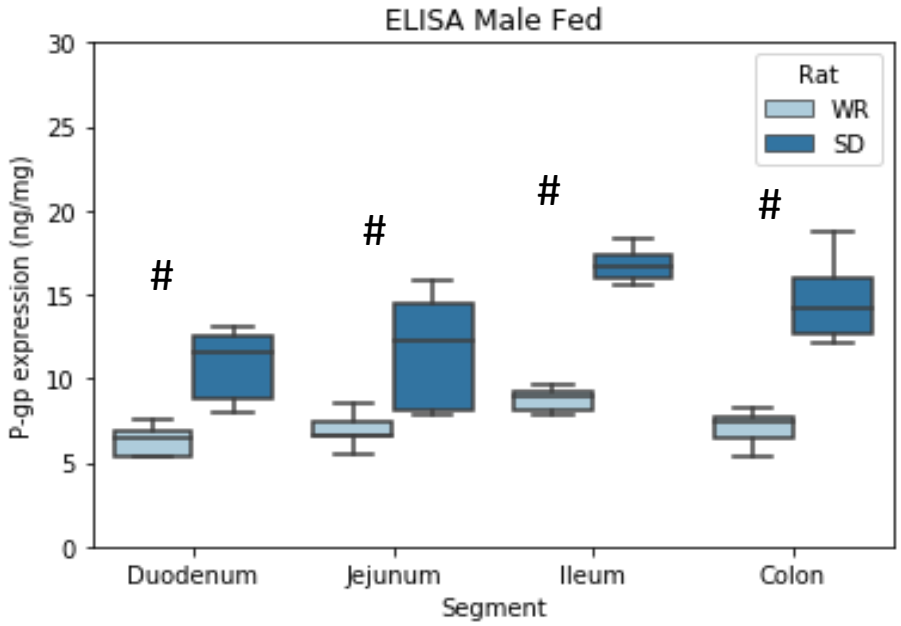

(B)

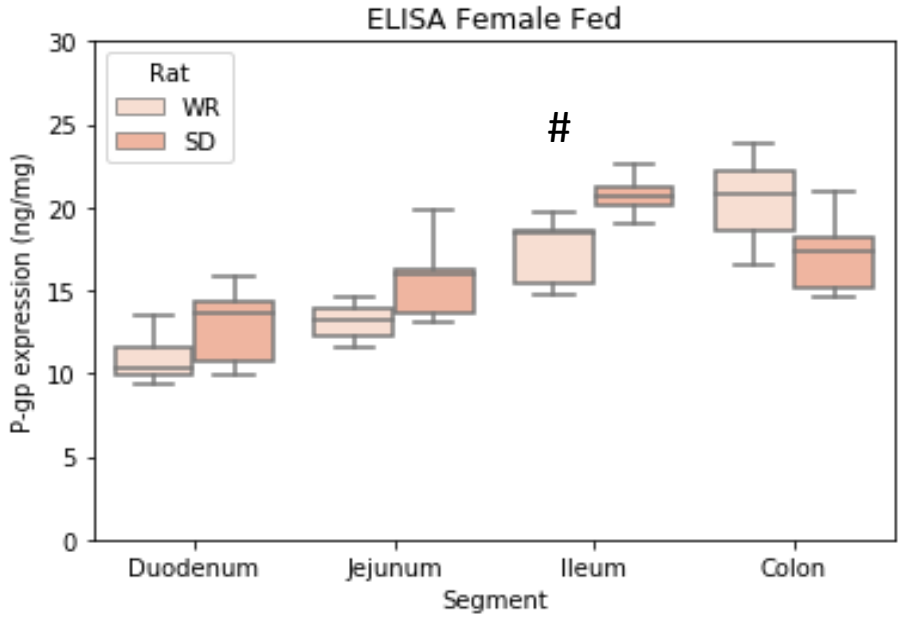

Figure 2-8 Strain differences in P-gp expression in fed male and female Wistar and Sprague Dawley rats quantified by ELISA (n = 5). The symbol # denotes statistical significance between the two strains at an intestinal region ($p < 0.05$).

(A)

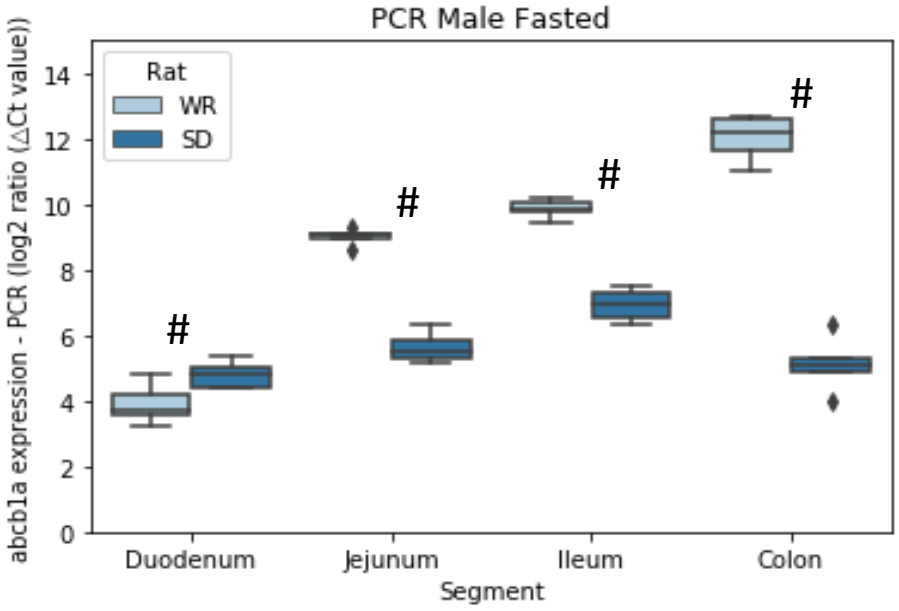

(B)

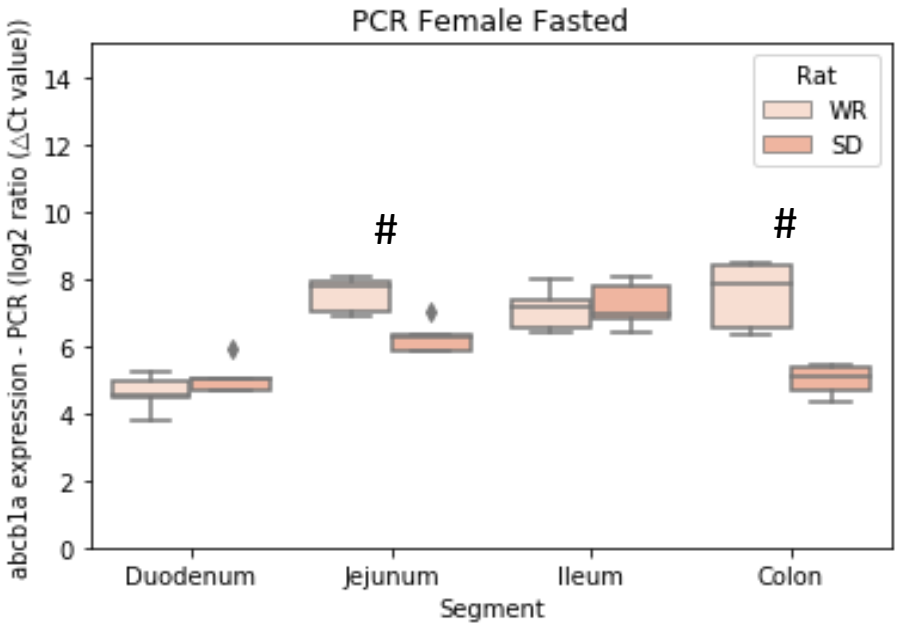

Figure 2-9 Strain differences in *abcb1a* expression in fasted female Wistar and Sprague Dawley rats quantified by PCR (n = 5). The symbol # denotes statistical significance between the two strains at an intestinal region ($p < 0.05$).

(A)

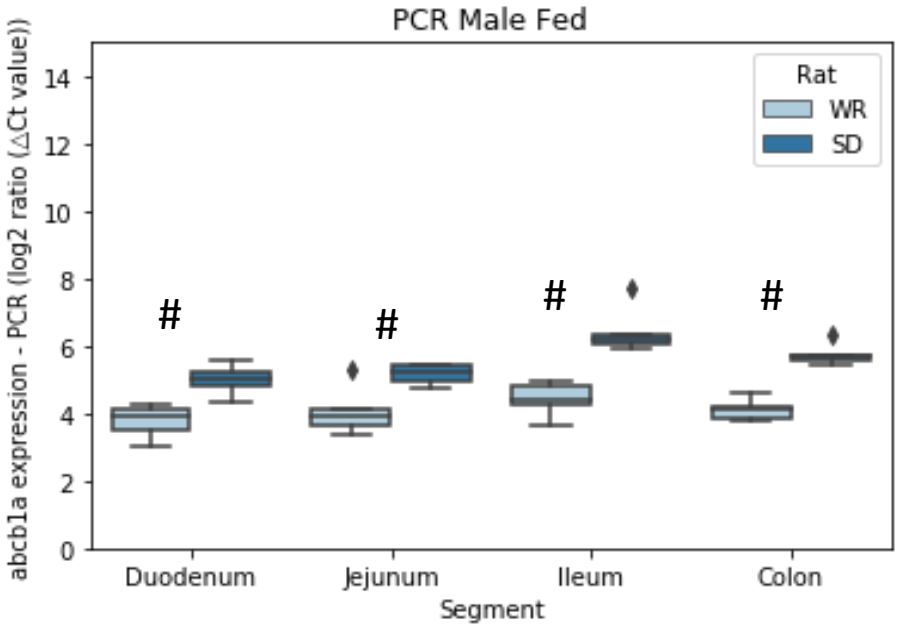

(B)

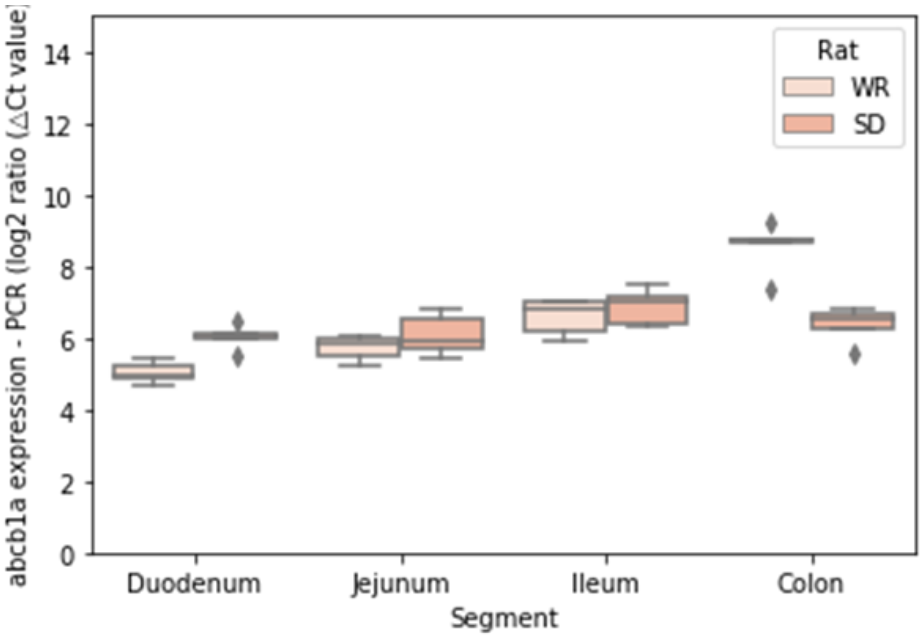

Figure 2-10 Strain differences in *abcb1a* expression in fasted female Wistar and Sprague Dawley rats quantified by PCR (n = 5). The symbol # denotes statistical significance between the two strains at an intestinal region ($p < 0.05$).

2.5.3 Intestinal BCRP and *abcg2* quantification

2.5.3.1 Intestinal BCRP and *abcg2* quantification in Wistar rats

The intestinal BCRP expression in male and female Wistar rats in the fasted and fed state quantified by ELISA is reported in Figure 2-11. The feeding intervention increased the BCRP expression in both sexes. In the male Wistar rats, feeding increased the BCRP expression by +77%, +172%, and +206% in the jejunum, ileum and colon, respectively. A similar trend was observed in the female Wistar rat, where feeding increased the BCRP expression by +22%, +26%, and +39% in the duodenum, ileum, and colon, respectively. Regional differences were observed across the intestine with the ELISA methodology. In the fed state, BCRP expression significantly increased from the duodenum to the ileum, then dropped in the colon. However, in the male fasted state BCRP decreased from the jejunum to the ileum (9.71 ± 0.80 ng/mg to 7.81 ± 1.30 ng/mg) and the ileum to the colon (7.81 ± 1.30 ng/mg to 5.86 ± 1.36 ng/mg). In the female fasted state, BCRP significantly increased from the duodenum to the ileum by 2.5 times, then decreased from the ileum to the colon (16.75 ± 1.03 ng/mg to 12.47 ± 0.70 ng/mg).

A)

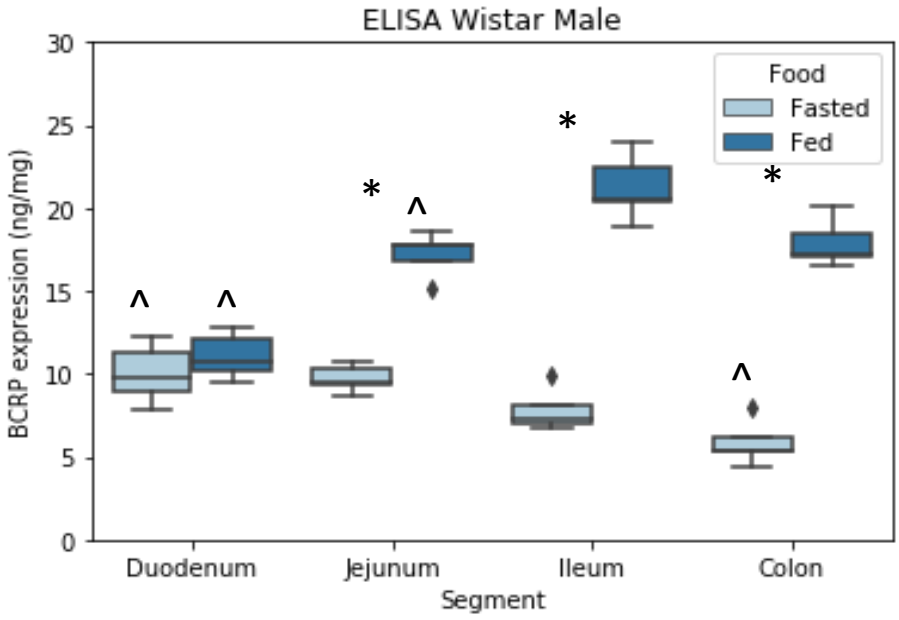

(B)

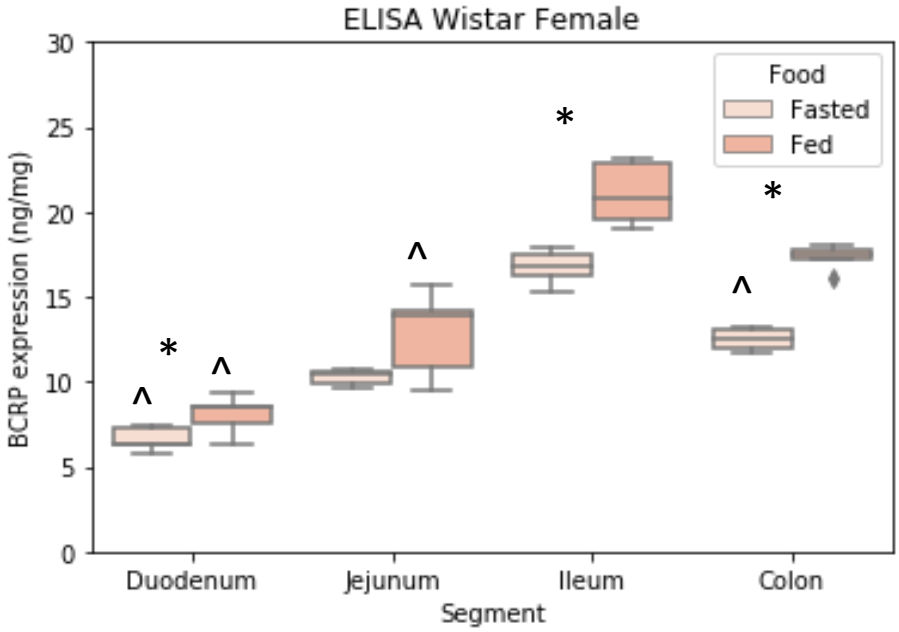

Figure 2-11 BCRP expression in fasted and fed (A) male and (B) female Wistar rats quantified by ELISA (n=5). The * symbol denotes statistical significance between the feeding state and ^ denotes a statistical significance between the sexes in an intestinal region ($p < 0.05$).

A sex difference was observed in the *abcg2* expression of the fasted duodenum, ileum, and colon (Figure 2-12). The fasted male duodenal *abcg2* was higher than in the female than the male (3.14 ± 0.58 ng/mg versus 2.23 ± 0.43 ng/mg, respectively). Whereas, the ileal *abcg2* was higher in the female fasted ileum and colon (3.64 ± 0.30 ng/mg versus 2.48 ± 0.57 ng/mg and 2.30 ± 0.36 ng/mg and 2.06 ± 0.18 ng/mg). In addition, for the male rat, feeding increased the *abcg2* expression by +24%, +62% and +58% in the jejunum, ileum, and colon, respectively.

(A)

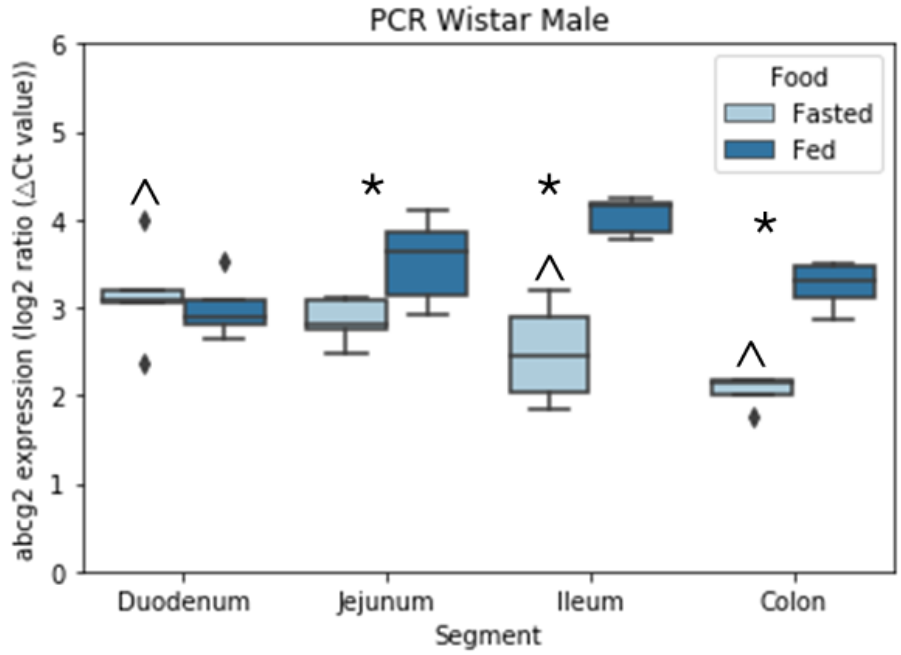

B)

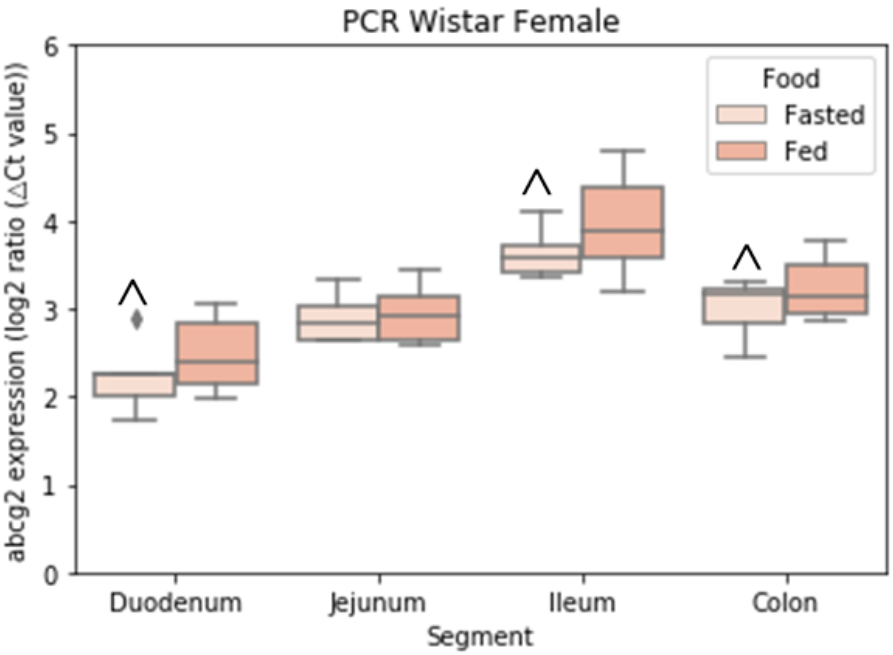

Figure 2-12 *abcg2* expression in male and female Wistar rats quantified PCR (n = 5). The * symbol denotes statistical significance between the sexes in an intestinal region and ^ denotes a statistical significance between the feeding types ($p < 0.05$).

The *abcg2* expression in Wistar rats quantified by PCR showed a similar trend to the BCRP expression quantified by ELISA, reflected in the good correlation between the methods (r = 0.816) (Figure 2-13).

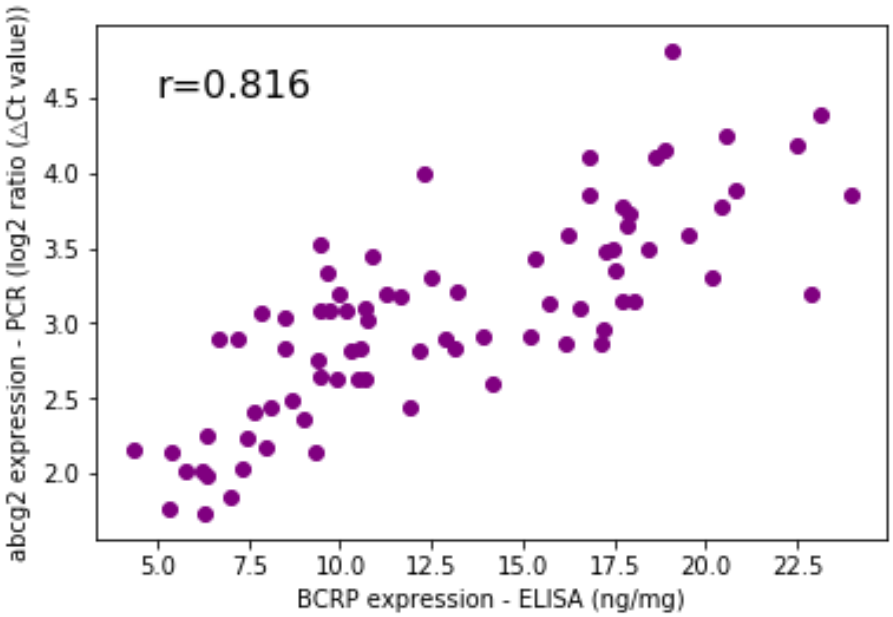

Figure 2-13 Correlation of intestinal BCRP expression quantified by ELISA and *abcg2* expression quantified by PCR in Wistar rats

2.5.3.2 Intestinal BCRP and *abcg2* quantification in Sprague Dawley rats

The BCRP expression in Sprague Dawley rats is reported in Figure 2-14. A comparable pattern was observed between the sexes in the fed state, except in the ileum. In the male rats, the BCRP expression gradually rose from the duodenum to the ileum; by +103% in the fasted state and +128% in the fed state. A similar trend was seen in the female rat from the duodenum to the ileum, where the BCRP expression was +107% higher in the fasted state and +29% higher in the fed state. Sex differences were seen in the ileum, where the BCRP in the male rat increased by +13% but decreased the BCRP expression by -23% in the female rat in the fed state, compared with the fasted state

(A)

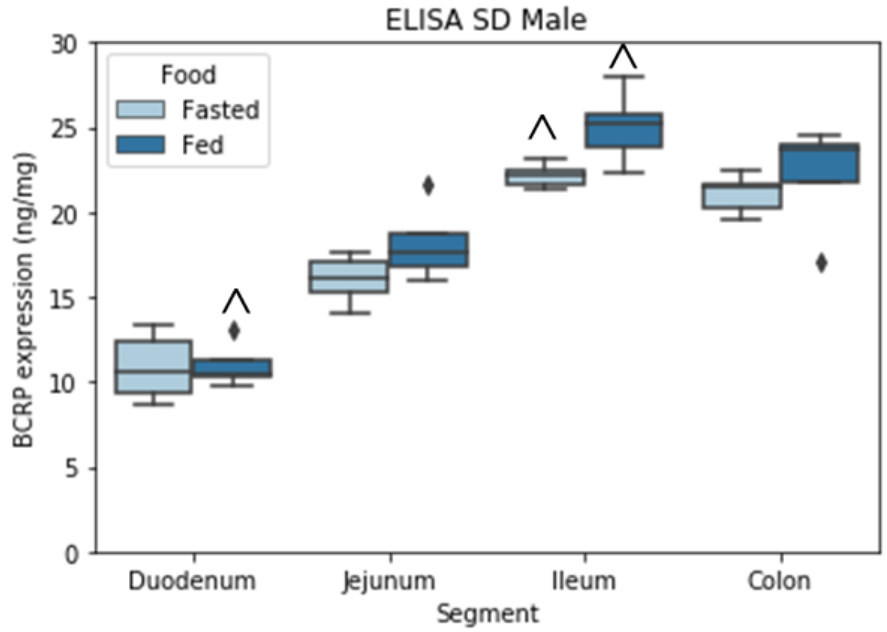

(B)

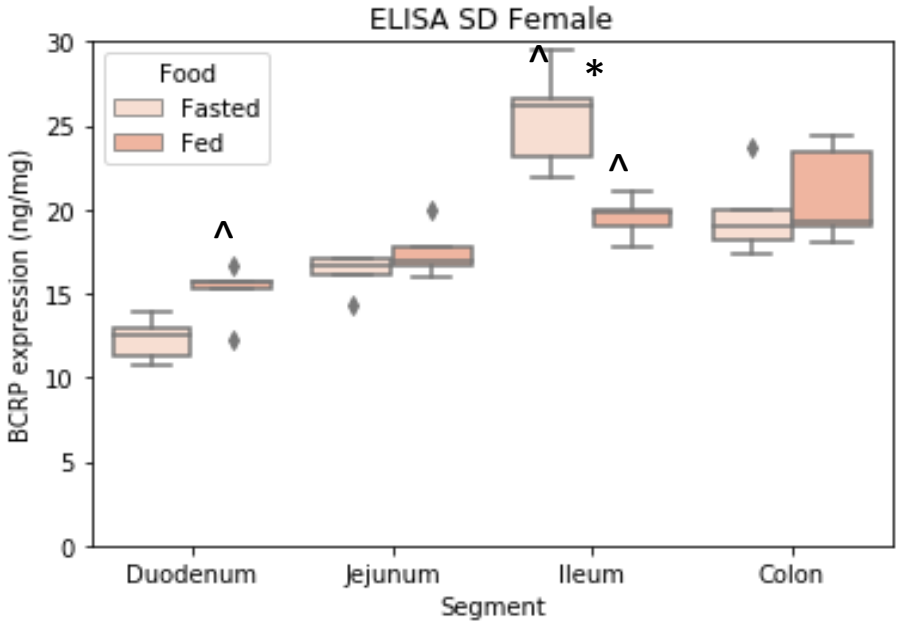

Figure 2-14 BCRP expression in male and female Sprague Dawley rats quantified by ELISA (n = 5). The * symbol denotes statistical significance between the sexes in an intestinal region and ^ denotes a statistical significance between the feeding types ($p < 0.05$).

(A)

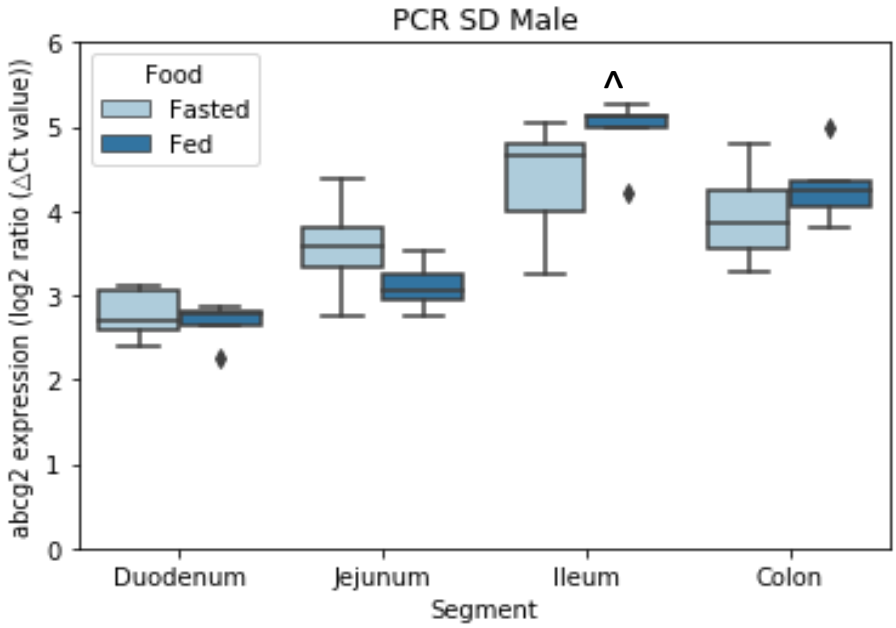

(B)

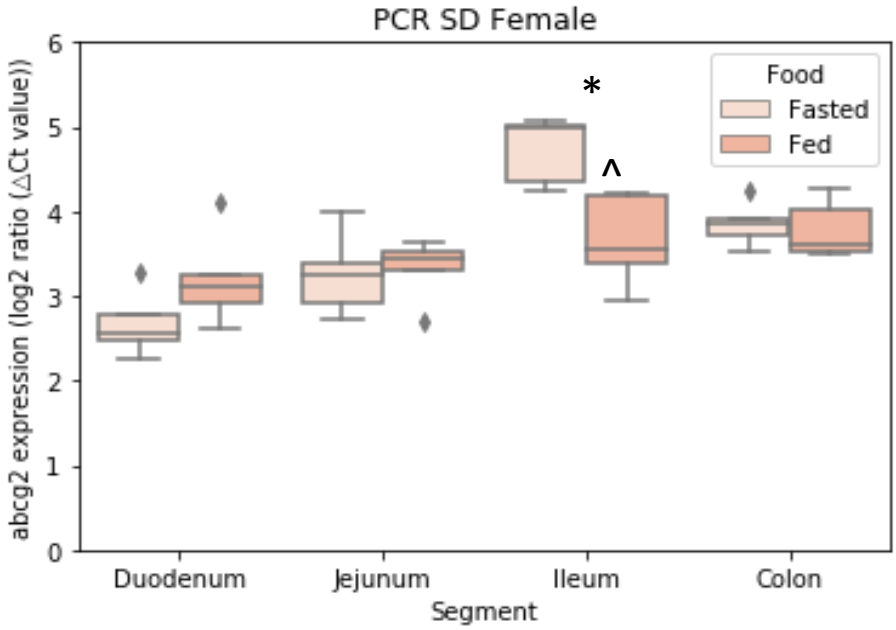

Figure 2-15 *abcg2* expression in male and female Sprague Dawley rats quantified by PCR (n = 5). The * symbol denotes statistical significance between the sexes in an intestinal region and ^ denotes a statistical significance between the feeding types ($p < 0.05$).

Figure 2-15 reports the *abcg2* expression in the Sprague Dawley rat. The feeding intervention significantly decreased the *abcg2* expression in the female by -23%.

A comparable profile was seen compared to the BCRP expression reported, which is reflected in the good correlation seen between the ELISA and PCR methods (r = 0.773) (Figure 2-16).

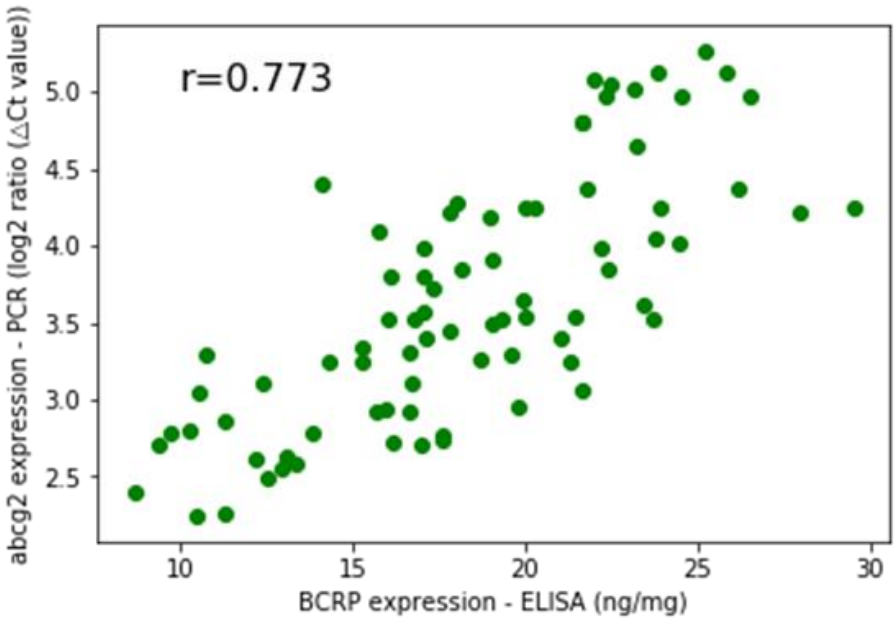

Figure 2-16 Correlation of intestinal BCRP expression quantified by ELISA and abcg2 expression quantified by PCR in Sprague Dawley rats

2.5.3.3 Strain Differences in Intestinal BCRP and *abcg2* quantification between Wistar and Sprague Dawley Rats

Figure 2-17, Figure 2-18, Figure 2-19, and Figure 2-20 display the BCRP and *abcg2* expression across the intestinal tract between Wistar and Sprague Dawley rats. Higher BCRP expression was seen in the male Sprague Dawley rat; 1.7 and 2.8 times higher in the fasted jejunum and ileum and 1.2 times higher in the fed ileum. In the female Sprague Dawley rat, higher BCRP was also seen in the fasted duodenum, jejunum, and fed jejunum, compared with the Wistar rat. For the PCR quantification, higher *abcg2* expression was observed in the Sprague Dawley rat in the male fasted jejunum (+25%), ileum (+75%), and colon (+92%), female fasted ileum (+30%) and colon (+28%), and male fed ileum (+22%), than in the Wistar rat counterpart.

(A)

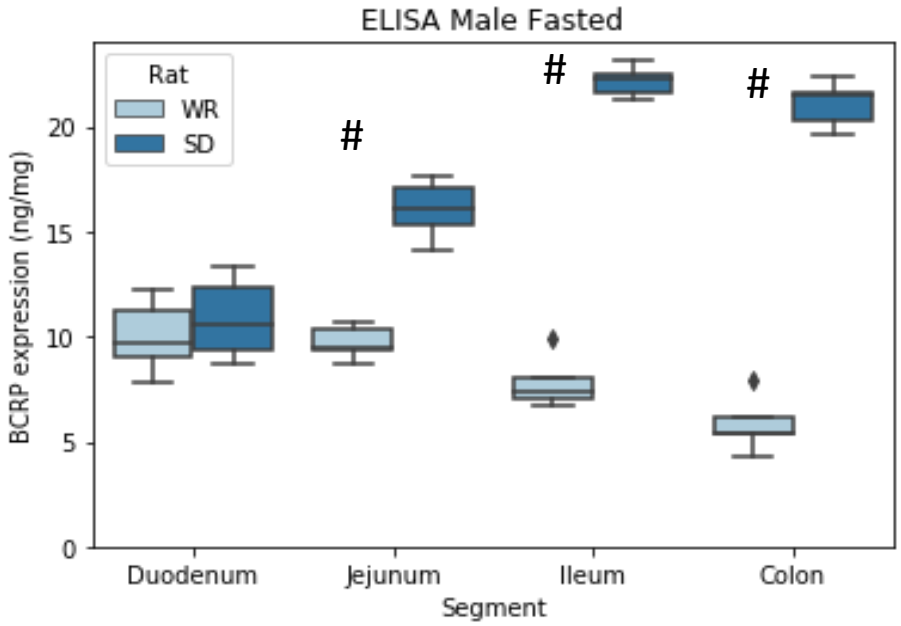

(B)

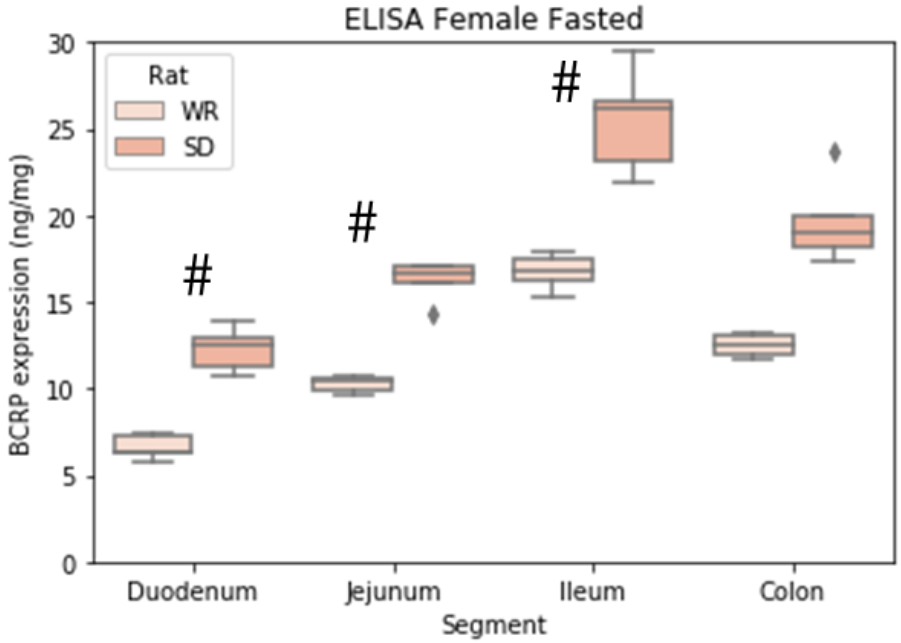

Figure 2-17 Strain differences in BCRP expression in fasted male and female Wistar and Sprague Dawley rats quantified by ELISA (n = 5). The symbol # denotes statistical significance between the two strains at an intestinal region ($p < 0.05$).

(A)

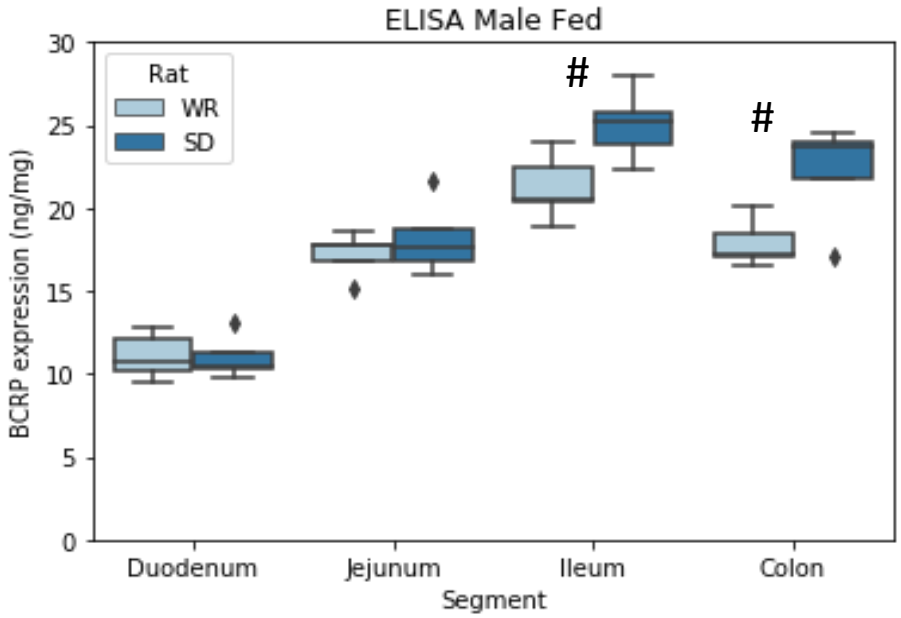

(B)

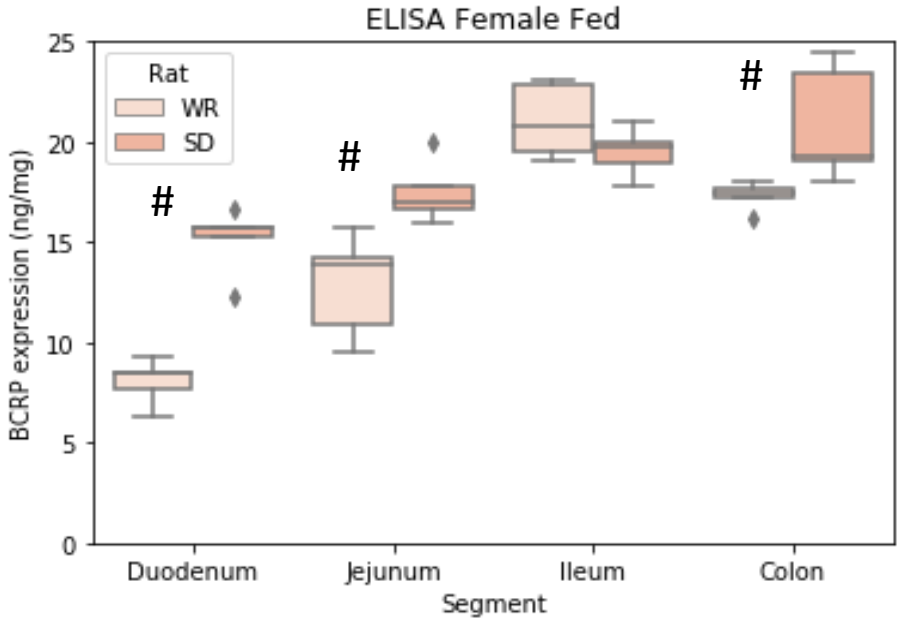

Figure 2-18. Strain differences in BCRP expression in fed (A) male and (B) female Wistar and Sprague Dawley rats quantified by ELISA. Data is represented as mean ± SD, n = 5. The symbol # denotes statistical significance between the two strains at an intestinal region ($p < 0.05$).

(A)

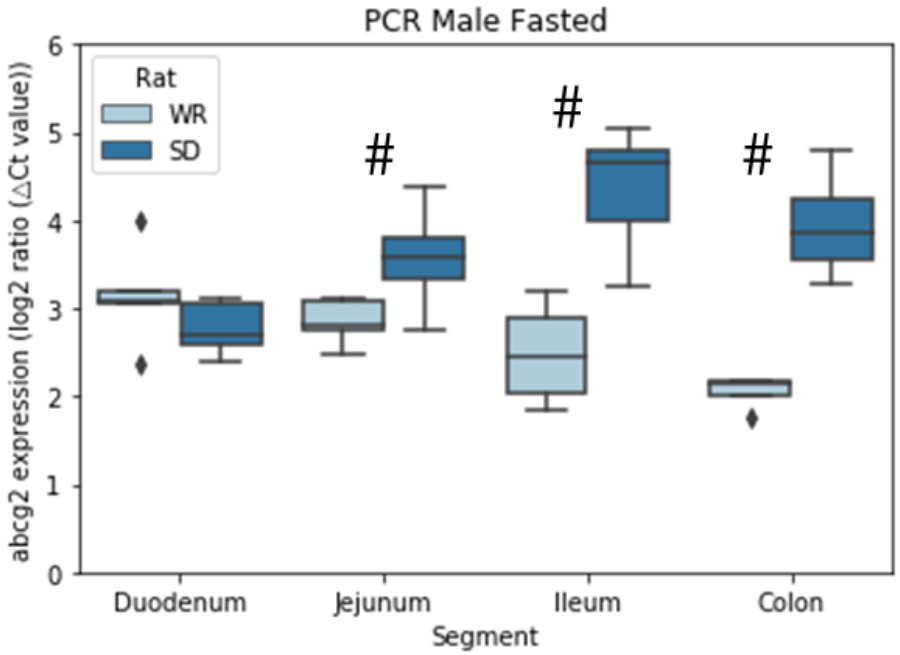

(B)

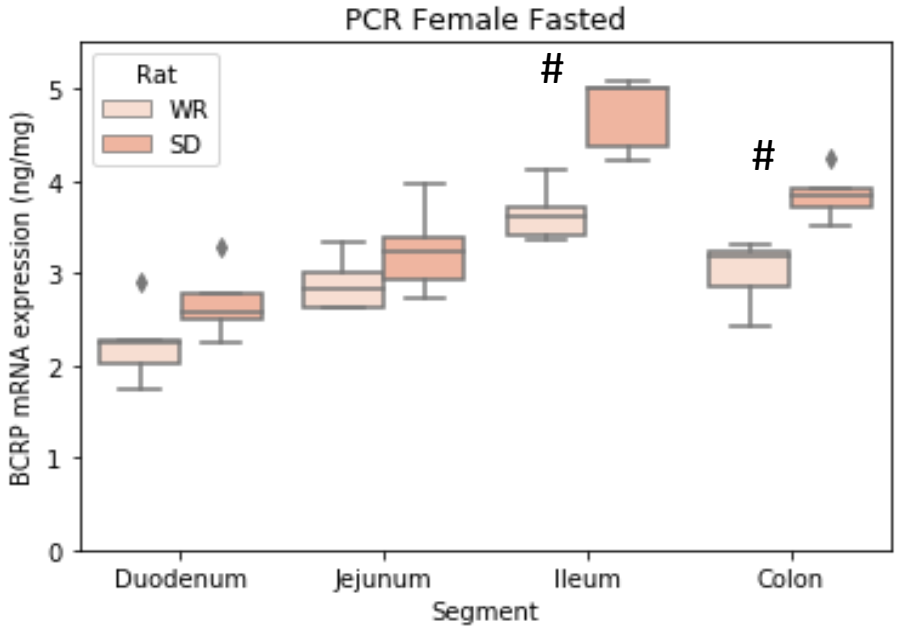

Figure 2-19 Strain differences in *abcg2* expression in fasted (A) male and (B) female Wistar and Sprague Dawley rats quantified by PCR (n = 5). The symbol # denotes statistical significance between the two strains at an intestinal region ($p < 0.05$).

(A)

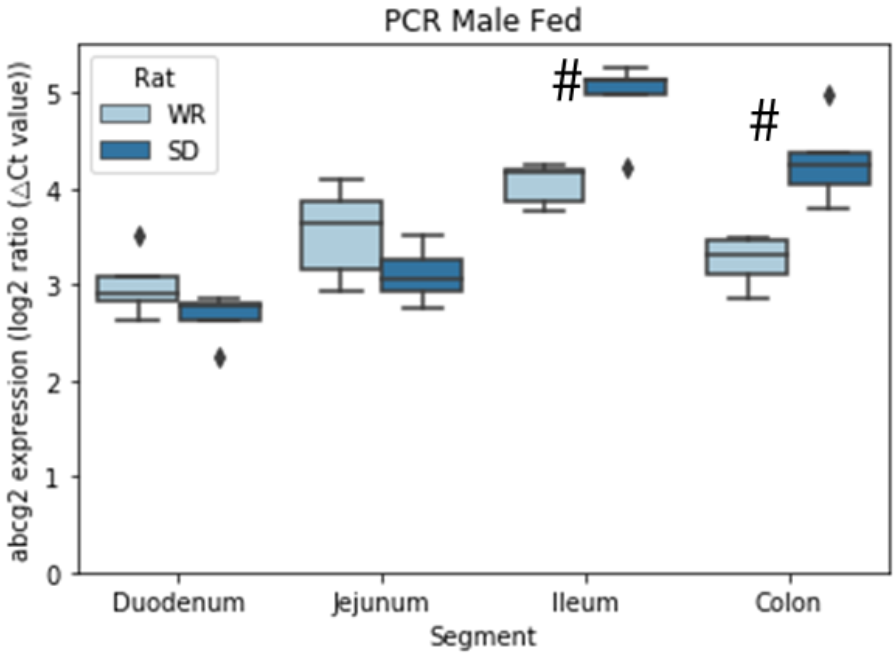

(B)

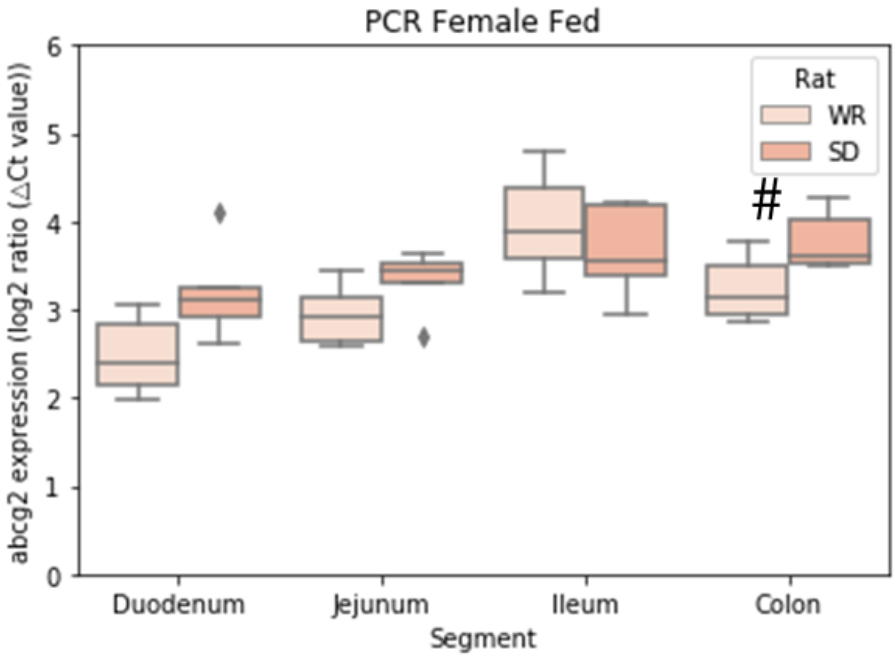

Figure 2-20 Strain differences in *abcg2* expression in fed (A) male and female Wistar and Sprague Dawley rats quantified by PCR (n = 5). The symbol # denotes statistical significance between the two strains at an intestinal region ($p < 0.05$).

2.5.4 Intestinal MRP2 and *abcc2* quantification

2.5.4.1 Intestinal MRP2 and *abcc2* quantification in Wistar rats

Figure 2-21 displays the MRP2 expression in male and female Wistar rats in the fasted and fed states. Feeding caused a significant increase in MRP2 expression in both sexes. Specifically, in the male rats feeding caused an increase in the duodenum (+50%), jejunum (+136%), ileum (+50%), and colon (132%). Feeding also resulted in a MRP2 increase in the female rat; jejunum (+101%), ileum (+156%), and colon (+157%). Sex differences were observed in the fasted duodenum, jejunum, and colon.

(A)

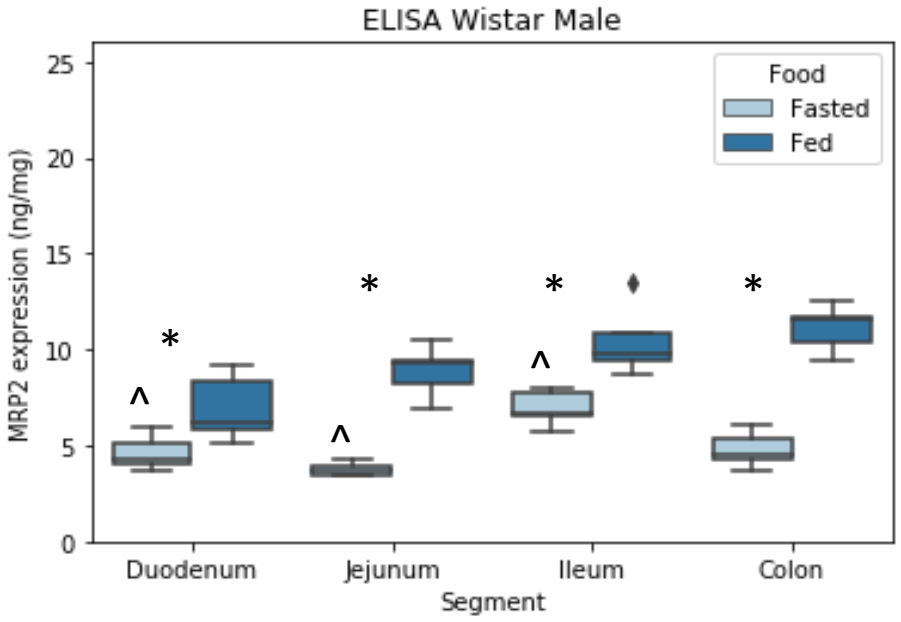

(B)

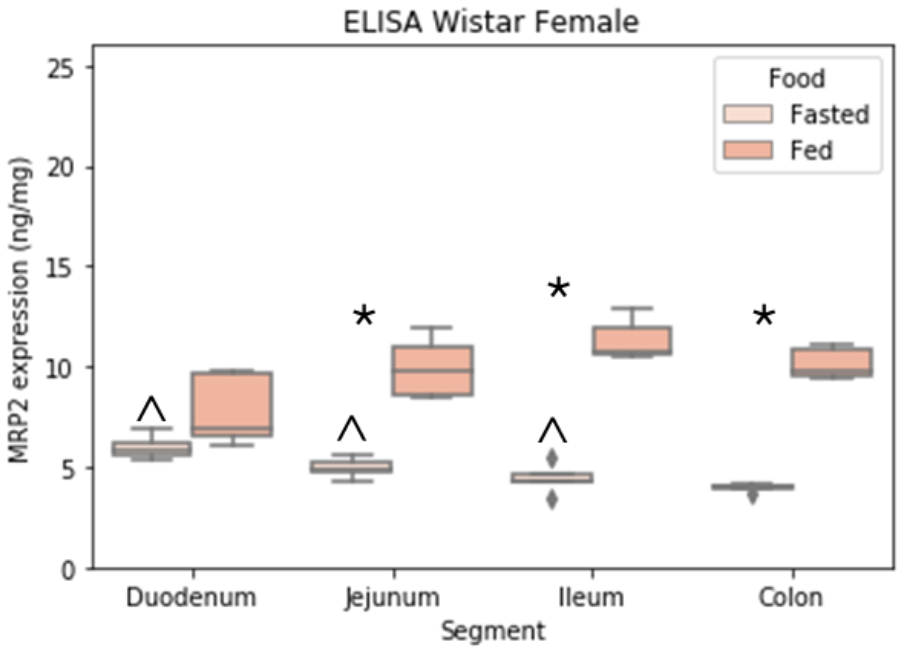

Figure 2-21 MRP2 expression in (A) male and (B) female Wistar rats quantified by ELISA (n = 5). The * symbol denotes statistical significance between the sexes in an intestinal region and ^ denotes a statistical significance between the feeding types ($p < 0.05$).

The *abcc2* expression levels quantified by PCR (Figure 2-22) reflected the MRP2 protein levels quantified by ELISA. In the male rat, feeding caused a significant rise in the *abcc2* levels with a 1.5-, 2.1-, 2.1-, and 1.8- fold increase in the duodenum, jejunum, ileum, and colon. In the female rat, feeding also caused a change in the *abcc2* expression, with a 1.7-, 2.3-, and 2.4-fold increase in the jejunum, ileum, and colon, respectively. Sex differences were observed in both prandial states in the duodenum and the jejunum, with the greatest difference in the jejunum; a 1.3-times increase in the fasted state and 1.0- times increase in the fed state, between the male and female Wistar rats.

(A)

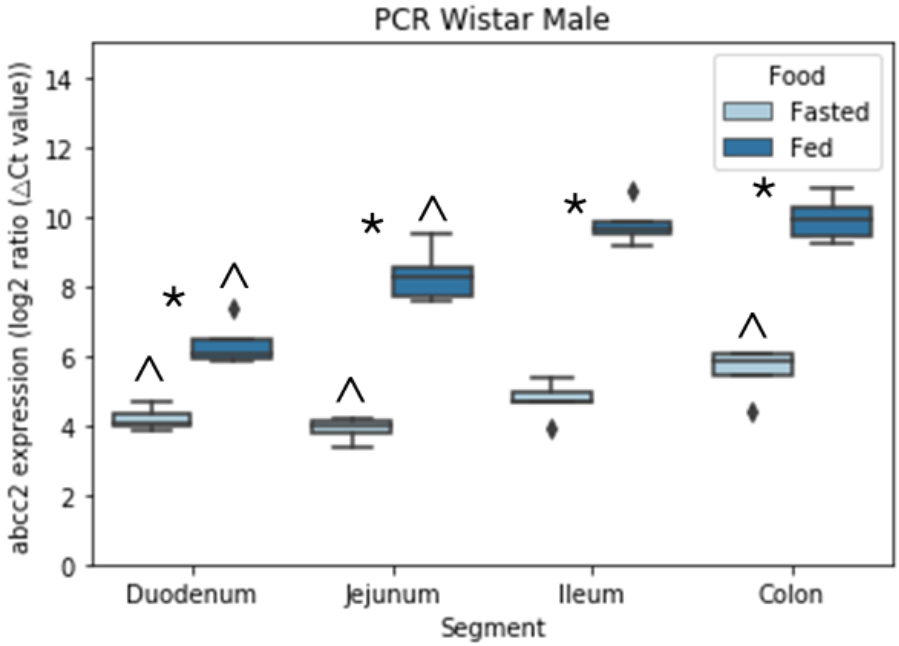

(B)

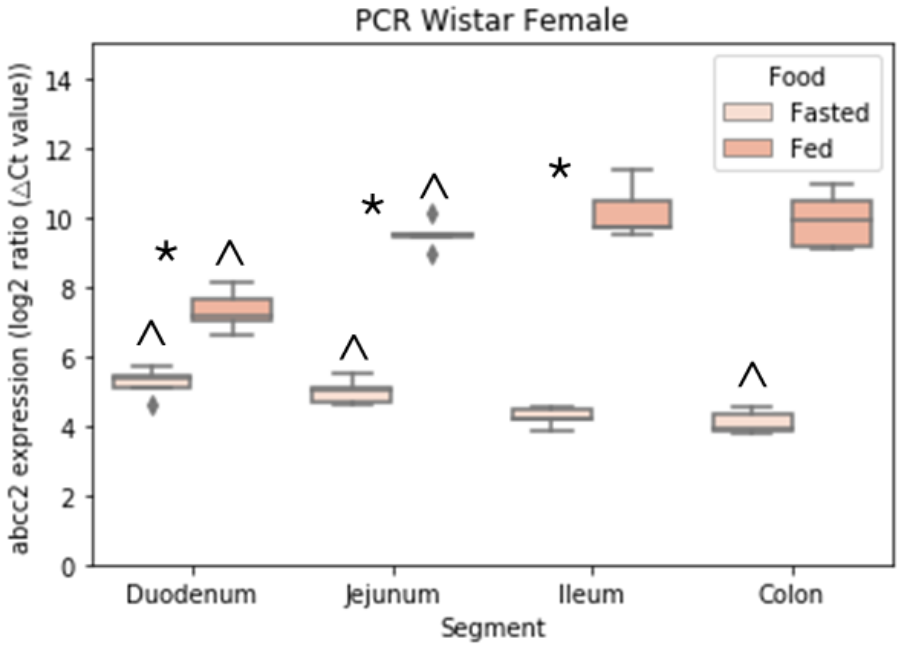

Figure 2-22 *abcc2* expression in male and female Wistar rats quantified by PCR (n = 5). The * symbol denotes statistical significance between the sexes in an intestinal region and ^ denotes a statistical significance between the feeding types ($p < 0.05$).

In fact, a good correlation of r = 0.881 was found between MRP2 measured by ELISA and *abcc2* measured by PCR (Figure 2-23).

2.5.4.2 Intestinal MRP2 and *abcc2* quantification in Sprague Dawley rats

The MRP2 quantification levels in the Sprague Dawley rats is shown in Figure 2-24Figure *2-23*. The intake of food significantly increased the MRP2 expression in both sexes. The male Sprague Dawley rat showed a +134%, +121%, +80% and +113% increase between the prandial states in the duodenum, jejunum, ileum, and colon, respectively. A similar trend was observed in the female rat, where feeding caused a +108%, +128%, +78%, and +107% increase in the duodenum, jejunum, ileum, and colon, respectively. A sex difference was found in the jejunum in both states; a +30% and +26% higher in the male rat compared with the female rat, in fasted and fed states, respectively.

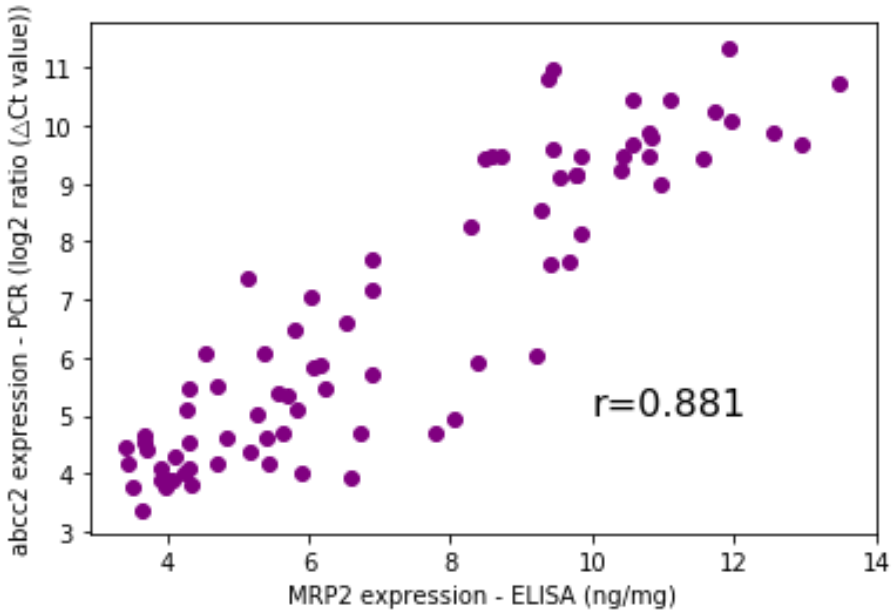

Figure 2-23 Correlation of intestinal MRP2 expression quantified by ELISA and *abcc2* expression quantified by PCR in Wistar rats

(A)

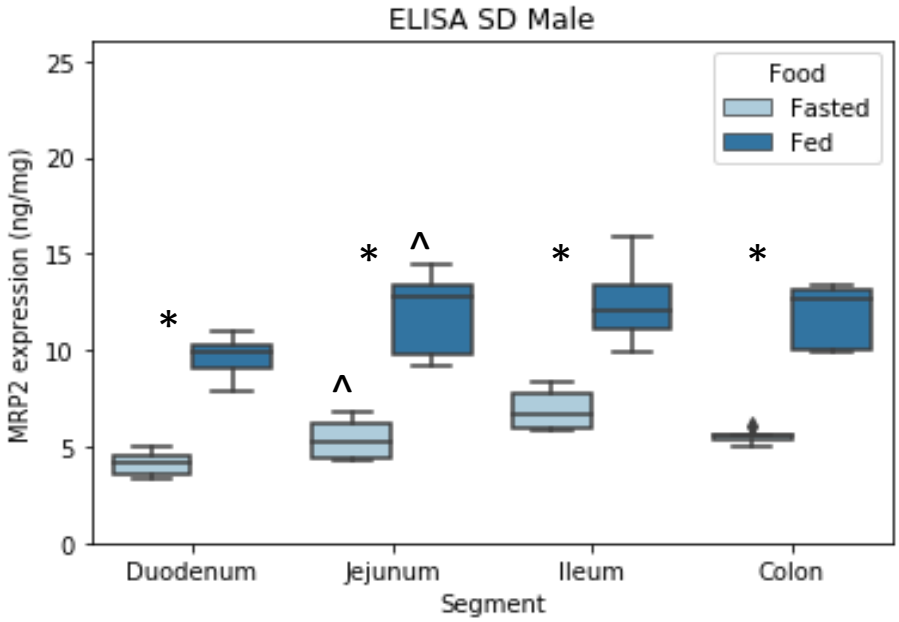

(B)

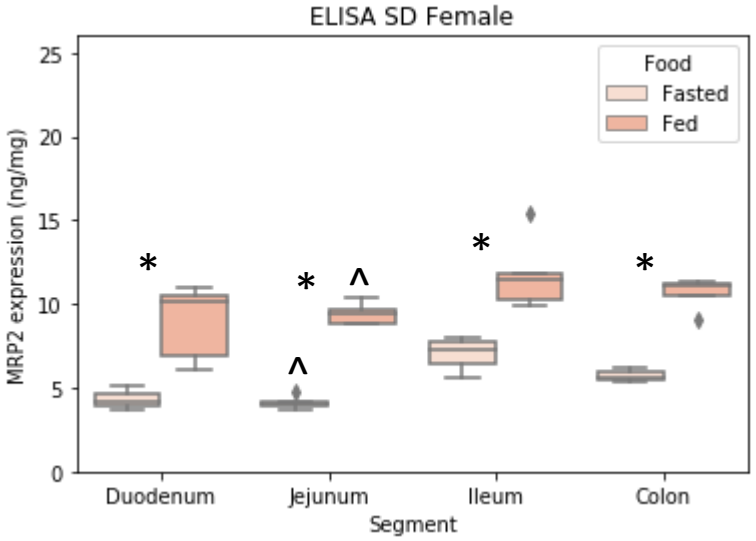

Figure 2-24 MRP2 expression in (A) male and (B) female Sprague Dawley rats quantified by ELISA (n = 5). The * symbol denotes statistical significance between the sexes in an intestinal region and ^ denotes a statistical significance between the feeding types ($p < 0.05$).

The *abcc2* expression in male and female Sprague Dawley rats is reported in Figure *2-25* Here, feeding caused an increase of 2.4-, 2.2-, 1.7-, and 2.0-fold in the male rats across the intestine (duodenum, jejunum, ileum, and colon). Feeding in the female rat also showed an increase in the *abcc2* expression –2.0-, 2.3-, 1.5-, and 1.9-times higher in the duodenum, jejunum, ileum, and colon, respectively. Sex differences were also shown in the main site of absorption – the jejunum. To be specific, the *abcc2* level was 1.2- and 1.2-times higher in the fasted and fed male jejunum.

(A)

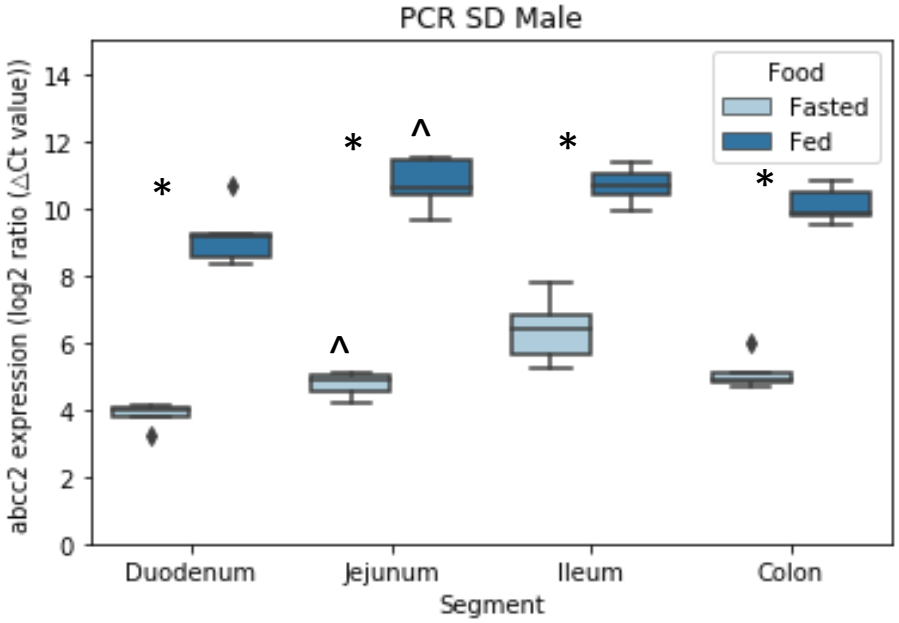

(B)

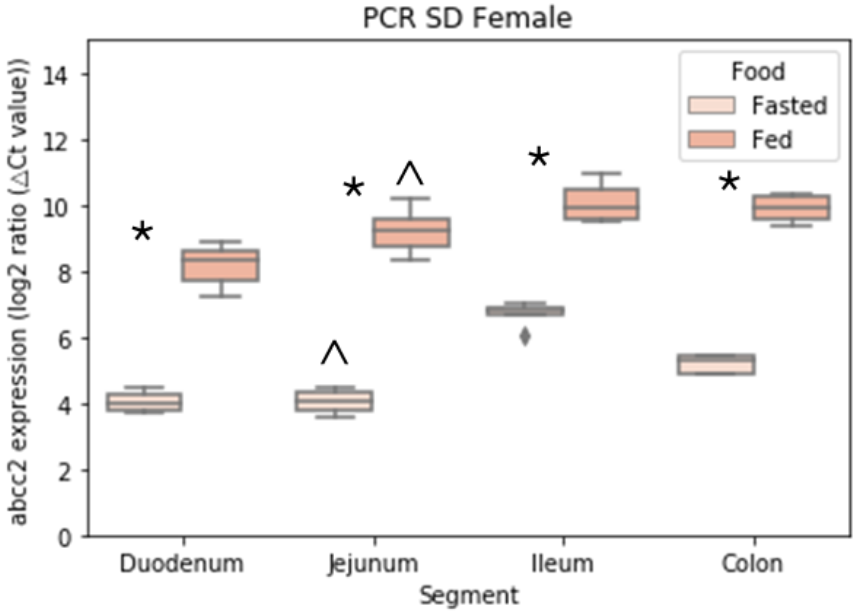

Figure 2-25 *abcc2* expression in (A) male and (B) female Sprague Dawley rats quantified by PCR (n = 5). The * symbol denotes statistical significance between the sexes in an intestinal region and ^ denotes a statistical significance between the feeding types ($p < 0.05$).

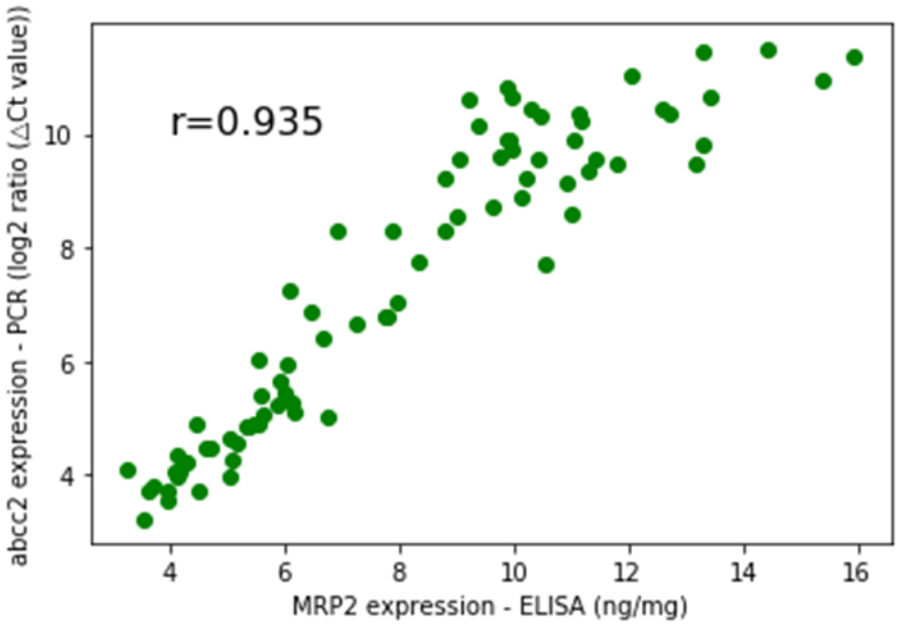

Figure 2-26 Correlation of intestinal MRP2 expression quantified by ELISA and *abcc2* expression quantified by PCR in Sprague Dawley rats

Importantly, similar trends were shown between the MRP2 protein levels and the *abcc2* mRNA levels. In fact, a strong correlation of r = 0.935 was calculated between the MRP2 and the *abcc2* (Figure *2-26*).

2.5.4.3 Strain Differences in Intestinal MRP2 and *abcc2* between Wistar and Sprague Dawley Rats

Figure 2-27, Figure 2-28, Figure 2-29, and Figure 2-30 present the comparative plots of the MRP2 and *abcc2* levels between the Wistar and Sprague Dawley rats. Strain differences were found in the fasted female rat for the MRP2 and *abcc2* levels. Here, in the duodenum and jejunum MRP2 was 15% and 6% higher in the Wistar rat, respectively. Whereas, in the ileum and colon, the MRP2 was 3.5% and 4.7% higher in the Sprague Dawley rat. No strain differences were seen in the fed female rats. For the male rats, strain differences were seen for MRP2 in the fasted jejunum and fed duodenum and jejunum. The PCR quantification showed strain differences in the male fasted jejunum and ileum and the male fed small intestine.

(A)

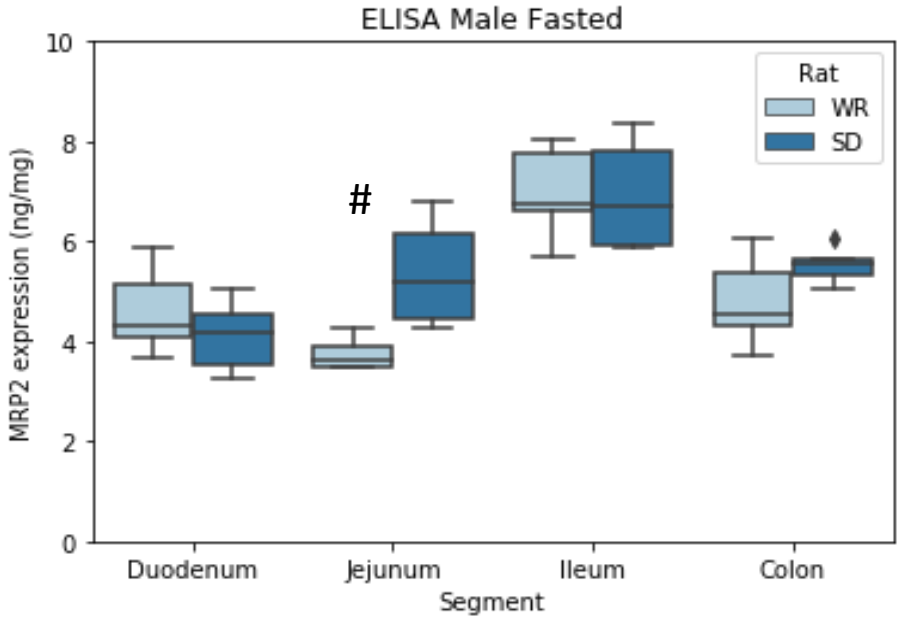

(B)

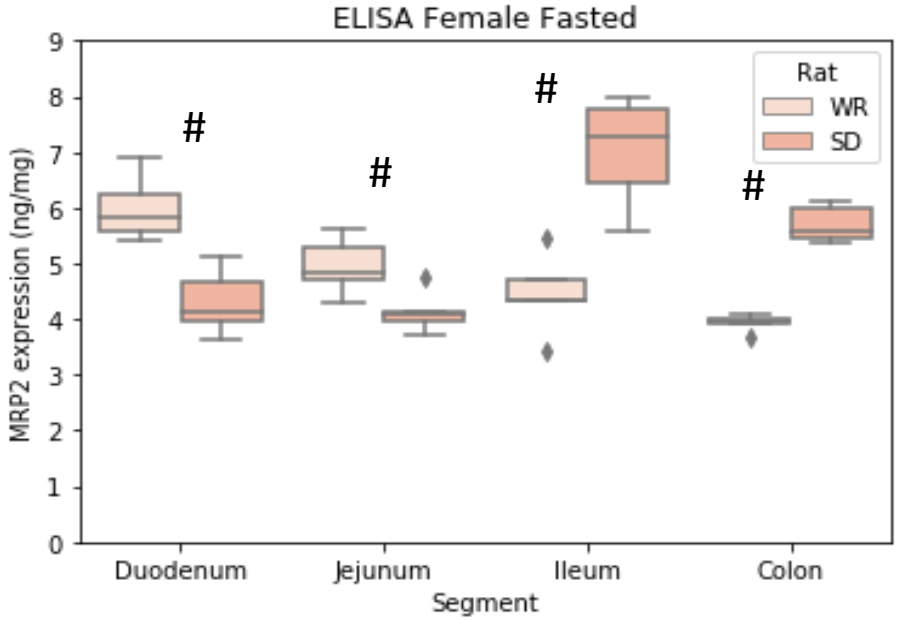

Figure 2-27 Strain differences in MRP2 expression in fasted (A) male and (B) female Wistar and Sprague Dawley rats quantified by ELISA (n = 5). The symbol # denotes statistical significance between the two strains at an intestinal region ($p < 0.05$).

(A)

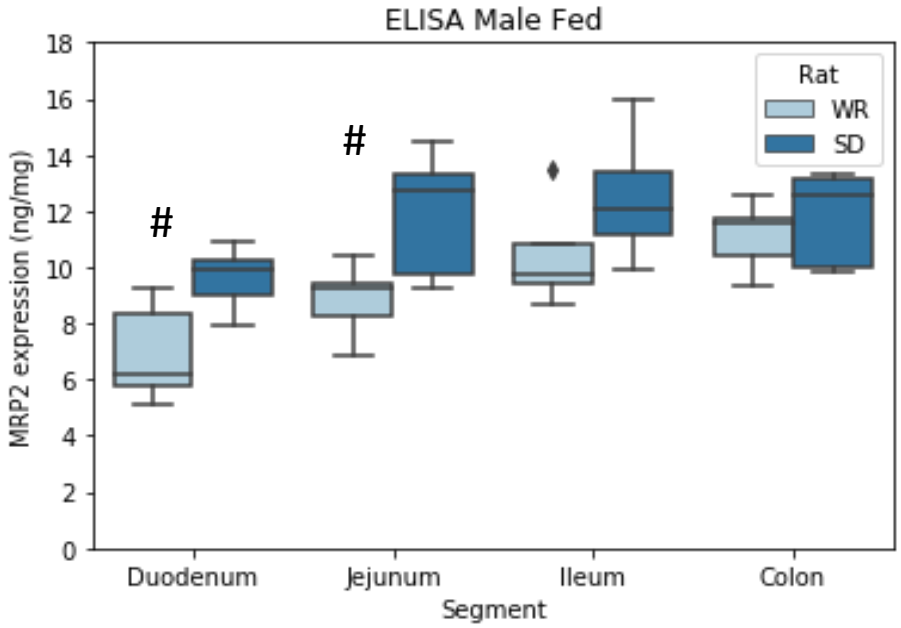

(B)

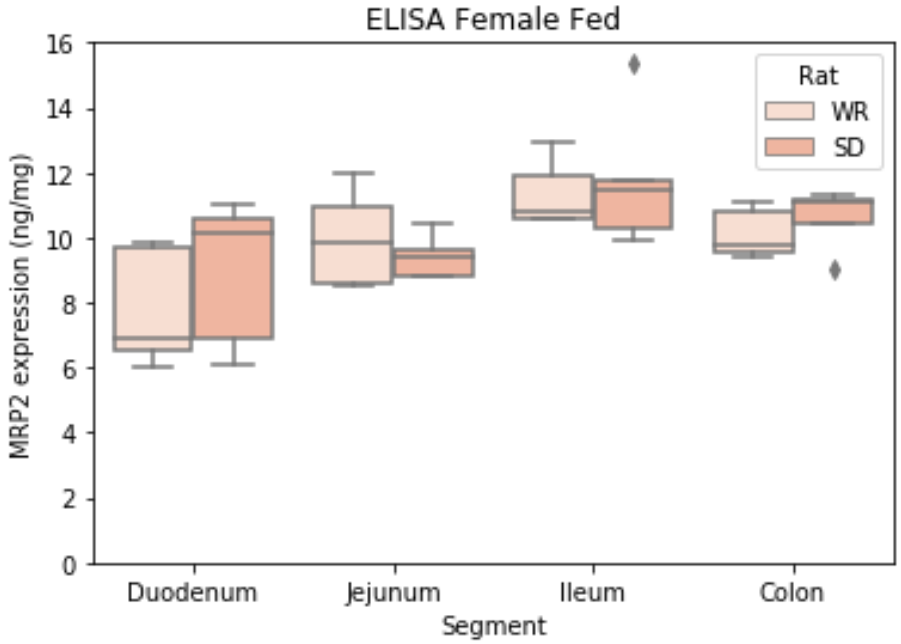

Figure 2-28 Strain differences in MRP2 expression in fed female (A) Wistar and (B) Sprague Dawley rats quantified by ELISA (n = 5). The symbol # denotes statistical significance between the two strains at an intestinal region ($p < 0.05$).

(A)

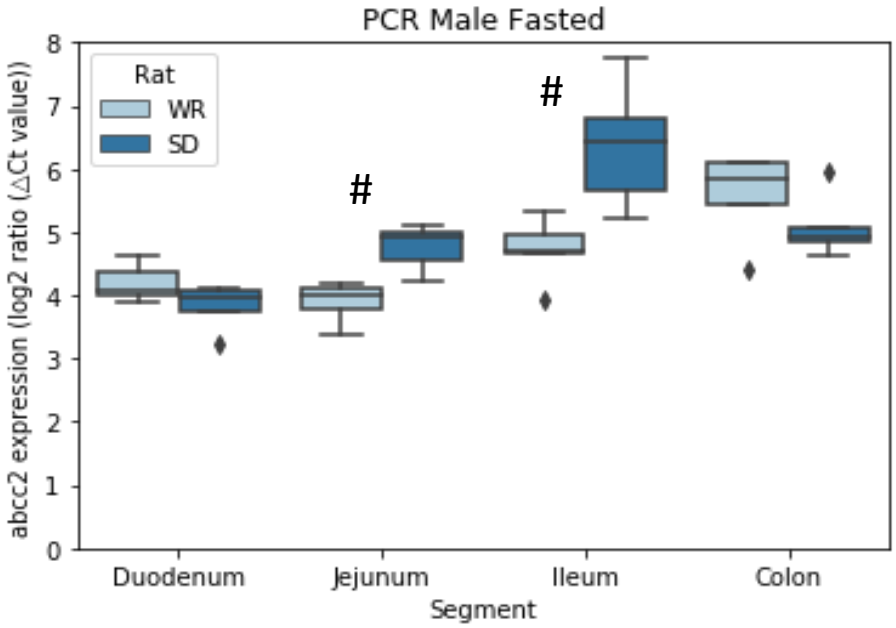

(B)

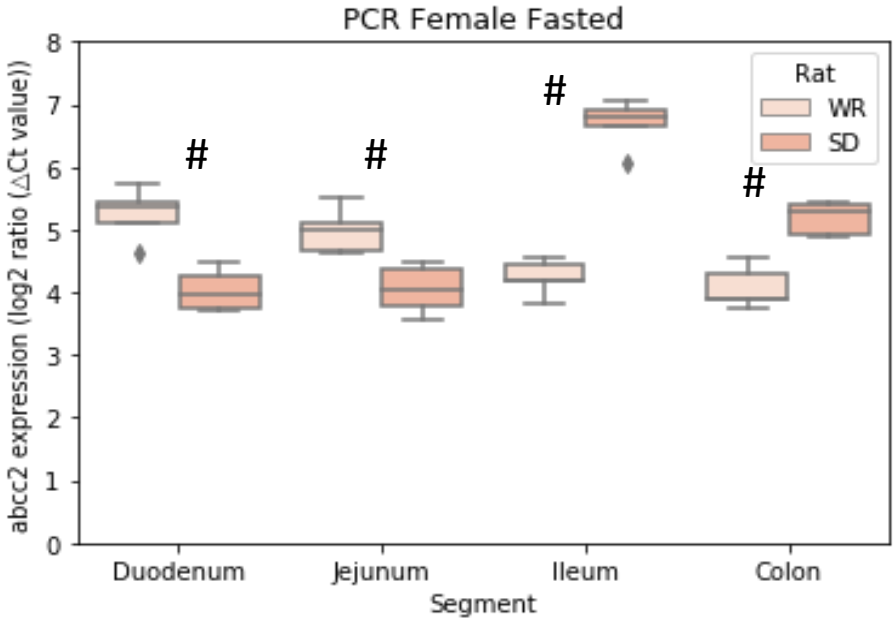

Figure 2-29 Strain differences in abcc2 expression in fasted male and female Wistar and Sprague Dawley rats quantified by PCR (n = 5). The symbol # denotes statistical significance between the two strains at an intestinal region ($p < 0.05$).

(A)

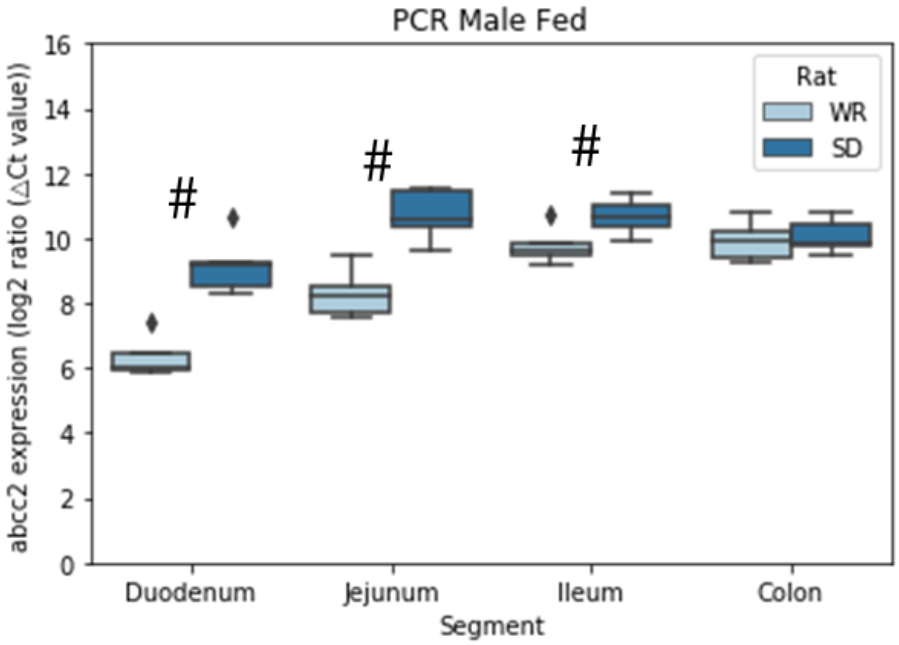

(B)

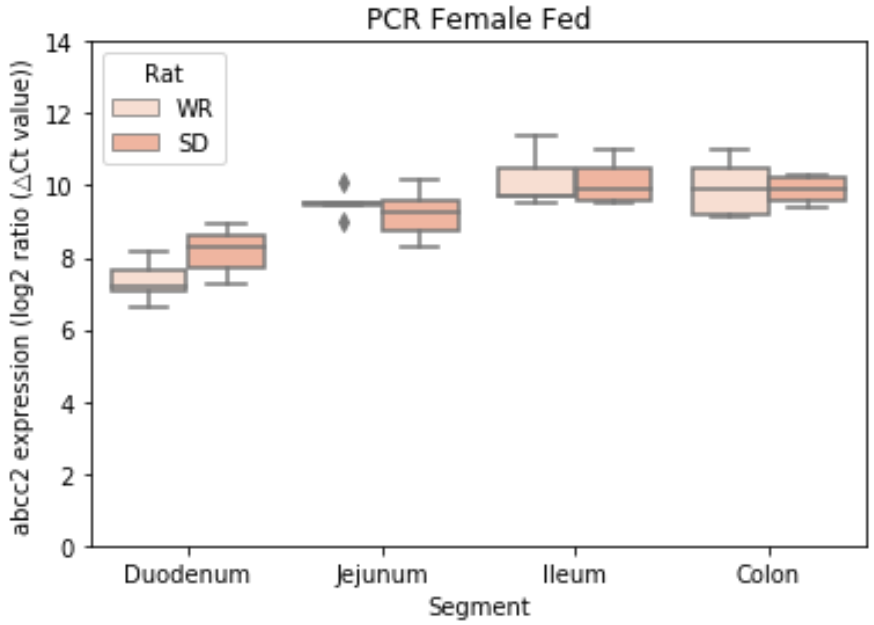

Figure 2-30 Strain differences in abcc2 expression in fed male and female Wistar and Sprague Dawley rats quantified by PCR (n = 5). The symbol # denotes statistical significance between the two strains at an intestinal region ($p < 0.05$).

2.5 Discussion

Efflux transporters provide useful protection from xenobiotics at biological barriers, which include the blood-brain barrier and the intestinal tract. However, from a drug delivery perspective, efflux transporters can prevent effective pharmacotherapy by limiting the absorption of therapeutic drug substrates with clinical implications. Knowledge of the intricacies of GI tract, such as the expression of efflux transporters, should be understood in order to choose the most appropriate animal model for preclinical testing of new drug products. While there are several investigations on the expression of ABC transporters in rodent models in the literature, due to the heterogeneity in the studies in the methodologies, strains, feeding status and sexes, it is difficult to find a conclusive message [204,205]. Here, a full library of the efflux transporters P-gp, BCRP, and MRP2 were characterised in both prandial states (fasted and fed), the sexes (males and females), and the most used strains (Wistar and Sprague Dawley) by established PCR and ELISA technologies. Food, sex, and strain were shown to alter the expression of P-gp, BCRP and MRP2 in contrasting ways.

Drug molecules and food products use the same biochemical pathways to permeate through the GI tract. Therefore, food-drug interactions at the sites of the intestinal monolayer are expected, although not fully understood [9]. It is known that several food-derived compounds may alter efflux transporter activity through inhibition in the intestinal tract [68]. Experimental testing using several *in vitro* models such as the Caco-2 cell line have shown that food-derived compounds can inhibit intestinal efflux transporters. However clinical studies in this area are limited. It is rational that food intake would increase the expression of efflux transporters as a protective mechanism to protect the body from xenobiotics, seen for P-gp in female Wistar rats, male and female Sprague Dawley rats and for MRP2 and BCRP male and female rats of both strains. The increase of the P-gp expression in the female rat could be explained by the innate protection that females have for successful reproduction. P-gp, BCRP, and MRP2 are found the maternal-foetus barrier [206]. However, it is less clear why food intake causes the P-gp expression level to decrease in the male Wistar rat. Differences in

protein expression may be due to signalling by nuclear receptors, which are induced by a variety of xenobiotics and physiological cues [65].

Our results showed that rodent P-gp expression increased from the proximal small intestine, and then decreased in the colon. This reflects our groups' previous findings, that of the literature, and the pattern seen in humans [51,202,204,207]. Data in the literature have reported that BCRP increases from the duodenum to the ileum, and then decreases in the colon in humans [194]. Our study reflected this, except for the fasted male Wistar rat where the BCRP/*abcg2* levels decreased along the intestinal tract. For MRP2, studies have reported that intestinal expression in male Wistar rats was highest in the duodenum then decreases directionally from the jejunum to the ileum and the colon [202,208,209]. Although, the feeding status was not reported. In contrast, Drozdzik and colleagues found in human intestinal tissue that the protein abundance of MRP2 peaked in the jejunum [194]. Our findings found a decrease between the jejunum and ileum of MRP2 in the female fasted Wistar rats, however in the male fasted rats, an increase was reported between the jejunum and ileum. Feeding was seen to increase MRP2 across the intestinal tract in both strains and sexes. Our study also found that P-gp/*abcb1a* and BCRP/*abcg2* expression levels were the highest and of similar values, whereas the MRP2/*abcc2* levels were the lowest.

Sprague Dawley rats showed innately higher P-gp levels compared with Wistar rats, in corroboration with our previous study, and as well as the novel finding of higher BCRP and MRP2 levels as well [210]. These differences in P-gp, BCRP, and MRP2 transcript and protein expression levels highlight that the sex, strain, feeding status, and quantification method should be clearly stated when reporting transporter expression abundances. Although, importantly protein levels may not be representative of the transport activity [65]. A limitation of this study is that efflux transporter functionality was not explored. These transporters are reported to function differently, where P-gp is thought to be a primary active transporter of drugs, whereas other ATP-dependent transporters such as MRP2 function through a co-transport mechanism with reduced glutathione [211].

ELISA and PCR are gold-standard analytical techniques used to quantify protein and mRNA expression, respectively. Both techniques are high-throughput in nature as 96 samples can be analysed at a time in 96-well plates. Sample preparation takes longer for PCR, whereas ELISA has longer incubation times. ELISA can suffer from comparatively low sensitivity and specificity [212]. Here, PCR appears to be more sensitive than ELISA to variability, shown as the significant differences between the sexes and feeding state are more pronounced with PCR. A limitation of PCR is that it measures the relative expression of mRNA, using the housekeeping protein, beta-actin, as a control. Furthermore, it is not known which parts of the efflux transporters the food binds to, and whether it has implications for their functional activity. Several *in vitro* studies have shown that food-derived compounds are capable of inhibiting efflux transporters [213]. In contrast, PCR measures the total mRNA in a sample and can provide early detection and insights into the transcription process in a tissue [214]. However, it is the relative expression of the mRNA relative to beta-actin, a housekeeping protein, that is expressed ubiquitously in every tissue and is essential for the maintenance of normal cellular function [215]. Although, variability may exist in the expression of beta-actin questioning its role as a control [216]. To the authors' knowledge, it is not known if food intake affects beta-actin expression in preclinical rodent models or humans. The use of another technique, LC-MS/MS-based quantitative proteomics, has expanded to quantify transporter abundance [207,210,217]. Our recent comparison of ELISA and LC-MS/MS concluded that these methods produced similar trends in P-gp expression. Another key message of the article was that while LC-MS/MS was more sensitive, ELISA allowed for faster data acquisition [210]. Targeted LC-MS/MS works by measuring proteospecific peptides generated by a tryptic digest as surrogates for the respective protein [218]. Our recent comparison of ELISA and LC-MS/MS concluded that the methods produced similar trends in P-gp expression. While LC-MS/MS is more sensitive, ELISA allows for faster data acquisition [210]. It was also suggested that the complex method development associated with LC-MS/MS may limit its use.

Strong to moderate positive correlation was found between ELISA to PCR; r=0.615 and r=0.741 for P-gp/*abcb1a*, r = 0.816 and r = 0.773 for BCRP/*abcg2*, and r = 0.881 and r = 0.935 for MRP2/*abcc2* (Figure 2-3, Figure 2-6, Figure 2-13, Figure 2-16, Figure 2-23 and Figure 2-26). Drozdzik et al also found significant positive correlation in human small intestinal tissue between mRNA level and protein abundance for P-gp/*abcb1a*, BCRP/*abcg2*, and MRP2/*abcc2* [219]. The differing correlations between mRNA/protein expression suggest that predictive power of transcript analysis should be examined on a gene-by-gene basis [62]. The expression of a protein can be regulated at multiple stages; the initiation of transcription, splicing of the primary transcript, initiation of translation, post-translational modifications, subcellular redistribution, and degradation of the protein [220]. The lowest correlation between the methods was for P-gp/*abcb1a*, suggesting downstream processes affect the P-gp expression. PCR and ELISA should be used together for comprehensive insights into transcript and protein expression.

The strain, sex, and prandial state of preclinical animals are often selected based on cost, convenience, ease-of-handling, and experience, as opposed to for biological reasons. Anecdotally, experimental animal models are chosen to yield clean, homogenous, and predictable data, which may fail to consider intra-individual variability. However, this study and findings in the literature suggest that the experimental groups should be carefully selected based on the most appropriate physiological characteristics for that experimental measurement [210]. A prominent commentary by Clause noted that due to its uniformity, quality, efficiency of production and application to scientific practice, the Wistar rat is the best choice for a standardised animal model for translation to humans [221]. There are key differences in the physiology, behaviour, and appearance. Sprague Dawley rats are seen to grow faster, exhibit higher testosterone levels, and have a higher reproductive potential, compared with Wistar rats [188]. Sprague Dawley rats also show increased motor activity and explorative levels in comparison to Wistar rats, which may contribute to their higher reproduction rates [188]. A recent investigation from our research group proposed that the Wistar rats should be the chosen animal model for preclinical studies using P-gp drug substrates as both Wistar rats and humans

show sex differences in P-gp expression [210]. Sprague Dawley rats, on the other hand, did not show sex differences in the P-gp expression, which our results corroborate.

Transporter-knockout animal models are commonly used to evaluate the impact of a single transporter on the ADME of an investigational new drug [222]. However, the majority of knockout animal models are mice. Unfortunately, it can be logistically challenging to conduct pharmacokinetic studies with mice and can lead to high variation. In addition, knockout rats can be very expensive, and it was found that suppliers only had male rats available and no females, so potential sex differences could not be investigated. This could be a future experiment when appropriate knockout rat animal models become available.

The use of *in vivo* animal models serve as a primary tool to guide development into novel active pharmaceutical ingredients (APIs) [136]. Biopharmaceutics investigations are largely, empirical, rather than based on an in-depth mechanistic approach. Here, the heterogenous nature of efflux transporter expression in commonly used animal models has been characterised. For investigations into P-gp, BCRP, and MRP2 substrates as the drug of interest, these fundamental differences in transporter expression should be used to guide the choice of the animal model. There are limited studies using human intestinal tissue examining the BCRP and MRP2 expression between the sexes that assess the most appropriate animal model to understand the oral absorption of substrates. Furthermore, the influence of feeding on these key efflux transporters should be assessed at the human level. The intra- and inter-variability in drug substrate response seen in the clinic may be attributed to differing efflux transporter expression seen between the sexes, ethnicities, and food intake.

2.6 Conclusion

The intake of food was found to modulate the expression of P-gp, BCRP, and MRP2 in frequently used Wistar and Sprague Dawley animal models. Sex differences were reported in the P-gp, BCRP, and MRP2 expression in Wistar rats, but not Sprague Dawley rats. Similar profiles were seen between the protein and transcript expression, quantified by ELISA and PCR, respectively. The comprehensive characterisation offered by this study can be used in the extrapolation of preclinical studies to the design of clinical trials and inputted into physiologically based pharmacokinetic models for early predictions.

Chapter 3 Influence of a fibre meal on the expression of efflux transporters in the gastrointestinal tract

This chapter contains material adapted from the following publication:

Y Mai *, FKH Gavins *, L Dou, J Liu, F Taherali, ME Alkahtani, S Murdan, AW Basit, M Orlu. A Non-Nutritive Feeding Intervention Alters the Expression of Efflux Transporters in the Gastrointestinal Tract. Pharmaceutics. 2021 Oct 26;13(11):1789. doi: 10.3390/pharmaceutics13111789

*These authors contributed equally to the manuscript.

3. 1 Introduction

3.1.1 Efflux transporters

At the intestinal layer, efflux transporters shuttle substrates from intestinal epithelia, into the GI lumen, providing a protective barrier and limiting their absorption into systemic circulation. These transporters are located on the apical surface of the intestinal epithelial cells. Substrates for these efflux transporters can include several endogenous compounds (sterols, bile acids and hormones), nutrients (sugars, fatty acids and vitamins), and drug products [223]. The efflux transporters P-gp (*abcb1*) and BCRP (*abcg2*), in particular, are considered clinically relevant and can contribute to poor absorption and low oral bioavailability of many drugs [224]. Multidrug resistance-associated proteins (MRP) are a key group of human ABC transporters that are relevant for drug transport. Here, MRP2 (*abcc2*) was examined as it is expressed at high levels in barrier tissues [48]. P-gp substrates include antineoplastic drugs (docetaxel, etoposide, vincristine), calcium channel blockers (amlodipine), digoxin, macrolide antibiotics (clarithromycin), and protease inhibitors [225]. BCRP substrates, amongst others, include prazosin, glyburide, cimetidine, sulfasalazine, rosuvastatin, and chemotherapeutic agents such as methotrexate, topotecan, imatinib, and irinotecan [46,226]. MRP2 substrates include pravastatin, temocaprilat, etoposide, vinblastine, vincristine, doxorubicin, epirubicin, and cisplatin [51].

3.1.2 Food intake

The effects of food intake can occur at different stages of drug absorption in the body [143] and the key mechanism for such effects is often unknown [24,227,228]. Food-mediated changes include: chemical interaction with the drug substances [67]; alterations to the luminal conditions (fluid volume, motility, pH); and modulations to the intestinal monolayer, metabolism, or transporters [9]. The effect of food on efflux transporters has been extensively studied, focusing on the inhibiton of transporters by of dietary compounds [63]. The main food components investigated by *in vitro* studies

are herbal and fruit products, such as grapefruit juice [229], orange juice [230], and St John's Wort [231] Although, the effect of food on the pharmacokinetic profile of an orally administered drug substrate is not necessarily caused by specific interactions with the efflux transporters and can also be caused by a change in luminal conditions [9].

The properties of a meal can affect the GI luminal fluid, and in turn, drug absorption. These properties includes the calorie content (low versus high calorie meals), nutrient composition (protein, carbohydrate-rich, or high fat meals), volume of food, temperature of the meal itself, and fluid co-ingestion [21]. Solid food is initially kept in the proximal stomach, whereas liquids are distributed throughout the stomach. The gastric emptying of liquids is faster, than for solids. Non-nutritive liquids empty from the stomach into the duodenum exponentially [232]. Whereas, more linear emptying is reported with increasing nutrient and calorie content of the liquid phase [233]. Several hormones influence the motor processes, which include CCK by affecting the gallbladder contraction, bile, and pancreatic secretions.

Sex differences exist in the body's digestion of food, which in turn can affect drug performance between males and females in the postprandial state [73]. For example, following a fat-rich meal sex differences were reported in the bioavailability of a P-gp substrate cyclosporine A. In females, a decreased oral bioavailability was seen, whereas an increased oral bioavailability was shown in male humans [86]. Sex hormones were recently found to affect passive diffusion and active transport of drugs to different extents in males and females [234].

3.1.3 Food and transporter interactions

As mentioned, food can dynamically interact with transport in the epithelia of the GI tract [9]. The interaction may not necessarily be caused by specific interactions but could also be due to changes in the luminal conditions. Dou et al., observed that food consumption resulted in a change in the intestinal P-gp expression to different extents in male and female rats using Western Blot (relative expression) and proteomics methods (absolute expression) [217,235]. However, the mechanism for the food-

mediated phenomenon was unknown and not fully understood. The hypothesis was that the sex-dependent food effect in the modulation of P-gp may be multifactorial; an interplay between food components in a meal and the release of GI hormones and sex hormones [217].

Firstly, several components in the food matrix are shown to modulate the intestinal absorption of P-gp substrates [63]. Monoglycerides and bile salts were observed *in vitro* to show an inhibitory effect on both uptake and efflux transporters (Custodio et al., 2008). Therefore, some researchers hypothesise that high-fat meals may inhibit efflux and uptake transporters (Won et al., 2012). Dietary fibres are present in meals as well as in over the counter and prescription laxatives such as Fybogel®. Fibres can beneficially modulate GI activity by altering transit time and stool formation in humans [236]. In addition, dietary fibres can also alter the expression and functions of intestinal P-gp and BCRP in humans [237], cell-lines, and male rats [238]. Secondly, gastrointestinal hormones may increase P-gp membrane localization [239]. Thirdly, testosterone, the primary male sex hormone, and estradiol, a female hormone, were shown to inhibit or induce P-gp, respectively [240,241]. Previous studies in the literature predominantly focused on the expression of P-gp [242,243], whereas other intestinal transporters such as BCRP and MRP2 also play significant roles in drug absorption.

3.2 Aims

To understand the effects of three feeding interventions – fasted, housing food (normal meal) and a non-nutritive 'food' (fibre meal) – on clinically relevant efflux transporters in the rat Wistar animal model.

Objectives

- To characterise the luminal characteristics (pH and buffer capacity) in the stomach, small intestine, and colon following food intake
- To investigate the intestinal expression of P-gp, BCRP, and MRP2 with three feeding interventions (fasted, housing pellets [termed normal food], and non-nutritive fibre pellet [termed fibre food])
- To explore if sex differences are seen in the transporter expression (P-gp, BCRP, and MRP2) between male and female rats
- To explore the plasma concentration of sex hormones (testosterone and estradiol) and gastrointestinal hormone (cholecystokinin)
- To investigate the trends in transporter expression (P-gp, BCRP, and MRP2) over time (0 to 2 h)

3.3 Materials and Methods

3.3.1 Materials

KBR, pH 7.4, was freshly prepared before the experiment at room temperature and was kept at 37 °C. KBr was composed of 10 mM D-glucose, 1.2 mM $CaCl_2$, 1.2 mM $MgCl_2$, 115 mM NaCl, 25 mM $NaHCO_3$, 0.4 mM KH_2PO_4 and 2.4 mM K_2HPO_4 [244]. Lysis buffer was freshly prepared with 50 mM Tris, 250 mM NaCl, 5 mM ethylenediaminetetraacetic acid (EDTA), 1 mM Na_3VO_4, 1mM PMSF, 1% Nonidet P40 and protease inhibitor cocktail from Sigma in phosphate-buffered saline (PBS) and stored at 4 °C.

ELISA kits were purchased from MEIMAN Biotech (Guangzhou, China). The ELISA kits were as follows rat P-gp ELISA Kit (MM-0604R2), rat BCRP ELISA kit (MM-0606R2), rat MRP2 ELISA kit (MM-0607R2), rat CCK ELISA Kit (MM-0034R2), rat testosterone ELISA kit (MM-0577R1) and rat estradiol ELISA kit (MM-0567R2). Cellulose pellets (Solka-Floc® 200 FCC) were purchased from Envigo – Teklad custom diet (TD.85467) (Madison, WI, USA). Normal meal was housing food was provided in the animal housing unit.

3.3.2. Animals

Male and female Wistar rats (healthy 8- to 13-week-old) were used as the animal models and each experimental unit used 6 rats. The rats were housed at room temperature (25 °C) in a light-dark cycle of 12h. The rats acclimatized to the animal unit for at least 7 days. An overnight fast of 12 hours was conducted prior to the experiments the following morning at 8 am. All animal work was conducted in accordance with the project license (8002536), approved by the Home Office under the Animals (Scientific Procedures) Act 1986 on 7 June 2012. The fasted group was the control group, and the animals were sacrificed at t=0 h. The rats were administered normal meal and fibre meal suspensions by oral gavage and were sacrificed at t= 0.5 h, t= 1 h and t= 2 h. A timeframe of 2 hours was chosen for animal welfare reasons after the overnight fast. The rats were sacrificed by CO_2 asphyxiation. Blood was taken by cardiac puncture and kept on ice until further preparation.

3.3.3 Tissue preparation

The intestines of the rats were immediately excised and stored in ice-cold KBR solution. Roughly 2 cm pieces of the small intestine; duodenum (1 cm from the ligament of Treitz), jejunum (10 cm from the ligament of Treitz) and ileum (1 cm from the cecum) were opened along their mesenteric border. The tissues were gently washed with KBR solution to remove the intestinal contents.

3.3.4 Meal characterisation

The suspensions were prepared in the concentration of 0.125 g/ml by mixing 0.5 g of meal (normal meal and fibre meal) with 4 ml deionized water as it was a suitable consistency for oral gavage. Fibre meal was composed of cellulose pellets (section 3.3.1), which were non-fermentable in the GI tract. A description of the fibre meal is provided in the Table *3-1*. Normal housing food was provided in the animal housing unit and the composition is listed (Table *3-2*).

Table 3-1 Fibre meal composition

Name of diet	Envigo Teklad custom diet TD.85467, cellulose pelleted	
Key features	Purified diet, cellulose, non-fermentable fibre	
Formula (g/Kg)	Cellulose (1000)	
Footnote	Pelleted cellulose. Cellulose is considered non-fermentable for rats and mice	
Purchased from	Envigo Teklad	
Selected Nutrient Information		
	% by weight[1]	%kcal
Protein	0	0
Carbohydrate[2]	0	0
Fat	0	0

Kcal/g	0	0
[1]Values are calculated from ingredient analysis or manufacturer data [2]Estimated digestible carbohydrate		

Table 3-2 Normal housing food

Composition	Corn, Wheat middling, Wheat, Soybean meal, Peru fish meal, Chicken meing, Pre-mixed materials, Limestone, Wheat gluten, Soybean oil.
Selected Nutrient Information	
Composition	Amount (g/kg)
Water	91
Crude protein	186.7
Crude fat	53.7
Crude fibre	28.1
Crude ash	54.8
Calcium	10.4
Total phosphorus	7.1
Calcium:Total phosphorus	1.46:1
Lysine	14
Methionine + Cystine	11.5

The crushed pellets were assessed as powder for swelling properties. The powder (0.5g) was suspended in deionised water (4ml) under magnetic stirring for 4 hours. Filter paper was used to gently remove water after 4 hours. Equation 3.1 was used to calculate the swelling capacity of the cellulose powder, where W_s was the weight of the suspension and W_p was the weight of the powder.

Equation 3-1 Swelling capacity

$$Swelling\ capacity = \frac{W_s - W_p}{W_p}$$

Images were taken using an iPhone 12 camera and light microscopy images were taken using an EVOS M5000 microscope.

3.3.5 Transporter extraction from the small intestine

The mucosal tissues (approximately 50 mg) were cut into small pieces and homogenized in 0.5 mL RIPA lysis buffer at 30 Hz for 30s with a TissueLyser (QIAGEN) and repeated twice at intervals of 30 s for complete homogenisation. The tissue homogenates were incubated at 4°C for 2 h, and then centrifuged at 12,000 g for 5 min. The total tissue protein was collected in the supernatants, and its concentration was subsequently determined with the Pierce™ BCA Protein Assay kit (Beyotime Biotechnology) according to the manufacturer's instructions. To measure the target transporter protein level, P-gp, BCRP and MRP2 were quantified by ELISA kits (Meimian Biotech) using the method described in section 3.3.7.

3.3.6 Preparation of hormone blood samples

Blood samples were centrifuged at 10,000 rpm for 10 minutes within 24 h of sampling. The supernatant (plasma samples) was collected and placed in a 1.5 mL Eppendorf tube and immediately stored at -20°C prior to analysis. To measure the hormone levels; CCK, testosterone and estradiol concentrations were quantified by ELISA kits using the method described in section 3.3.7.

3.3.7 ELISA Assay Procedure

Beta-actin was chosen as the internal control protein which was measured by ELISA Assay kit (RTDL00014, Assay Genie). Briefly, 50 µL of serially titrated standards, diluted samples and blanks were added to the standard wells of the i) P-gp; ii) BCRP; iii) MRP2;

iv) testosterone and v) estradiol microplates in duplicates, respectively. 100 µL of HRP-conjugate reagent was then added to each well apart from the blank wells. The plate was covered with a plate sealer membrane and incubated for 60 min at 37°C. The plate sealer was then removed and the liquid discarded by rigorously flicking into an acceptable waste receptacle. The washing buffer solution provided in the assay kit was diluted 20-fold with distilled water. It was then added to each well, shaken on a plate stirrer for 3 s and drained. This was repeated 5 times and wells were blotted dry using a paper towel to remove any remaining liquid. 50 µL Chromogen Solution A and 50 µL Chromogen Solution B was added to each well, covered and incubated for 15 min at 37°C. 50 µL of the Stop Solution was added to each well; a blue colour change to a yellow solution would have indicated a stop in the reaction. Upon analysis, the blank well is taken as zero. Absorbance was then measured at 450 nm in a plate reader following the addition of the Stop Solution within 15 min.

A linear calibration line was constructed using P-gp; BCRP; MRP2; CCK; testosterone and estradiol, and appropriately diluted in 50 mM carbonate buffer (pH 9.5). Tissue supernatants for protein transporter quantification, and plasma supernatants for hormone quantification were also appropriately diluted to 50 mM carbonate buffer (pH 9.5). Absorbance was measured at 450 nm after the reaction and the protein and hormone expression was calculated according to the standard protein calibration curve. Protein and hormone concentrations in all unknown and standard preparations were measured as per instructions of the ELISA kit in duplicate.

3.3.8 Characterisation of Luminal Fluids in the GI Tract

As mentioned in section 3.3.5, the rats were sacrificed by CO2 asphyxiation in the morning of the experiment. The pH of the GI tract was measured *in situ* using a pH meter equipped with an FC202 electrode, designed for measurements in viscous and semi-solid materials (HI99161, Hanna Instruments). pH was determined by introducing the pH probe into the opening created by sectioning parts of the intestinal tract (duodenum,

jejunum, and ileum). The entire intestinal tract was then promptly extracted and separated into the duodenum, jejunum, and ileum within 10 min. The sections were placed into 1.5 mL Eppendorf tubes and centrifuged at 13000 rpm for 20 min (Centrifuge 5415D, Eppendorf AG). The supernatant obtained was kept at −80 °C until the buffer capacity analysis.

Buffer capacity was measured at pH changes of 0.5 and 1.0 units by adding aliquots (10 µL) of 0.1 M HCl (for intestinal fluids) or 0.1 M NaOH (for gastric fluids) to a 300 µL supernatant pooled sample from GI fluid to achieve the desired pH change. Buffer capacity was then calculated using the following Equation (1):

Equation 3-2 Buffer capacity

$$\beta(mmol/L/\Delta pH) = \frac{(M_a \times V_a)}{\Delta pH} \times \frac{1000}{V_b}$$

where β is the buffer capacity, M_a is the molarity of the acid, V_a is the volume of acid in mL, V_b is the volume of buffer in mL and ΔpH is the change in pH unit.

Due to the small amount of fluid available in some of the intestinal segments, the measurements were conducted using pooled samples, where fluids from the same segment of different rats were mixed to increase the available volume.

3.3.4 Statistical Analysis & Data Presentation

The data were analysed by an ANOVA in each segment, followed by a Tukey post-hoc analysis with a 95% confidence interval using the scipy.stats package in Python. A significance value of $p < 0.05$ was used for all tests. The line graph plots were expressed as mean ± standard deviation (SD) (n = 6) using the Matplotlib package version 3.4.3 [203]. Pearson correlation (r) were also calculated in Python. Boxplots were constructed in the Seaborn package version in Python [245]. Box plots consisted of a central line indicative of the median, the box indicative of the interquartile range, the whiskers being

1.5 times the 25th and 75th percentile, respectively and diamond shapes representing the outliers. Python version 3.9.0 on Jupyter Notebook version 6.0.3.

3.5 Results

3.5.1 Meal characterisation

Figure 3-1 and Figure 3-2 shows images of the normal housing meal and fibre meal, respectively. The fibre meal powder was composed of cellulose fibres, off-white in colour.

Figure 3-1 Images of left housing food pellet and right powdered housing food

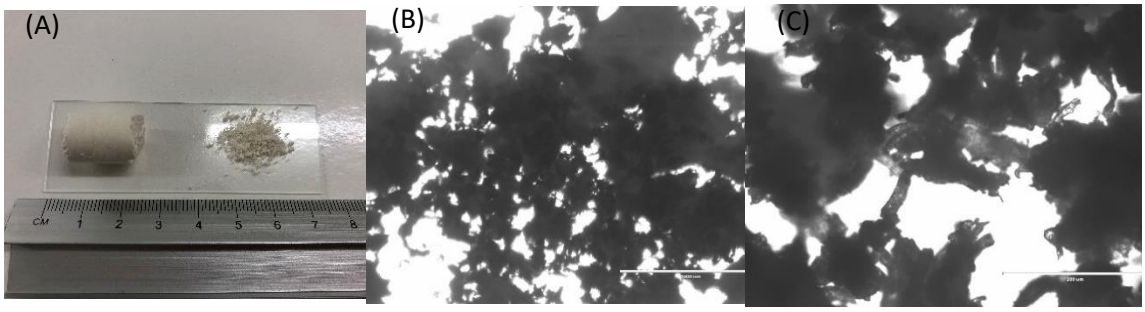

Figure 3-2 Images of (A) left cellulose pellet and right powdered cellulose, (B) and (C) light microscope images

The fibre meal has a swelling capacity of 160% and the housing meal has a swelling capacity of 66%. Figure 3-3 shows the fibre meal suspension.

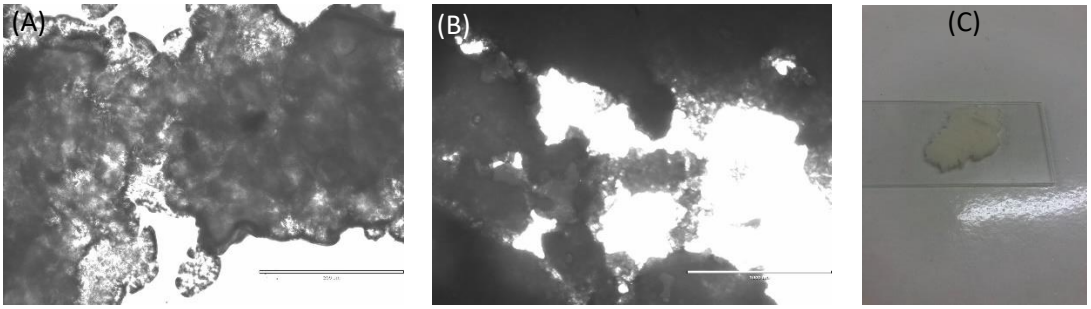

Figure 3-3 (A), (B) and (C) Images of fibre meal after magnetic stirring in deionised water at t=4 h. (A) image and (B) are light microscope images.

3.5.2 Luminal fluid characterisation

The GI pH profile will affect drug ionisation, which can in turn affect the drug solubility, stability, absorption, and bioavailability. The buffer capacity of the GI luminal fluid will affect the rate and extent of dissolution for drugs. Buffer capacity will depend on the pH, buffer species, pKa, and concentration of the buffer species, which are key parameters affecting the drug solubility [246].

3.5.2.1 pH measurements

Figure 3-4 shows no statistically significant differences ($p < 0.05$) in the pH of the stomach and small intestines for both feeding interventions. However, a statistically significant difference was reported the pH of colon after 1 h between the female normal and fibre meals and at 2 h between the male normal and fibre meals. An increase in the inter-individual variability was observed in the colon. The lowest pH was reported in the stomach 30 min following both feeding interventions and the highest pH was reported in the colon 1 hour following administration of the fibre meal.

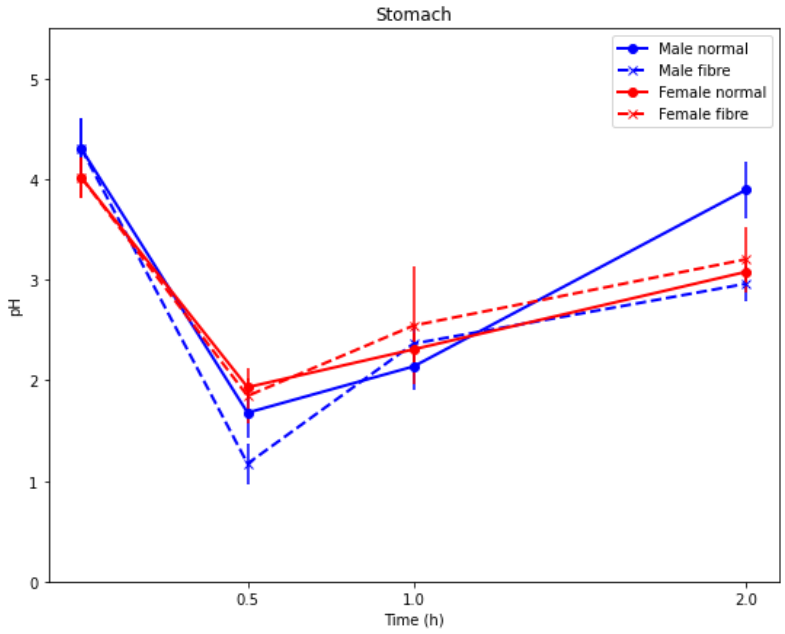
Stomach
Male normal
Male fibre
Female normal
Female fibre
pH
Time (h)
0
1
2
3
4
5
0.5
1.0
2.0

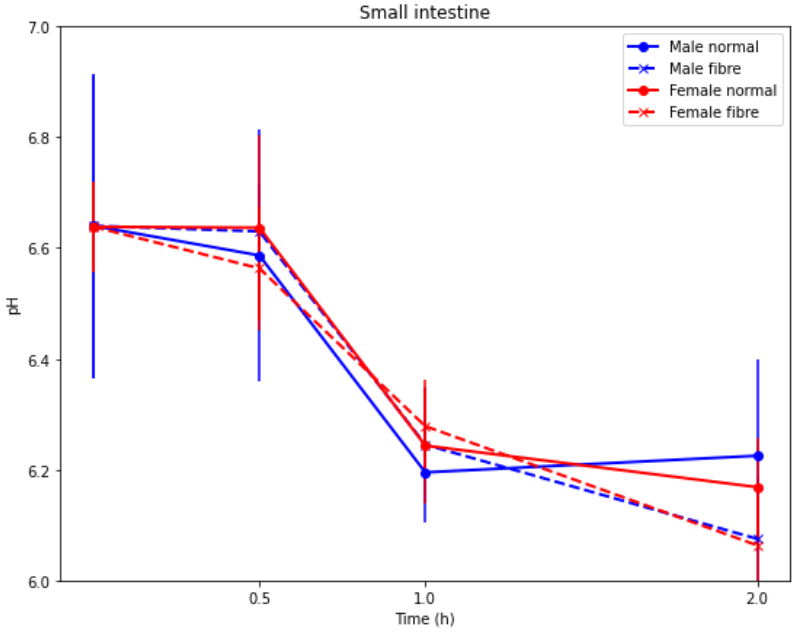
Small intestine
Male normal
Male fibre
Female normal
Female fibre
pH
Time (h)
6.0
6.2
6.4
6.6
6.8
7.0
0.5
1.0
2.0

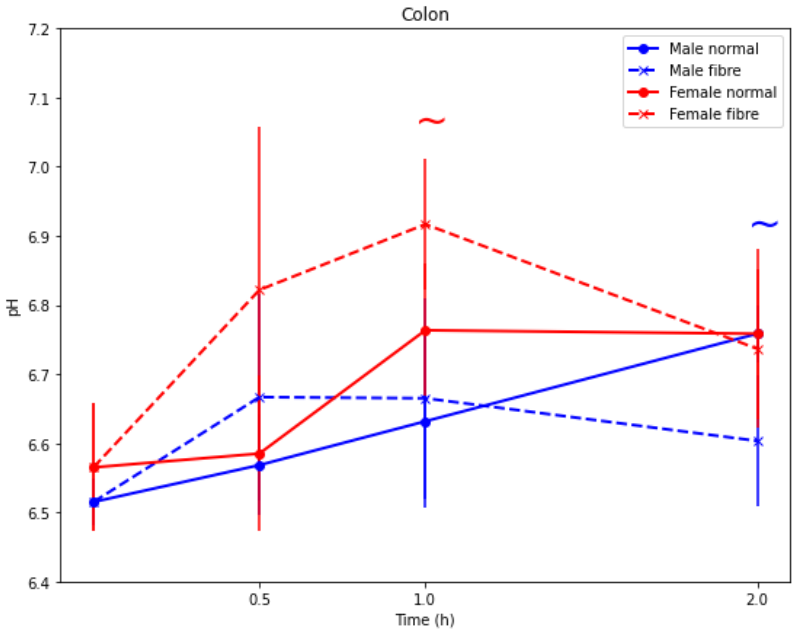

Figure 3-4 pH change in the luminal environment along the gastrointestinal (GI) tract (stomach, small intestine, and colon) over time (h) from the fasted state to the fed state (normal housing food and fake food intervention) in male and female Wistar rats measured in situ (mean ± SD, n = 6).

3.5.2.1 Buffer capacity measurements

As shown in Figure 3-5, the buffer capacity measurements were comparable between the groups. The highest buffer capacity was observed in the stomach. The buffer capacity of small intestine was slightly reduced, and the buffer capacity of the colon was the lowest. The greatest inter-individual variability was seen in the small intestine after 1 h.

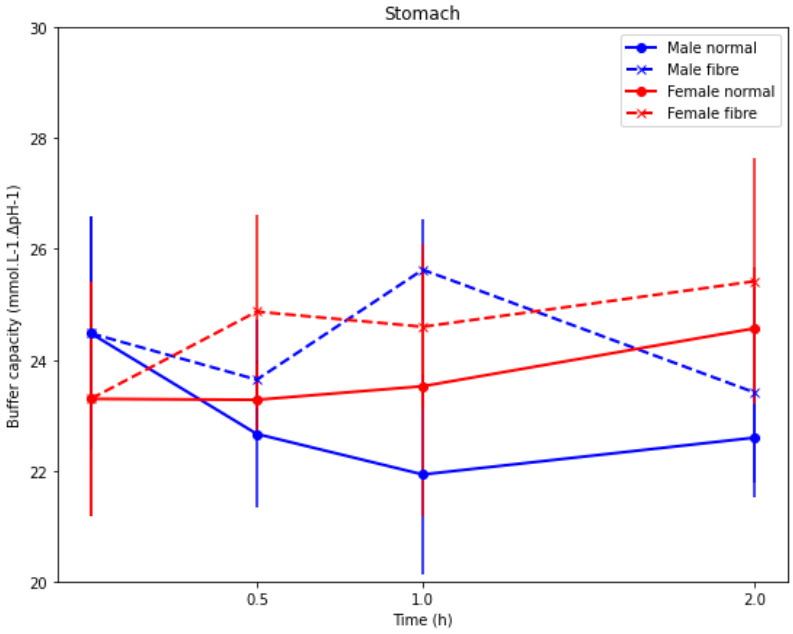
Stomach
Male normal
Male fibre
Female normal
Female fibre
Buffer capacity (mmol.L-1.ΔpH-1)
Time (h)
30
28
26
24
22
20
0.5
1.0
2.0

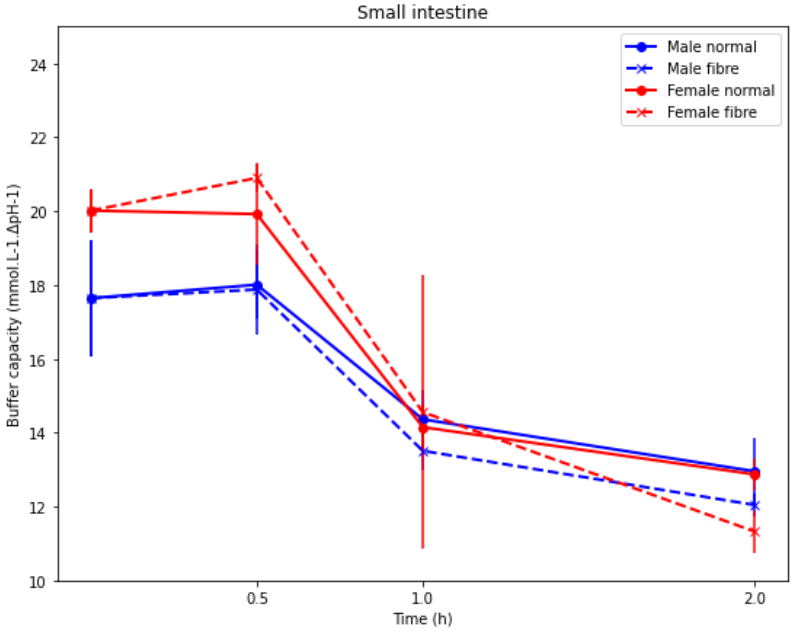
Small intestine
Male normal
Male fibre
Female normal
Female fibre
Buffer capacity (mmol.L-1.ΔpH-1)
Time (h)
24
22
20
18
16
14
12
10
0.5
1.0
2.0

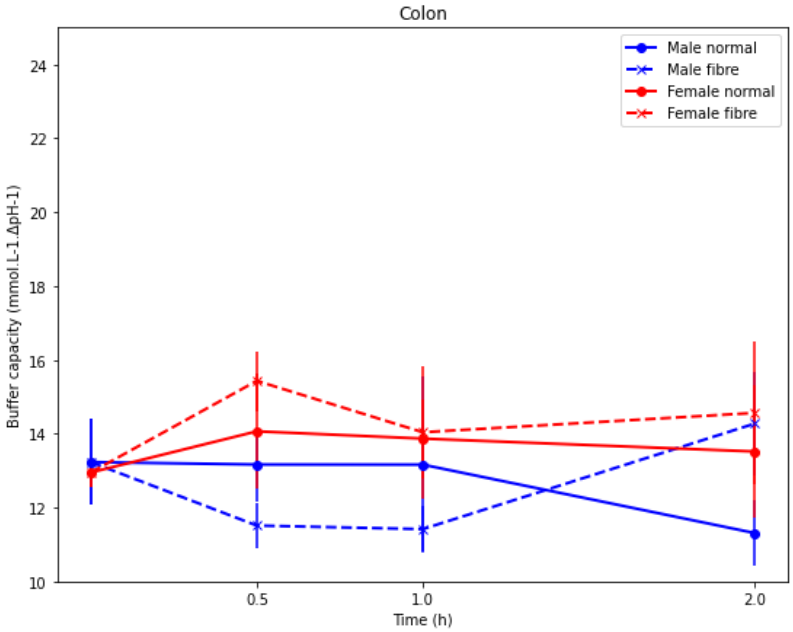

Figure 3-5 Buffer capacity change in the luminal environment along the gastrointestinal (GI) tract over time (h) from the fasted state to the fed state (normal housing food and fake food intervention) in male and female Wistar rats (mean ± SD, n = 6).

3.5.3 Efflux transporter expression

3.5.3.1 ELISA calibration curves

Figures S0.1-6 (Appendix) report the ELISA calibration curves of P-gp, BCRP, MRP2, CCK, testosterone, and estradiol, respectively, with R^2 over 0.99.

3.5.3.2 P-gp expression

The change in P-gp expression with the feeding interventions are illustrated in Figure 3-6. In the fasted state, a significant sex difference was reported; the P-gp expression was 17% higher in male rats than in females. On the other hand, in the normal meal fed state, a contrasting trend was seen where the P-gp expression was 102% higher in female rats than male rats. Interestingly, in the fibre meal group, male rats showed a significantly higher P-gp expression than in the normal meal group; 18.54 ± 0.38 ng/mg and 8.58 ± 0.23 ng/mg, respectively. Whereas, for female rats, the P-gp expression was

not significantly different between the normal meal and fibre meal groups, 17.30 ± 1.32 ng/mg and 16.68 ± 1.33 ng/mg, respectively.

Figure 3-6C reports the influence of food interventions on P-gp expression over time. Significant sex differences were seen in the jejunum with all feeding interventions (fasted, normal meal and fibre meal). An interesting trend was observed in male rats, where the normal meal feeding intervention caused a decrease in P-gp expression from 12.4 ± 0.70 ng/mg to 8.6 ± 0.23 ng/mg. In contrast, the fibre meal caused an increase in P-gp expression from 12.4 ± 0.7 ng/mg to 18.5 ± 0.38 ng/mg. On the other hand, in females P-gp expression increased for both food interventions in the first hour. Between 1 to 2 hours, the P-gp expression decreased in female rats with the normal meal from 17.3 ± 1.32 ng/mg to 12.97 ± 1.17 ng/mg, whereas in the fibre meal intervention, the P-gp expression increased from 16.68 ± 1.33 ng/mg to 18.38 ± 0.90 ng/mg.

(A)

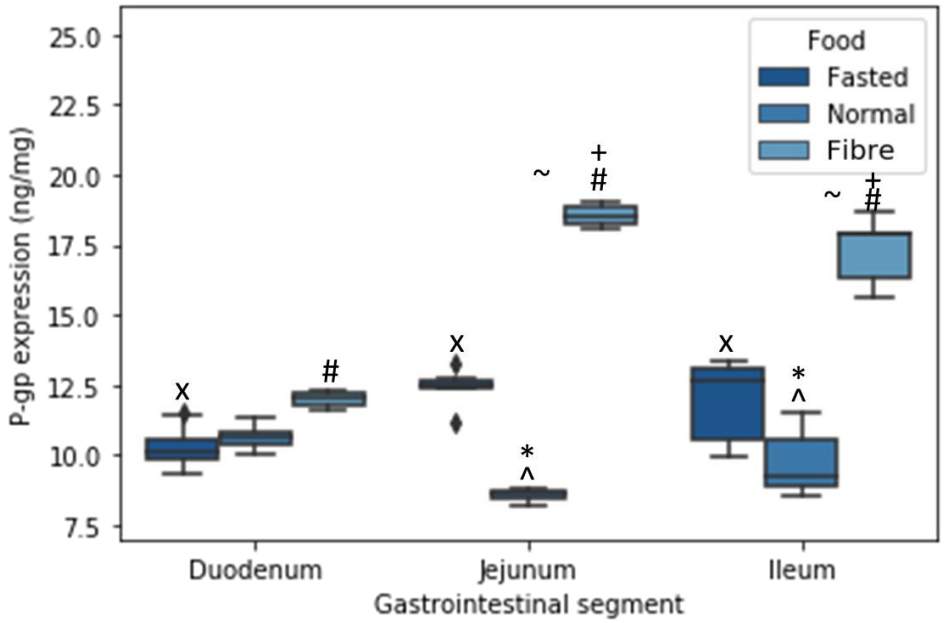

(B)

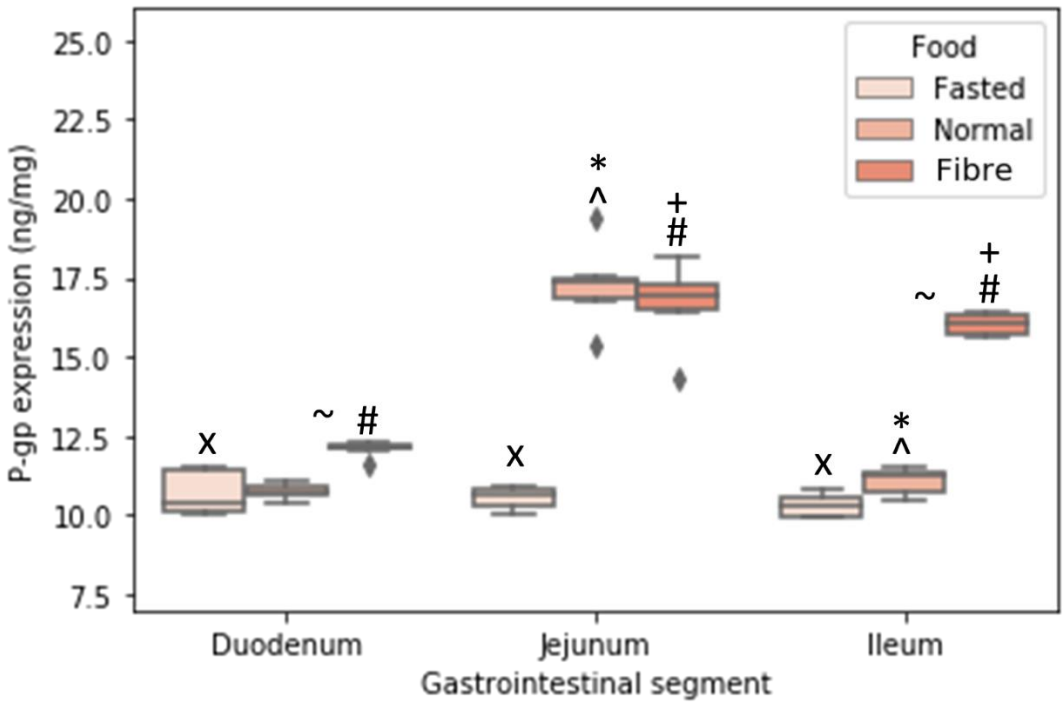

(C)

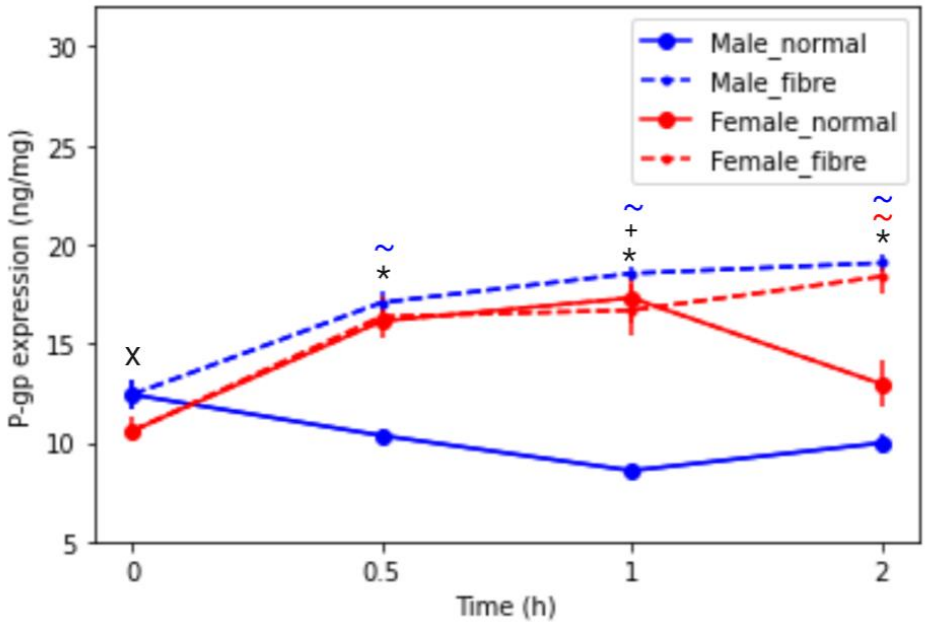

Figure 3-6 P-gp expression across the intestinal tract under three feeding interventions (i) fasted, (ii) normal meal, and (iii) fibre meal quantified by ELISA in (A) male and (B) female Wistar rats (n=6).

(C) P-gp expression (ng/mg) in the jejunum from time 0 to 2h under fasted and fed states (normal meal and fibre meal) (mean ± SD), (n=6).

The following symbols denote a statistical significance ($p < 0.05$) showing a sex difference between male and female rats; fasted state (x), normal meal (*) and fibre meal (+); and a food effect between the feeding interventions; fasted and fibre (#), fasted and normal (^) and normal and fibre (~).

3.5.3.3 BCRP expression

Figure 3-7A and B reported a statistically significant difference in BCRP expression between the fasted and the fibre meal interventions in both sexes along the small intestine. Female rats showed a higher level of expression in the duodenum (9.32 ng/mg, 11.40 ng/mg and 12.08 ng/mg, compared to 8.24 ng/mg, 8.79 ng/mg and 11.15 ng/mg), for the fasted, normal meal and fibre meal groups, respectively. Furthermore, Figure 3-7C showed that the fibre meal intervention significantly increased the jejunal BCRP levels after 30 minutes, 50% in males and 57% in females. In contrast for the normal meal group, the female BCRP levels increased by 19% in the first 30 minutes by and then gradually decreased after two hours. The male normal meal intervention showed the greatest increase of 18% between the 1 and 2h time-interval.

(A)

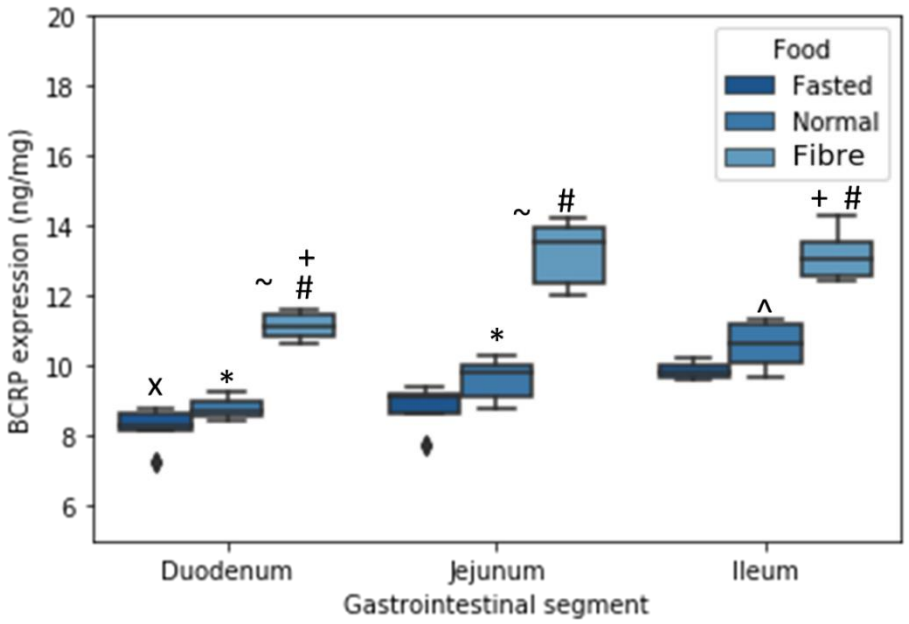
Food
Fasted
Normal
Fibre
BCRP expression (ng/mg)
20
18
16
14
12
10
8
6
Duodenum
Jejunum
Ileum
Gastrointestinal segment

(B)

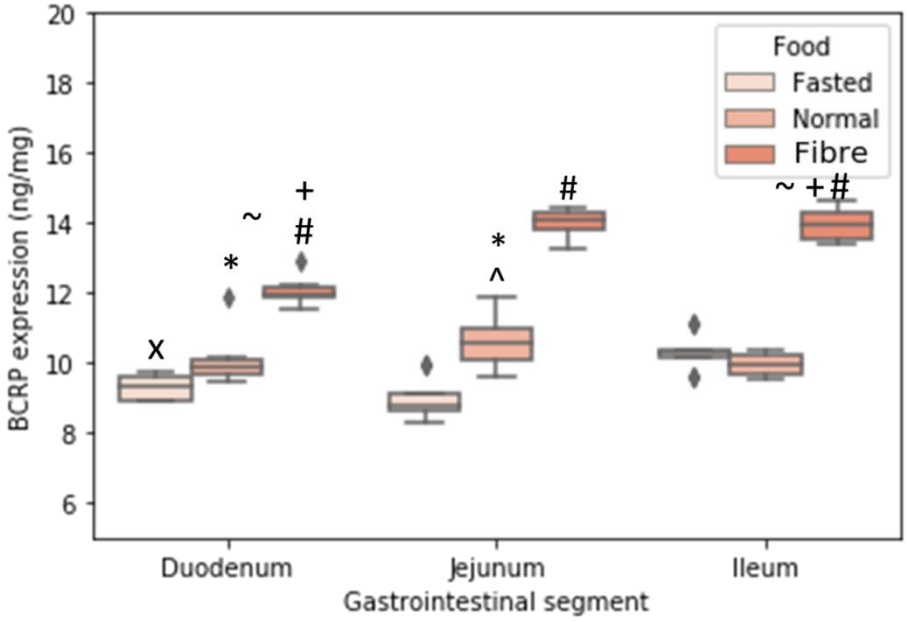
Food
Fasted
Normal
Fibre
BCRP expression (ng/mg)
20
18
16
14
12
10
8
6
Duodenum
Jejunum
Ileum
Gastrointestinal segment

(C)

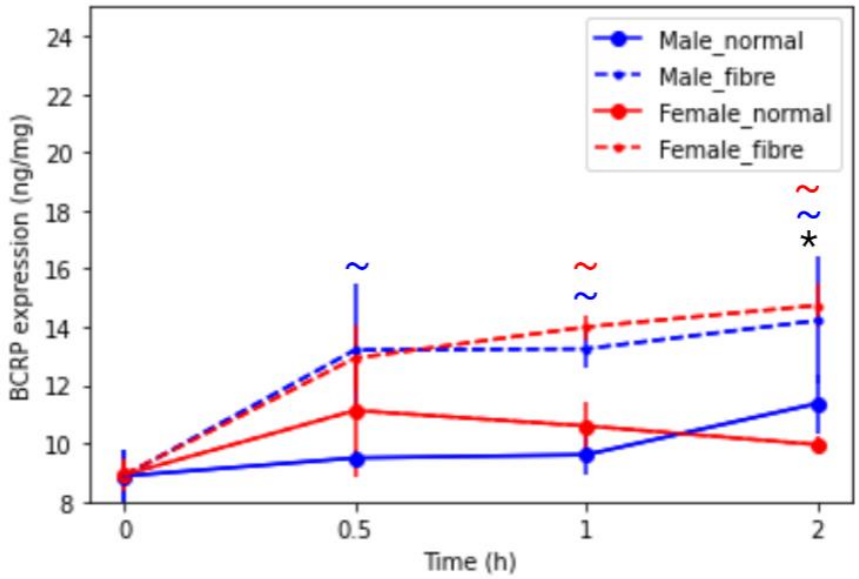

Figure 3-7 BCRP expression across the intestinal tract under three feeding interventions (i) fasted, (ii) normal meal, and (iii) fibre meal quantified by ELISA in (A) male and (B) female Wistar rats (n=6).

(C) BCRP expression (ng/mg) in the jejunum from time 0 to 2h under fasted and fed states (normal meal and fibre meal (mean ± SD), (n=6).

The following symbols denote a statistical significance ($p < 0.05$) showing a sex difference between male and female rats; fasted state (x), normal meal (*) and fibre meal (+); and a food effect between the feeding interventions; fasted and fibre (#), fasted and normal (^) and normal and fibre (~).

3.1.3. MRP2 expression

MRP2 expression in males and female rats along the small intestine is reported in Figure 3-8A and B. Significant differences ($p < 0.05$) were reported between the fasted and fibre meal interventions in both sexes along the small intestine; the largest increase was 103% in the male jejunum. Interestingly, normal meal caused an increase in the MRP2 expression of male rats; 1.6-fold in the duodenum, 1.7-fold in the jejunum and 1.5-fold in the ileum, compared to the fasted state. Although, this housing food-mediated effect was not seen in female rats. Figure 3-8C showed a similar jejunal MRP2 expression at 30 minutes in the fibre meal and male normal meal interventions. Significantly, following normal meal intake, the female MRP2 expression was lower than in males. In addition,

the female MRP2 expression in the normal meal intervention was similar (4.23 ± 0.57 ng/mg at 0h, 4.46 ± 0.49 ng/mg at 0.5h, 4.28 ± 0.72 ng/mg at 1 h and 4.51 ± 0.57 ng/mg).

(A)

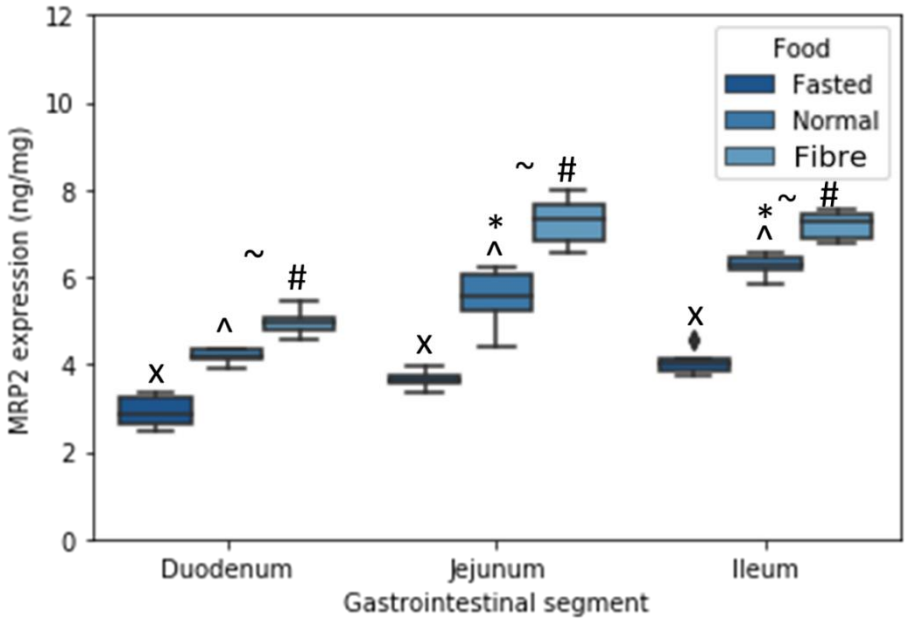

(B)

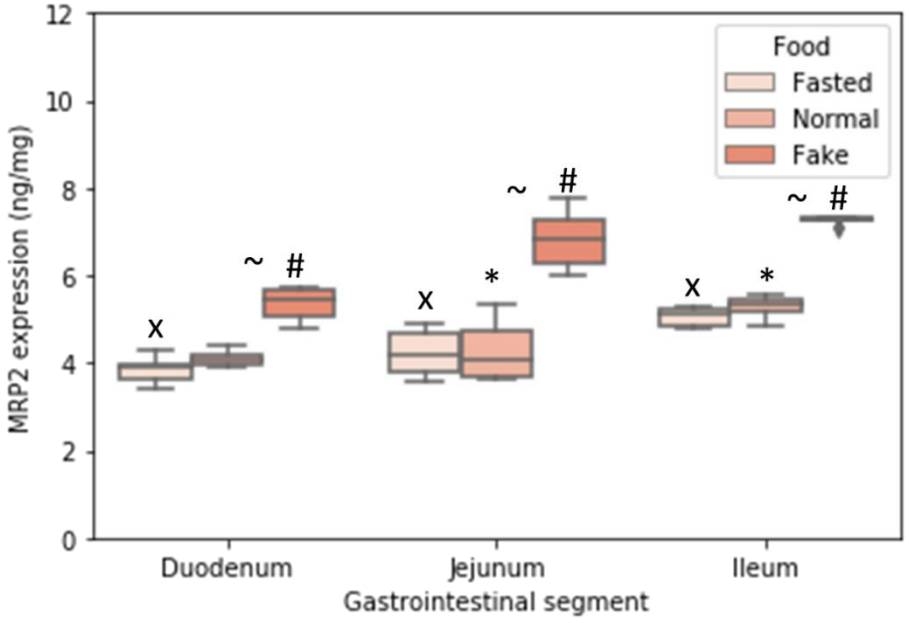

(C)

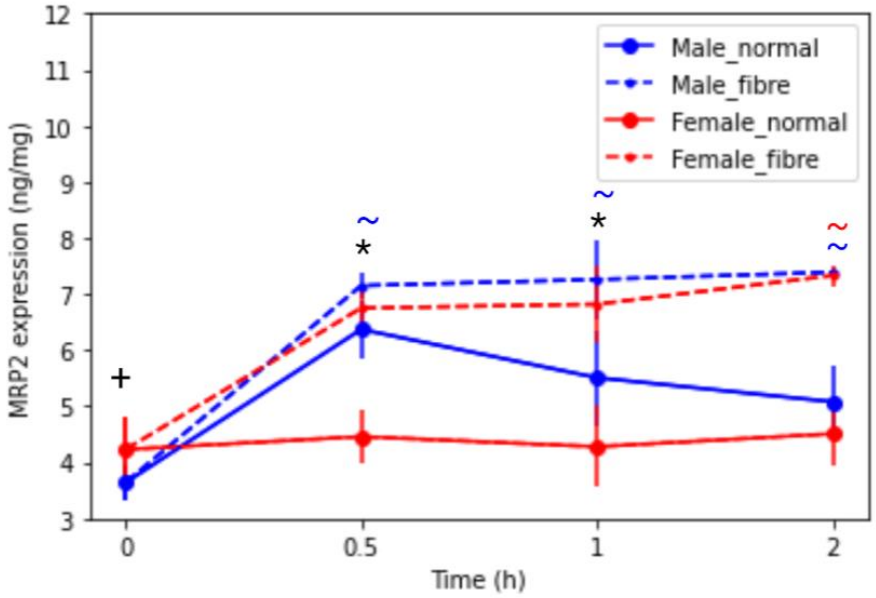

Figure 3-8 BCRP expression across the intestinal tract under three feeding interventions (i) fasted, (ii) normal meal, and (iii) fibre meal quantified by ELISA in (A) male and (B) female Wistar rats (n=6).

(c) BCRP expression (ng/mg) in the jejunum from time 0 to 2h under fasted and fed states (normal meal and fibre meal) (mean ± SD), (n=6).

The following symbols denote a statistical significance ($p < 0.05$) showing a sex difference between male and female rats; fasted state (x), normal meal (*) and fibre meal (+); and a food effect between the feeding interventions; fasted and fibre (#), fasted and normal (^) and normal and fibre (~).

3.2. Hormone concentration

3.2.1 Gastrointestinal hormones; cholecystokinin (CCK)

Figure 3-9 displays the CCK plasma concentration (pg/ml) over time in hours in male and female rats under fasted state and fed (normal meal and fibre meal) states. A significant sex difference was seen in the fasted state at t=0, in the normal meal state at each time points and in the fibre meal fed state at 2 h. Interestingly, a clear statistical difference ($p < 0.05$) was seen between the normal meal and the fibre meal intervention in male rats. An increase of 75% was seen in the CCK plasma concentration between 0 h and 0.5 h in the fibre meal intervention, with a decrease of 32 % in the normal meal intervention.

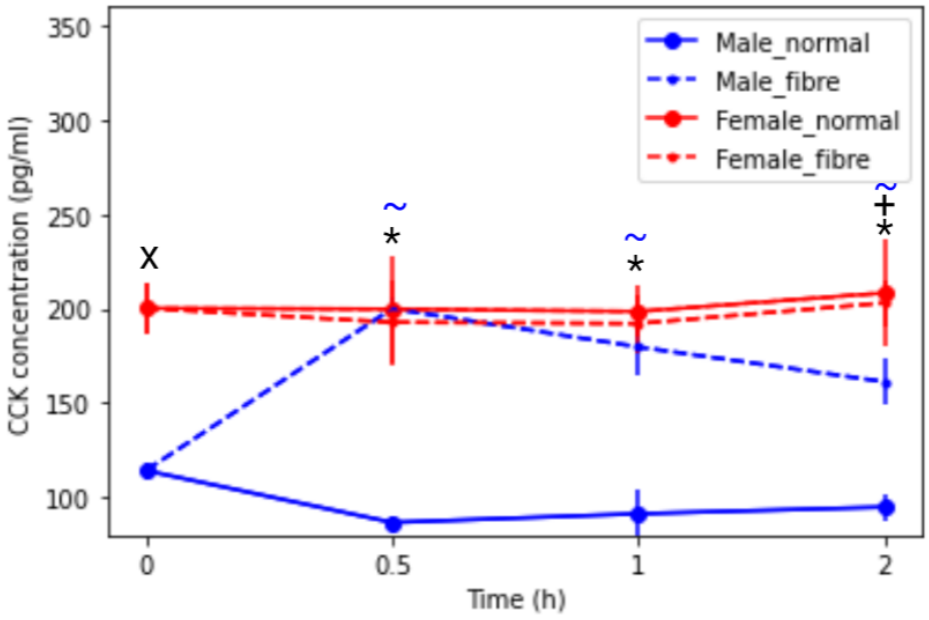

Figure 3-9 CCK concentration (pg/ml) over time of male and female rats under fasted and fed states (normal housing food and fibre meal, (mean ± SD, n=6). The following symbols denote a statistical significance ($p<0.05$) showing a sex difference between male and female rats; fasted state (x), normal meal (*) and fibre meal (+); and a food effect between the feeding interventions; fasted and fibre (#), fasted and normal (^) and normal and fibre (~).

3.2.2. Sex hormone concentrations; testosterone and estradiol

Interestingly, the basal testosterone was shown to be higher in female rats than in male rats. Additionally, in female rats, the testosterone concentration decreased until 1 h for the normal meal intervention, then increased (Figure 3-10)**.** Whereas the testosterone continued to decrease with the fibre meal. A contrasting trend was observed for testosterone concentration between the feeding groups in male rats; the normal meal showed an increase of 23% up to 2 h and the fibre meal showed a decrease of 54%. The basal estradiol was higher in females than males. Significant sex differences ($p < 0.05$) were seen for the estradiol concentration (Figure 3-11), but the type of meal did not affect the plasma concentration.

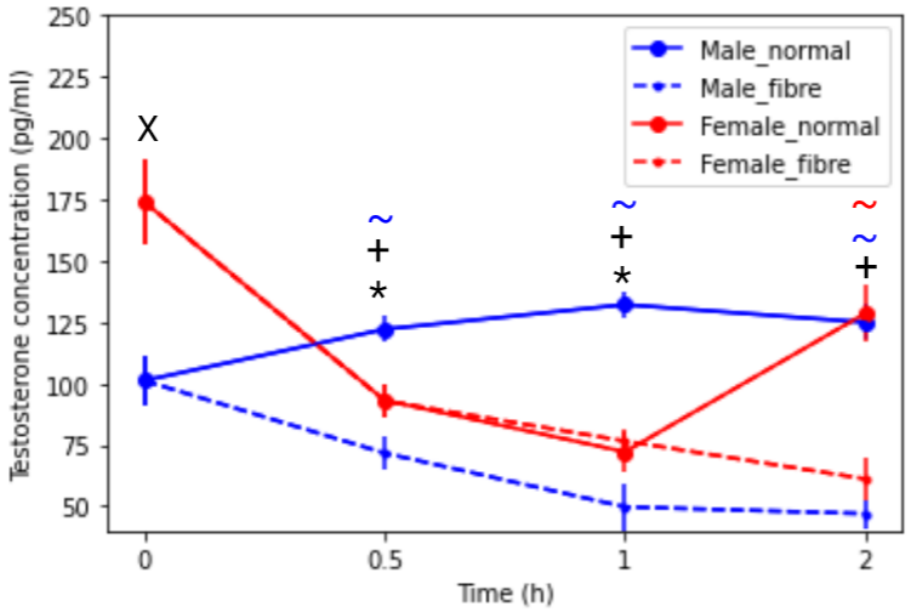

Figure 3-10 Plasma testosterone concentration (pg/ml) (pg/ml) over time (0 to 2 h) in male and female rats under fasted and fed states (normal meal and fibre meal (mean ± SD, n=6). The following symbols denote a statistical significance ($p < 0.05$) of a sex difference between male and female rats; fasted state (x), normal meal (*) and fibre meal (+); and a food effect between the feeding interventions; fasted and fibre (#), fasted and normal (^) and normal and fibre (~).

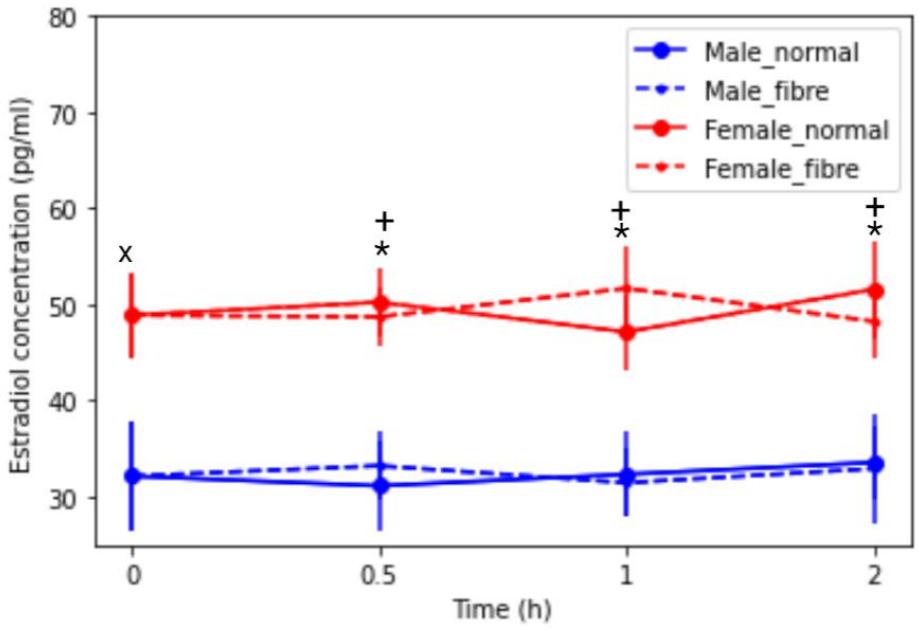

Figure 3-11 Plasma estradiol concentration (pg/ml) over time (0 to 2 h) in male and female rats under fasted and fed states (normal meal and fibre meal (mean ± SD, n=6). The following symbols denote a statistical significance ($p < 0.05$) of a sex difference between male and female rats; fasted state (x), normal meal (*) and fibre meal (+); and a food effect between the feeding interventions; fasted and fibre (#), fasted and normal (^) and normal and fibre (~).

3.4. Correlation between efflux transporter expression and hormone expression

Figure 3-12 explores the correlation between the expression of P-gp, BCRP and MRP2 transporters and concentration of testosterone, estradiol, and CCK hormones. The highest correlation were the negative correlations shown between testosterone and P-gp (r= -0.99, r= -0.99, r= -0.99 and r= -0.92 for males and females in the normal and fibre meals, respectively). For BCRP, testosterone showed a strong negative correlation with the female fibre group (r= -0.99) and estradiol showed a strong positive correlation with the male normal group (r= 0.89). CCK concentration was moderately correlated with male P-gp expression (r= 0.81 and 0.75 for normal and fibre, respectively). In addition, estradiol was moderately correlated with MRP2 in the female normal meal group (r=0.85).

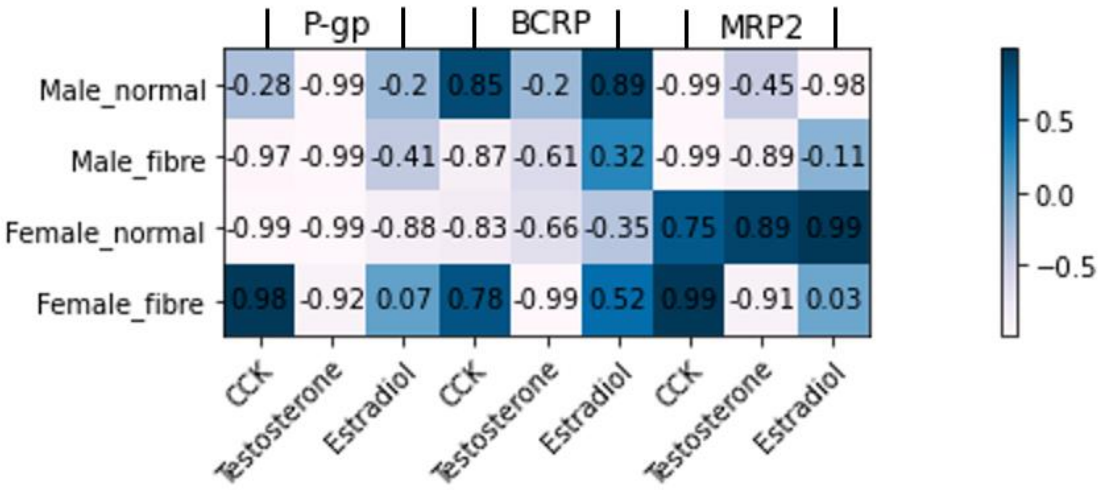

Figure 3-12 Correlation between transporter and hormone concentration for; P-gp, BCRP, and MRP2 expression in the jejunum with CCK gastrointestinal hormone and testosterone and estradiol sex hormones.

3.4 Discussion

3.4.1 Luminal fluid

Following oral drug administration, a drug product will be exposed to the fluid in the GI tract, where it will undergo disintegration, dissolution, and diffusion, followed by permeation into the systemic circulation. The rate and extent of absorption will depend on the drug product's physicochemical properties as well as the GI physiological conditions, including the luminal fluid composition. Key properties of the luminal fluid that will influence the drug's behaviour, include the pH and buffer capacity, almost other properties such as surface tension and osmolality.

As shown in Figure 3-4 and Figure 3-5, the luminal fluid properties in the rat models were variable depending on the location of the GI segment. The pH of the GI fluid affects drug ionisation, by influencing the drug solubility, stability, and absorption. Studies have reported that the gastric rat pH is higher than in humans [115,119], which these current findings reflected. The lowest pH value was expected in the stomach due to the active secretion of hydrochloric acid by parietal cells. Interestingly, the pH of the stomach was lower in the fed state after 30 minutes due to the release of gastric acid to digest the food 'chyme' mixture. The extent of the acidification of the stomach will depend on the buffer capacity of the meal as well as the rate of gastric emptying [247]. In the postprandial state of humans, peak acid secretion was measured as 42 ± 22 mmol/h, which was around ten times higher than the basal acid output rate [248]. Variations in the pH within the stomach may occur due to the different mixing conditions in the fundus and antrum. There are distinct physiological differences between humans and rats, which should be considered in preclinical studies. For example in rats, the fundus is a reservoir for food, with no glands [121]. The fundus has a relatively low shearing mixing zone, lined by stratified epithelium, with convoluted rugal, showing higher fundal variability in pH values. In the antrum, high shear conditions from intensive contractions with linear rugal, results in less variation in pH [249]. In addition, the human gastric microarchitecture differs from the rats as the entire organ is secretory [121]. Rat jejunal

permeability shows strong correlation with human jejunum permeability, concluded from investigations using *in situ* single pass perfusion models [120,250].

A rise in pH was seen from the stomach to the small intestine, which may be due to the presence of bicarbonate ions, bile, and other products of digestion. The slight reduction of the pH in the colon could be due to fermentation and acidic species production by bacteria, as the proximal large intestine is a common site for colonic microbiota [249]. These findings were similar to previous studies investigating the pH of GI luminal fluids in rats [117,118,251] and to studies in fed state male and female rats [252]. The overall trend in the GI pH profile found in this study in the rat is comparable to the human GI pH profile described here and the pH value, except for the stomach pH as mentioned.

The buffer capacity is known to determine the microclimate pH in the diffusion boundary layer next to a dissolving surface, here considering the dissolution of a drug product [253]. The buffer capacity was lower in the small intestine than the stomach, which was unexpected as the presence of bile salts in both the fasted and fed states is expected to increase the buffer capacity. Small intestinal pH and buffer capacity is dependent on the pancreatic and mucosal cell secretion of bicarbonate ions. The lack of gall bladder in rodents is compensated for by the enlargement of the duct system [254]. Without the storage of bile, which occurs in humans, bile acids are continually excreted into the duodenum via the duodenal papilla. In comparison, humans secrete concentrated bile from the gall bladder, around 2-22 ml of bile per kg of body weight each day [255], whereas rats secrete 48 ml of dilute bile per kg of body weight each day from the liver [256]. The trend in the buffer capacity profile measured here is similar to trend found in the literature for rats [257]. The buffer capacity measurements were comparable between the feeding interventions and sexes.

3.4.2 Transporter expression

This study showed feeding interventions, sex, time, and hormone concentration influenced the expression of intestinal efflux transporters in male and female rats. In the drug delivery arena, intestinal transporters are key determinants of the

pharmacokinetics of many drug substrates [194]. Interestingly, inter- and intra-variability exists in their expression and activity with implications for drug substrate performance. A key external factor influencing the variability of drug absorption is food consumption for certain drugs [4]. In food effect studies in a clinical trial setting with human subjects, a high-fat diet is used as suggested by the FDA to maximise the potential for drugs to show a food effect [11]. In preclinical animal studies, specific high-fat diets have been designed for dog and pig models [105,114]. Whereas in studies using small rodents, housing food as opposed to a specific high-fat diet is normally used to study the fed state [217]. High-fat rodent food are available in the market and used in biomedical studies to induce obesity, with 30-78% of total energy intake from fat [258]. However, anecdotally in some cases the rats will not eat high-fat diets, thought to be due to the consistency, the smell, and texture of the pellets. It could be interesting to develop a palatable high-fat rodent diet to simulate the FDA high-fat breakfast to be used in preclinical rodent studies. Here, another approach was tested using a fibre meal. To the authors' knowledge, the effects of a non-nutritive type of fibre on efflux transporters have not been thoroughly explored by *in vivo* male and female animal model studies.

An interesting result was seen with the fibre meal intervention in the efflux transporters examined here; P-gp, BCRP and MRP2. The fibre meal in the GI tract increased transporter expression in both sexes across the small intestine. The largest percentage change was the increase in the P-gp expression in female jejunum (+58%) after the fibre meal. In the male distal small intestine (jejunum and ileum), increases of 50% and 40% from the fasted state were found. A hypothesis for these findings is that the presence of the insoluble foodstuff, the fibre cellulose, in the GI tract will add bulk to the lumen, and contribute to the increased gastric luminal pressure, leading to the distension of the stomach, a delay in gastric emptying, and the subsequent release of GI hormones. A protective function may exist in the GI tract, where the epithelia of intestinal tract increases the expression of the efflux transporters as a barrier mechanism to prevent the absorption of potentially toxic ingested compounds. Housing food, here termed the

normal meal, on the other hand, will undergo digestion and be broken down into products of digestion, followed by the absorption of key nutrients across the GI epithelia.

These protective mechanisms could be a complex interplay between the modulation of efflux transporter expression, neurohormonal feedback mechanisms, enzyme reactions, and the defence ability of epithelial cells, which could be further influenced by sex hormones and the components in food. An Ussing Chamber experiment exposed male and female ileal rat tissues to harsh conditions (hypoxia for 40 minutes and acidosis at pH 6.8) to evaluate the immune-inflammatory response [259]. Fluorescein Isothiocyanate-dextran (FITC-dextran, molecular weight 4300 Da) was used to assess the barrier function of the intestinal lumen. Interestingly, the female intestinal tissue showed a higher anti-inflammatory response and an enhanced intestinal barrier function, in comparison to the male tissue. Estradiol is an endogenous oestrogen that rapidly conjugates with glucuronic acid in intestinal epithelial cells. The addition of estradiol in male rats relieved the intestinal injury and enhanced their anti-inflammatory ability. In terms of transporters, the modulation of ABC transporters has been previously investigated, with the majority of the studies focussing on P-gp [260-262]. The extent of the effects were reported to be dependent on hormone concentrations, protein, and cell type. A finding from Coles et al found that the addition of estradiol increased the P-gp expression, in a concentration dependent manner, using NCI/ADR-RES cells that overexpressed P-gp [263]. Furthermore, estrogen conjugates are strong and specific substrates for BCRP, with a higher affinity for transport than was is observed for MRP2 [264].

Significant sex differences were observed in the expression of P-gp and MRP2 in the jejunum following the feeding of the normal meal. In male rats, a decrease in the expression of jejunal P-gp (-45%) was seen, with the normal feeding intervention, compared with the male fasted rats. On the other hand, in females, a higher expression of P-gp (+64%) was shown, compared with the fasted state. For MRP2, a sex difference was reported in the jejunum with the normal meal, and in the duodenum in the fasted state. The normal meal caused an increase from the fasted state for males (+50%), but

not for females where MRP2 expression was similar (4.23 ± 0.57 ng/mg and 4.28 ± 0.72 ng/mg). The P-gp-related findings for the fasted and housing food (normal meal) were similar to previous findings in my research group using a validated LC-MS/MS method [217], a Western Blot method [235] and PCR [207]. Significantly, the inter-individual variations were low in these results, shown by narrow standard deviation, in comparison to the Western Blot and LC-MS/MS methods reported by Dou et al [207,217,235], which could suggest that the sensitivity of detection is lower for the ELISA method, as discussed in Chapter 2.

Traditionally, oral drug absorption studies focus on the upper small intestine, the jejunum, as it is the first main site of drug absorption. However, more recently the pharmaceutical industry has growing interest in the proximal intestine - the ileum and the colon - for potential sites for targeted drug delivery of extended-release formulations. There are several studies in preclinical animal models [204,265,266], but there is a knowledge gap in the number and function of drug transporters in the ileum and colon in humans [227].

Differing results were found in the literature for some of the data. MacLean et al reported no sex differences in P-gp, BCRP, and MRP2 in fed male and female Han-Wistar rats using immunohistochemistry [202]. MacLean's study showed relative P-gp expression increased from proximal to distal regions, BCRP showed an arcuate pattern with highest expression toward the end of small intestine, and MRP2 decreased along the intestinal axis from proximal to distal parts [202]. In another study, Dahan and Amidon, using a Western Blot method, reported an increase in the P-gp expression in the distal ileum, compared with the proximal jejunum in the fasted male Wistar rats [211]. This study found that BCRP and MRP2 expression showed statistically significant increases between the duodenum and jejunum for the fibre meals, and the male fasted and housing meal groups. Here, no statistically significant increases were reported for the fasted or normal meal female rat. The aforementioned studies used Western Blot methodologies which reply on an internal standard protein. Here an ELISA method was used with specific antibodies, as discussed in Chapter 2. Our findings are similar to my

group's recent article [207]. In the male fasted state, statistically significant differences were reported between the duodenum and jejunum and no statistically significant difference between the jejunum and the ileum. In contrast, in the female fasted state, there was no statistically significant difference between the duodenum, jejunum, and ileum.

Fast and reversible modulation of the function of efflux transporters is of interest to formulation scientists and pharmacologists to enhance the oral absorption of transporter substrates [69]. A prominent review stated that changes to the transporter expression can be caused by (i) changes in their protein expression (long-term regulation), or (ii) changes that does not modify the total amount of protein (acute regulation) [69], by transcriptional or post-transcriptional changes. Vine et al., evaluated the effects of a fatty acid diet (saturated fatty acids, monounsaturated fatty acids, ω-3 and ω-6 polyunsaturated fatty acids) on the jejunal permeability for marker drugs, in this case mannitol, diazepam, glucose, and digoxin, in a long-term study over 30 days [267]. The diet of dietary fatty acids did not alter the passive paracellular permeability of mannitol. However, the efflux of digoxin, a P-gp substrate, was decreased by 20% in the rats. In addition, the permeability of glucose (active absorption) was significantly changed with the dietary change [267]. My hypothesis is that dietary components may modulate micro-RNA expression present in the epithelial cells, which may in turn control gene expression [268-271].

Significant changes were seen in the P-gp, BCRP, and MRP2 expression half an hour after the feeding interventions. Potent BCRP, MRP2 and P-gp inhibitors have been reported in the literature, although most studies use *in vitro* cell lines [272]. These findings suggest that targeted release drug products could be designed, which first releases a specific transporter inhibitor to reversibly block their activity [273], followed by the chosen drug substrate. This reversibility mechanism of the transporter in a short-term time frame could safeguard the normal physiological functioning of the intestinal tract as a barrier after the API has been absorbed [69]. A suggested mechanism for P-gp inhibition is the inhibition of ATPase activity as P-gp is believed to be an energy-activated protein [274].

Studies suggest that the transporter substrate will bind to the binding site, and then ATP will then bind to the two binding sites in the nucleotide-binding domains for ATP. This is then followed by hydrolysis of ATP, which causes conformational change, where the substrate is released from the protein. The second molecule of ATP is hydrolysed, allowing a conformational reset and the substrate and ATP can bind again [60]. Furthermore, MRP2 and BCRP are also shown to be ATP-dependent transporter for the cellular extrusion of their substrates [51,275].

CCK is a GI hormone that plays a significant role in the digestion of nutrients in response to food intake [276]. There are suggested links in the literature between CCK and efflux transporters. For example, Yano and co-workers reported that the CCK hormone levels increased the P-gp localisation and transporter activity in Caco-2 cells [239]. Another study from Karhunen and colleagues reported that fibre intake cause an increase in CCK in humans [277]. CCK is reported to delay gastric emptying in order to reduce the quantity of nutrients entering the duodenum. Delaying gastric emptying by prolonging the gastric residence may be one of the GI's responses to a non-nutritive foodstuff so that the maximum nutrients can be digested by the digestive enzymes. CCK evokes an inhibitory effect on food intake and acts by reducing meal size and duration. The effect of CCK is seen to be short-lived, lasting less than 30 min [278]. Here, a sharp rise in CCK over 30 minutes, was found in the male rats from the fibre experimental group, followed by the subsequent decrease in CCK concentration, reflecting the short-lived nature of this hormone. Furthermore, CCK can increase satiation to terminate feeding and reduce meal duration as a result of the presence of 'foodstuff' in the GI tract [277].

In the housing food (normal meal) intervention in males, a reduction in the P-gp expression was observed (Figure 3-6). A contributing factor to this change in P-gp could be that a nutrient in the housing food could influence the expression of P-gp in males, but not in female rats due to physiological differences. The laboratory rodent diet is formulated for growth and is rich in phytoestrogens, including genistein, a component in soy (soybean is listed in the normal meal, Table 3-2). A study from Arias et al., reported that ethynylestradiol and genistein, nutrients that are associated with soy ingestion,

influenced the expression and activity of P-gp, BCRP, and MRP2 transporters in the Caco-2 cell model (a male cell line) [279]. A further finding here was that the testosterone concentration decreased in the male normal meal (Figure 3-10). Testosterone was highly correlated to P-gp expression (Figure 3-12). In the literature, testosterone was found to be both a substrate and inhibitor of P-gp [280]. A study in the literature found that testosterone administration decreased the functionality of P-gp in male rabbits [281]. A hypothesis could be that the reduction in male testosterone concentration may be related to the decrease in P-gp. Interestingly the testosterone concentration increased after the male fibre meal group.

The normal housing meal-mediated increase in P-gp in females could be the female innate protection present in the intestinal epithelial layer. No significant hormonal changes were reported in the female rats for both food interventions. Higher concentrations of CCK were seen in female rats, with no statistically significant differences between the normal meal and fibre meal. Bitter ligands were shown to increase the release of the satiety hormone CCK [282]. The cellulose-based fibre meal could be bitter, although it was not tested in this study. Unexpectedly as shown in Figure 3-10, the basal testosterone concentration was higher in females than in males. This could be a causative factor for the female rats showing lower P-gp expression in fasted state, compared to males. The sex hormones estrogen and testosterone have been shown to impact *abcg2* expression, although the data are inconclusive [283].

No sex differences in the transporter expression were reported for the fibre meal intervention. Although, sex differences were observed in the testosterone and CCK hormone concentrations. Additional studies are needed to explore the changes in efflux transporter functionality with the feeding interventions by assessing substrate activity with different concentrations of a P-gp, BCRP, or MRP2 inhibitors. Furthermore, the acute effects of different diets could be explored by investigating the effects of different meal components (fats, proteins, and carbohydrates) on the intestinal tract, with a focus on transporter expression, to understand how these food types will affect the delivery of drug products.

3.5 Conclusions

This chapter has shown the P-gp, BCRP and MRP2 expression along the small intestinal tract, with two acute feeding interventions; fed with a normal meal, and fed with fibre meal as well as the fasted state, in male and female Wistar rats. The intake of the fibre meal increased the P-gp, BCRP, and MRP2 transporter expression along the small intestinal tract in both sexes. No significant sex or food effect differences were observed for the BCRP expression. Significant sex differences were seen in the jejunal P-gp and MRP2 expression with normal meal. For the MRP2, significant increases were seen for the male jejunal and ileal expression. For P-gp, on the other hand, the housing food meal caused differing effects between the sexes, where the male jejunal P-gp expression significantly decreased and in contrast, the female jejunal P-gp expression significantly increased. Changes in testosterone and CCK concentrations were observed in the male rat with the fibre meal compared to the normal housing meal, but not in the female rat. Our findings suggest that the products of digestion may modulate P-gp and MRP2 expression in a sex-dependent manner. This is the first study that demonstrates that a non-nutritive fibre meal influences transporter expression differently in the intestinal tract of male and female rats.

Chapter 4 : Machine learning to predict the effect of food on oral drug absorption

This chapter contains material adapted from the following publication:

FKH Gavins, Z Fu, M Elbadawi, AW Basit, MRD Rodrigues, M Orlu. Machine learning predicts the effect of food on orally administered medicines. Int J Pharm. 2022 Jan 5;611:121329. doi: 10.1016/j.ijpharm.2021.121329

4. 1 Introduction

4.1.1 Food effect

Mealtimes can serve as a reminder for patients to administer their medicines, and with the rise in snacking between meals, patients can remain in the postprandial state in waking hours. However, food intake can cause dynamic changes to the physiology of the GI tract, that include a delay in GI transit time, an increase in bile acid release, a decrease in first pass metabolism, and an increase in lymphatic drainage. The co-administration of drugs with food can, in turn, significantly impact drug pharmacokinetics and bioavailability, compared to the fed state, referred to as the food effect.

The FDA and EMA regulatory bodies have supplied guidelines detailing how to design human clinical trials to investigate food effects, requiring fasted and fed subjects. A food effect is classified if the 90% confidence intervals for the ratio of population geometrics means, based on log-transformed data, for either $AUC_{0-\infty}$ or C_{max} are outside of the 80-125% bioequivalences limits, relative to the fasted state [11,19]. A high-fat, high-calorie 'FDA' breakfast is given to the fed state subjects, designed to maximise the potential of a food effect occurring [11]. A positive food effect describes an increase in overall bioavailability, whereas a negative food effect describes a decrease in overall bioavailability.

If a food effect is discovered for an API, it can considerably affect the time, cost, and strategy for bringing a drug to market. The pharmaceutical scientists may need to explore other lead drug molecules, explore formulation types that are food effect-resistant, or add specific instructions for administration in relation to food intake [10]. In fact, a recent analysis found 40% of the drugs licensed between 2010 and 2017 by the EMA and FDA display a significant food effect or contain a label restriction in relation to dosing with or without food in the dossier [10]. These instructions can be inconvenient to the patient and lead to poor adherence.

A number of *in vitro*, *in vivo*, and *in silico* tools have been developed to predict the food effect. However, the effect of food on the absorption of orally administered medicines

can be hard to predict at the early preclinical drug development stage. Biorelevant dissolution media are used to simulate the conditions of the human GI tract, with the development of FaSSGF, FaSSIF, FeSSGF, and FeSSIF.

Despite the growing number of tools, limitations exist in their predictive abilities. Challenges such as supersaturation, and precipitation often leave traditional *in vitro* and *in silico* tools inadequate for predicting the behaviour of drugs after ingestion [227].

4.1.2 Modelling and simulation

Pharmaceutical drug development expenditure and timelines continue to increase, and disruptive innovations are needed to improve the making of therapeutic products. Traditional research and development experiments depend on iterative, trial-and-error investigations, which are time-consuming and can be resource-intensive. In the biopharmaceutics field, there is heterogeneity in the approaches to predicting the food effect across the pharmaceutical field. A number of *in vitro* models based on fasted and fed state simulated biorelevant media have been developed to predict drug performance [94,97,98]. Preclinical *in vivo* animal models, in particular canine and porcine animal species, are used to predict the impact of food on drug absorption in humans [111,114]. Although, distinct limitations exist with these models, and there is no universal, regulatory approved method.

The BCS and BDDCS are used as simple rules for predicting the food effect based on the drug's solubility and permeability/metabolism [67,125,284]. In general, for a high-fat meal, BCS/BDDCS Class I drugs do not show a food effect but there may be an increase T_{max} due to the delay in gastric emptying. BCS/BDDCS Class II drugs, where solubility is the limiting factor for bioavailability, tend to show a positive food effect due to an increase in solubilisation by bile and products of digestion such as lipids. BCS/BDDCS Class III, where permeability is the limiting factor for bioavailability, show a negative food effect due to transporters effects and there is insufficient evidence for Class IV [285]. While this rule of thumb approach is clear and easy to understand, it is poorly predictive.

PBPK modelling is evolving, with multiple applications in predicting drug product performance [286-290]. In the food effect field, PBPK models are used to mechanistically simulate a drug's pharmacokinetic profile under fasted or fed conditions [16,18,132,291]. Extensive physicochemical and physiological data are needed and inputted into the PBPK models, although these data may not be available at early-stage drug development. In addition, biopharmaceutics scientists can spend a considerable amount of time optimising the inputs, and PBPK models perform poorly in the prediction of negative food effects [135].

An integrated approach of linking large amounts of data, with advanced analytical techniques could drive transformation, enable decision making, and translate drug products into the clinic. In recent years, machine learning has become more powerful in its ability to recognise patterns with enhanced automation, and may provide useful insights at the early drug development stage [292]. Machine learning is increasingly being used in pharmaceutical industry in the drug discovery stages [153]. Although, its uptake in pharmaceutics and pharmacokinetics has been slower. Machine learning models can handle large-scale, complex datasets and discern patterns with quick computer speed [154]. Given the highly complex nature of the GI tract, machine learning could potentially offer tools for the prediction of dynamic biopharmaceutics processes.

Previous studies have investigated machine learning in the prediction of the food effect classification on smaller datasets with different methodologies (Bennett-Lenane et al., 2021, Gatarić and Parojčić, 2019, Gu et al., 2007).

The machine learning models used in this thesis are summarised below.

Random forest

Random forest (RF) generates a number of decision trees based on various subsamples of the dataset using a vector of random parameters, independent for each tree. It uses averaging to improve the predictive accuracy and to control overfitting. The error estimate for RF is known as out-of-bag (OOB) error.

An additional tool of RF is that it can provide a *rank of the importance of features*, which can be used to discriminate between input features by observing deviations in the OOB when the values of each individual feature are permitted in the training data. The rank of importance can be provided for binary tasks.

Logistic regression (LR)

Logistic regression is a type of analysis that is used to predict the probability of a classification outcome based on a set of independent variables. It uses the logistic function, also known as the sigmoid function. Despite its name, logistic regression is an example of a classification-based machine learning algorithm.

k-Nearest Neighbors (kNN)

k-nearest neighbor (kNN) is a non-parametric that classifies data based on a similarity measure. It uses the majority vote of its neighbors, with the data being assigned to the class most common among its k-nearest neighbors measured by a distance function.

Support vector machines/support vector regression (SVM/SVR)

A Support Vector Machine (SVM) splits the set of input features by defining a decision boundary. The decision boundary consists of one or more hyperplanes with the largest separation margin from the target variable and support vectors that determines the margin of the decision boundary [293]. SVM can be used for both linear and non-linear datasets. For non-linear datasets, the *kernel* trick projects the data onto a high-dimensional feature space, and then a linear hyperplane is fitted [124]. A Support Vector Regression (SVR) was used in part 2.

AdaBoost (ADA)

AdaBoost is an ensemble learning technique that begins by fitting a regressor on the original dataset then fits additional copies on the same dataset [294]. The weights adjusted according to the output of weak learners. The ultimate learner contains the results of each weak learner. The weak learners' weights and error rate of the samples are key concepts.

Gradient Boosting (GB)

A gradient boosting machine is an ensemble learning that aggregates the output of weak learners [295]. Gradient Boosting can deal with the discrete and continuous values, it has strong robustness to outlier if using the Huber or quantile loss function. The strong connection of each weak learner makes it hard to train the data parallelly and time-consuming.

Extreme gradient boosting (XGB)

XGBoost (eXtreme Gradient Boosting) is an algorithm based on GB. The 'extreme' refers to fast running speed, as the data is stored in blocks and allows for parallel learning. XGB also includes a split-finding algorithm to optimize trees with built-in regularization that reduces overfitting.

Least Absolute Shrinkage and Selection Operator (LASSO)

Least Absolute Shrinkage and Selection Operator (LASSO) is a modification of linear regression that includes a L1 penalty [296]. The loss function is modified to minimize the complexity of the model by adding a penalty (shrinkage quantity) to limit the sum of the absolute values of the model coefficients.

Multi-layer Perceptron (MLP)

Multilayer perceptron (MLP) is a type of artificial neural network algorithm, which consists of at least three layers of nodes: an input layer, a hidden layer, and an output layer. Except for the input nodes, each node is a neuron that uses a nonlinear activation function. MLP uses backpropagation techniques for training. It can distinguish data that is not linearly separable.

4.2 Part 1

Machine learning to predict the effect of food on drugs using classification tasks

4.2.1 Aims

The study aimed to use machine learning technologies to predict the food effect classification (positive versus negative versus no food effect) from an extensive database of over 300 drugs with a diverse set of chemical features and over 20 drug properties or features.

Objectives

- To conduct exploratory data analysis on the dataset [175]
- To perform data cleaning on the dataset
- To use a toolkit of linear and non-linear machine learning algorithms (RF, LR, SVM, and kNN)
- To train and test machine learning tasks
- To achieve an optimal task performance

4.2.2 Materials and methods

4.2.2.1 Compilation of Features/Physicochemical Properties

Drug physicochemical properties were compiled from the literature, mostly from the publication 'BDDCS Applied to Over 900 Drugs' [175] chosen as it is a comprehensive set of drug physiochemical properties. Drug physicochemical descriptors will be referred to here as features. Features not listed in Benet et al. were obtained from PubChem, Lombardo et al [297] or calculated by RDKit (version 2021.03.1). RDKit is an open-source chemoinformatics software that can derive drug molecular information [298]. The tools in RDKit processed the simplified molecular input line entry system (SMILES) of each of the drugs, a line notation for describing chemical structures. The final set of features is listed below (Table 4-1). It should be noted that our approach is based on molecular rather than biopharmaceutical properties which are available at the early stages of drug development. However, dose number and the BDDCS class are often not available until later stages of drug development.

Table 4-1 Features used in the machine learning tasks

Features	Abbreviation	Definition
Biopharmaceutics Drug Disposition Classification System	BDDCS Class	A biopharmaceutics classification system which divides compounds into four classes based on their permeability and solubility.
Maximum strength dose value	MSD	Highest unit dose of the drug (mg)
% Excreted Unchanged in Urine	% U	The proportion of drug unchanged in the body and excreted in the urine
Molecular Weight	MW Drug	Molecular Mass of the drug
pDose (mol/L)	pDose	$-\log_{10}$(Maximum Dose Strength) (molar)

ALOGPS 2.1 solubility	ALOGPS2.1 Sol	Solubility of each drug in its neutral form using Tetko's solubility in water calculated using ALOGPS 2.1
cDose Number (ALOGPS based)	cDose (ALOGPS)	cDose Number calculated using ALOGPS (Maximum Strength Dose (mg) / 250) / (10^ALOGPS2.1) * MWSol
minVSLgS 3-7.5	minVSLgS 3-7.5	Log of the lowest water solubility calculated over the pH range 3–7.5 calculated using VolSurf+
cDose Number (minVSLgS based)	cDose (minVSLgS)	cDose Number calculated by VolSurf+ (Maximum Strength Dose (mg) / 250) / ((10^minVSLgS3-7.5) * MWSol)
Calculated Log Permeability	CLogP	Logarithm of a molecules partition coefficient between *n*-octanol and using the method of Leo
Hydrogen Bond Acceptors	HBA	Electronegative ion or molecule that must possess a lone electron pair in order to form a hydrogen bond
Hydrogen Bond Donors	HBD	Heteroatom with at least one bonded hydrogen
Polar surface area ($Å^2$)	PSA	The sum of the fractional contributions to the surface area of all nitrogen and oxygen atoms calculated using the method of Clark
Rule of Five Violations	Ro5	Number of Lipinski's Rule-of-Five violations which predicts poor absorption or permeation
Polar Surface Drug Area	PSDA	Molecular weight (MW Drug) divided by polar surface area (PSA)
Single bond	Single Bond	Number of single bonds calculated by RDKit
Double Bond	Double Bond	Number of double bonds calculated by RDKit
Aromatic Bond	Aromatic Bond	Number of aromatic bonds calculated by RDKit

Number of atom	No. of atoms	Number of atoms calculated by RDKit
Total atom	Total atom	Total atomic number calculated by RDKit
Average atom	Average atom	Average number of protons = total atom/number of atom calculated by RDKit
Molecularly calculated Log Permeability	MoKa.LogP	MoKa.LogP calculated by Molecular Discovery
Molecularly calculated Log Distribution at pH 7.4	MoKa.LogD7.4	MoKa.LogD7.4 calculated by Molecular Discovery

4.2.2.2 Food effect classification

A dataset was collated from literature sources [175,297]. The food effect was classified by literature searches (no food effect, positive food effect or negative food effect) in humans (shown in Appendix, Table 0-1). The inclusion criteria were orally administered drugs.

Food effect studies for all orally administered products are required in drug development in the form of a human phase I pilot trial and a pivotal food effect study, using fasted and fed state groups [17]. Positive food effect describes an increase in the overall extent (area under the curve [AUC]) of oral drug bioavailability as a result of the intake of the high-fat FDA meal. Conversely, negative food effect describes a decrease in the oral drug bioavailability. AUC was chosen instead of C_{max} as C_{max} data were not always found in the data sources. A positive or negative food effect was classified if the 90% confidence intervals for the ratio of population geometric means, did not fall within the ratio of AUC_{fed}/AUC_{fasted} in reference to the bioequivalence limits of 80-125%, according to the FDA guidance on food-effect bioavailability and fed equivalence [11].

4.3.2.3 Design of the Machine Learning Tasks

The pilot task over-predicted the number of drugs with no food effect and a poor performance was found in the specificity evaluation metric. Therefore, three prediction tasks were considered; i) task one: binary classification of drugs without food effect (F0) versus with food effect (F- & F+), ii) task two: binary classification of drugs with negative food effects (F-) versus positive food effects (F+), and iii) task three: three-class classification of drugs with no food effects (F0) versus negative food effect (F-) versus positive food effect (F+). The classification of the drugs were imbalanced (F0: 235, F-: 44 and F+: 32) and therefore the accuracy of the model may be detrimentally affected [299].

In task one, the dataset was split into two groups; no food effect (F0) versus with food effect (F- & F+), Figure 4-1. The same random states were used throughout for consistency. The dataset was then split into 80:20 with stratification for training and testing using the machine learning algorithms. The majority class (F0) was split into three sub-datasets using sampling without replacement, and individual sub-tasks (sub-task 1, 2 and 3) were trained with 1/3 of the majority class data (F0) and the whole set of the minority class data (F- & F+). The task then predicted the test results according to the majority vote from every individual task. This was performed as the no food effect group (F0) was approximately three-times the size of the combination of food effect (F- & F+).

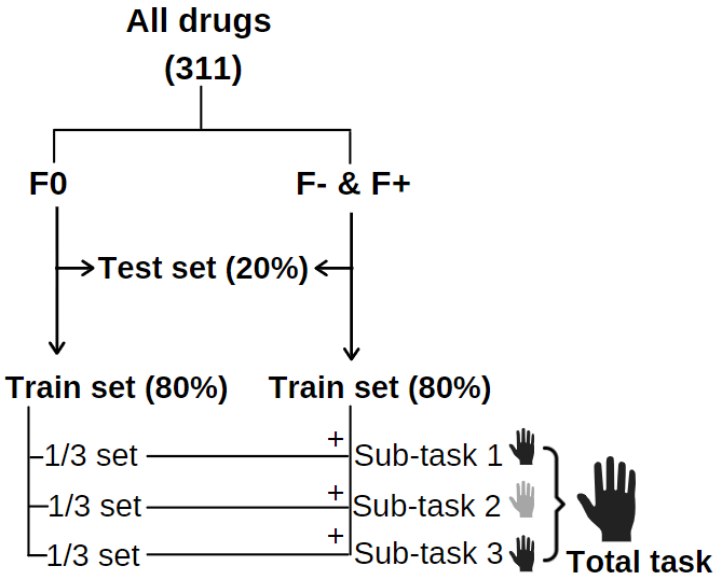

Figure 4-1 Task one; no food effect (F0) & food effect (F+ & F-)

In task two first the drugs with no food effect (F0) were removed. The resulting dataset two contained drugs with a food effect; classified into negative (F-) versus positive (F+) food effect (Figure 4-2). The dataset was then machine learning split into 80:20 with stratification for training and testing and then the machine learning algorithms were trialled.

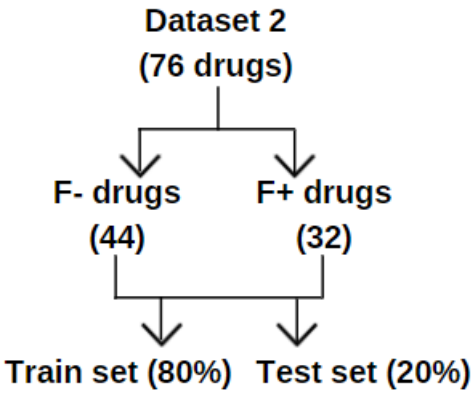

Figure 4-2 Task two showing classification of negative food effect (F-) and positive food effect (F+)

Task three was then built, which is a combination of task one and task two. The process is shown in Figure 4-3. First, a task was tested to distinguish the food effect (F- & F+) versus without food effect (F0), using the majority vote predictions from task one. Then, for the drugs predicted to have a food effect, another task was tested to distinguish between positive food versus negative food effect, using the trained and predictive model, task two.

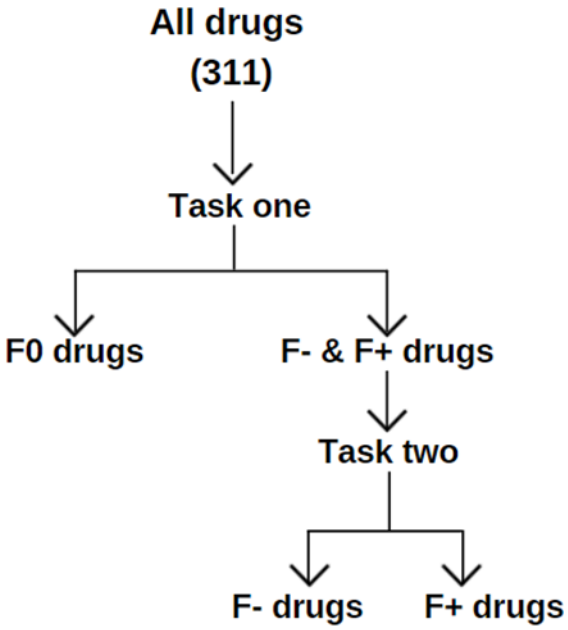

Figure 4-3 Task 3; combination of task one and task two – classifying food effect (F0) negative food effect (F-) and positive food effect (F+)

4.2.2.4 Task implementation

RF, LR, SVM, and kNN algorithms were tested. Other machine learning algorithms, such neural networks, were not chosen as they often perform poorly on datasets with small number of examples per group [300,301]. Tasks were performed and developed using python 3.7 (Python Software Foundation). All of the tasks were performed using the machine learning library for the Python programming language (scikit-learn package, v0.23.2). The tasks were built using classification algorithms with consistent random states throughout. The RF task used 30 trees for each task, with the Gini impurity for the quality of split measurement. No hyperparameters were specified for LR. SVM used a fixed kernel called the radial basis function (RBF). For kNN, k was defined as 3 (n_neighbors=3).

4.2.2.5 Tasks evaluation metrics

All plots were constructed in Python using the Matplotlib, tSNE and Seaborn packages [203,302]. For the evaluation of the tasks, the study used a number of metrics which included: (i) accuracy; (ii) sensitivity; and (iii) specificity.

The confusion matrices capture various performance measurements. The rows represent the real values of the dataset, whereas the columns represent the predicted values by the classifier. False positive (FP) represent the actual negative values that were incorrectly predicted to be positive values. True positive (TP) represent the actual positive values that were correctly predicted to be positive values. True negatives (TN) represent the actual negative values that were correctly predicted to be negative values. False negative (FN) represent the actual positive values that were incorrectly predicted to be negative values. The confusion matrix for binary classification is shown in Figure 4-4.

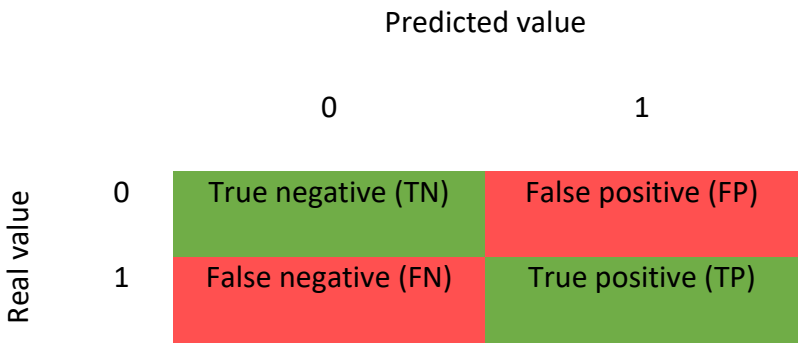

Figure 4-4 Confusion matrix for binary classification

The confusion matrix for three-class classification is shown in Figure 4-5. The TP, TN, FP and FN should be calculated for each individual class (-1, 0 and 1) [303]. For example, for class -1, TP-1 is the number of true positive samples in class -1 correctly classified in class -1. FN-1 in class -1 is the sum of all class -1 that were incorrectly classified as 1 or 0; the sum of $E_{-1,0}$ and $E_{-1,1}$. The FN of each class can be calculated by adding the errors in that

class/row. Whereas, the FP for any predicted class, located in a column, represents the sum of all errors in that column. For example, the FP-1 in class -1 was calculated by FP-1 = E0,-1 + E1,-1. Finally the TN is the sum of all true negative samples that are not in class -1 and are correctly predicted as not in class -1; for TN-1 = TP0 + E0,1, + E1,0 + TP1.

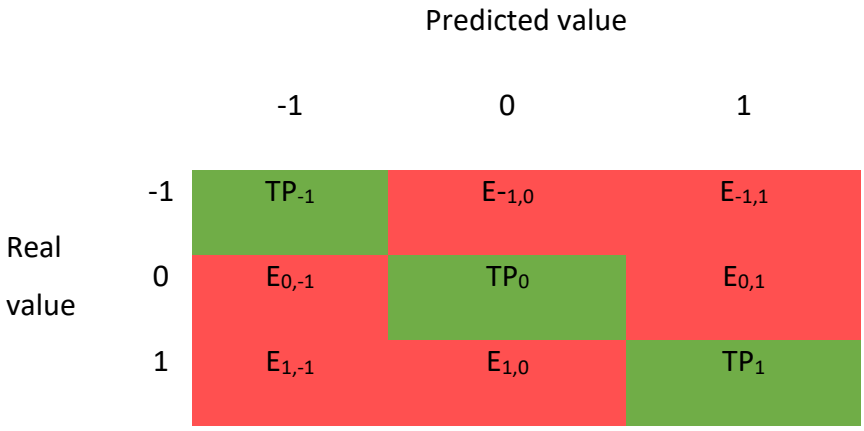

Figure 4-5 Confusion matrix for three-class classification, adapted from [303]

The accuracy refers to the proportion of the number of drug samples, which were correctly predicted, true positives plus true negatives divided by total values, Equation *4-1*. The overall accuracy shows the ability of the machine learning technique to correctly predict the outputs.

Equation 4-1 Accuracy

$$Accuracy = \frac{TP+TN}{TP+FP+FN+TN} = \frac{Correctly\ predicted}{Total\ predicted}$$

Sensitivity and specificity were calculated using the weighted average. Weighted accounts for the class imbalance by computing the average of binary in which each class's score is weighted by its presence in the true data sample [163]. The main aim of the study was to predict the probability of the three classifications; no food effect, a

positive food effect or a negative food effect and the dataset was imbalanced where the majority class was no food effect. Therefore, weighted average was used as the imbalanced class could affect the calculation of the measurement.

Sensitivity, also known as recall, is a measure of the proportion of positive values that were predicted as true positive (TP), Equation *4-2*. There can be a number of positive cases, which will be predicted incorrectly as false negative (FN). A higher value of sensitivity reports a higher value of true positive and a lower value of false negatives, whereas a lower value of sensitivity reports the opposite. Here, the weighted average sensitivity was shown, where the weighted contribution of sensitivity for each label was averaged by the number of samples (Equation *4-3*).

Equation 4-2 Sensitivity

$$sensitivity = \frac{TP}{TP+FN}$$

Equation 4-3 Weighted average sensitivity

$$Weighted\ average\ sensitvity = \frac{1}{\sum|c_i|} \times \sum \frac{TP_{c_i=positive}}{TP_{c_i=positive}+FN_{c_i=positive}} \times |c_i|$$

Specificity is the proportion of negative values, which were predicted as true negatives (TN), Equation *4-4*. There will be a number of negative cases, which were incorrectly predicted as false positives. Specificity could be termed a false positive (FP) rate. A higher value of specificity shows a higher value of true negative and lower false positive rate, in contrast a lower value shows the opposite. Here, the weighted average specificity was used, where the weighted contribution of specificity for each label was averaged by the number of samples (Equation *4-5*).

Equation 4-4 Specificity

$$specificity = \frac{TN}{TN + FP}$$

Equation 4-5 Weighted specificity

$$Weighted\ average\ specificity = \frac{1}{\sum|c_i|} \times \sum \frac{TN_{c_i=positive}}{TN_{c_i=positive} + FP_{c_i=positive}} \times |c_i|$$

4.2.2.6 Feature importance

Next, feature importance was also assessed using RF. RF provided a rank of the importance of various features to perform the classification tasks, with a computationally light algorithm compared to other methods [304]. The feature importance was performed for task one and task two.

4.2.3 Results

4.2.3.1. Exploratory Data Analysis

An exploratory data analysis was performed prior the machine learning tasks to explore the distribution of the features and the food effect classifications. An imbalanced dataset was shown where drugs classified with no food effect made up 75.6% of the dataset, whereas 24.4% of the drugs showed a food effect (Figure 4-6). In addition, for the drugs with a food effect, a further imbalanced dataset was found, with 57.9% showing a negative food effect and 42.1% showing a positive food effect. Drugs used in this study cover a diverse chemical space showing a broad range of physicochemical properties; maximum strength dose value 0-1200 mg, MW Drug 100- 850 and cLogP -7 to 9.

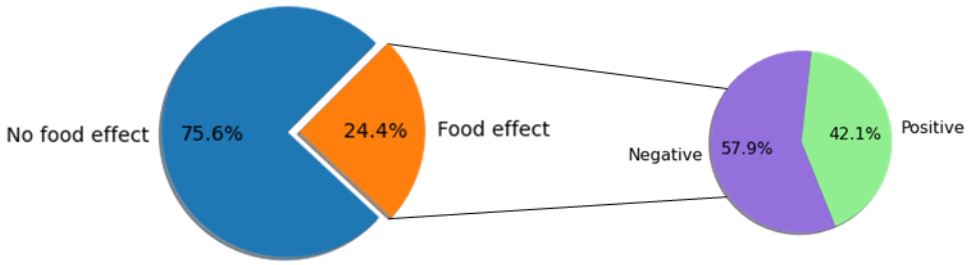

Figure 4-6 Food effect classification

Figure 4-7 shows a representation of the dataset in the chemical space of the over 600 orally approved drugs from Benet et al. The represented drugs are shown in shades of blue, whereas the not classified drugs are shown in grey, reflecting that the drugs in the dataset are from a broad chemical space.

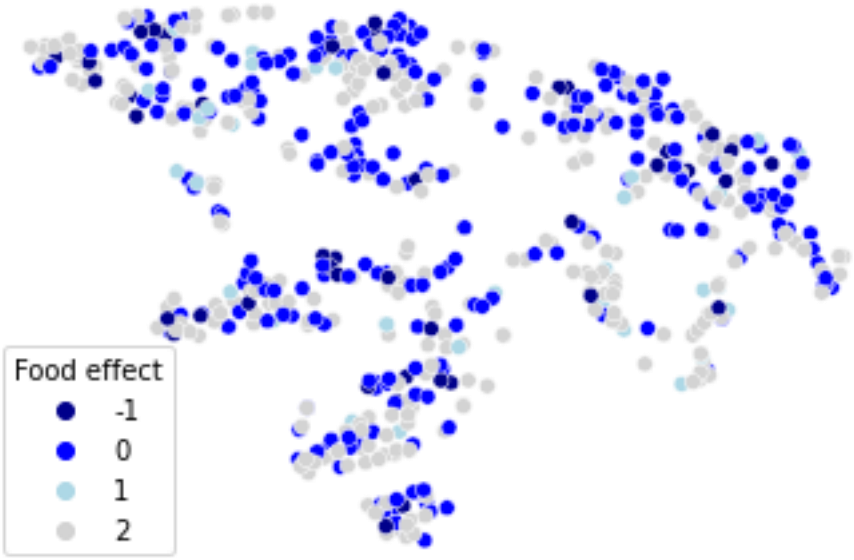

Figure 4-7 A t-distributed stochastic neighbour embedding (tSNE) scatterplot of drugs classified by food effect classification; negative food effects (-1), no food effect (0), positive food effect (1) and not classified (2)

Figure 4-8 shows that there is no food effect for the majority of drugs in all BDDCS classes and reflects Figure 4-6. showing that the majority of the drugs showed no food effect.

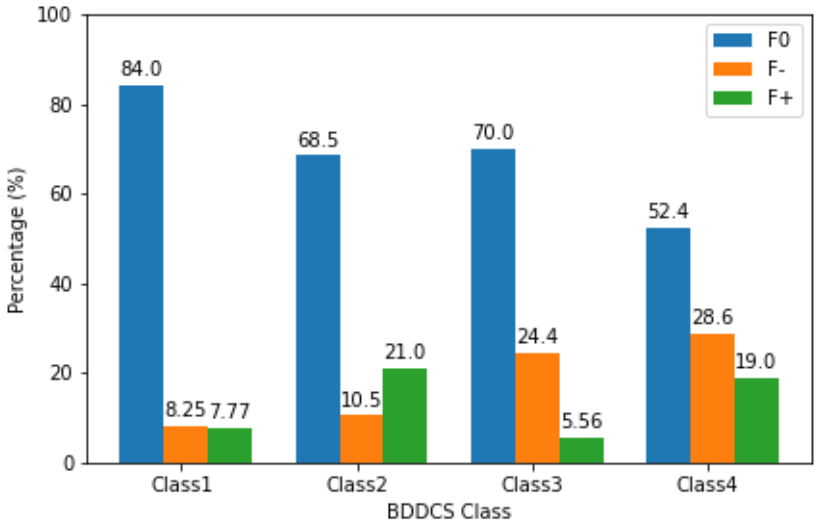

Figure 4-8 Distribution of drugs in the feature sets by BDDCS Class and food effect classification

Pearson correlation between the features were assessed and is shown in Figure 4-9. Interestingly, a moderate correlation was seen between % Excreted Unchanged in Urine (% U) and the BDDCS Class (0.71). MoKa.LogP was strongly correlated with MoKa.LogD74 (0.8), cLogP (0.91), ALOGPS 2.1 sol (-0.74). For the structural features, significant correlations were seen between the molecular weight of the drug (MW Drug) and total atom (0.96), no. of atom (0.95), single bond (0.83) and rule of 5 (Ro5) (0.73). In addition, strong correlations were seen between polar surface area (PSA) and hydrogen bond donor (HBD) (0.8) and hydrogen bond acceptor (0.87).

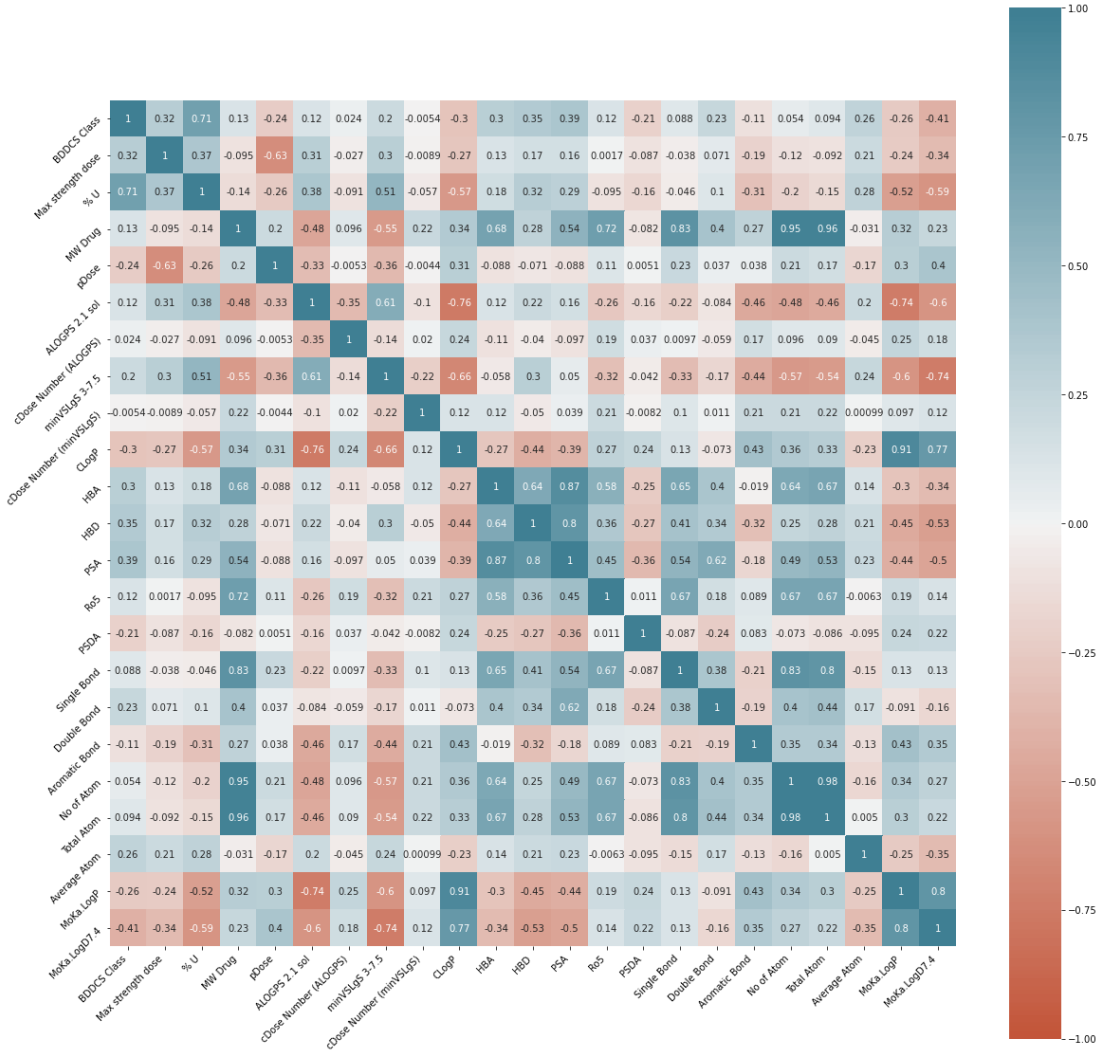

Figure 4-9 Correlation plot between the features

4.3.3.2. Pilot study

Here, this approach to building a predictive model, first utilised a toolkit of machine learning algorithms with a standard machine learning pipeline. Here, the data was randomly split 80:20 into training and testing sets, respectively, with stratification where the testing set used blind data to test the robustness of the trained model from the dataset. Using this approach resulted in the task over predicting drugs with no food effect, shown in Figure 4-10. The confusion matrices showed that the majority of drugs were predicted as no food effect. While high accuracies and sensitivities were reported, the specificities were low (below 45%).

(A)

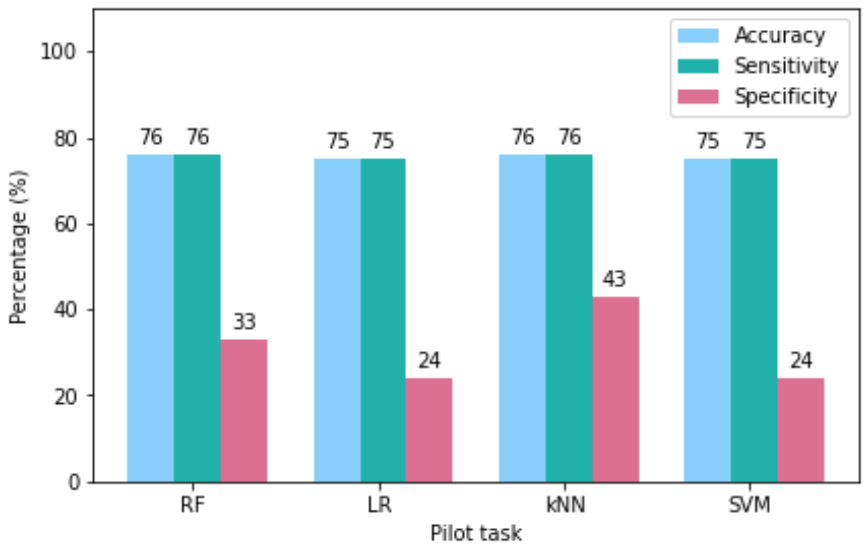

(B)

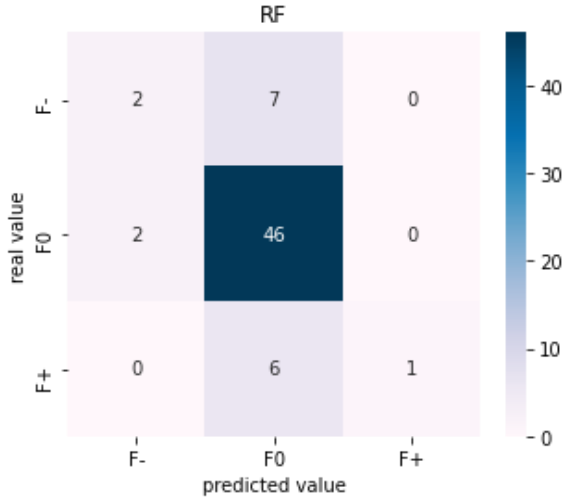
RF
real value
F-
F0
F+
2
7
0
2
46
0
0
6
1
F-
F0
F+
predicted value
40
30
20
10
0

(C)

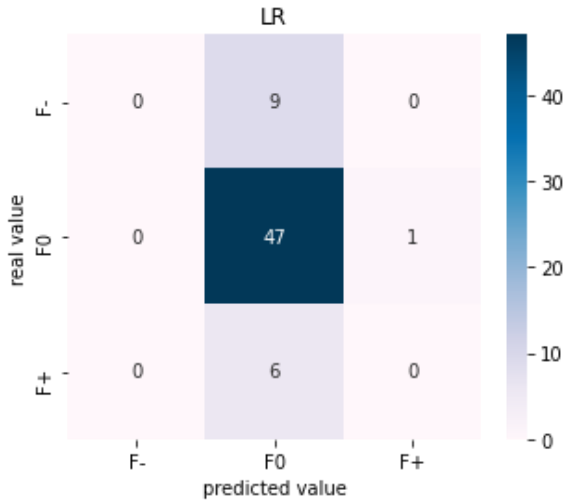
LR
real value
F-
F0
F+
0
9
0
0
47
1
0
6
0
F-
F0
F+
predicted value
40
30
20
10
0

(D)

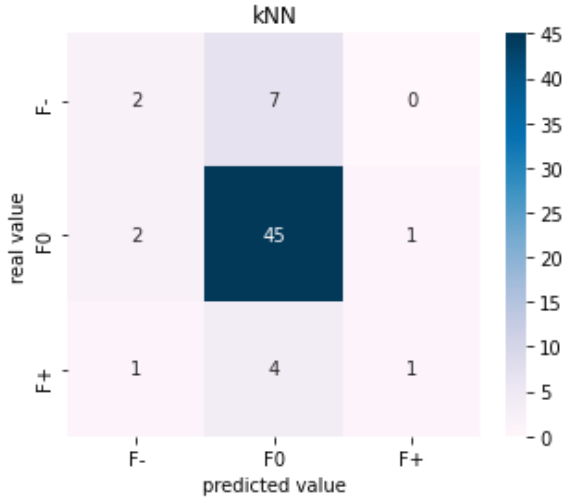
kNN
real value
F-
F0
F+
2
7
0
2
45
1
1
4
1
F-
F0
F+
predicted value
45
40
35
30
25
20
15
10
5
0

(E)

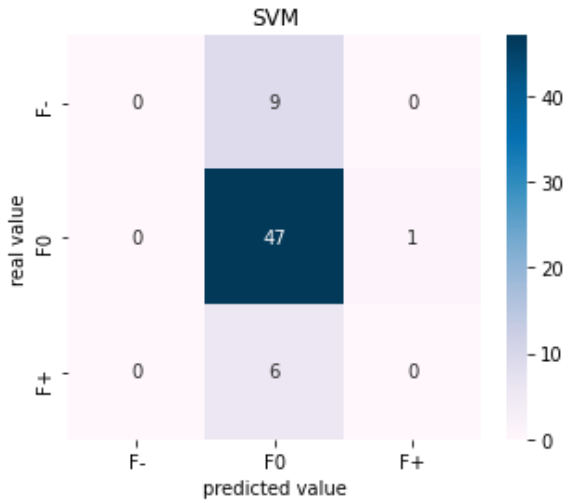

Figure 4-10 Predictive performance of the pilot task (F0 versus F- versus F+]) in (A) bar plot and confusion matrices of (B) RF, (C) LR, (D) kNN, and (E) SVM

4.2.3.3 Task Analysis

Bespoke tasks were developed with the aim of surpassing the predictions obtained from the pilot task and to leverage the characteristics of the dataset. The first task, referred to as task one, sought to determine how well a model can distinguish between no food effect (F0) vs food effect (F+/-) and hence a binary classification task was modelled. In addition, given that the dataset consisted of three times as many F0 drugs than F+/- drugs, three small sub-tasks were modelled containing a third of the F+/- samples. Consequently, three different models were developed on each sub-task training dataset before being applied to the test dataset, which was consistent for each sub-task. A majority vote was taken from the three smaller sub-tasks. Figure 4-11 presents the findings of task one, binary classification of F0 vs (F- & F+), where the results focus on the total task. The training accuracy was 100%. SVM showed the highest accuracy and sensitivity of 75%, although the specificity was low at 23%. The SVM confusion matrix reported that the drugs were over-predicted as no food effect. Overall RF performed the best with an accuracy and sensitivity of 70% and a specificity of 71%.

(A)

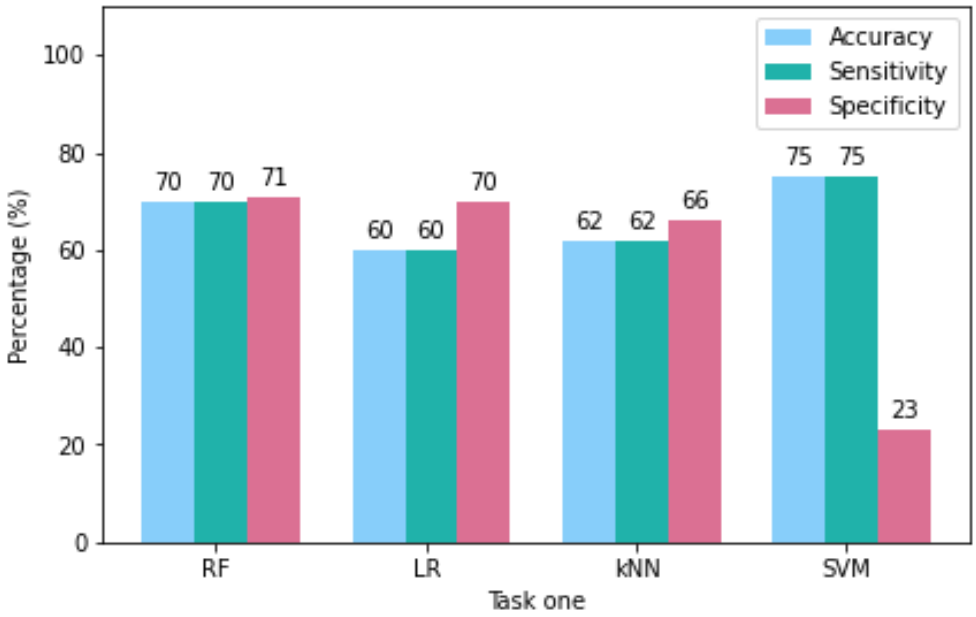
Accuracy
Sensitivity
Specificity
Percentage (%)
100
80
60
40
20
0
70 70 71
60 60 70
62 62 66
75 75 23
RF
LR
kNN
SVM
Task one

(B)

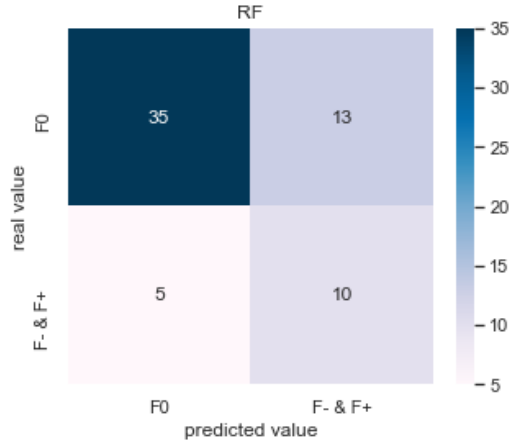
RF
F0
F- & F+
real value
35
13
5
10
F0
F- & F+
predicted value
35
30
25
20
15
10
5

(C)

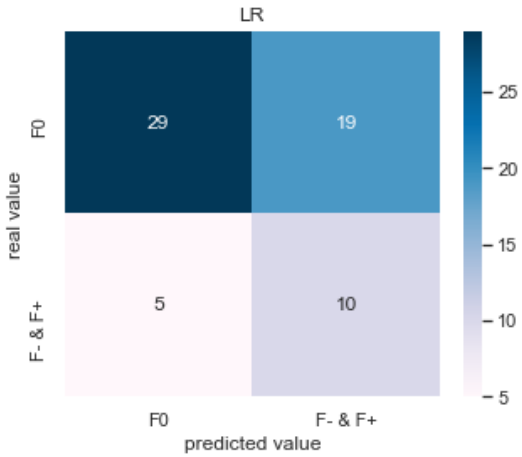
LR
F0
F- & F+
real value
29
19
5
10
F0
F- & F+
predicted value
25
20
15
10
5

(D)

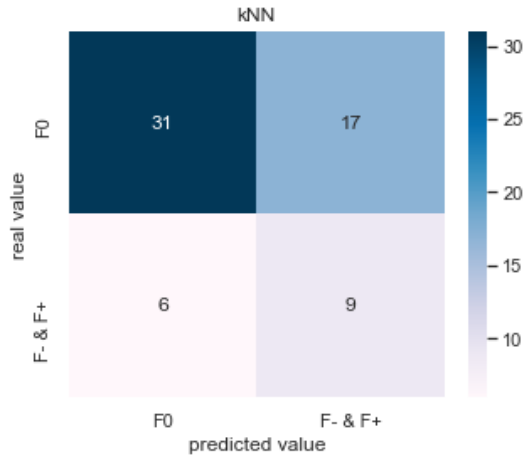

(E)

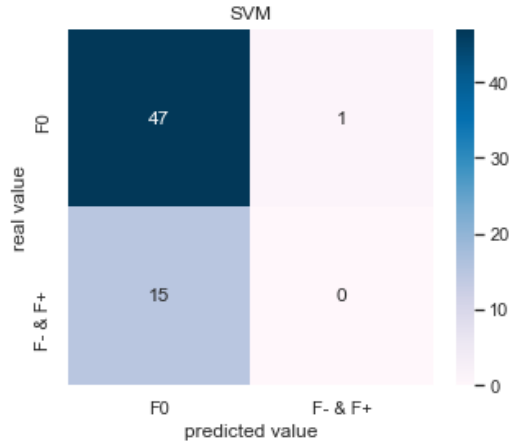

Figure 4-11 Predictive performance of Task one (F0 versus [F-/+]) in (A) bar plot and (B) confusion matrices of (B) RF, (C) LR, (D) kNN, and (E) SVM

The second task investigated how well the model was able to distinguish between F+ versus F-, also a binary classification task. Figure 4-12 shows the evaluation results of task two (F- versus F+). The training accuracy was 100%. The accuracies, sensitivities and specificities of the binary classification reached 80%, whereas the specificity was lower at 76% for RF, LR and kNN. SVM on the other hand, showed a lower performance and achieved 60% for the accuracy and sensitivity and 40% for the specificity.

(A)

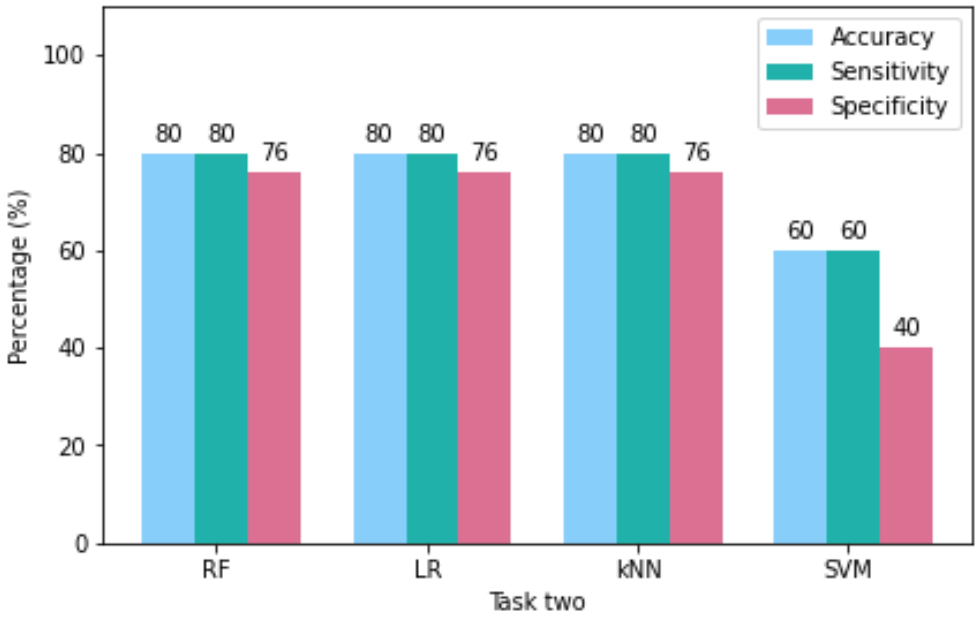
Accuracy
Sensitivity
Specificity
Percentage (%)
100
80
60
40
20
0
80 80 76
80 80 76
80 80 76
60 60 40
RF
LR
kNN
SVM
Task two

(B)

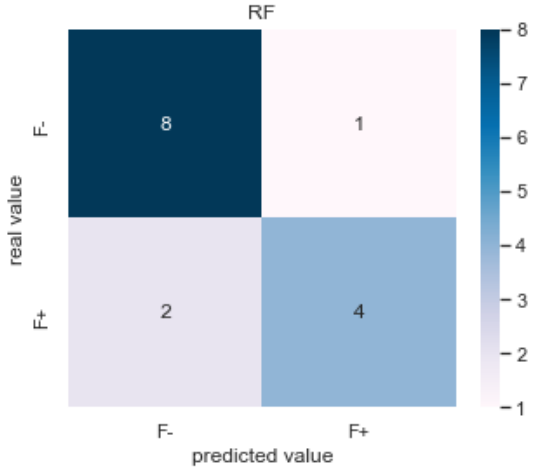
RF
real value
F-
F+
8
1
2
4
F-
F+
predicted value
8
7
6
5
4
3
2
1

(C)

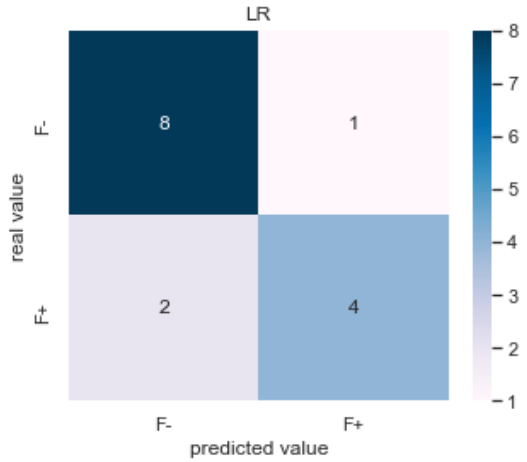
LR
real value
F-
F+
8
1
2
4
F-
F+
predicted value
8
7
6
5
4
3
2
1

(D)

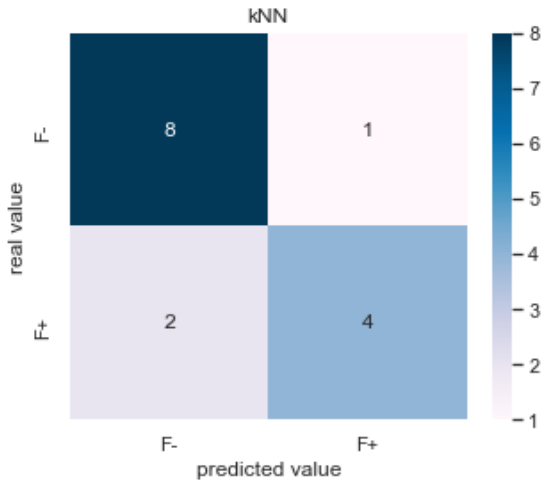

(E)

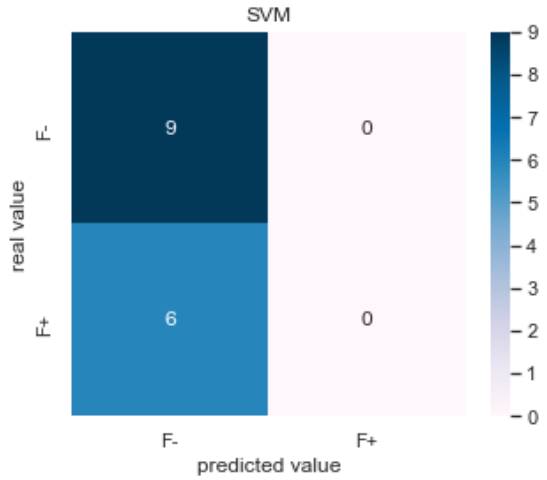

Figure 4-12 Predictive performance of Task two (F0 vs [F-/+]) in (A) bar plot and (B) confusion matrices of (B) RF, (C) LR, (D) kNN and (E) SVM

The third task was a sequential task, an amalgamation of task ones and two, chosen as both tasks yielded high accuracies in comparison to the baseline task. First, the task distinguishes between F0 versus F+/-. Next, based on the drugs predicted have an effect, the task then predicted whether the drugs will have a positive or negative effect. The final accuracy will be compared to the original ground truth. Figure 4-13 showed the results of task three, F0 versus F- versus F+, which is a multiple classification task. For RF, the task reported a 70% accuracy and sensitivity and a slightly higher specificity at 71%. This sequential methodology yielded a higher specificity than the pilot task (Figure 4-10). LR and kNN showed poorer performance. SVM, on the other hand, showed good

accuracy and sensitivity of 75%, but however the specificity was low at 23% and showed the same performance as the pilot task (Figure 4-10).

(A)

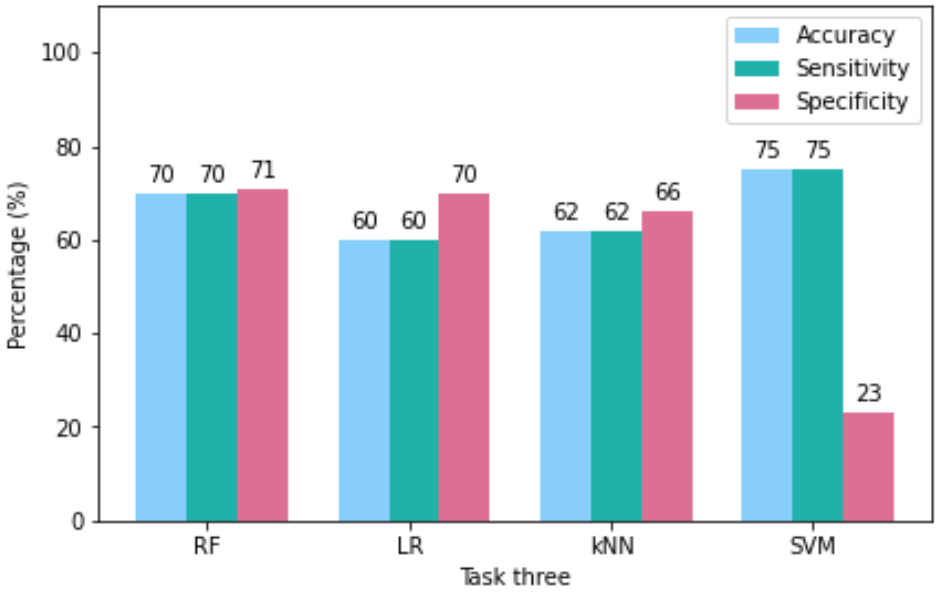

(B)

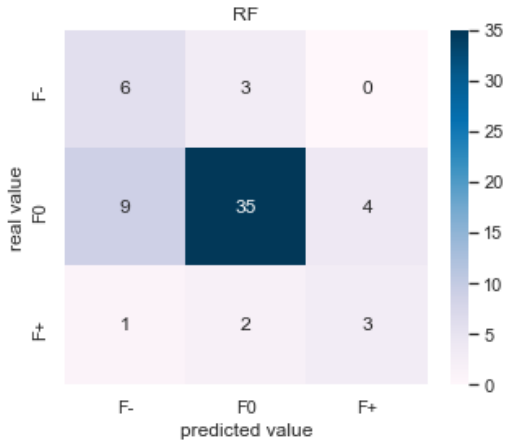

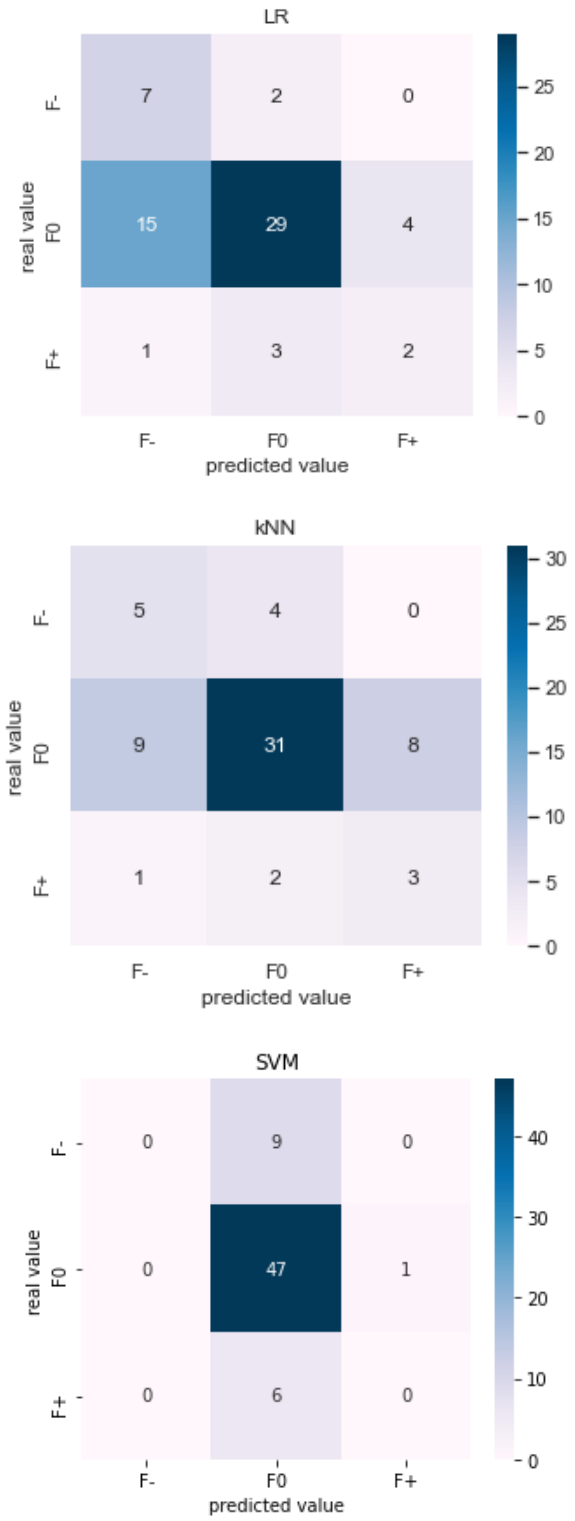

Figure 4-13 Predictive power of Task three (F0 versus F- versus F+) in (A) bar plot and (B) confusion matrices of (B) RF, (C) LR, (D) kNN, and (E) SVM

4.2.3.4 Feature importance

Feature importance analyses were performed to identify key features in task one and task two. As shown in Figure 4-14 and Figure 4-15, certain features were calculated by RF to be more important than others in the building of the prediction tasks one and two. Interestingly, the most important features were different for task one and task two. For task one, shown in Figure 4-14, cDose were the most important features (minVSLgS based then ALOGPS based). In task two, the most important feature was cDose (ALOGPS based) then PSDA, as shown in Figure 4-15.

These are all features calculated by *in silico* software. This could be useful in deciding which features should be determined in early-stage drug development. The least important feature in both tasks were Ro5, determined by the Lipinski's rule of five, and the BDDCS class feature.

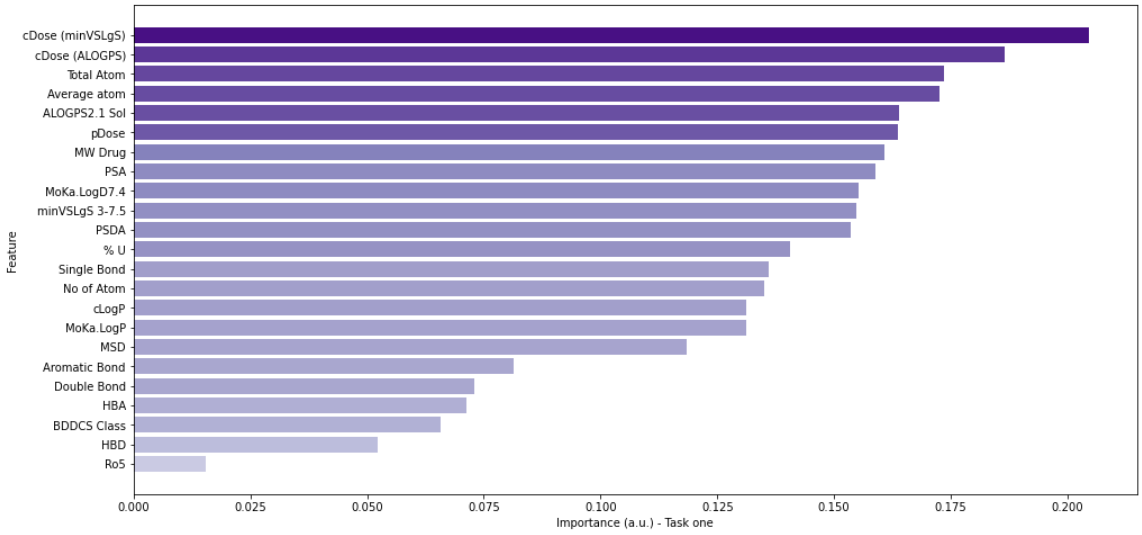

Figure 4-14 Feature importance analysis for 23 features calculated from the feature set used in task one. The ranking function reflects the importance of each feature in the predictive model.

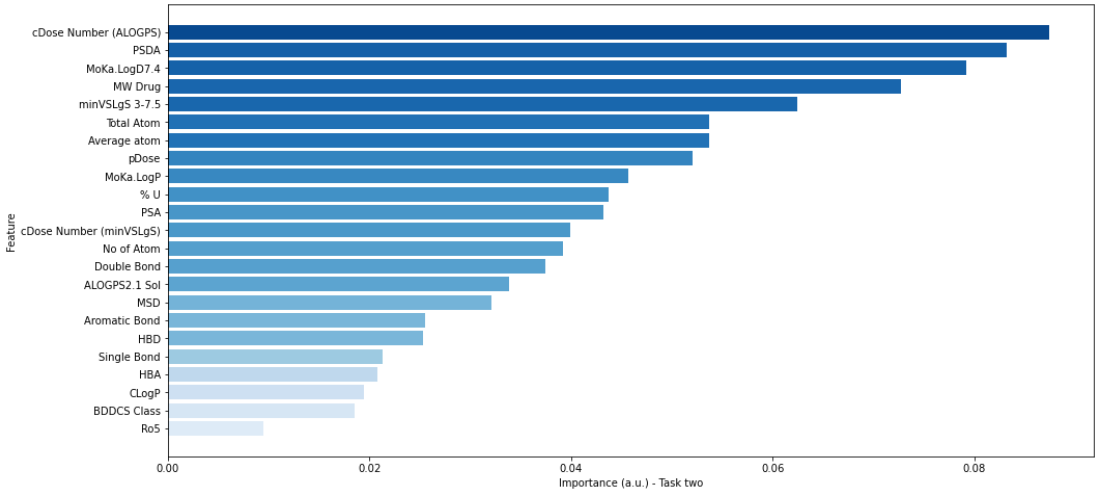

Figure 4-15 Feature importance analysis for 23 features calculated from the feature set used in task two. The ranking function reflects the importance of each feature in the predictive model.

4.3 Part 2
Machine learning to predict the effects of food on drugs using regression tasks

4.3.1 Aims

- To predict the food-mediated percentage changes between the fasted and fed state to key pharmacokinetic properties (AUC and C_{max}).

Objectives

- To conduct exploratory data analysis on dataset [176]
- To perform data cleaning on the feature sets – RDKit, ADMET and MFP feature sets
- To use a toolkit of machine learning algorithms – ADA, GB, XGB, kNN, LASSO, RF, MLP, and SVR
- To train and test machine learning tasks
- To achieve an optimal task performance

4.3.2. Materials and methods

4.3.2.1 Food-mediated changes to AUC and C_{max}

A dataset was collated from the literature [176] with 311 drugs. The dataset contained the SMILES and food-mediated changes to the AUC and C_{max} as a percentage change (%) from the fasted state to the fed state. The two outputs were the food-mediated percentage change (%) to the AUC and C_{max}. Regression tasks were used to predict the quantitative values. Following data cleaning, 291 drugs remained for the prediction of C_{max} and AUC.

4.3.2.2 Compilation of Features/Physicochemical Properties

Molecular descriptors were generated using the SMILES of each drug. Three different packages were used to derive features: (i) RDKit, (ii) Morgan Fingerprint (MFP), and (iii) ADMET Predictor. RDKit generated 201 physicochemical property-based features (version 2021.03.1) [298]. MFP (radius 2, 2048 bits) is a popular chemical descriptor package used for small molecules and provided a 2048 features based on multiple substructures around each atom in a molecule [305]. ADMET Predictor is a commercially available software and physiochemical property features (version 9.8.3). The ADMET properties are listed in Table 0-2 (Appendix). Three feature sets were created: (i) ADMET, (ii) MFP + RDKit, and (iii) ADMET + MFP + RDKit.

4.3.2.3 Data cleaning

The dataset contained several missing values and outliers. The outliers were values of C_{max} and AUC of over 600%. Together with the null values, the outliers were deleted. The following steps were performed to clean the feature values. First, some features of the ADMET were not numeric, these data also cannot be used. Here, the LabelEncoder function transferred the string variables into integer numbers (ECCS_Class and S+Cl_Mech). The ‘S+Acidic_pKa’ feature and the ‘S+Basic_pKa’ contained multiple

numbers and to include them as inputs 'S+Acidic_pKa' feature was split into four and 'S+Basic_pKa' was split into seven. The 'ADMET_Code' feature consisted of 45 properties, it was therefore split into 45 columns, each representing one of the properties, if the drug possessed this property, it was allocated a 1, if not, it was allocated a 0.

The MFP did not need to be scaled. RDKit and ADMET was scaled using MinMaxScaler to rescale the value to between 0 and 1 as a negative float number cannot be trained in Python.

SelectKBest was used as a feature selection algorithm to find the 15 best features [306].

4.3.2.4 Machine learning algorithms

Tasks were performed and developed using python 3.7 (Python Software Foundation). All of the tasks were performed using the machine learning library for the Python programming language (scikit-learn package, v0.23.2). AdaBoost (ADA), gradient boosting (GB), extreme gradient boosting (XGB), random forest (RF), k nearest neighbour (kNN), least absolute shrinkage and selection operator (LASSO), multilayer perceptron (MLP), support vector machine regressor (SVR) were used. The dataset was split into training and testing (85:15). A grid search was performed using GridSearchCV function and the hyperparameters used are listed in Table 0-3 (Appendix).

4.3.2.5 Task evaluation metrics

All plots were constructed in Python using the matplotlib and Seaborn package [203,245]. R2 score is the residual between actual and predicted values. The equation is shown as Equation 4-6.

Equation 4-6 R2 score

$$R^2 = 1 - \frac{\sum_{i=1}^{n_{samples}}(y_i - \hat{y_i})^2}{\sum_{i=1}^{n_{samples}}(y_i - \bar{y})^2}$$

where $\hat{y}$ is the predicted value of the i-th sample, y_i is the corresponding actual value and $\bar{y}$ is the mean value of all the actual values. The closer the r2 score to 1, the better performance of the model. A negative r2 means that the model's predictions are worse than a constant function, which predicts the mean of the actual values.

The explained variance is a measure of the proportion of the variability of the prediction of a machine learning model and is represented as Equation 4-7.

Equation 4-7 Explained variance

$$explained_{variance(y,\hat{y})} = 1 - \frac{Var\{y, \hat{y}\}}{Var\{y\}}$$

where Var is the variance, $\hat{y}$ is the estimated target value and y is the actual value. If the error of prediction is unbiased, the r2 and explained variance will be the same.

Mean square error (MSE) is the average of the squared difference between the actual and the predicted values. It measures the variance of the residuals and is represented as Equation *4-8*.

Equation 4-8 Mean square error (MSE)

$$MSE = \frac{1}{n_{samples}} \sum_{i=1}^{n_{samples}} (y_i - \hat{y})^2$$

Mean absolute error (MAE) is the average error between the predicted values and actual values. It measures the average of the residuals and is represented as Equation *4-9*.

Equation 4-9 Mean absolute error (MAE)

$$MAE = \frac{1}{n_{samples}} \sum_{i=1}^{n_{samples}} |y_i - \hat{y}|$$

The closer the MSE and MAE are to 0, the better the model is.

4.3.3 Results

4.3.3.1 Exploratory Data Analysis

Figure 4-16 shows the target output values before and after data cleaning.

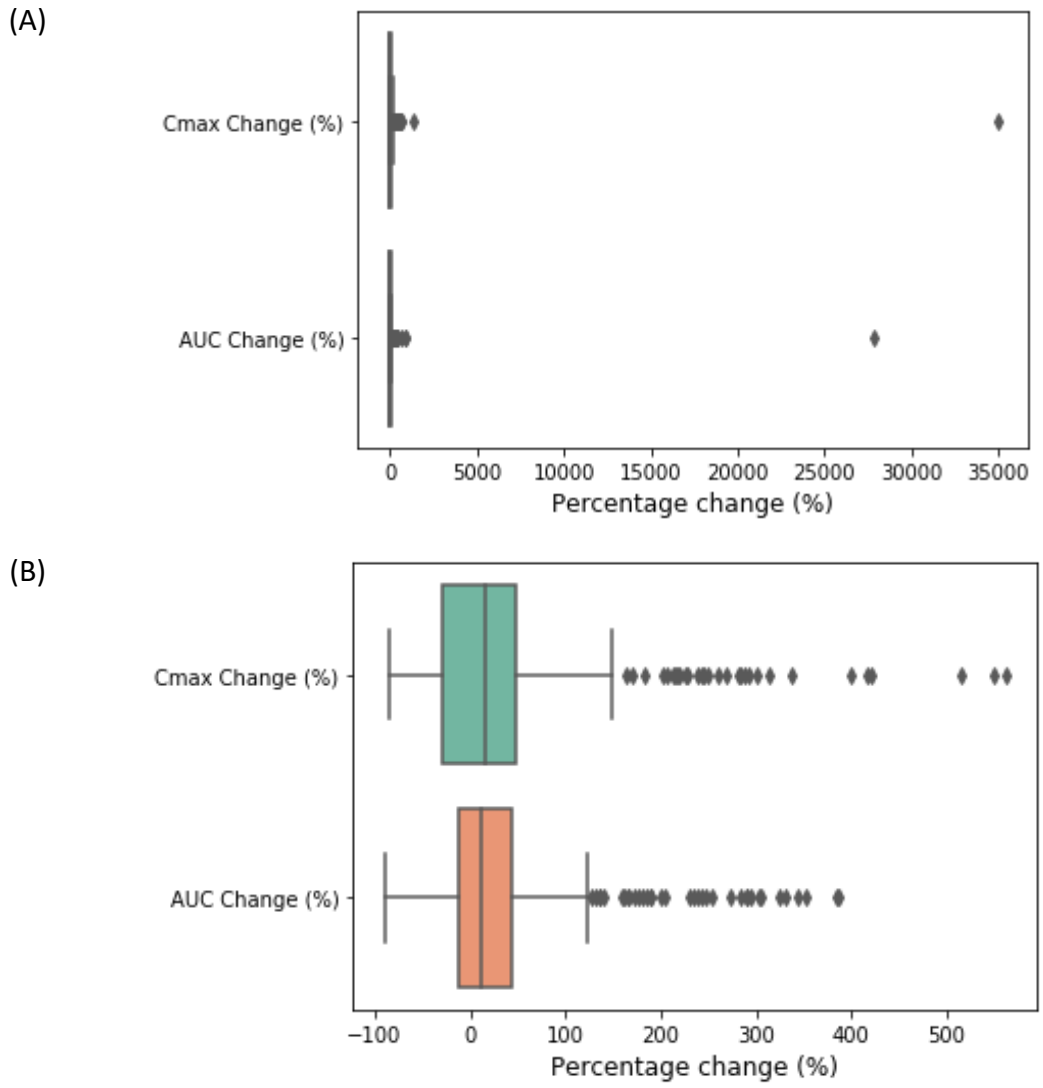

Figure 4-16 Boxplots showing the distribution of target outputs (a) before, and (b) after data cleaning

4.3.3.2 Predictive performance

4.3.3.2.1 Food-mediated changes to AUC

ADMET feature set

Figure 4-17 shows the performance metrics for the prediction of the food-mediated changes to AUC. Most of the machine learning algorithms report negative r2 and explained variance, except for XGB and RF. XGB was the best performing algorithm, reporting a r2 and explained variance of 0.13. In addition, the MSE and MAE were consistently high. The lowest MSE was found for the XGB machine learning algorithm.

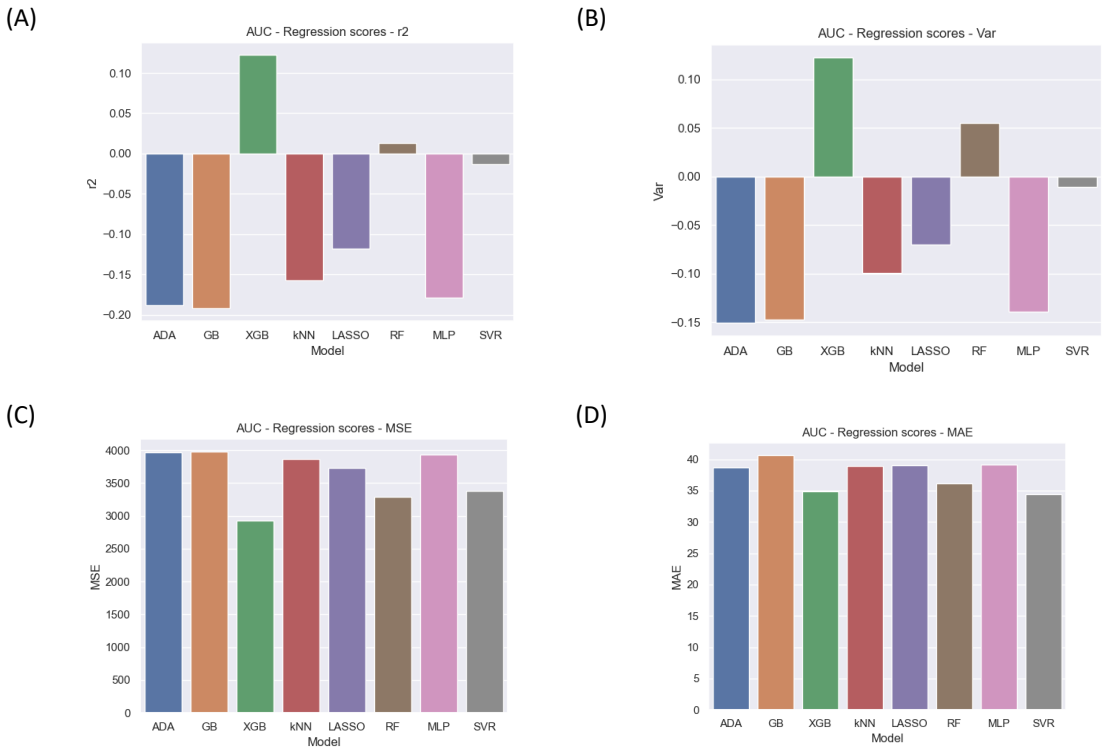

Figure 4-17 Predictive performance for food-mediated changes to AUC with ADMET feature set; (A) r2 score, (B) explained variance, (C) MSE, and (D) MAE.

MFP + RDKit feature set

Figure 4-18 reports the r2, explained variance, MSE, and MAE for the predicted food-mediated changes to Cmax. The majority of the models reported a positive r2 score, except for RF. Overall, LASSO was the best performing machine learning algorithm, followed by SVR, then MLP. The other machine learning algorithms reported a r2 score less than 0.1. The MAE values were similar for all of the machine learning algorithms. As shown by Figure 2C, LASSO reported the best MSE score.

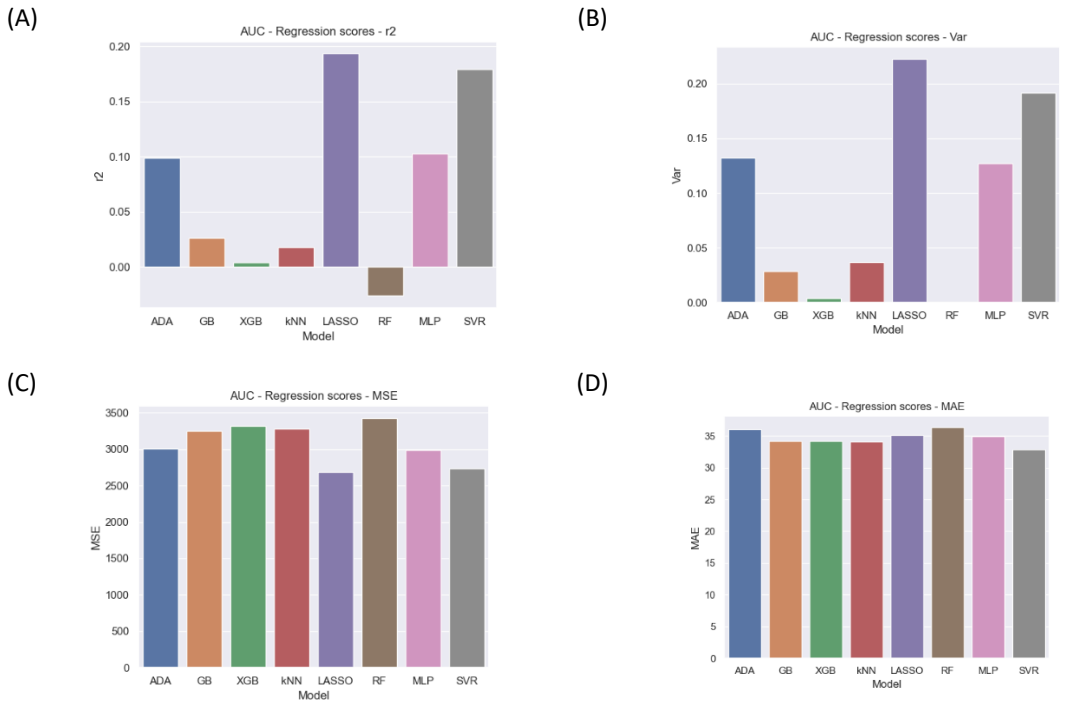

Figure 4-18 Predictive performance for food-mediated changes to AUC with MFP + RDKit feature set; (A) r2 score, (B) explained variance, (C) MSE, and (D) MAE.

ADMET + MFP + RDKit feature set

Figure 4-19 shows the performance metrics using the combined feature sets, that used the ADMET, MFP, and RDKit feature sets. Interestingly, ADA and RF showed negative r2 scores, whereas the other machine learning algorithms showed positive r2 scores. Using

the MFP feature sets, ADA and RF showed positive scores. Therefore, adding the ADMET and RDKit scores resulted in a worse performance. Overall, MLP performed the best, with a r2 and explained variance of 0.28 and the lowest MSE score.

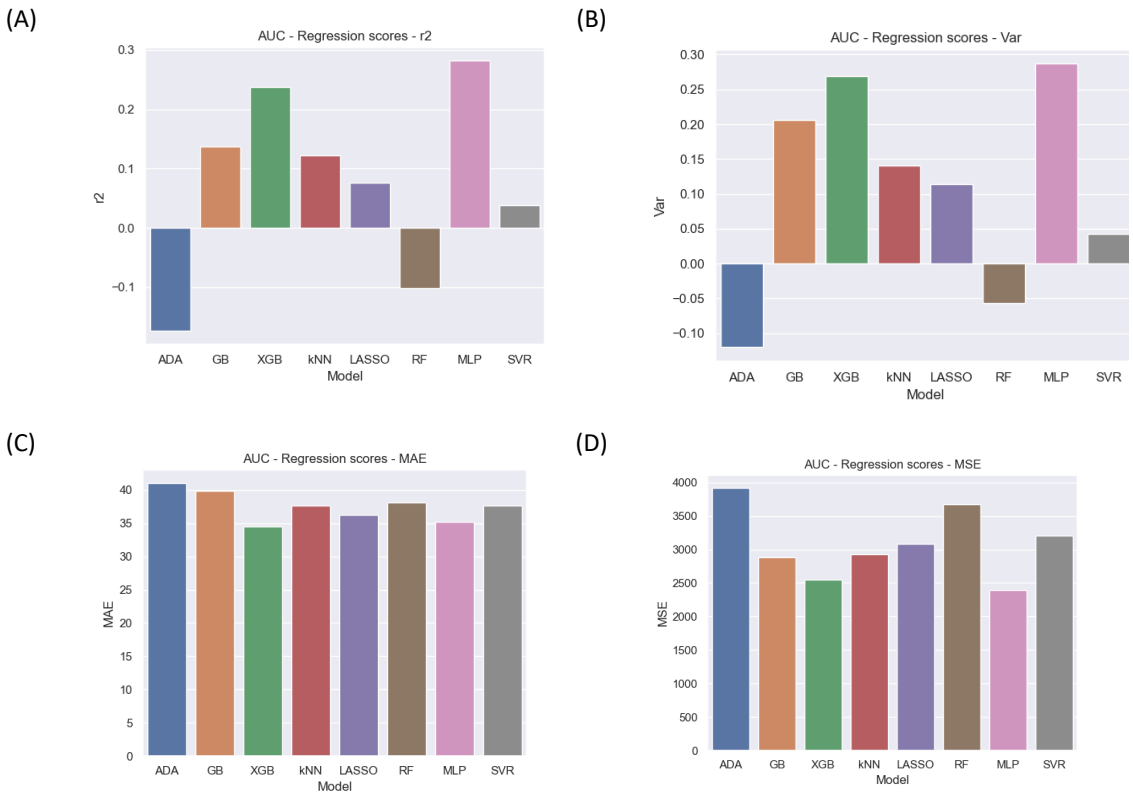

Figure 4-19 Predictive performance for food-mediated changes to Cmax with ADMET + MFP + RDKit feature set; (A) r2 score, (B) explained variance, (C) MSE, and (D) MAE.

4.3.3.2.2 Food-mediated changes to Cmax

ADMET feature set

Figure 4-20 reports the food-mediated changes to Cmax using the ADMET feature set. Low scores were found for the r2 and explained variance, with ADA showing the lowest r2 score of -0.3, and XGB showing the highest score of 0.25. RF and SVR also showed

positive score, although both r2 scores were below 0.05. The MSE and MAE are high, with the best MSE found for the XGB machine learning algorithm.

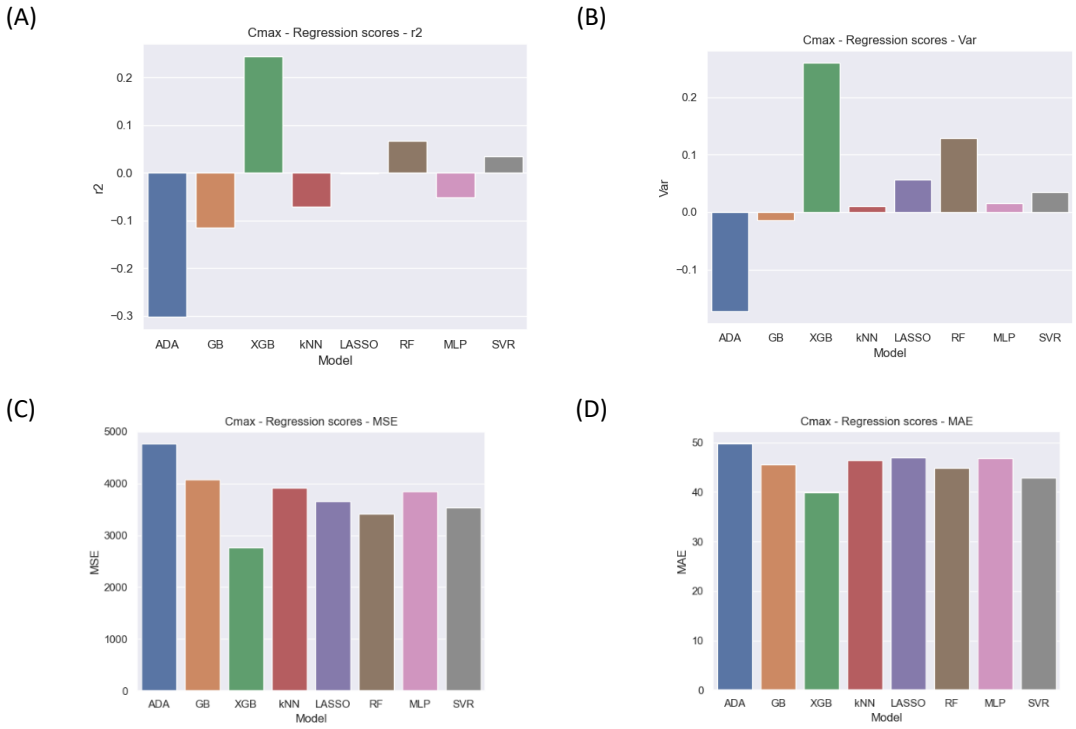

Figure 4-20 Predictive performance for food-mediated changes to AUC with ADMET feature set; (A) r2 score, (B) explained variance, (C) MSE, and (D) MAE.

MFP + RDKit feature set

Figure 4-21 showed the r2, explained variance, MAE, and MSE for the machine learning algorithms for the prediction of food-mediated changes to Cmax using the MFP + RDKit feature set. ADA was the highest scoring machine learning algorithm

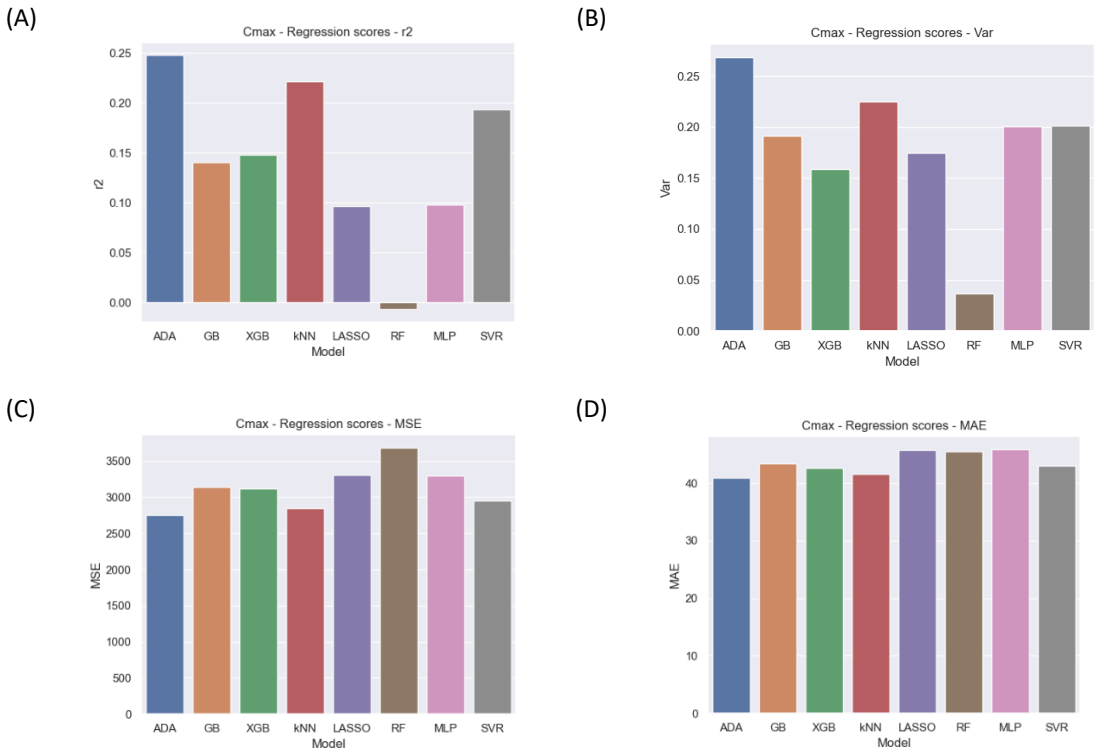

Figure 4-21 Figure 5 Predictive performance for food-mediated changes to Cmax with MFP + RDKit feature set; (A) r2 score, (B) explained variance, (C) MSE, and (D) MAE.

ADMET + MFP + RDKit feature set

The performance metrics for the prediction of the food-mediated changes to Cmax are reported in Figure 4-22. ADA performed poorly, showing a negative r2 score. The highest performing machine learning algorithm was XGB, although the r2 was low at 0.11. Here, combining the MFP with ADMET and RDKit resulted in worse performance metrics than the MFP + RDKit feature set.

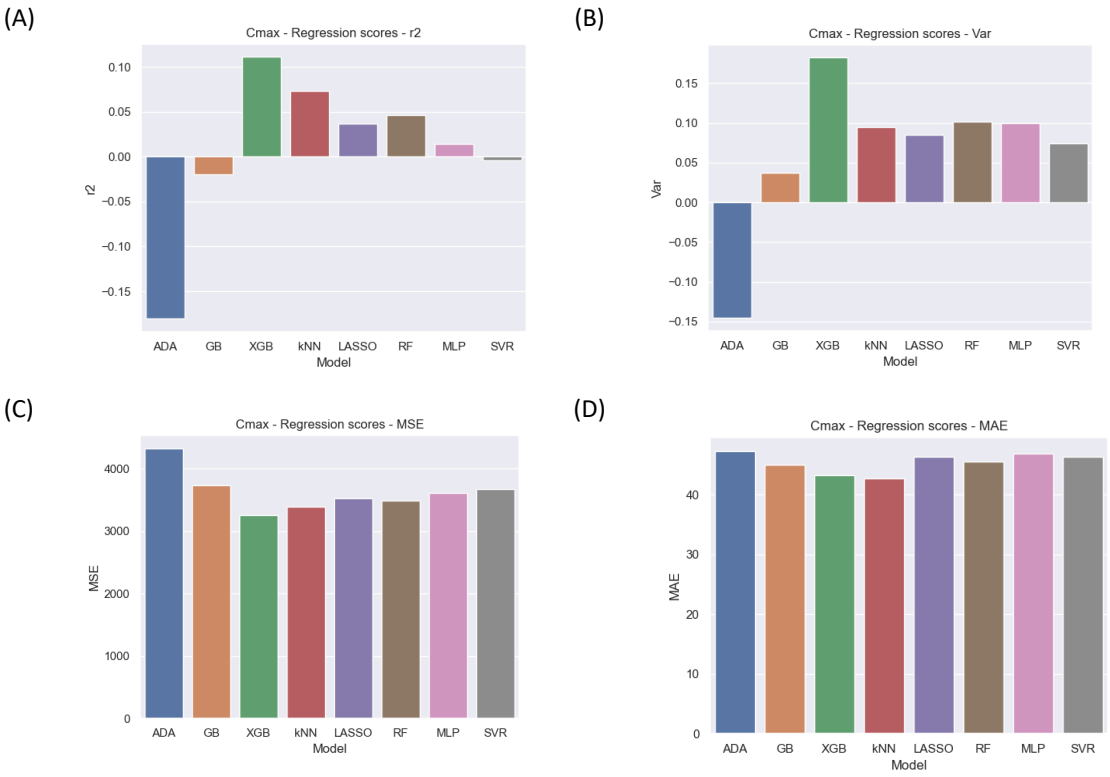

Figure 4-22 Predictive performance for food-mediated changes to Cmax with ADMET + MFP+ RDKit feature set; (A) r2 score, (B) explained variance, (C) MSE, and (D) MAE

4.4. Discussion

Prediction of the food effect is one of the key requirements for estimating the suitability of potential drug candidates. Presence of a food effect for a medicine complicates the process of bringing a drug product to market and can affect the safety and efficacy profile of the drug. Two machine learning projects were conducted. For part one and part two, the feature sets included *in silico* structural and activity data of small molecule drugs. For part one, the evaluation metrics of the tasks were the confusion matrices and the prediction metrics. The RF tasks performed the best overall compared to LR, kNN and SVM, suggesting that an ensemble-based method was needed for strong predictive performance. Importantly, the training accuracies were 100% for task one and task two. The SVM tasks reported high accuracies and sensitivities which may be due to the smaller size of the dataset and as there were only three classes [307]. Although, the specificities were consistently low as the algorithm under-predicted the food effect.

The RF task two achieved the highest accuracy and sensitivity of 80%, followed by task one with 71%, then task three with 70%. For binary classification, task two showed an improved performance compared with task one. The specificity of task two was high at 76%, whereas in task one the specificity was 68%**.** It must be highlighted that the accuracy of task three is lower than that of task one and two. This is due to the coding method of task three, where first task one was used, followed by task two. If these tasks incorrectly classifies the drugs or samples, it will therefore affect performance of task three. Several reasons may contribute to the high accuracies seen here with RF. First, the dataset was moderately large with 311 drugs and 23 features. Second, the RF algorithm has the ability to integrate a number of decision trees to train the models and solve classification issues without too much hyper-parameter tuning [308]. The performance of kNN was less accurate. This may be caused by the distance between the predictions and the actual points. If the distance is very similar from one sample to two or three classes, then the final prediction can be wrong.

The task validation stage is crucial for all machine learning techniques, as they have a high tendency for overfitting. This was observed in the obtained results in tasks one, two and three, as accuracy, specificity and sensitivity were always higher for the training set than for the testing set. Furthermore, relatively small databases can show overfitting, where the machine learning models do not generalize well if presented with new data. Data splitting techniques, such as the method used in task one, can help to prevent this. In addition, due to the smaller size of the dataset, the tasks can be sensitive to changes in the methodologies. Recently, newer machine learning techniques are emerging which are able to handle small databases, such as Bayesian Neural networks [309].

Most of the machine learning studies in formulation development have also focused on prediction accuracy [148]. In part two, the focus instead was the prediction of regression tasks. Algorithms can be referred to as 'black boxes' where the predictive tasks are not transparent or interpretable. Another term used is 'a messy glass box' when it is too complicated and therefore indecipherable [227]. An important approach used in part one was the feature importance analyses, part of a set of techniques called explainable machine learning [148], where scientific insights can be found from multi-dimensional datasets. The prediction accuracy of the tasks is limited by the features used in models and may not represent all of the factors contributing to the effect of food on oral drug absorption. Key properties not included in these datasets may include biopharmaceutical and human physiological data. Another limitation of the dataset used in part one is that the pKa of the drug was not included as a feature. This was included in part two in the ADMET feature set. The pH of the GI tract is significantly affected by food intake [249,310], and therefore, pKa of the drug is a key property in predicting food effects. For example, Marasanapallea et al., found that furosemide, an acidic drug with low permeability and a pKa of 3, exhibits pH-dependent dissolution rates and showed negative food effects [311]. Importantly, all of the feature sets from part one and part two did not include the type of formulation, which can influence food-mediated changes in drug absorption. In drug development, formulation approaches can be developed to overcome the food effect [10,24]. The minimum number of features that is necessary

for an accurate prediction model development will be a subject of future work in both parts. Part one and part two used *in silico* calculated features that may be the only data available at early-stage drug development. Furthermore, in drug development, early datasets tend to be small with an imbalanced features space due to limited experimental data. Importantly, machine learning tools can be combined with other tools such as PBPK [287,312]

The feature analyses in part one revealed that different features were important in the prediction of the binary classification of task one; no food effect (F0) versus a food effect (F-&F+), and task two; a negative food effect (F-) versus a positive food effect (F+). Drug solubility is a key property to aid the understanding of drug absorption through the gastrointestinal tract. Drugs with lower intestinal solubilities can show an increased absorption in the presence of food, due to the increased secretion of bile. For example, oral oncology drugs frequently show positive food effect due to their poor aqueous solubility [313]. Regional differences exist in the luminal fluid properties along the gastrointestinal tract [3], therefore determining the solubility across a range of pH values, as calculated by minVSLgS 3-7.5 may be useful to determine the food effect, the fifth most important feature in task two.

The feature MoKa.LogD7.4 represents the lipophilicity of the drug, the third most important feature in task two. Positive food effects are associated with drug lipophilicity by lipid emulsification and an increase in luminal solubilisation [314,315]. Abiraterone, for example, shows a dramatic positive food effect depending on the lipidic content of the meal [316]. Its positive food effect is attributed to its high lipophilicity, where it is highly solubilized in the lipophilic, micelle-abundant fed state gastrointestinal fluid containing bile salts and exogenous solubilizing species [24].

The two most important features in task one were cDose number (minVSLgS 3-7.5 and ALOGPS based). These features were calculated by software from the SMILES drug structure, which is available in early drug development. Although, it must be acknowledged that the experimentally derived dose number is not usually available in

early drug development. Dose number is an indicator of solubility-dose relationship. When the dose number is low, the drug is considered to have high solubility; when the dose number is high, the drug is considered to have low solubility. For drugs that cannot be absorbed from the GI tract because of poor solubility or slow dissolution rate, food can enhance their oral absorption by solubilisation [317]. In the high fat meal used in the food effect study, the products of digestion introduce a higher concentration of bile salts than in the fasted state which leads to higher solubility and dissolution rate of lipophilic compounds. Importantly, food components can inhibit both influx and efflux transporters [217,235,285].

Whilst RF can select the most important features that can be useful for determining which features should be experimentally validated, the relationship between the features is hidden inside the many decision trees. Importantly, the model interpretation should be intuitive to a pharmaceutical scientist, as well as a machine learning data scientist and the rank of importance appears to highlight the most important physicochemical features for food effect prediction in an easy-to-interpret manner. The BCS/BDCCS Class has been used as an indicator for food effect prediction [285], although it is not always available in early drug development. Therefore, it might not necessarily be available to input into a computational prediction model. The BDDCS/BCS tool was estimated to be accurate in 70% of cases [285]. In addition, it suggests that food effect can be predicted from *in vitro* drug physicochemical properties.

In part one study, however, the majority of the drugs did not display a food effect. Therefore, the BDDCS/BCS tool was not appropriate for this dataset. This was reflected in the feature importance where the BDDCS was one of the lowest ranked features in task one and task two. Although, for the drugs with a food effect (Figure 4.2.9), drugs in Class I reported a food effect in less than 10% of drugs. Class II drugs displayed a higher proportion of 21% with positive food effect, compared with 11% reporting a negative food effect. Class III drugs showed a higher percentage of 24% with a negative food effect, compared with 6% with a negative food effect. Class IV drugs showed less of a

percentage difference between positive and negative food effects than drugs in the other classes.

Few studies have used mathematical modelling to predict and understand the food effect [318]. One study built a dataset of 92 drugs and achieved an accuracy of 80% for food effect prediction [317]. However, only LR was used, a basic statistical technique, which can only handle linear relationships between input and output data, whereas the non-linear machine learning approaches used here can handle more complex relationships between inputs and outputs. A further study used a RF for food effect prediction and reported with a moderate Kappa (a metric comparing the observed accuracy with the expected accuracy) from the modelling of a dataset of 53 drugs and 11 drug properties [319]. Another study reported using correlation analysis that the food-stimulated increase in bile flow caused the increased elimination of biliary excreted drugs, resulting in negative food effects [320]. The most recent study used artificial neural networks and support vector machines to predict the food effect using a dataset of 141 drug compounds brought to market in the last 5 years. These models demonstrated higher food effect prediction accuracy (72% and 69%) than the BCS prediction which showed an accuracy of 46% [321]. In addition, for the positive food effect and no food effect groups, the specificities of the testing sets were 80% and 78% (SVM) and 80% and 90% (ANN), and the sensitivities were 62% and 71% (SVM) and 73% and 71% (ANN). The specificity and sensitivity of the test set for negative food effect group was not reported. Comparisons to these studies is not possible as different drugs and features were used to build these predictive models. However, our strategic machine learning pipeline approach based on three tasks shown in part 1 found that RF could accurately predict the food effect over 300 drugs from a diverse chemical space.

Prediction of pharmacokinetic properties is common practice for assessing the suitability of potential drug candidates. The druggability of a drug is mainly dependent on the metabolism and the pharmacokinetic properties (termed the DMPK) [322]. Importantly, there are some successful examples in the literature [323-325]. Zhang et al trained a light gradient boosting machine learning model using 1719 molecular descriptors with a

dataset of 246 chemicals and achieved a correlation coefficient of 0.6 – 0.8 comparing rat and humans for several pharmacokinetic metrics (C_{max} and AUC) [326]. Predicting pharmacokinetic parameters using regression techniques (part two) are a more complex set of tasks, compared with the classification tasks as shown in part one. Overall, the tasks showed poor performance, with the r2 score and the explained variance below 0.3 for all the machine learning algorithms (ADA, GB, XGB, kNN, LASSO, RF, MLP, and SVR) with the three different feature sets (ADMET, MFP + RDKit, and ADMET + MFP + RDKit). The poorest performing feature set were the features derived from the ADMET predictor software. For instance, the prediction of the C_{max} and AUC with the ADMET feature set showed negative r2 score and explained variance. The best performing task was prediction of the AUC by MLP with a r2 score of 0.28. The worse performing task was the prediction of C_{max} by ADA with a score of -0.3. The quality and quantity (size) of the dataset and feature sets may limit the performance of the machine learning algorithms.

These studies considers the influence of a high fat meal on drug absorption which is the regulatory requirement in bioavailability and bioequivalence testing [11]. However, there are a number of specific food-drug interactions that occur between drugs and the food components in the meal. Due to the ever-growing number of nutrients and dietary supplements, interactions may remain undetected [9,327] and a predictive machine learning tool could be developed to give further insight in specific nutrient-drug interactions. In addition to interactions occurring in the luminal fluids, food can interact with the intestinal layer in a specific manner. Reker et al used machine learning to predict the biological interaction between food and the efflux transporter P-gp and the enzyme uridine diphosphate-glucuronosyltransferase-2B7 which uncovered an interaction that was validated by *in vitro* and *in vivo* assays [143].

Food consumption can affect the drug absorption through many different mechanisms, such as changes in the GI physiology, bile-mediated enhanced solubilisation of lipophilic drugs, inhibition of drug metabolising enzymes and transporters [63] and by direct food-drug mechanisms. However, the key mechanisms that causes the food effect for a particular drug are often unknown [227]. While these machine learning approaches

cannot yet identify the mechanism of the food effect, if a food effect is predicted for a new drug candidate using these tasks, follow-up *in vitro*, PBPK and preclinical studies could then be designed to provide further insights into the potential mechanism of the food effect.

4.5 Conclusions

These studies assessed the application of machine learning-powered tasks for the prediction of the food effect. Part one used classification-based machine learning algorithms to predict the class of food effect (no food effect versus positive food effect versus negative food effect) for an extensive dataset of over 311 drugs with more than 20 drug physicochemical properties. As opposed to a 'plug-and-play' standard machine learning approach, a strategic approach was trained and tested. The RF algorithm was able to predict the food effect with accuracies of over 70% in three prediction tasks: food effect versus no food effect, negative food effect versus positive food effect, and no food effect versus negative food effect versus positive food effect, respectively. Feature importance revealed that calculated dose number was the most important feature underlying the development of the machine learning tasks.

Part two tested regression-based machine learning algorithms to predict food-mediated changes to key pharmacokinetic properties - AUC and C_{max} for a dataset of 291 drugs. Three different feature sets were used as inputs – ADMET properties, MFP + RDKit features, and a combination of ADMET, MFP, and RDKit. Overall, the best performance was a r2 score of 0.28 for the prediction of the AUC with the MFP + RDKit feature set using the MLP algorithm. The ADMET feature set was the poorest performing feature set showing negative r2 values. Consistently high MAE and MSE were reported. The performance is limited by the small size of the dataset and the complexity of predicting pharmacokinetic parameters.

These studies combined machine learning tools and biopharmaceutical sciences. The proposed approaches could enable a potential reduction in the number of animals of and humans required in food effect studies. Furthermore, it offers a useful insight at the early drug discovery and development stage and could prevent costly reformulation strategies or the failure of lead compounds at later stages if food-drug interactions are found.

Chapter 5 : General discussion, conclusions, and future work

The research described in this thesis serves to demonstrate the importance of predicting the food effect early in pharmaceutical development and strives to offer novel tools and the understanding of this area. This chapter provides a general discussion of the research; it begins with a justification for research into the food effect on pharmaceuticals, before discussing the key findings, limitations, and future work.

5.1 The importance of food effect assessment

A wealth of knowledge exists on the effect of food intake on intestinal drug absorption. However, despite over 40 years of research in the area, it remains a problem in pharmaceutical research and key gaps still exist. The mechanisms of the food effect are often not known, and therefore this thesis focussed both on further understanding of the mechanisms as well as prediction method development.

The aims of this PhD were to: 1) review the current knowledge in the food effect field, focusing on the current tools used to assess the food effect, and identify where developments are needed; 2) explore the influence of food intake, sex (male versus female), strain (Wistar versus Sprague Dawley) on the expression of three clinically relevant efflux transporters P-gp, BCRP, and MRP2; 3) investigate the influence of a fibre meal on the luminal contents, expression of P-gp, BCRP, and MRP2, and key GI and sex hormones over time; and 4) expand the machine learning toolkit for predicting food-mediated changes to drug pharmacokinetics.

5.2 Overview of research contributions

The main findings of the research documented in this thesis are summarised below in relation to the aims and objectives outlined.

Review of the scientific literature in the food effect field was presented in chapter 1. The chapter focused on biopharmaceutics considerations and machine learning technologies, reflecting the aims and objectives of the thesis. Multiple key knowledge

gaps were identified where developments were needed. This thesis endeavoured to offer novel insights to bridge the knowledge gaps.

Oral drug absorption is subject to high inter- and intra-individual variability, which can be attributed in part to patient-specific internal and external factors. Among patient-specific factors such as disease state, pregnancy, and ethnicities, the sex of a patients and their choice of diet are associated with alterations in the physiology of the GI tract. These factors can, in turn, influence the oral bioavailability of many commonly prescribed medications. In the preclinical arena, the strain of the animal model is usually selected based on cost, convenience, or traditional. However, physiological differences between strains could influence intestinal permeability properties. Chapter 2 examines the influence of food intake on three clinically relevant efflux transporters with a focus on the intestines (duodenum, jejunum, and ileum); P-gp, BCRP, and MRP2, which are responsible for the efflux of many drug substrates. The influence of sex and strain was also considered. The study found food-mediated sex differences in P-gp expression, whereby feeding decreased P-gp expression in male Wistar rats but increased P-gp expression in their female counterparts. Food intake increased the BCRP/*abcg2* expression in both male and female Wistar rats. In contrast, no sex differences or food effect differences were seen in the Sprague Dawley rats for the P-gp/*abcb1a* and BCRP/*abcg2* expression. Feeding increased the MRP2/ *abcc2* expression in male and female Wistar and Sprague Dawley rats, with sex differences in the fasted state. Moderate to strong positive linear correlations were found between ELISA and PCR quantification methods. Significantly, strain differences were reported for P-gp/*abc1a*, BCRP/*abcg2*, and MRP2/abcc2 expression. Therefore, researchers must carefully consider the sex, strain, and feeding status in their preclinical studies into P-gp, BCRP, and MRP2 drug substrates.

It is known that intestinal interactions with nutrients, xenobiotics, and endogenous hormones can influence the expression of the clinically relevant membrane transporters P-gp, BCRP, and MRP2. These changes in the GI physiology can in turn affect the absorption of numerous drug substrates. Several studies have examined the effect of

food on intestinal transporters in male and female humans and animal models. However, to our knowledge no studies have investigated the influence of a non-nutritive fibre meal on intestinal efflux transporters and key sex and GI hormones. Non-nutritive fibre can be found in commonly consumed meals, in legumes, nuts, and seeds. Furthermore, patients experiencing constipation often take fibre-based laxatives. Here, the findings in chapter 2 show that a fibre meal increased the acute expression of P-gp, BCRP, and MRP2 in small intestinal segments in both male and female Wistar rats. From the findings in chapter 1, ELISA was used for protein quantification of the efflux transporters and hormonal plasma concentration, and the Wistar rat strain was used. In male rats, the fibre meal caused the plasma concentration of the GI hormone CCK to increase by 75% and the sex hormone testosterone to decrease by 50%, whereas, in contrast, the housing food meal caused a decrease in CCK by 32% and testosterone saw an increase of 31%. No significant changes in the hormonal concentrations, however, were seen in female rats. A deeper understanding of the modulation of efflux transporters by sex, food intake, and time can improve our understanding of inter- and intra-variability in the pharmacokinetics of drug substrates.

Computational tools have been embraced in the drug discovery field. However, in drug development, their full potential is yet to be realised. Furthermore, it can be challenging to predict biopharmaceutics and pharmacokinetic parameters due to the complex GI environment. Machine learning provides a powerful set of tools for data analysis and prediction. Part one shows a machine learning-based approach that aimed to predict the food effect based on an extensive dataset of over 311 drugs with more than 20 drug physicochemical properties. First a standard ML pipeline using a 80:20 split for training and testing was tried to predict no food effect, negative food effect and positive food effect, however this lead to specificities of less than 40%. Next, a strategic machine learning pipeline was built to predict food effect classification – no food effect, positive food effect, and negative food effect. A range of machine learning tools were tried – LR, SVM, kNN, and RF. RF achieved the best score with accuracies, specificities, and sensitivities of over 70%. RF also provided a ranking system of the most importance

features, termed feature importance. The calculated dose number was the most importance feature. Here, machine learning has provided an effective screening tool for predicting the food effect, with the potential to select lead compounds with no food effect, reduce the number of animal studies, and accelerate oral drug development studies.

In part two, regression machine learning supervised tasks were tested to predict the AUC and C_{max} of a drugs following food intake. ADMET, MFP, and RDKit were used to generate three feature sets, and a dataset of 291 drugs were used as outputs. A toolkit of machine learning technologies were tested - ADA, GB, XGB, XGB, kNN, LASSO, RF, MLP, and SVR. MLP was the best performing algorithm for the prediction of the AUC with the MFP + RDKit feature set. The machine learning algorithms using the ADMET feature set performed poorly, and negative r2 values were found for 6/8 of the machine learning algorithms predicting the AUC and 5/8 of the machine learning algorithms predicting the C_{max}. A larger dataset may improve the performance of the algorithms.

Overall, this PhD has offered insights and tools to enhance the prediction of the effect of food on orally administered medicines using preclinical *in vivo* models and machine learning technologies. This will advance the toolkit available to pharmaceutical scientists, with the ultimate aim of benefitting patients.

5.3 Future works

These findings raise more questions, and extensive work is still needed to fully understand the mechanisms of the food effect and to integrate novel tools in pharmaceutical drug development.

One key aim of this PhD was to enhance our understanding of the physiological characteristics of the GI tract in the pre- and postprandial states. This thesis explored the expression of key efflux transporters in the fasted and fed states, as well as with a fibre meal intervention. The GI epithelia expresses both uptake and efflux transporters, which

are both significant for oral drug absorption and bioavailability. The solute carrier (SLC) superfamily is made up of the organic anion transporting polypeptides (OATP) that act as uptake transporters. These uptake transporters should be assessed in the fasted and fed states and between the sexes. Here, the role of intestinal metabolising enzymes was also not considered and are frequently overlooked in view of the intestinal epithelial. CYP 450 3A and 2C9 are the most abundant CYPs and are located on the villous tips, with the highest expression in the duodenum and proximal jejunum. The CYP expression decreases along the human intestinal tract. This pattern contrasts with the P-gp profile, which increases along the human intestinal tract. The small intestinal metabolism by CYP3A enzymes contributes to the first-pass metabolism of many P-gp substrates, such as cyclosporine, verapamil, or tacrolimus. The interplay between intestinal metabolism by CYP and the efflux mechanism and the implications for oral drug delivery should be studied further.

The epithelium of the intestinal barrier provides a controlled homeostatic system to regulate the interactions between the luminal contents and the systemic circulation. The interactions between the digestion of food, the microbiota, and the absorption of drug products were not examined in this thesis and is an emerging topic of interest in the field. A recent paper by Foley et al., 2021 found that short chain fatty acids and secondary bile acid production synergistically upregulate P-gp expression [328]. It would be interesting to unpiece the multidimensional relationships between the luminal contents and the epithelial barrier.

This thesis used targeted approaches to quantify the transcription and protein expression in the intestinal tract, in the form of PCR and ELISA, respectively. More advanced techniques exist in the biomedical space. For example, global proteomics provides comprehensive proteome-wide quantification of a large number of proteins (100s–1,000s) in a biological sample [195]. While global shotgun proteomics can be less sensitive and reproducible, compared with targeted proteomics, its ability to quantify and identify all the proteins from a given sample. Future experiments could use these

advanced analytical tools to measure the genes and proteins present in the intestinal epithelia in the fasted and fed states and between the sexes.

Digital tools are being embraced in the pharmaceutics field, creating a new discipline - computational pharmaceutics. Here, machine learning technologies have enabled the prediction of a complex biopharmaceutics – the food effect. Future studies could use larger 'clean' datasets, which could enable the use of deep learning models. These predictive models should also be experimentally validated. As more data is gathered, other patient-specific pharmacokinetic properties could be predicted, such as sex differences in drug response and the impact of age, ethnicity, pregnancy, and disease states in drug product performance.

The findings in this PhD and the future research avenues identified could help forecast and predict food-mediated changes to oral drug absorption.

Publications and Communications

Related to this thesis

Research articles

Christine M. Madla, Yujia Qin, **Francesca K. H. Gavins**, Jing Liu, Liu Dou, Mine Orlu, Sudaxshina Murdan, Yang Mai, Abdul W. Basit. Sex differences in intestinal P-glycoprotein expression in Wistar versus Sprague Dawley rats. Pharmaceutics. 2022. 14(5), 1030.

Francesca KH Gavins, Zihao Fu, Moe Elbadawi, Abdul W Basit, Miguel RD Rodrigues, Mine Orlu. Machine learning predicts the effect of food on orally administered medicines. International Journal of Pharmaceutics. 2022. 611 121329.

Yang Mai, **Francesca KH Gavins**, Liu Dou, Jing Liu, Farhan Taherali, Manal E Alkahtani, Sudaxshina Murdan, Abdul W Basit, Mine Orlu. A Non-Nutritive Feeding Intervention Alters the Expression of Efflux Transporters in the Gastrointestinal Tract. Pharmaceutics. 2021. 13 11 1789.

Yang Mai, Liu Dou, Zhicheng Yao, Christine M Madla, **Francesca KH Gavins**, Farhan Taherali, Heyue Yin, Mine Orlu, Sudaxshina Murdan, Abdul W Basit. Quantification of P-Glycoprotein in the Gastrointestinal Tract of Humans and Rodents: Methodology, Gut Region, Sex, and Species Matter. Molecular Pharmaceutics. 2021. 18 5 1895-1904.

Liu Dou, **Francesca KH Gavins**, Yang Mai, Christine M Madla, Farhan Taherali, Mine Orlu, Sudaxshina Murdan, Abdul W Basit. Effect of food and an animal's sex on p-glycoprotein expression and luminal fluids in the gastrointestinal tract of wistar rats. Pharmaceutics. 2020. 12 4 296.

Reviews

Christine M Madla, **Francesca KH Gavins**, Hamid A Merchant, Mine Orlu, Sudaxshina Murdan, Abdul W Basit. Let's talk about sex: Differences in drug therapy in males and females. Advanced Drug Delivery Reviews. 2021. 175 113804.

Oral Presentations

Francesca KH Gavins. Towards the prediction of the effect of food on orally administered medicines using preclinical in vivo models and machine learning technologies. UCL School of Pharmacy Research Day. September 2022.

Francesca KH Gavins. Machine Learning for the prediction of food effect. Understanding Gastrointestinal Absorption-related Processes (UNGAP) Webinar 2022.

Liu Dou, **Francesca KH Gavins**, Yang Mai, Christine M Madla, Farhan Taherali, Mine Orlu, Sudaxshina Murdan, Abdul W Basit. Effect of food and sex on P-glycoprotein expression and luminal fluids in the gastrointestinal tract of rats. UNGAP Spring Meeting Ljubljana 2020.

Poster Presentations

Francesca KH Gavins. A Non-Nutritive Fibre Meal Alters the Expression of Efflux Transporters in the Gastrointestinal Tract. 13th World Meeting on Pharmaceutics, Biopharmaceutics and Pharmaceutical Technology in Rotterdam 2022.

Francesca KH Gavins. Machine Learning predicts the effect of food on orally administered medicines. 13th World Meeting on Pharmaceutics, Biopharmaceutics and Pharmaceutical Technology in Rotterdam 2022.

Liu Dou, **Francesca KH Gavins**, Yang Mai, Christine M Madla, Farhan Taherali, Mine Orlu, Sudaxshina Murdan, Abdul W Basit. Effect of food and sex on P-glycoprotein expression and luminal fluids in the gastrointestinal tract of rats. UNGAP Spring Meeting Ljubljana 2020.

Book chapters

Francesca KH Gavins, Christine M Madla, Sarah J Trenfield, Laura E McCoubrey, Abdul W Basit, Mark McAllister. Impact of Anatomy and Physiology. Pages 165-188. Biopharmaceutics: From Fundamentals to Industrial Practice. John Wiley & Sons, Ltd. 2022.

Christine M Madla, **Francesca KH Gavins**, Sarah J Trenfield, Abdul W Basit. Special Populations. Pages 205-237. Biopharmaceutics: From Fundamentals to Industrial Practice. John Wiley & Sons, Ltd. 2022.

External to this thesis

Reviews

Atheer Awad, Christine M Madla, Laura E McCoubrey, Fabiana Ferraro, **Francesca KH Gavins**, Asma Buanz, Simon Gaisford, Mine Orlu, Florence Siepmann, Juergen Siepmann, Abdul W Basit. Clinical translation of advanced colonic drug delivery technologies. Advanced drug delivery reviews. 2021. 114076.

Moe Elbadawi, Laura E McCoubrey, **Francesca KH Gavins**, Jun J Ong, Alvaro Goyanes, Simon Gaisford, Abdul W Basit. Disrupting 3D printing of medicines with machine learning. 2021. 42 9 745-757.

Moe Elbadawi, Laura E McCoubrey, **Francesca KH Gavins**, Jun Jie Ong, Alvaro Goyanes, Simon Gaisford, Abdul W Basit. Harnessing artificial intelligence for the next generation of 3D printed medicines. 2021. 175 113805.

Oral Presentations

Francesca KH Gavins. The Ageing Gut: Biopharmaceutical Considerations. Academy of Pharmaceutical Sciences (APS) Webinar 2021.

Francesca KH Gavins. The Ageing Gut: Biopharmaceutical Considerations. Controlled Release Society (CRS) Conference Webinar 2021.

Book chapters

Neel Desai, Laura E. McCoubrey, Christine M. Madla, **Francesca K.H. Gavins** and Mine Orlu. Geriatric Pharmaceutics. Pages 230-258. Specialised Pharmaceutical Formulation: The Science and Technology of Dosage Forms. Royal Society of Chemistry. 2022.

Atheer Awad, Christine M Madla, **Francesca KH Gavins**, Nour Allahham, Sarah J Trenfield, Abdul W Basit. Liquid dosage forms. Remington. Academic Press. 2021

Ana Cristina Freire, **Francesca K.H. Gavins,** and Abdul W. Basit. Dissolution testing of solid dosage forms. Aulton's Pharmaceutics: The Design and Manufacture of Medicines, 6th Edition. Elsevier. 2021.

News & Views

Abdul W Basit, Christine M Madla, **Francesca KH Gavins**. Robotic screening of intestinal drug absorption. Nature Biomedical Engineering. 2020 4 5 485-486.

Appendices

Appendix for Chapter 2 & 3

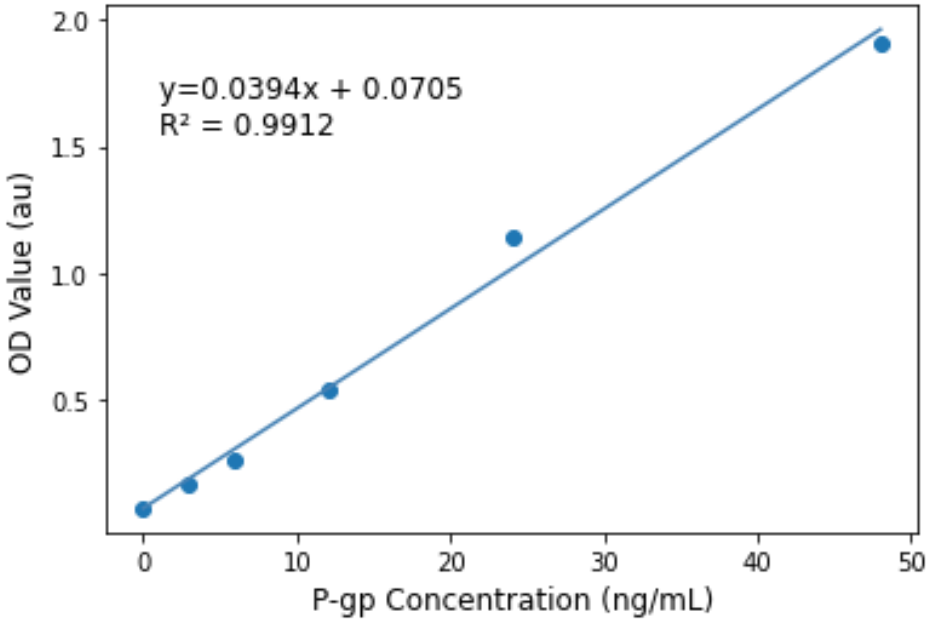

Figure 0-1 ELISA calibration curve of P-gp concentration (ng/mL) against OD value (au)

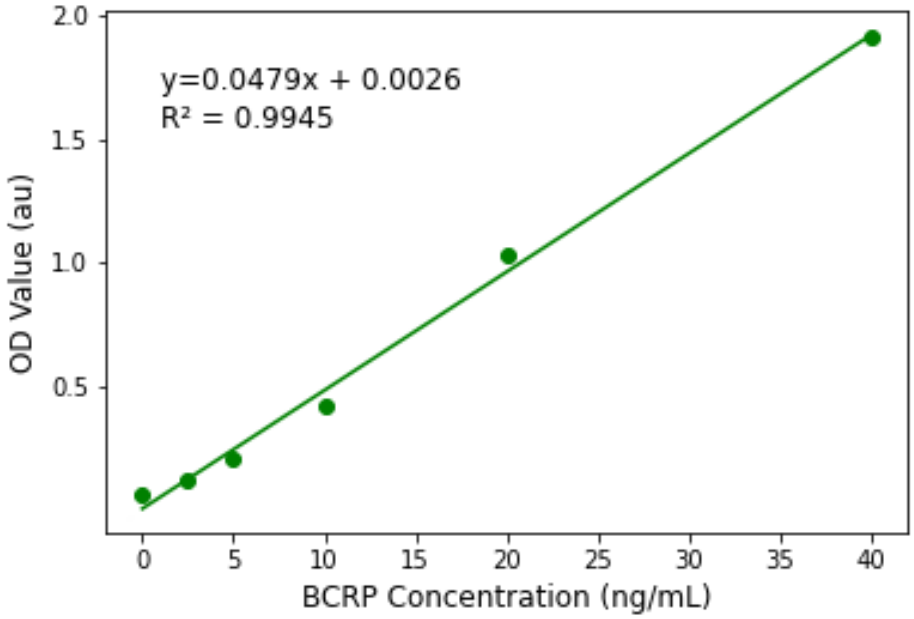

Figure 0-2 ELISA calibration curve of BCRP concentration (ng/mL) against OD value (au)

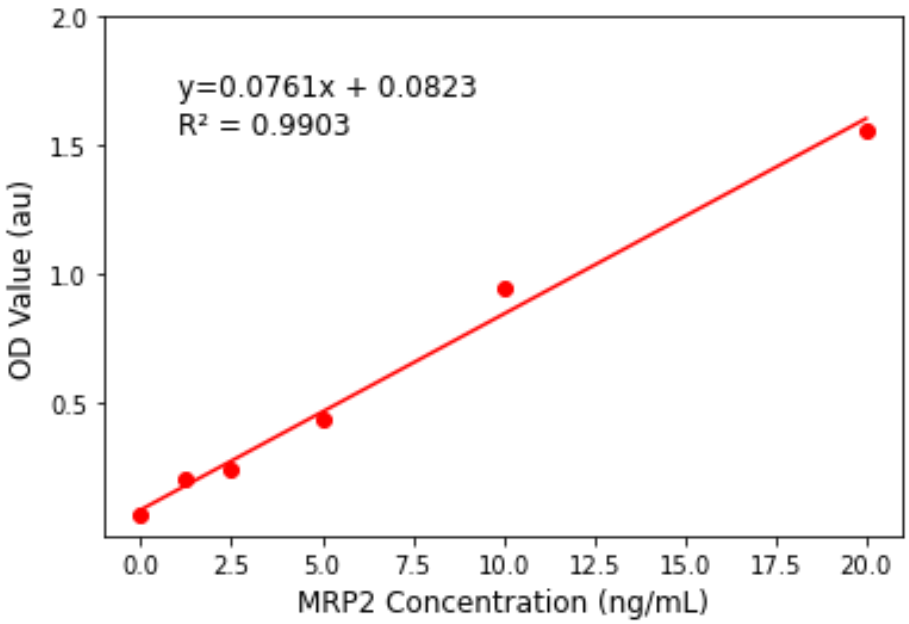

Figure 0-3 ELISA calibration curve of MRP2 concentration (ng/mL) against OD value (au)

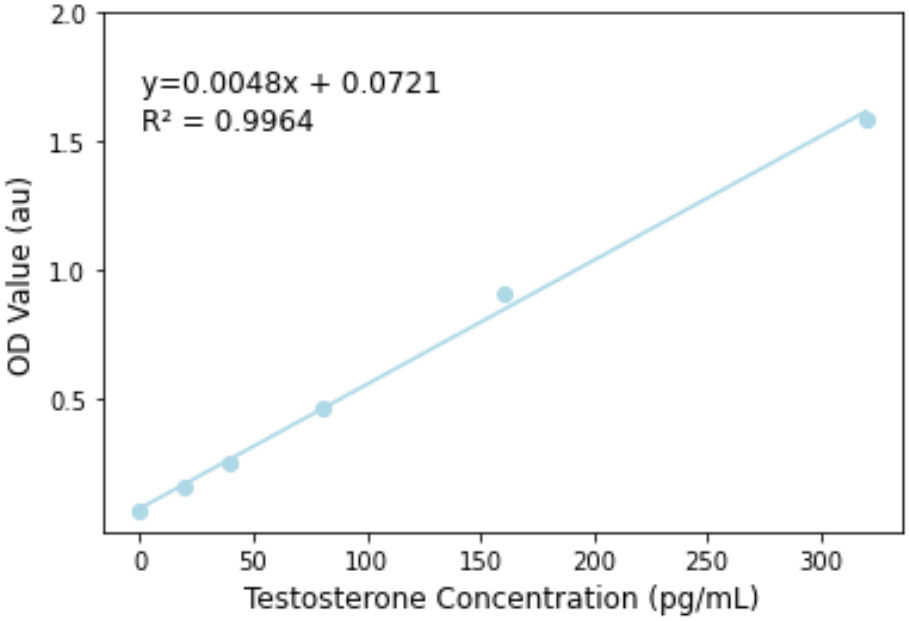

Figure 0-4 ELISA calibration curve of sex hormone testosterone concentration (pg/mL) against OD value (au)

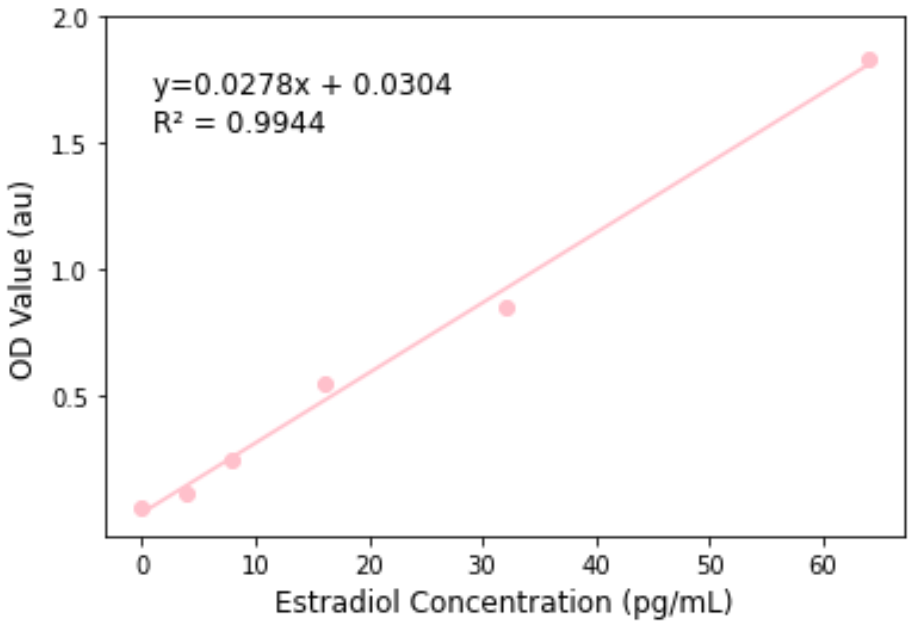

Figure 0-5 ELISA calibration curve of sex hormone estradiol concentration (pg/mL) against OD value (au).

Appendix for Chapter 4

Table 0-1 Drugs with food effect classification; no food effect (F0), positive food effect (F+) and negative food effect (F-). The * denotes 'controversial' food effect data

Generic Name	Food effect	Reference
Abacavir Sulfate	F0	[329]
Acarbose	F0*	[330]
Acebutolol	F0	[331]
Acetaminophen/Paracetamol	F0*	[332]
Acetylsalicylic Acid; Aspirin	F0	[333]
Acyclovir	F0*	[334]
Alendronate Sodium	F-	[335]
Alfacalcidol	F0	[336]
Alfuzosin	F0*	[337]
Allopurinol	F0	[338]
Almotriptan	F0	[339]
Alosetron	F0*	[340]
Alprazolam	F0*	[341]
Alprenolol	F0	[342]
Amantadine	F0	[343]
Amiodarone	F+	[344]
Amitriptyline	F0	[345]
Amlodipine	F0	[346]
Amoxicillin	F0	[347]
Ampicillin	F-	[348]
Aprepitant	F0	[349]
Aripiprazole	F0	[350]
Atenolol	F-	[351]
Atomoxetine	F0	[352]
Atovaquone	F+	[353]

Azithromycin	F0	[354]
Bambuterol	F0	[355]
Betaxolol	F0	[356]
Bevantolol	F0	[357]
Bosentan	F0	[358]
Budesonide	F0	[359]
Bumetanide	F0	[360]
Calcitriol	F0	[361]
Candesartan	F0	[362]
Captopril	F-	[363]
Carbenicillin	F-	[364]
Carvedilol	F-	[365]
Cefadroxil	F0	[366]
Cefamandole	F0	[364]
Cefixime	F0	[367]
Cefprozil	F0	[368]
Cefuroxime	F+	[369]
Cephalexin	F0	[370]
Cephradine	F0	[366]
Chloroquine	F+	[371]
Chlorpheniramine	F0	[372]
Chlorpromazine	F0	[373]
Chlorthalidone	F0	[374]
Cimetidine	F0	[375]
Cinacalcet	F+	[376]
Ciprofloxacin	F0	[377]
Citalopram	F0	[378]
Clarithromycin	F0	[379]
Clodronate	F-	[380]
Clonazepam	F0	[381]
Clonidine	F0	[382]

Clozapine	F0	[383]
Codeine	F0	[384]
Cyclizine	F0	[385]
Cyclophosphamide	F0	[386]
Dabigatran	F0	[387]
Dantrolene	F0	[388]
Dapsone	F0	[389]
Darifenacin	F0	[390]
Darunavir	F+*	[391]
Desipramine	F0	[392]
Dexamethasone	F0	[393]
Dexmethylphenidate	F0	[394]
Diazepam	F+*	[395]
Diazoxide	F0	[396]
Diclofenac	F0	[397]
Dicloxacillin	F-	[398]
Didanosine	F-	[399]
Diflunisal	F0	[400]
Digoxin	F0	[401]
Dilevalol	F0	[402]
Diltiazem	F0	[403]
Diphenhydramine	F0	[404]
Dipyridamole	F0	[405]
Disopyramide	F0	[406]
Dofetilide	F0	[407]
Dolasetron	F0	[408]
Domperidone	F-	[409]
Doxepin	F+	[410]
Doxycycline	F0	[411]
Duloxetine	F0	[412]
Eletriptan	F0	[413]

Enoxacin	F0	[414]
Entacapone	F0	[415]
Eprosartan	F0	[416]
Erlotinib	F+	[417]
Erythromycin	F0	[418]
Esomeprazole	F-	[419]
Estradiol	F0	[420]
Ethambutol	F0	[421]
Ethinylestradiol	F0	[317]
Etoposide	F0	[422]
Etoricoxib	F0	[398]
Famotidine	F0	[423]
Felodipine	F0	[424]
Finasteride	F0	[425]
Flecainide	F0	[426]
Fluconazole	F0	[427]
Flucytosine	F0	[428]
Flunitrazepam	F0	[429]
Fluphenazine	F0	[430]
Fluvastatin	F0	[431]
Fluvoxamine	F0	[432]
Fosfomycin	F0	[433]
Frovatriptan	F0	[434]
Furosemide	F-	[360]
Gabapentin	F+*	[435]
Ganciclovir	F+	[436]
Gefitinib	F0	[437]
Gliclazide	F0	[438]
Glimepiride	F0	[439]
Glipizide	F0	[440]
Glyburide	F0	[441]

Granisetron	F0	[442]
Guanfacine	F+	[443]
Haloperidol	F0	[444]
Hexobarbital	F0	[445]
Hydralazine	F-	[317]
Hydromorphone	F0	[446]
Hydroxychloroquine Sulfate	F0	[447]
Ibandronate	F-	[448]
Ibuprofen	F0	[449]
Imatinib	F0	[450]
Imipramine	F0	[451]
Indomethacin	F-*	[452]
Indoramin	F0	[453]
Irbesartan	F0	[454]
Isoniazid	F-	[317]
Isosorbide 5-Mononitrate	F0	[455]
Isradipine	F0	[456]
Itraconazole	F+	[457]
Ivabradine	F+	[458]
Ketanserin	F0	[459]
Ketoprofen	F-	[460]
Ketorolac	F0	[461]
Labetalol	F+	[462]
Lacosamide	F0	[463]
Lamivudine	F0	[464]
Lansoprazole	F0*	[317]
Letrozole	F0	[465]
Levetiracetam	F0	[466]
Levodopa	F0	[467]
Levofloxacin	F0	[468]
Linezolid	F0	[469]

Lisinopril	F0	[470]
Lomefloxacin	F0	[471]
Lorazepam	F0	[429]
Lorcainide	F0	[472]
Losartan	F0	[473]
Lovastatin	F+*	[474]
Maprotiline	F0	[475]
Maraviroc	F-	[476]
Meloxicam	F0	[477]
Melphalan	F-	[478]
Meperidine;	F0	[479]
6-Mercaptopurine	F-	[480]
Metformin	F-*	[481]
Methadone	F0	[482]
Methotrexate	F0	[483]
Methyldopa	F0	[484]
Methylprednisolone	F0	[485]
Metoclopramide	F0	[486]
Metoprolol	F+	[487]
Metronidazole	F0	[488]
Mexiletine	F0	[398]
Mianserin	F0	[489]
Milnacipran	F0	[490]
Minocycline	F0	[491]
Minoxidil	F0	[492]
Mirtazapine	F0	[493]
Mizolastine	F0	[494]
Montelukast	F0	[495]
Morphine	F0	[496]
Moxifloxacin	F0	[497]
Nadolol	F-*	[498]

Naloxone	F0	[499]
Naltrexone	F+	[500]
Naproxen	F0	[501]
Naratriptan	F0	[502]
Nateglinide	F0	[503]
Nefazodone	F+*	[504]
Nefopam	F0	[505]
Nicardipine	F0	[506]
Nicorandil	F0	[507]
Nifedipine	F0	[508]
Nimodipine	F-	[509]
Nitrazepam	F0	[510]
Nitrendipine	F0	[511]
Nitrofurantoin	F+	[512]
Nizatidine	F0	[513]
Norfloxacin	F0*	[514]
Nortriptyline	F0	[345]
Ofloxacin	F0	[515]
Olmesartan	F0	[516]
Omeprazole	F-	[517]
Ondansetron	F+	[518]
Oseltamivir	F0	[519]
Oxazepam	F0	[511]
Oxprenolol	F0	[520]
Oxybutynin	F0	[521]
Oxycodone	F0	[522]
Paliperidone	F+*	[523]
Pantoprazole	F0	[524]
Paricalcitol	F0	[525]
Paroxetine	F0	[526]
Pefloxacin	F0	[527]

Pentazocine	F0	[528]
Pentoxifylline	F0	[529]
Phenobarbital	F0	[530]
Phenytoin	F+	[531]
Pindolol	F0	[532]
Pramipexole	F0	[533]
Pravastatin	F-*	[317]
Prazosin	F0	[534]
Prednisolone	F0	[535]
Prednisone	F0	[536]
Primaquine	F+	[537]
Probenecid	F0	[538]
Prochlorperazine	F0	[539]
Promazine	F0	[540]
Promethazine	F+	[541]
Propafenone	F+	[542]
Propranolol	F+	[543]
Pyridostigmine	F0	[544]
Quinapril	F0	[545]
Quinine	F0	[546]
Rabeprazole	F0	[547]
Raloxifene	F+	[548]
Ramelteon	F+	[549]
Ranitidine	F0	[550]
Ranolazine	F0	[551]
Reboxetine	F0	[552]
Repaglinide	F-*	[553]
Ribavirin	F+	[554]
Rifabutin	F0	[555]
Rifampin	F-	[556]
Riluzole	F0*	[557]

Risedronate	F-	[558]
Risperidone	F0	[559]
Rivastigmine	F+	[560]
Rizatriptan	F0	[561]
Rofecoxib	F0	[562]
Ropinirole	F0	[563]
Rosiglitazone	F0	[564]
Rosuvastatin	F0	[565]
Saquinavir	F+	[566]
Saxagliptin	F0	[567]
Scopolamine	F0	[568]
Selegiline	F+	[569]
Sildenafil	F0	[570]
Sitafloxacin	F0	[571]
Sitagliptin	F0	[572]
Solifenacin	F0	[573]
Sotalol	F-*	[574]
Sparfloxacin	F0	[575]
Stavudine	F0	[576]
Sulfamethoxazole	F0	[577]
Sulfasalazine	F0	[578]
Sulfinpyrazone	F0	[579]
Sumatriptan	F0	[580]
Tacrine	F-	[581]
Tacrolimus	F-	[582]
Tamsulosin	F-	[583]
Tegaserod	F-	[584]
Telithromycin	F0	[585]
Telmisartan	F0	[586]
Temozolomide	F-	[587]
Tenofovir	F+	[588]

Tenoxicam	F0	[589]
Terazosin	F0	[590]
Terbutaline	F-	[398]
Tetracycline	F-	[591]
Theophylline	F0	[592]
Thioguanine	F0	[593]
Tiagabine	F0	[398]
Tiaprofenic Acid	F0	[594]
Tiludronate	F-	[398]
Timolol	F0	[534]
Tinidazole	F0	[595]
Tolbutamide	F0	[596]
Tolcapone	F0	[597]
Tolfenamic Acid	F0	[598]
Tolterodine	F0*	[599]
Topiramate	F0	[600]
Topotecan	F0	[601]
Torsemide	F0*	[602]
Tramadol	F0	[603]
Trazodone	F0*	[604]
Triamterene	F0	[605]
Triazolam	F0	[606]
Trimethoprim	F0	[364]
Tropisetron	F0	[607]
Trospium	F-	[608]
Valproic Acid	F-*	[609]
Valsartan	F0*	[610]
Vardenafil	F0	[611]
Venlafaxine	F0	[612]
Verapamil	F0	[613]
Voriconazole	F-	[614]

Warfarin	F0*	[615]
Zalcitabine	F-	[616]
Zidovudine	F0	[617]
Ziprasidone	F+	[618]
Zolmitriptan	F-	[619]
Zolpidem	F-	[620]
Zopiclone	F0	[621]

Table 0-2 ADMET Features

Absn_Risk	LogBB	S+FaSSIF	UNCR:hum_fup%
ADMET_Code	logHLC	S+FeSSIF	UNCR:LogBB
ADMET_Risk	MlogP	S+fumic	UNCR:logHLC
AP_FWeight	Perm_Cornea	S+logD	UNCR:rat_fup%
BBB_Filter	Perm_Skin	S+logP	UNCR:RBP
CONF:BBB_Filter	rat_fup%	S+MDCK	UNCR:RBP_rat
CONF:S+CL_Metab	RBP	S+MDCK-LE	UNCR:S+FaSSIF
CONF:S+CL_Renal	RBP_rat	S+Peff	UNCR:S+fumic
CONF:S+CL_Uptake	RuleOf5	S+pH_Satd	UNCR:S+logP
CONF:S+MDCK-LE	S+Acidic_pKa	S+S_Intrins	UNCR:S+MDCK
CONF:n	S+Basic_pKa	S+S_pH	UNCR:S+Peff
DiffCoef	S+CL_Mech	S+Sw	UNCR:S+Sw
ECCS_Class	S+CL_Metab	SolFactor	UNCR:Vd
HIVI-ST	S+CL_Renal	n	Vd
HIVI-TC	S+CL_Uptake	UNCR:HIVI-ST	
hum_fup%	S+FaSSGF	UNCR:HIVI-TC	

Table 0-3 Hyperparameters used in Part 2

Algorithm	**C_{max}**	**AUC**
ADA	learning_rate=0.05, loss="square", n_estimators=20	learning_rate=0.01, n_estimators=10
GB	learning_rate=0.02, max_depth=8, min_samples_leaf=2,	learning_rate=0.02, max_depth=8, min_samples_leaf=2,

	min_samples_split=6, subsample=0.1,	min_samples_split=6, subsample=0.1
XGB	base_score=0.5, booster="gbtree", callbacks=None, colsample_bylevel=1, colsample_bynode=1, colsample_bytree=1, early_stopping_rounds=None, enable_categorical=False, eval_metric=None, gamma=0, gpu_id=-1, grow_policy="depthwise", importance_type=None, interaction_constraints="", learning_rate=0.001, max_bin=256, max_cat_to_onehot=4, max_delta_step=0, max_depth=2, max_leaves=0, min_child_weight=5, monotone_constraints="()", n_estimators=1100, n_jobs=0, num_parallel_tree=1, predictor="auto", random_state=0, reg_alpha=0, reg_lambda=1	base_score=0.5, booster="gbtree", callbacks=None, colsample_bylevel=1, colsample_bynode=1, colsample_bytree=1, early_stopping_rounds=None, enable_categorical=False, eval_metric=None, gamma=0, gpu_id=-1, grow_policy="depthwise", importance_type=None, interaction_constraints="", learning_rate=0.001, max_bin=256, max_cat_to_onehot=4, max_delta_step=0, max_depth=2, max_leaves=0, min_child_weight=5, monotone_constraints="()", n_estimators=1100, n_jobs=0, num_parallel_tree=1, predictor="auto", random_state=0, reg_alpha=0, reg_lambda=1,
kNN	n_neighbors=14, p=1	algorithm="brute", n_neighbors=29, p=1
LASSO	Default	default
RF	max_depth=20, max_features="log2", min_samples_leaf=0.1, min_samples_split=0.2, n_estimators=400	max_depth=20, max_features="log2", min_samples_leaf=0.1, min_samples_split=0.2, n_estimators=400
MLP	activation="identity", hidden_layer_sizes=(100, 1), learning_rate="adaptive"	activation="identity", hidden_layer_sizes=(100, 1), learning_rate="adaptive"
SVR	C=100, gamma=0.1, kernel="sigmoid"	C=100, gamma=0.1, kernel="sigmoid"

References

1. Homayun, B.; Lin, X.; Choi, H.-J. Challenges and recent progress in oral drug delivery systems for biopharmaceuticals. *Pharmaceutics* 2019, *11*, 129.

2. von Erlach, T.; Saxton, S.; Shi, Y.; Minahan, D.; Reker, D.; Javid, F.; Lee, Y.-A.L.; Schoellhammer, C.; Esfandiary, T.; Cleveland, C.; et al. Robotically handled whole-tissue culture system for the screening of oral drug formulations. *Nature Biomedical Engineering* 2020, *4*, 544-559.

3. Vertzoni, M.; Augustijns, P.; Grimm, M.; Koziolek, M.; Lemmens, G.; Parrott, N.; Pentafragka, C.; Reppas, C.; Rubbens, J.; Van Den Alphabeele, J.; et al. Impact of regional differences along the gastrointestinal tract of healthy adults on oral drug absorption: An UNGAP review. *European Journal of pharmaceutical sciences* 2019, *134*, 153-175, doi:10.1016/j.ejps.2019.04.013.

4. Stillhart, C.; Vucicevic, K.; Augustijns, P.; Basit, A.W.; Batchelor, H.; Flanagan, T.R.; Gesquiere, I.; Greupink, R.; Keszthelyi, D.; Koskinen, M.; et al. Impact of gastrointestinal physiology on drug absorption in special populations - An UNGAP review. *European Journal of Pharmaceutical Sciences* 2020, *147*, 105280, doi:10.1016/j.ejps.2020.105280.

5. McConnell, E.L.; Fadda, H.M.; Basit, A.W. Gut instincts: explorations in intestinal physiology and drug delivery. *International Journal of Pharmaceutics* 2008, *364*, 213-226, doi:10.1016/j.ijpharm.2008.05.012.

6. Jamei, M.; Turner, D.; Yang, J.; Neuhoff, S.; Polak, S.; Rostami-Hodjegan, A.; Tucker, G. Population-Based Mechanistic Prediction of Oral Drug Absorption. *The AAPS Journal* 2009, *11*, 225-237, doi:10.1208/s12248-009-9099-y.

7. Feeney, O.M.; Crum, M.F.; McEvoy, C.L.; Trevaskis, N.L.; Williams, H.D.; Pouton, C.W.; Charman, W.N.; Bergström, C.A.; Porter, C.J. 50 years of oral lipid-based formulations: provenance, progress and future perspectives. *Advanced Drug Delivery Reviews* 2016, *101*, 167-194.

8. Rangaraj, N.; Sampathi, S.; Junnuthula, V.; Kolimi, P.; Mandati, P.; Narala, S.; Nyavanandi, D.; Dyawanapelly, S. Fast-Fed Variability: Insights into Drug Delivery, Molecular Manifestations, and Regulatory Aspects. *Pharmaceutics* 2022, *14*, 1807.

9. Koziolek, M.; Alcaro, S.; Augustijns, P.; Basit, A.W.; Grimm, M.; Hens, B.; Hoad, C.L.; Jedamzik, P.; Madla, C.M.; Maliepaard, M.; et al. The mechanisms of pharmacokinetic food-drug interactions – A perspective from the UNGAP group. *European Journal of Pharmaceutical Sciences* 2019, *134*, 31-59, doi:https://doi.org/10.1016/j.ejps.2019.04.003.

10. O'Shea, J.P.; Holm, R.; O'Driscoll, C.M.; Griffin, B.T. Food for thought: formulating away the food effect – a PEARRL review. *Journal of Pharmacy and Pharmacology* 2019, *71*, 510-535, doi:10.1111/jphp.12957.

11. FDA. Guidance for Industry: Food-Effect Bioavailability and Fed Bioequivalence Studies. Available online: https://www.fda.gov/files/drugs/published/Food-Effect-Bioavailability-and-Fed-Bioequivalence-Studies.pdf (accessed on 14/08/2020).

12. Camilleri, M. Integrated upper gastrointestinal response to food intake. *Gastroenterology* 2006, *131*, 640-658, doi:10.1053/j.gastro.2006.03.023.

13. Welling, P.G. Influence of food and diet on gastrointestinal drug absorption: A review. *Journal of Pharmacokinetics and Biopharmaceutics* 1977, *5*, 291-334, doi:10.1007/BF01061694.

14. Welling, P.G. Effects of food on drug absorption. *Pharmacology & therapeutics* 1989, *43*, 425-441.

15. Fleisher, D.; Li, C.; Zhou, Y.; Pao, L.-H.; Karim, A. Drug, Meal and Formulation Interactions Influencing Drug Absorption After Oral Administration. *Clinical Pharmacokinetics* 1999, *36*, 233-254, doi:10.2165/00003088-199936030-00004.

16. Pepin, X.J.H.; Huckle, J.E.; Alluri, R.V.; Basu, S.; Dodd, S.; Parrott, N.; Emami Riedmaier, A. Understanding Mechanisms of Food Effect and Developing Reliable PBPK Models Using a Middle-out Approach. *The AAPS Journal* 2021, *23*, 12, doi:10.1208/s12248-020-00548-8.

17. FDA. Assessing the Effects of Food on Drugs in INDs and NDAs — Clinical Pharmacology Considerations. Draft Guidance for Industry. Available online: https://www.fda.gov/media/121313/download (accessed on 01/03/2021).

18. Kesisoglou, F. Can PBPK Modeling Streamline Food Effect Assessments? *The Journal of Clinical Pharmacology* 2020, *60*, S98-S104, doi:https://doi.org/10.1002/jcph.1678.

19. EMA. Guideline on the Investigation of Drug Interactions. Available online: https://www.ema.europa.eu/documents/scientific-guideline/guideline-investigation-drug-interactions_en.pdf (accessed on

20. Goetze, O.; Steingoetter, A.; Menne, D.; van der Voort, I.R.; Kwiatek, M.A.; Boesiger, P.; Weishaupt, D.; Thumshirn, M.; Fried, M.; Schwizer, W. The effect of macronutrients on gastric volume responses and gastric emptying in humans: a magnetic resonance imaging study. *American Journal of Physiology-Gastrointestinal and Liver Physiology* 2007, *292*, G11-G17.

21. Lentz, K.A. Current methods for predicting human food effect. *The AAPS journal* 2008, *10*, 282-288.

22. Meola, T.R.; Bremmell, K.E.; Williams, D.B.; Schultz, H.B.; Prestidge, C.A. Bio-enabling strategies to mitigate the pharmaceutical food effect: A mini review. *International Journal of Pharmaceutics* 2022, *619*, 121695, doi:https://doi.org/10.1016/j.ijpharm.2022.121695.

23. Dahan, A.; Altman, H. Food-drug interaction: grapefruit juice augments drug bioavailability--mechanism, extent and relevance. *European journal of clinical nutrition* 2004, *58*, 1-9, doi:10.1038/sj.ejcn.1601736.

24. Varum, F.J.O.; Hatton, G.B.; Basit, A.W. Food, physiology and drug delivery. *International Journal of Pharmaceutics* 2013, *457*, 446-460, doi:10.1016/j.ijpharm.2013.04.034.

25. Abuhelwa, A.Y.; Foster, D.J.R.; Upton, R.N. A Quantitative Review and Meta-Models of the Variability and Factors Affecting Oral Drug Absorption—Part I: Gastrointestinal pH. *The AAPS Journal* 2016, *18*, 1309-1321, doi:10.1208/s12248-016-9952-8.

26. Schiller, C.; Fröhlich, C.-P.; Giessmann, T.; Siegmund, W.; Mönnikes, H.; Hosten, N.; Weitschies, W. Intestinal fluid volumes and transit of dosage forms as assessed by magnetic resonance imaging. *Alimentary Pharmacology & Therapeutics* 2005, *22*, 971-979, doi:10.1111/j.1365-2036.2005.02683.x.

27. Kalantzi, L.; Goumas, K.; Kalioras, V.; Abrahamsson, B.; Dressman, J.B.; Reppas, C. Characterization of the Human Upper Gastrointestinal Contents Under Conditions Simulating Bioavailability/Bioequivalence Studies. *Pharmaceutical Research* 2006, *23*, 165-176, doi:10.1007/s11095-005-8476-1.

28. Koziolek, M.; Grimm, M.; Garbacz, G.; Kühn, J.-P.; Weitschies, W. Intragastric volume changes after intake of a high-caloric, high-fat standard breakfast in healthy human subjects investigated by MRI. *Pharmaceutics* 2014, *11*, 1632-1639.

29. Sommers, D.K.; van Wyk, M.; Moncrieff, J.; Schoeman, H.S. Influence of food and reduced gastric acidity on the bioavailability of bacampicillin and cefuroxime axetil. *British journal of clinical pharmacology* 1984, *18*, 535-539, doi:10.1111/j.1365-2125.1984.tb02501.x.

30. Derendorf, H.; VanderMaelen, C.P.; Brickl, R.S.; MacGregor, T.R.; Eisert, W. Dipyridamole bioavailability in subjects with reduced gastric acidity. *The journal of clinical pharmacology* 2005, *45*, 845-850, doi:10.1177/0091270005276738.

31. Bartholomé, R.; Salden, B.; Vrolijk, M.F.; Troost, F.J.; Masclee, A.; Bast, A.; Haenen, G.R. Paracetamol as a Post Prandial Marker for Gastric Emptying, A Food-Drug Interaction on Absorption. *PLoS One* 2015, *10*, e0136618, doi:10.1371/journal.pone.0136618.

32. Schmidt, L.E.; Dalhoff, K. Food-Drug Interactions. *Drugs* 2002, *62*, 1481-1502, doi:10.2165/00003495-200262100-00005.

33. Clarysse, S.; Tack, J.; Lammert, F.; Duchateau, G.; Reppas, C.; Augustijns, P. Postprandial evolution in composition and characteristics of human duodenal fluids in different nutritional states. *Journal of pharmaceutical sciences* 2009, *98*, 1177-1192.

34. Watts, A.; Williams III, R. Formulation and production strategies for enhancing bioavailability of poorly absorbed drugs. In *Preclinical Drug Development*; CRC Press: 2016; pp. 173-207.

35. Morcos, P.N.; Guerini, E.; Parrott, N.; Dall, G.; Blotner, S.; Bogman, K.; Sturm, C.; Balas, B.; Martin-Facklam, M.; Phipps, A. Effect of Food and Esomeprazole on the Pharmacokinetics of Alectinib, a Highly Selective ALK Inhibitor, in Healthy Subjects. *Clinical Pharmacology in Drug Development* 2017, *6*, 388-397, doi:https://doi.org/10.1002/cpdd.296.

36. Radwan, A.; Zaid, A.N.; Jaradat, N.; Odeh, Y. Food effect: The combined effect of media pH and viscosity on the gastrointestinal absorption of ciprofloxacin tablet. *European Journal of Pharmaceutical Sciences* 2017, *101*, 100-106, doi:https://doi.org/10.1016/j.ejps.2017.01.030.

37. Marasanapalle, V.P.; Boinpally, R.R.; Zhu, H.; Grill, A.; Tang, F. Correlation between the systemic clearance of drugs and their food effects in humans. *Drug Development and Industrial Pharmacy* 2011, *37*, 1311-1317.

38. Porter, C.J.; Charman, W.N. Intestinal lymphatic drug transport: an update. *Advanced drug delivery reviews* 2001, *50*, 61-80.

39. Melander, A.; McLean, A. Influence of food intake on presystemic clearance of drugs. *Clinical pharmacokinetics* 1983, *8*, 286-296, doi:10.2165/00003088-198308040-00002.

40. Schubert, M.L.; Peura, D.A. Control of gastric acid secretion in health and disease. *Gastroenterology* 2008, *134*, 1842-1860.

41. Gribble, F.M.; Reimann, F. Nutrient sensing in the gut and the regulation of appetite. *Current Opinion in Endocrine and Metabolic Research* 2022, *23*, 100318, doi:https://doi.org/10.1016/j.coemr.2022.100318.

42. Farré, R.; Tack, J. Food and symptom generation in functional gastrointestinal disorders: physiological aspects. *Official journal of the American College of Gastroenterology| ACG* 2013, *108*, 698-706.

43. Weitschies, W.; Blume, H.; Mönnikes, H. Magnetic Marker Monitoring: High resolution real-time tracking of oral solid dosage forms in the gastrointestinal tract. *European Journal of Pharmaceutics and Biopharmaceutics* 2010, *74*, 93-101, doi:https://doi.org/10.1016/j.ejpb.2009.07.007.

44. Fadda, H.M.; McConnell, E.L.; Short, M.D.; Basit, A.W. Meal-induced acceleration of tablet transit through the human small intestine. *Pharmaceutical research* 2009, *26*, 356-360, doi:10.1007/s11095-008-9749-2.

45. Schinkel, A.H.; Jonker, J.W. Mammalian drug efflux transporters of the ATP binding cassette (ABC) family: an overview. *Advanced drug delivery reviews* 2003, *64*, 138-153.

46. Giacomini, K.M.; Huang, S.-M.; Tweedie, D.J.; Benet, L.Z.; Brouwer, K.L.R.; Chu, X.; Dahlin, A.; Evers, R.; Fischer, V.; Hillgren, K.M.; et al. Membrane transporters in drug development. *Nature Reviews Drug Discovery* 2010, *9*, 215-236, doi:10.1038/nrd3028.

47. FDA. *In Vitro Drug Interaction Studies — Cytochrome P450 Enzyme- and Transporter-Mediated Drug Interactions Guidance for Industry*; 2020.

48. Fricker, G.; Miller, D.S. Relevance of Multidrug Resistance Proteins for Intestinal Drug Absorption in vitro and in vivo. *Pharmacology & Toxicology* 2002, *90*, 5-13, doi:https://doi.org/10.1034/j.1600-0773.2002.900103.x.

49. Fu, S.; Yu, F.; Sun, T.; Hu, Z. Transporter-mediated drug–drug interactions – Study design, data analysis, and implications for in vitro evaluations. *Medicine in Drug Discovery* 2021, *11*, 100096, doi:https://doi.org/10.1016/j.medidd.2021.100096.

50. FDA. Drug Development and Drug Interactions | Table of Substrates, Inhibitors and Inducers. Available online: https://www.fda.gov/drugs/drug-interactions-labeling/drug-development-and-drug-interactions-table-substrates-inhibitors-and-inducers (accessed on 01/06/2022).

51. Suzuki, H.; Sugiyama, Y. Role of metabolic enzymes and efflux transporters in the absorption of drugs from the small intestine. *European journal of pharmaceutical sciences* 2000, *12*, 3-12, doi:10.1016/S0928-0987(00)00178-0.

52. Egido, E.; Müller, R.; Li-Blatter, X.; Merino, G.; Seelig, A. Predicting activators and inhibitors of the breast cancer resistance protein (ABCG2) and P-glycoprotein

(ABCB1) based on mechanistic considerations. *Molecular pharmaceutics* 2015, *12*, 4026-4037.

53. Seelig, A. P-Glycoprotein: One Mechanism, Many Tasks and the Consequences for Pharmacotherapy of Cancers. *Frontiers in Oncology* 2020, *10*, doi:10.3389/fonc.2020.576559.

54. Tarling, E.J.; de Aguiar Vallim, T.Q.; Edwards, P.A. Role of ABC transporters in lipid transport and human disease. *Trends in endocrinology and metabolism: TEM* 2013, *24*, 342-350, doi:10.1016/j.tem.2013.01.006.

55. Juliano, R.L.; Ling, V. A surface glycoprotein modulating drug permeability in Chinese hamster ovary cell mutants. *Biochimica et Biophysica Acta (BBA)-Biomembranes* 1976, *455*, 152-162, doi:10.1016/0005-2736(76)90160-7.

56. Buchler, M.; Konig, J.; Brom, M.; Kartenbeck, J.; SPRING, H. cDNA cloning of the hepatocyte canalicular isoform of the multidrug resistance protein, cMrp, reveals a novel conjugate export pump deficient in hyperbilirubinemic mutant rats. *Journal of Biological Chemistry* 1996, *271*, 15091-15098.

57. Borst, P.; Evers, R.; Kool, M.; Wijnholds, J. A Family of Drug Transporters: the Multidrug Resistance-Associated Proteins. *JNCI: Journal of the National Cancer Institute* 2000, *92*, 1295-1302, doi:10.1093/jnci/92.16.1295.

58. Doyle, L.A.; Yang, W.; Abruzzo, L.V.; Krogmann, T.; Gao, Y.; Rishi, A.K.; Ross, D.D. A multidrug resistance transporter from human MCF-7 breast cancer cells. *Proceedings of the National Academy of Sciences* 1998, *95*, 15665-15670.

59. Basit, A.W.; Madla, C.M.; Gavins, F.K.H. Robotic screening of intestinal drug absorption. *Nature Biomedical Engineering* 2020, *4*, 485-486, doi:10.1038/s41551-020-0551-8.

60. Robey, R.W.; Pluchino, K.M.; Hall, M.D.; Fojo, A.T.; Bates, S.E.; Gottesman, M.M. Revisiting the role of ABC transporters in multidrug-resistant cancer. *Nature Reviews Cancer* 2018, *18*, 452-464, doi:10.1038/s41568-018-0005-8.

61. Vasiliou, V.; Vasiliou, K.; Nebert, D.W. Human ATP-binding cassette (ABC) transporter family. *Human genomics* 2009, *3*, 281-290, doi:10.1186/1479-7364-3-3-281.

62. Taipalensuu, J.; Törnblom, H.; Lindberg, G.; Einarsson, C.; Sjöqvist, F.; Melhus, H.; Garberg, P.; Sjöström, B.; Lundgren, B.; Artursson, P. Correlation of gene expression of ten drug efflux proteins of the ATP-binding cassette transporter family in normal human jejunum and in human intestinal epithelial Caco-2 cell monolayers. *Journal of Pharmacology and Experimental Therapeutics* 2001, *299*, 164-170.

63. Deferme, S.; Augustijns, P. The effect of food components on the absorption of P-gp substrates: a review. *J Pharm Pharmacol* 2003, *55*, 153-162, doi:10.1211/002235702603.

64. Shugarts, S.; Benet, L.Z. The role of transporters in the pharmacokinetics of orally administered drugs. *Pharmaceutical research* 2009, *26*, 2039-2054, doi:10.1007/s11095-009-9924-0.

65. Dietrich, C.G.; Geier, A.; Oude Elferink, R.P. ABC of oral bioavailability: transporters as gatekeepers in the gut. *Gut* 2003, *52*, 1788-1795, doi:10.1136/gut.52.12.1788.

66. Evers, R.; Piquette-Miller, M.; Polli, J.W.; Russel, F.G.M.; Sprowl, J.A.; Tohyama, K.; Ware, J.A.; de Wildt, S.N.; Xie, W.; Brouwer, K.L.R. Disease-Associated Changes in Drug Transporters May Impact the Pharmacokinetics and/or Toxicity of Drugs: A White Paper From the International Transporter Consortium. *Clinical Pharmacology & Therapeutics* 2018, *104*, 900-915, doi:10.1002/cpt.1115.

67. Custodio, J.M.; Wu, C.-Y.; Benet, L.Z. Predicting drug disposition, absorption/elimination/transporter interplay and the role of food on drug absorption. *Advanced drug delivery reviews* 2008, *60*, 717-733.

68. Won, C.S.; Oberlies, N.H.; Paine, M.F. Mechanisms underlying food–drug interactions: inhibition of intestinal metabolism and transport. *Pharmacology & therapeutics* 2012, *136*, 186-201.

69. Domínguez, C.J.; Tocchetti, G.N.; Rigalli, J.P.; Mottino, A.D. Acute regulation of apical ABC transporters in the gut. Potential influence on drug bioavailability. *Pharmacological Research* 2020, 105251, doi:10.1016/j.phrs.2020.105251.

70. Fleisher, B.; Unum, J.; Shao, J.; An, G. Ingredients in fruit juices interact with dasatinib through inhibition of BCRP: a new mechanism of beverage-drug interaction. *Journal of Pharmaceutical Sciences* 2015, *104*, 266-275, doi:10.1002/jps.24289.

71. Whitley, H.P.; Lindsey, W. Sex-based differences in drug activity. *American family physician* 2009, *80*, 1254-1258.

72. Pirmohamed, M.; James, S.; Meakin, S.; Green, C.; Scott, A.K.; Walley, T.J.; Farrar, K.; Park, B.K.; Breckenridge, A.M. Adverse drug reactions as cause of admission to hospital: prospective analysis of 18 820 patients. *BMJ* 2004, *329*, 15-19.

73. Madla, C.M.; Gavins, F.K.H.; Merchant, H.; Orlu, M.; Murdan, S.; Basit, A.W. Let's Talk About Sex: Differences in Drug Therapy in Males and Females. *Advanced Drug Delivery Reviews* 2021, doi:10.1016/j.addr.2021.05.014.

74. FDA. Guideline for the Study and Evaluation of Gender Differences in the Clinical Evaluation of Drugs. Available online: https://www.fda.gov/media/71107/download (accessed on 01/01/2019).

75. Beery, A.K.; Zucker, I. Sex bias in neuroscience and biomedical research. *Neuroscience & Biobehavioral Reviews* 2011, *35*, 565-572.

76. Parekh, A.; Fadiran, E.O.; Uhl, K.; Throckmorton, D.C. Adverse effects in women: implications for drug development and regulatory policies. *Expert review of clinical pharmacology* 2011, *4*, 453-466.

77. McBride, W.G. Thalidomide and congenital abnormalities. *Lancet* 1961, *2*, 90927-90928.

78. NIH. Policy and Guidelines on The Inclusion of Women and Minorities as Subjects in Clinical Research. Available online: https://grants.nih.gov/policy/inclusion/women-and-minorities/guidelines.htm (accessed on 01/01/2019).

79. NIH. Consideration of sex as a biological variable in NIH-funded research. Available online: :grants.nih.gov/grants/guide/notice-files/NOT-OD-15-102.html (accessed on 01/01/2019).

80. MRC. Guidance for Applicants. 2022.

81. Pardue, M.-L.; Wizemann, T.M. *Exploring the biological contributions to human health: does sex matter?*; National Academies Press: 2001.

82. Schiebinger, L.; Klinge, I. Gendered Innovations 2: How Inclusive Analysis Contributes to Research and Innovation. 2020.

83. Scandlyn, M.J.; Stuart, E.C.; Rosengren, R.J. Sex-specific differences in CYP450 isoforms in humans. *Expert opinion on drug Metabolism & toxicology* 2008, *4*, 413-424, doi:10.1517/17425255.4.4.413.

84. Tanaka, E. Gender-related differences in pharmacokinetics and their clinical significance. *Journal of clinical pharmacy and therapeutics* 1999, *24*, 339-346.

85. Smirnova, O. Sex differences in drug action: The role of multidrug-resistance proteins (MRPs). *Fiziologiia Cheloveka* 2012, *38*, 124-136.

86. Kees, F.; Bucher, M.; Schweda, F.; Gschaidmeier, H.; Faerber, L.; Seifert, R. Neoimmun versus Neoral: a bioequivalence study in healthy volunteers and influence of a fat-rich meal on the bioavailability of Neoimmun. *Naunyn-Schmiedeberg's archives of pharmacology* 2007, *375*, 393-399.

87. Klein, S.L.; Roberts, C.W. *Sex and gender differences in infection and treatments for infectious diseases*; Springer: 2015.

88. Prewett, E.; Smith, J.; Nwokolo, C.; Sawyerr, A.; Pounder, R. Twenty-four hour intragastric acidity and plasma gastrin concentration profiles in female and male subjects. *Clinical Science* 1991, *80*, 619-624.

89. Freire, A.C.; Basit, A.W.; Choudhary, R.; Piong, C.W.; Merchant, H.A. Does sex matter? The influence of gender on gastrointestinal physiology and drug delivery. *International Journal of Pharmaceutics* 2011, *415*, 15-28, doi:10.1016/j.ijpharm.2011.04.069.

90. McGregor, A.J.; Markowitz, J.S.; Forrester, J.; Shader, R.I. Joining the effort: the challenges in establishing guidelines for sex-and gender-specific research design in clinical therapeutic studies. *Clinical Therapeutics* 2017, *39*, 1912-1916.

91. Bhupathy, P.; Haines, C.D.; Leinwand, L.A. Influence of sex hormones and phytoestrogens on heart disease in men and women. *Women's health* 2010, *6*, 77-95.

92. Beery, A.K. Inclusion of females does not increase variability in rodent research studies. *Curr Opin Behav Sci* 2018, *23*, 143-149, doi:10.1016/j.cobeha.2018.06.016.

93. Jantratid, E.; Janssen, N.; Reppas, C.; Dressman, J.B. Dissolution media simulating conditions in the proximal human gastrointestinal tract: an update. *Pharmaceutical research* 2008, *25*, 1663-1676, doi:10.1007/s11095-008-9569-4.

94. Klein, S. The use of biorelevant dissolution media to forecast the in vivo performance of a drug. *The AAPS journal* 2010, *12*, 397-406, doi:10.1208/s12248-010-9203-3.

95. Klumpp, L.; Leigh, M.; Dressman, J. Dissolution behavior of various drugs in different FaSSIF versions. *European Journal of Pharmaceutical Sciences* 2020, *142*, 105138, doi:https://doi.org/10.1016/j.ejps.2019.105138.

96. Sassene, P.; Kleberg, K.; Williams, H.D.; Bakala-N'Goma, J.-C.; Carrière, F.; Calderone, M.; Jannin, V.; Igonin, A.; Partheil, A.; Marchaud, D. Toward the establishment of standardized in vitro tests for lipid-based formulations, part 6: effects of varying pancreatin and calcium levels. *The AAPS journal* 2014, *16*, 1344-1357.

97. Borbás, E.; Kádár, S.; Tsinman, K.; Tsinman, O.; Csicsák, D.; Takács-Novák, K.; Völgyi, G.; Sinkó, B.; Pataki, H. Prediction of Bioequivalence and Food Effect Using Flux- and Solubility-Based Methods. *Molecular Pharmaceutics* 2019, *16*, 4121-4130, doi:10.1021/acs.molpharmaceut.9b00406.

98. Mathias, N.; Xu, Y.; Vig, B.; Kestur, U.; Saari, A.; Crison, J.; Desai, D.; Vanarase, A.; Hussain, M. Food Effect in Humans: Predicting the Risk Through In Vitro Dissolution and In Vivo Pharmacokinetic Models. *The AAPS Journal* 2015, *17*, 988-998, doi:10.1208/s12248-015-9759-z.

99. Gamsiz, E.D.; Ashtikar, M.; Crison, J.; Woltosz, W.; Bolger, M.B.; Carrier, R.L. Predicting the effect of fed-state intestinal contents on drug dissolution. *Pharmaceutical research* 2010, *27*, 2646-2656.

100. Shono, Y.; Jantratid, E.; Janssen, N.; Kesisoglou, F.; Mao, Y.; Vertzoni, M.; Reppas, C.; Dressman, J.B. Prediction of food effects on the absorption of celecoxib based on biorelevant dissolution testing coupled with physiologically based pharmacokinetic modeling. *European Journal of Pharmaceutics and Biopharmaceutics* 2009, *73*, 107-114.

101. Dahlgren, D.; Venczel, M.; Ridoux, J.P.; Skjöld, C.; Müllertz, A.; Holm, R.; Augustijns, P.; Hellström, P.M.; Lennernäs, H. Fasted and fed state human duodenal fluids: Characterization, drug solubility, and comparison to simulated fluids and with human bioavailability. *European Journal of Pharmaceutics and Biopharmaceutics* 2021, *163*, 240-251, doi:https://doi.org/10.1016/j.ejpb.2021.04.005.

102. Dressman, J.B.; Reppas, C. In vitro–in vivo correlations for lipophilic, poorly water-soluble drugs. *European journal of pharmaceutical sciences* 2000, *11*, S73-S80.

103. Russell, W.M.S.; Burch, R.L. *The principles of humane experimental technique*; Methuen: 1959.

104. Zhao, Y.H.; Abraham, M.H.; Le, J.; Hersey, A.; Luscombe, C.N.; Beck, G.; Sherborne, B.; Cooper, I. Evaluation of rat intestinal absorption data and correlation with human intestinal absorption. *European Journal of Medicinal Chemistry* 2003, *38*, 233-243, doi:https://doi.org/10.1016/S0223-5234(03)00015-1.

105. Lentz, K.A.; Quitko, M.; Morgan, D.G.; Grace, J.E., Jr.; Gleason, C.; Marathe, P.H. Development and validation of a preclinical food effect model. *Journal of pharmaceutical sciences* 2007, *96*, 459-472, doi:10.1002/jps.20767.

106. Cook, C.; Hauswald, C.; Grahn, A.; Kowalski, K.; Karim, A.; Koch, R.; Schoenhard, G.; Oppermann, J. Suitability of the dog as an animal model for evaluating

theophylline absorption and food effects from different formulations. *International journal of pharmaceutics* 1990, *60*, 125-132.

107. Lui, C.Y.; Amidon, G.L.; Berardi, R.R.; Fleisher, D.; Youngberg, C.; Dressman, J.B. Comparison of gastrointestinal pH in dogs and humans: implications on the use of the beagle dog as a model for oral absorption in humans. *Journal of pharmaceutical sciences* 1986, *75*, 271-274.

108. Paulson, S.K.; Vaughn, M.B.; Jessen, S.M.; Lawal, Y.; Gresk, C.J.; Yan, B.; Maziasz, T.J.; Cook, C.S.; Karim, A. Pharmacokinetics of celecoxib after oral administration in dogs and humans: effect of food and site of absorption. *Journal of Pharmacology and Experimental Therapeutics* 2001, *297*, 638-645.

109. Meyer, J.H.; Dressman, J.; Fink, A.; Amidon, G. Effect of size and density on canine gastric emptying of nondigestible solids. *Gastroenterology* 1985, *89*, 805-813.

110. Henze, L.J.; Koehl, N.J.; O'Shea, J.P.; Kostewicz, E.S.; Holm, R.; Griffin, B.T. The pig as a preclinical model for predicting oral bioavailability and in vivo performance of pharmaceutical oral dosage forms: a PEARRL review. *Journal of Pharmacy and Pharmacology* 2019, *71*, 581-602, doi:https://doi.org/10.1111/jphp.12912.

111. Henze, L.J.; Koehl, N.J.; O'Shea, J.P.; Holm, R.; Vertzoni, M.; Griffin, B.T. Combining species specific in vitro & in silico models to predict in vivo food effect in a preclinical stage - case study of Venetoclax. *European Journal of Pharmaceutical Sciences* 2021, *162*, 105840, doi:10.1016/j.ejps.2021.105840.

112. Christiansen, M.L.; Müllertz, A.; Garmer, M.; Kristensen, J.; Jacobsen, J.; Abrahamsson, B.; Holm, R. Evaluation of the use of Göttingen minipigs to predict food effects on the oral absorption of drugs in humans. *Journal of Pharmaceutical Sciences* 2015, *104*, 135-143.

113. Grove, M.; Müllertz, A.; Pedersen, G.P.; Nielsen, J.L. Bioavailability of seocalcitol: III. Administration of lipid-based formulations to minipigs in the fasted and fed state. *European journal of pharmaceutical sciences* 2007, *31*, 8-15.

114. Henze, L.J.; Koehl, N.J.; O'Shea, J.P.; Holm, R.; Vertzoni, M.; Griffin, B.T. Toward the establishment of a standardized pre-clinical porcine model to predict food effects - Case studies on fenofibrate and paracetamol. *International journal of pharmaceutics: X* 2019, *1*, 100017, doi:10.1016/j.ijpx.2019.100017.

115. Kararli, T.T. Comparison of the gastrointestinal anatomy, physiology, and biochemistry of humans and commonly used laboratory animals. *Biopharmaceutics & Drug Disposition* 1995, *16*, 351-380, doi:10.1002/bdd.2510160502.

116. Hauss, D.J. Oral lipid-based formulations. *Advanced drug delivery reviews* 2007, *59*, 667-676.

117. Hatton, G.B.; Yadav, V.; Basit, A.W.; Merchant, H.A. Animal Farm: Considerations in Animal Gastrointestinal Physiology and Relevance to Drug Delivery in Humans. *Journal of Pharmaceutical Sciences* 2015, *104*, 2747-2776, doi:10.1002/jps.24365.

118. Sjögren, E.; Abrahamsson, B.; Augustijns, P.; Becker, D.; Bolger, M.B.; Brewster, M.; Brouwers, J.; Flanagan, T.; Harwood, M.; Heinen, C.; et al. In vivo methods for drug absorption – Comparative physiologies, model selection, correlations with in vitro methods (IVIVC), and applications for formulation/API/excipient characterization including food effects. *European Journal of Pharmaceutical Sciences* 2014, *57*, 99-151, doi:10.1016/j.ejps.2014.02.010.

119. Davies, B.; Morris, T. Physiological Parameters in Laboratory Animals and Humans. *Pharmaceutical Research* 1993, *10*, 1093-1095, doi:10.1023/A:1018943613122.

120. Cao, X.; Gibbs, S.T.; Fang, L.; Miller, H.A.; Landowski, C.P.; Shin, H.-C.; Lennernas, H.; Zhong, Y.; Amidon, G.L.; Lawrence, X.Y. Why is it challenging to predict intestinal drug absorption and oral bioavailability in human using rat model. *Pharmaceutical research* 2006, *23*, 1675-1686.

121. DeSesso, J.M.; Jacobson, C.F. Anatomical and physiological parameters affecting gastrointestinal absorption in humans and rats. *Food and Chemical Toxicology* 2001, *39*, 209-228, doi:https://doi.org/10.1016/S0278-6915(00)00136-8.

122. Yu, P.; Lu, S.; Zhang, S.; Zhang, W.; Li, Y.; Liu, J. Enhanced oral bioavailability and diminished food effect of lurasidone hydrochloride nanosuspensions prepared by facile nanoprecipitation based on dilution. *Powder Technology* 2017, *312*, 11-20, doi:https://doi.org/10.1016/j.powtec.2017.02.038.

123. Mou, D.; Chen, H.; Wan, J.; Xu, H.; Yang, X. Potent dried drug nanosuspensions for oral bioavailability enhancement of poorly soluble drugs with pH-dependent solubility. *International Journal of Pharmaceutics* 2011, *413*, 237-244, doi:https://doi.org/10.1016/j.ijpharm.2011.04.034.

124. Elbadawi, M.; McCoubrey, L.E.; Gavins, F.K.H.; Jie Ong, J.; Goyanes, A.; Gaisford, S.; Basit, A.W. Harnessing Artificial Intelligence for the Next Generation of 3D Printed Medicines. *Advanced Drug Delivery Reviews* 2021, doi:10.1016/j.addr.2021.05.015.

125. Heimbach, T.; Xia, B.; Lin, T.-h.; He, H. Case studies for practical food effect assessments across BCS/BDDCS class compounds using in silico, in vitro, and preclinical in vivo data. *The AAPS journal* 2013, *15*, 143-158.

126. Zhang, T.; Wells, E. A review of current methods for food effect prediction during drug development. *Current Pharmacology Reports* 2020, *6*, 267-279.

127. Benet, L.Z. The Role of BCS (Biopharmaceutics Classification System) and BDDCS (Biopharmaceutics Drug Disposition Classification System) in Drug Development.

Journal of Pharmaceutical Sciences 2013, *102*, 34-42, doi:https://doi.org/10.1002/jps.23359.

128. Emami Riedmaier, A.; Lindley, D.J.; Hall, J.A.; Castleberry, S.; Slade, R.T.; Stuart, P.; Carr, R.A.; Borchardt, T.B.; Bow, D.A.; Nijsen, M. Mechanistic physiologically based pharmacokinetic modeling of the dissolution and food effect of a Biopharmaceutics Classification System IV compound—the venetoclax story. *Journal of pharmaceutical sciences* 2018, *107*, 495-502.

129. Xia, B.; Heimbach, T.; Lin, T.-h.; Li, S.; Zhang, H.; Sheng, J.; He, H. Utility of physiologically based modeling and preclinical in vitro/in vivo data to mitigate positive food effect in a BCS class 2 compound. *AAPS PharmSciTech* 2013, *14*, 1255-1266.

130. Jones, H.; Rowland-Yeo, K. Basic concepts in physiologically based pharmacokinetic modeling in drug discovery and development. *CPT: pharmacometrics & systems pharmacology* 2013, *2*, e63, doi:10.1038/psp.2013.41.

131. Pentafragka, C.; Symillides, M.; McAllister, M.; Dressman, J.; Vertzoni, M.; Reppas, C. The impact of food intake on the luminal environment and performance of oral drug products with a view to in vitro and in silico simulations: a PEARRL review. *Journal of Pharmacy and Pharmacology* 2019, *71*, 557-580, doi:10.1111/jphp.12999.

132. Emami Riedmaier, A.; DeMent, K.; Huckle, J.; Bransford, P.; Stillhart, C.; Lloyd, R.; Alluri, R.; Basu, S.; Chen, Y.; Dhamankar, V.; et al. Use of Physiologically Based Pharmacokinetic (PBPK) Modeling for Predicting Drug-Food Interactions: an Industry Perspective. *The AAPS Journal* 2020, *22*, 123, doi:10.1208/s12248-020-00508-2.

133. Pepin, X.J.H.; Huckle, J.E.; Alluri, R.V.; Basu, S.; Dodd, S.; Parrott, N.; Emami Riedmaier, A. Understanding Mechanisms of Food Effect and Developing Reliable PBPK Models Using a Middle-out Approach. *Aaps j* 2021, *23*, 12, doi:10.1208/s12248-020-00548-8.

134. Li, M.; Zhao, P.; Pan, Y.; Wagner, C. Predictive performance of physiologically based pharmacokinetic models for the effect of food on oral drug absorption: current status. *CPT: pharmacometrics & systems pharmacology* 2018, *7*, 82-89.

135. Cheng, L.; Wong, H. Food Effects on Oral Drug Absorption: Application of Physiologically-Based Pharmacokinetic Modeling as a Predictive Tool. *Pharmaceutics* 2020, *12*, 672.

136. Lennernäs, H.; Aarons, L.; Augustijns, P.; Beato, S.; Bolger, M.; Box, K.; Brewster, M.; Butler, J.; Dressman, J.; Holm, R.; et al. Oral biopharmaceutics tools – Time for a new initiative – An introduction to the IMI project OrBiTo. *European Journal of Pharmaceutical Sciences* 2014, *57*, 292-299, doi:https://doi.org/10.1016/j.ejps.2013.10.012.

137. Elbadawi, M.; Muñiz Castro, B.; Gavins, F.K.H.; Ong, J.J.; Gaisford, S.; Pérez, G.; Basit, A.W.; Cabalar, P.; Goyanes, A. M3DISEEN: A novel machine learning approach for predicting the 3D printability of medicines. *International Journal of Pharmaceutics* 2020, *590*, 119837, doi:https://doi.org/10.1016/j.ijpharm.2020.119837.

138. Schneckener, S.; Grimbs, S.; Hey, J.; Menz, S.; Osmers, M.; Schaper, S.; Hillisch, A.; Göller, A.H. Prediction of Oral Bioavailability in Rats: Transferring Insights from in Vitro Correlations to (Deep) Machine Learning Models Using in Silico Model Outputs and Chemical Structure Parameters. *Journal of Chemical Information and Modeling* 2019, *59*, 4893-4905, doi:10.1021/acs.jcim.9b00460.

139. Cabrera-Pérez, M.Á.; Pham-The, H. Computational modeling of human oral bioavailability: what will be next? *Expert Opinion on Drug Discovery* 2018, *13*, 509-521, doi:10.1080/17460441.2018.1463988.

140. Dey, S.; Luo, H.; Fokoue, A.; Hu, J.; Zhang, P. Predicting adverse drug reactions through interpretable deep learning framework. *BMC Bioinformatics* 2018, *19*, 476, doi:10.1186/s12859-018-2544-0.

141. Rohani, N.; Eslahchi, C. Drug-Drug Interaction Predicting by Neural Network Using Integrated Similarity. *Scientific Reports* 2019, *9*, 13645, doi:10.1038/s41598-019-50121-3.

142. Ryu, J.Y.; Kim, H.U.; Lee, S.Y. Deep learning improves prediction of drug–drug and drug–food interactions. *Proceedings of the National Academy of Sciences* 2018, *115*, E4304-E4311, doi:10.1073/pnas.1803294115.

143. Reker, D.; Shi, Y.; Kirtane, A.R.; Hess, K.; Zhong, G.J.; Crane, E.; Lin, C.-H.; Langer, R.; Traverso, G. Machine Learning Uncovers Food- and Excipient-Drug Interactions. *Cell Reports* 2020, *30*, 3710-3716.e3714, doi:10.1016/j.celrep.2020.02.094.

144. Zhou, H.; Cao, H.; Matyunina, L.; Shelby, M.; Cassels, L.; McDonald, J.F.; Skolnick, J. MEDICASCY: A Machine Learning Approach for Predicting Small-Molecule Drug Side Effects, Indications, Efficacy, and Modes of Action. *Molecular Pharmaceutics* 2020, *17*, 1558-1574, doi:10.1021/acs.molpharmaceut.9b01248.

145. Janssen, A.; Bennis, F.C.; Mathôt, R.A.A. Adoption of Machine Learning in Pharmacometrics: An Overview of Recent Implementations and Their Considerations. *Pharmaceutics* 2022, *14*, 1814.

146. Tang, J.; Liu, R.; Zhang, Y.-L.; Liu, M.-Z.; Hu, Y.-F.; Shao, M.-J.; Zhu, L.-J.; Xin, H.-W.; Feng, G.-W.; Shang, W.-J.; et al. Application of Machine-Learning Models to

Predict Tacrolimus Stable Dose in Renal Transplant Recipients. *Scientific reports* 2017, *7*, 42192-42192, doi:10.1038/srep42192.

147. Falcón-Cano, G.; Molina, C.; Cabrera-Pérez, M.Á. Reliable Prediction of Caco-2 Permeability by Supervised Recursive Machine Learning Approaches. *Pharmaceutics* 2022, *14*, 1998.

148. Bannigan, P.; Aldeghi, M.; Bao, Z.; Häse, F.; Aspuru-Guzik, A.; Allen, C. Machine learning directed drug formulation development. *Advanced Drug Delivery Reviews* 2021, *175*, doi:https://doi.org/10.1016/j.addr.2021.05.016.

149. Terranova, N.; Venkatakrishnan, K.; Benincosa, L.J. Application of machine learning in translational medicine: current status and future opportunities. *The AAPS Journal* 2021, *23*, 1-10.

150. Goldenberg, S.L.; Nir, G.; Salcudean, S.E. A new era: artificial intelligence and machine learning in prostate cancer. *Nature Reviews Urology* 2019, *16*, 391-403.

151. Hajjo, R.; Sabbah, D.A.; Bardaweel, S.K.; Tropsha, A. Identification of Tumor-Specific MRI Biomarkers Using Machine Learning (ML). *Diagnostics (Basel)* 2021, *11*, doi:10.3390/diagnostics11050742.

152. Pech-May, F.; Aquino-Santos, R.; Rios-Toledo, G.; Posadas-Durán, J.P.F. Mapping of Land Cover with Optical Images, Supervised Algorithms, and Google Earth Engine. *Sensors (Basel)* 2022, *22*, doi:10.3390/s22134729.

153. Schuhmacher, A.; Gatto, A.; Hinder, M.; Kuss, M.; Gassmann, O. The upside of being a digital pharma player. *Drug Discovery Today* 2020, *25*, 1569-1574, doi:https://doi.org/10.1016/j.drudis.2020.06.002.

154. Elbadawi, M.; Gaisford, S.; Basit, A.W. Advanced machine-learning techniques in drug discovery. *Drug Discovery Today* 2020, doi:https://doi.org/10.1016/j.drudis.2020.12.003.

155. Najm, M.; Azencott, C.A.; Playe, B.; Stoven, V. Drug Target Identification with Machine Learning: How to Choose Negative Examples. *Int J Mol Sci* 2021, *22*, doi:10.3390/ijms22105118.

156. Schuhmacher, A.; Gassmann, O.; Hinder, M.; Kuss, M. The present and future of project management in pharmaceutical R&D. *Drug Discovery Today* 2020, doi:https://doi.org/10.1016/j.drudis.2020.07.020.

157. Yang, Y.; Ye, Z.; Su, Y.; Zhao, Q.; Li, X.; Ouyang, D. Deep learning for in vitro prediction of pharmaceutical formulations. *Acta Pharmaceutica Sinica B* 2019, *9*, 177-185, doi:https://doi.org/10.1016/j.apsb.2018.09.010.

158. Kadhim, A.I. An evaluation of preprocessing techniques for text classification. *International Journal of Computer Science and Information Security (IJCSIS)* 2018, *16*, 22-32.

159. Rahm, E.; Do, H.H. Data cleaning: Problems and current approaches. *IEEE Data Engineering Bulletin* 2000, *23*, 3-13.

160. Ridzuan, F.; Zainon, W.M.N.W. A review on data cleansing methods for big data. *Procedia Computer Science* 2019, *161*, 731-738.

161. Singh, D.; Singh, B. Investigating the impact of data normalization on classification performance. *Applied Soft Computing* 2020, *97*, 105524, doi:https://doi.org/10.1016/j.asoc.2019.105524.

162. Elbadawi, M.; McCoubrey, L.E.; Gavins, F.K.H.; Ong, J.J.; Goyanes, A.; Gaisford, S.; Basit, A.W. Disrupting 3D printing of medicines with machine learning. *Trends Pharmacol Sci* 2021, doi:10.1016/j.tips.2021.06.002.

163. Pedregosa, F.; Varoquaux, G.; Gramfort, A.; Michel, V.; Thirion, B.; Grisel, O.; Blondel, M.; Prettenhofer, P.; Weiss, R.; Dubourg, V. Scikit-learn: Machine learning in Python. *Journal of Machine Learning Research* 2011, *12*, 2825-2830.

164. Chollet, F. Keras. Available online: https://www.sciencedirect.com/science/article/pii/S0169409X21001800?via%3Dihub#bib494 (accessed on 05/07/22).

165. Abadi, M.; Agarwal, A.; Barham, P.; Brevdo, E.; Chen, Z.; Citro, C.; Corrado, G.S.; Davis, A.; Dean, J.; Devin, M. Tensorflow: Large-scale machine learning on heterogeneous distributed systems. *arXiv preprint arXiv:1603.04467* 2016.

166. Bishop, C.M.; Nasrabadi, N.M. *Pattern recognition and machine learning*; Springer: 2006; Volume 4.

167. Shah, P.; Kendall, F.; Khozin, S.; Goosen, R.; Hu, J.; Laramie, J.; Ringel, M.; Schork, N. Artificial intelligence and machine learning in clinical development: a translational perspective. *npj Digital Medicine* 2019, *2*, 69, doi:10.1038/s41746-019-0148-3.

168. Yamada, H.; Liu, C.; Wu, S.; Koyama, Y.; Ju, S.; Shiomi, J.; Morikawa, J.; Yoshida, R. Predicting materials properties with little data using shotgun transfer learning. *ACS central science* 2019, *5*, 1717-1730.

169. Tarasova, O.A.; Biziukova, N.Y.; Filimonov, D.A.; Poroikov, V.V.; Nicklaus, M.C. Data mining approach for extraction of useful information about biologically active compounds from publications. *Journal of chemical information and modeling* 2019, *59*, 3635-3644.

170. Yegros-Yegros, A.; Leeuwen., T.N.v. Production and Uptake of Open Access Publications Involving the Private Sector: The Case of Big Pharma. 2019.

171. Xu, R.; Baracaldo, N.; Joshi, J. Privacy-Preserving Machine Learning: Methods, Challenges and Directions. *ArXiv* 2021, *abs/2108.04417*.

172. Molnar, C. *Interpretable machine learning*; Lulu. com: 2020.

173. Lundberg, S.M.; Lee, S.-I. A unified approach to interpreting model predictions. In Proceedings of the Proceedings of the 31st International Conference on Neural Information Processing Systems, Long Beach, California, USA, 2017; pp. 4768–4777.

174. Ribeiro, M.T.; Singh, S.; Guestrin, C. "Why Should I Trust You?": Explaining the Predictions of Any Classifier. In Proceedings of the Proceedings of the 22nd ACM SIGKDD International Conference on Knowledge Discovery and Data Mining, San Francisco, California, USA, 2016; pp. 1135–1144.

175. Benet, L.Z.; Broccatelli, F.; Oprea, T.I. BDDCS applied to over 900 drugs. *The AAPS Journal* 2011, *13*, 519-547, doi:10.1208/s12248-011-9290-9.

176. Sharma, S.; Prasad, B. Meta-Analysis of Food Effect on Oral Absorption of Efflux Transporter Substrate Drugs: Does Delayed Gastric Emptying Influence Drug Transport Kinetics? *Pharmaceutics* 2021, *13*, 1035.

177. ICH. M3 (R2) Nonclinical safety studies for the conduct of human clinical trials and marketing authorization for pharmaceuticals. Available online: https://www.ema.europa.eu/en/documents/scientific-guideline/ich-m-3-r2-non-clinical-safety-studies-conduct-human-clinical-trials-marketing-authorization_en.pdf (accessed on 01/01/2022).

178. Butler, L.D.; Guzzie-Peck, P.; Hartke, J.; Bogdanffy, M.S.; Will, Y.; Diaz, D.; Mortimer-Cassen, E.; Derzi, M.; Greene, N.; DeGeorge, J.J. Current nonclinical testing paradigms in support of safe clinical trials: an IQ consortium DruSafe perspective. *Regulatory Toxicology and Pharmacology* 2017, *87*, S1-S15.

179. Sengupta, P. The Laboratory Rat: Relating Its Age With Human's. *International journal of preventive medicine* 2013, *4*, 624-630.

180. Berkenhout, J. *Outlines of the natural history of Great Britain and Ireland, containing a systematic arrangement and concise description of all the animals,*

vegetables and fossiles which have hitherto been discovered in these kingdoms; Printed for P. Elmsly (Successor to Mr. Vaillant): London, 1769; Volume v.1 (1769).

181. Richter, C.P. The effects of domestication and selection on the behavior of the Norway rat. *Journal of the National Cancer Institute* 1954, *15*, 725-738.

182. Mayhew, H. *London labour and the London poor: A cyclopædia of the condition and earnings of those that will work, those that cannot work, and those that will not*; Cosimo, Inc.: 2009; Volume 1.

183. Hedrich, H.J. Taxonomy and stocks and strains. In *The laboratory rat*; Elsevier: 2006; pp. 71-92.

184. Brower, M.; Grace, M.; Kotz, C.M.; Koya, V. Comparative analysis of growth characteristics of Sprague Dawley rats obtained from different sources. *Lab Anim Res* 2015, *31*, 166-173, doi:10.5625/lar.2015.31.4.166.

185. Suckow, M.A.; Weisbroth, S.H.; Franklin, C.L. *The laboratory rat*; Elsevier: 2005.

186. White, W.J.; Cham, S. The Development and Maintenance of the Crl: CH!! J (SD) IGSBR Rat Breeding System. In *Biological Reference Data on CD (SD) IGS Rats*; 1998; pp. 8-14.

187. Musther, H.; Olivares-Morales, A.; Hatley, O.J.; Liu, B.; Rostami Hodjegan, A. Animal versus human oral drug bioavailability: do they correlate? *European Journal of Pharmaceutical Sciences* 2014, *57*, 280-291, doi:10.1016/j.ejps.2013.08.018.

188. Rybnikova, E.; Vetrovoi, O.; Zenko, M.Y. Comparative characterization of rat strains (Wistar, Wistar–Kyoto, Sprague Dawley, Long Evans, LT, SHR, BD-IX) by their behavior, hormonal level and antioxidant status. *Journal of Evolutionary Biochemistry and Physiology* 2018, *54*, 374-382.

189. Heemskerk, S.; Peters, J.G.; Louisse, J.; Sagar, S.; Russel, F.G.; Masereeuw, R. Regulation of P-glycoprotein in renal proximal tubule epithelial cells by LPS and TNF-α. *Journal of Biomedicine and Biotechnology* 2010, *2010*.

190. Luker, G.D.; Nilsson, K.R.; Covey, D.F.; Piwnica-Worms, D. Multidrug resistance (MDR1) P-glycoprotein enhances esterification of plasma membrane cholesterol. *Journal of Biological Chemistry* 1999, *274*, 6979-6991.

191. Foucaud-Vignault, M.; Soayfane, Z.; Ménez, C.; Bertrand-Michel, J.; Martin, P.G.P.; Guillou, H.; Collet, X.; Lespine, A. P-glycoprotein dysfunction contributes to hepatic steatosis and obesity in mice. *PLoS One* 2011, *6*, e23614.

192. Nakanishi, T.; Ross, D.D. Breast cancer resistance protein (BCRP/ABCG2): its role in multidrug resistance and regulation of its gene expression. *Chinese journal of cancer* 2012, *31*, 73-99, doi:10.5732/cjc.011.10320.

193. Harwood, M.D.; Zhang, M.; Pathak, S.M.; Neuhoff, S. The Regional-Specific Relative and Absolute Expression of Gut Transporters in Adult Caucasians: A Meta-Analysis. *Drug Metabolism and Disposition* 2019, *47*, 854-864, doi:10.1124/dmd.119.086959.

194. Drozdzik, M.; Gröer, C.; Penski, J.; Lapczuk, J.; Ostrowski, M.; Lai, Y.; Prasad, B.; Unadkat, J.D.; Siegmund, W.; Oswald, S. Protein Abundance of Clinically Relevant Multidrug Transporters along the Entire Length of the Human Intestine. *Molecular Pharmaceutics* 2014, *11*, 3547-3555, doi:10.1021/mp500330y.

195. Prasad, B.; Achour, B.; Artursson, P.; Hop, C.E.; Lai, Y.; Smith, P.C.; Barber, J.; Wisniewski, J.R.; Spellman, D.; Uchida, Y. Toward a consensus on applying quantitative liquid chromatography-tandem mass spectrometry proteomics in translational pharmacology research: a white paper. *Clinical Pharmacology & Therapeutics* 2019, *106*, 525-543.

196. Bass, J.J.; Wilkinson, D.J.; Rankin, D.; Phillips, B.E.; Szewczyk, N.J.; Smith, K.; Atherton, P.J. An overview of technical considerations for Western blotting applications to physiological research. *Scandinavian Journal of Medicine & Science in Sports* 2017, *27*, 4-25, doi:10.1111/sms.12702.

197. Li, W.; Jian, W.; Fu, Y. Basic Sample Preparation Techniques in LC-MS Bioanalysis. In *Sample Preparation in LC-MS Bioanalysis*; 2019; pp. 1-30.

198. Mennen, S.M.; Alhambra, C.; Allen, C.L.; Barberis, M.; Berritt, S.; Brandt, T.A.; Campbell, A.D.; Castañón, J.; Cherney, A.H.; Christensen, M.; et al. The Evolution of High-Throughput Experimentation in Pharmaceutical Development and Perspectives on the Future. *Organic Process Research & Development* 2019, *23*, 1213-1242, doi:10.1021/acs.oprd.9b00140.

199. Wegler, C.; Gaugaz, F.Z.; Andersson, T.B.; Wiśniewski, J.R.; Busch, D.; Gröer, C.; Oswald, S.; Norén, A.; Weiss, F.; Hammer, H.S. Variability in mass spectrometry-based quantification of clinically relevant drug transporters and drug metabolizing enzymes. *Molecular pharmaceutics* 2017, *14*, 3142-3151.

200. Shen, Y.; Prinyawiwatkul, W.; Xu, Z. Insulin: a review of analytical methods. *Analyst* 2019, *144*, 4139-4148, doi:10.1039/C9AN00112C.

201. Ginzinger, D.G. Gene quantification using real-time quantitative PCR: An emerging technology hits the mainstream. *Experimental Hematology* 2002, *30*, 503-512, doi:https://doi.org/10.1016/S0301-472X(02)00806-8.

202. MacLean, C.; Moenning, U.; Reichel, A.; Fricker, G. Closing the Gaps: A Full Scan of the Intestinal Expression of P-Glycoprotein, Breast Cancer Resistance Protein, and Multidrug Resistance-Associated Protein 2 in Male and Female Rats. *Drug Metabolism and Disposition* 2008, *36*, 1249, doi:10.1124/dmd.108.020859.

203. Hunter, J.D. Matplotlib: A 2D graphics environment. *Computing in Science & Engineering* 2007, *9*, 90-95, doi:10.1109/MCSE.2007.55.

204. Zimmermann, C.; Gutmann, H.; Hruz, P.; Gutzwiller, J.P.; Beglinger, C.; Drewe, J. Mapping of multidrug resistance gene 1 and multidrug resistance-associated protein isoform 1 to 5 mRNA expression along the human intestinal tract. *Drug metabolism and disposition* 2005, *33*, 219-224, doi:10.1124/dmd.104.001354.

205. Johnson, B.M.; Zhang, P.; Schuetz, J.D.; Brouwer, K.L. Characterization of transport protein expression in multidrug resistance-associated protein (Mrp) 2-deficient rats. *Drug metabolism and disposition* 2006, *34*, 556-562, doi:10.1124/dmd.105.005793.

206. Leslie, E.M.; Deeley, R.G.; Cole, S.P.C. Multidrug resistance proteins: role of P-glycoprotein, MRP1, MRP2, and BCRP (ABCG2) in tissue defense. *Toxicology and Applied Pharmacology* 2005, *204*, 216-237, doi:https://doi.org/10.1016/j.taap.2004.10.012.

207. Mai, Y.; Dou, L.; Yao, Z.; Madla, C.M.; Gavins, F.K.H.; Taherali, F.; Yin, H.; Orlu, M.; Murdan, S.; Basit, A.W. Quantification of P-Glycoprotein in the Gastrointestinal Tract of Humans and Rodents: Methodology, Gut Region, Sex, and Species Matter. *Molecular Pharmaceutics* 2021, *18*, 1895-1904, doi:10.1021/acs.molpharmaceut.0c00574.

208. Mottino, A.D.; Hoffman, T.; Jennes, L.; Vore, M. Expression and Localization of Multidrug Resistant Protein mrp2 in Rat Small Intestine. *Journal of Pharmacology and Experimental Therapeutics* 2000, *293*, 717.

209. Rost, D.; Mahner, S.; Sugiyama, Y.; Stremmel, W. Expression and localization of the multidrug resistance-associated protein 3 in rat small and large intestine. *American Journal of Physiology-Gastrointestinal and Liver Physiology* 2002, *282*, G720-G726, doi:10.1152/ajpgi.00318.2001.

210. Madla, C.M.; Qin, Y.; Gavins, F.K.H.; Liu, J.; Dou, L.; Orlu, M.; Murdan, S.; Mai, Y.; Basit, A.W. Sex Differences in Intestinal P-Glycoprotein Expression in Wistar versus Sprague Dawley Rats. *Pharmaceutics* 2022, *14*, 1030.

211. Dahan, A.; Amidon, G.L. Segmental Dependent Transport of Low Permeability Compounds along the Small Intestine Due to P-Glycoprotein: The Role of Efflux Transport in the Oral Absorption of BCS Class III Drugs. *Mol Pharm* 2009, *6*, 19-28, doi:10.1021/mp800088f.

212. Rijsman, L.H.; Monkelbaan, J.F.; Kusters, J.G. Clinical consequences of polymerase chain reaction-based diagnosis of intestinal parasitic infections. *Journal of gastroenterology and hepatology* 2016, *31*, 1808-1815.

213. Sjöstedt, N.; Holvikari, K.; Tammela, P.; Kidron, H. Inhibition of Breast Cancer Resistance Protein and Multidrug Resistance Associated Protein 2 by Natural Compounds and Their Derivatives. *Mol Pharm* 2017, *14*, 135-146, doi:10.1021/acs.molpharmaceut.6b00754.

214. Mo, Y.; Wan, R.; Zhang, Q. Application of reverse transcription-PCR and real-time PCR in nanotoxicity research. *Methods Mol Biol* 2012, *926*, 99-112, doi:10.1007/978-1-62703-002-1_7.

215. Eisenberg, E.; Levanon, E.Y. Human housekeeping genes, revisited. *TRENDS in Genetics* 2013, *29*, 569-574.

216. Fan, B.; Li, X.; Liu, L.; Chen, D.; Cao, S.; Men, D.; Wang, J.; Chen, J. Absolute Copy Numbers of β-Actin Proteins Collected from 10,000 Single Cells. *Micromachines (Basel)* 2018, *9*, doi:10.3390/mi9050254.

217. Dou, L.; Gavins, F.K.H.; Mai, Y.; Madla, C.M.; Taherali, F.; Orlu, M.; Murdan, S.; Basit, A.W. Effect of Food and an Animal's Sex on P-Glycoprotein Expression and Luminal Fluids in the Gastrointestinal Tract of Wistar Rats. *Pharmaceutics* 2020, *12*, doi:10.3390/pharmaceutics12040296.

218. Oswald, S.; Gröer, C.; Drozdzik, M.; Siegmund, W. Mass spectrometry-based targeted proteomics as a tool to elucidate the expression and function of intestinal drug transporters. *Aaps j* 2013, *15*, 1128-1140, doi:10.1208/s12248-013-9521-3.

219. Drozdzik, M.; Busch, D.; Lapczuk, J.; Muller, J.; Ostrowski, M.; Kurzawski, M.; Oswald, S. Protein Abundance of Clinically Relevant Drug-Metabolizing Enzymes in the Human Liver and Intestine: A Comparative Analysis in Paired Tissue Specimens. *Clinical pharmacology & therapeutics* 2018, *104*, 515-524, doi:10.1002/cpt.967.

220. Pradet-Balade, B.; Boulmé, F.; Beug, H.; Müllner, E.W.; Garcia-Sanz, J.A. Translation control: bridging the gap between genomics and proteomics? *Trends in biochemical sciences* 2001, *26*, 225-229.

221. Bonnie Tocher, C. The Wistar Rat as a Right Choice: Establishing Mammalian Standards and the Ideal of a Standardized Mammal. *Journal of the History of Biology* 1993, *26*, 329-349.

222. Doran, A.; Obach, R.S.; Smith, B.J.; Hosea, N.A.; Becker, S.; Callegari, E.; Chen, C.; Chen, X.; Choo, E.; Cianfrogna, J. The impact of P-glycoprotein on the disposition of drugs targeted for indications of the central nervous system: evaluation using the MDR1A/1B knockout mouse model. *Drug Metabolism and Disposition* 2005, *33*, 165-174.

223. Müller, J.; Keiser, M.; Drozdzik, M.; Oswald, S. Expression, regulation and function of intestinal drug transporters: an update. *Biological Chemistry* 2017, *398*, 175-192, doi:10.1515/hsz-2016-0259.

224. Glavinas, H.; Krajcsi, P.; Cserepes, J.; Sarkadi, B. The role of ABC transporters in drug resistance, metabolism and toxicity. *Current drug delivery* 2004, *1*, 27-42.

225. Finch, A.; Pillans, P. P-glycoprotein and its role in drug-drug interactions. *Australian Prescriber* 2014, *37*, 137-139.

226. Mao, Q.; Unadkat, J.D. Role of the breast cancer resistance protein (BCRP/ABCG2) in drug transport--an update. *The AAPS journal* 2015, *17*, 65-82, doi:10.1208/s12248-014-9668-6.

227. Vinarov, Z.; Abrahamsson, B.; Artursson, P.; Batchelor, H.; Berben, P.; Bernkop-Schnürch, A.; Butler, J.; Ceulemans, J.; Davies, N.; Dupont, D.; et al. Current challenges and future perspectives in oral absorption research: An opinion of the UNGAP network. *Advanced Drug Delivery Reviews* 2021, *171*, 289-331, doi:10.1016/j.addr.2021.02.001.

228. Fadda, H.M.; McConnell, E.L.; Short, M.D.; Basit, A.W. Meal-Induced Acceleration of Tablet Transit Through the Human Small Intestine. *Pharm Res* 2009, *26*, 356-360, doi:10.1007/s11095-008-9749-2.

229. Seden, K.; Dickinson, L.; Khoo, S.; Back, D. Grapefruit-drug interactions. *Drugs* 2010, *70*, 2373-2407, doi:10.2165/11585250-000000000-00000.

230. Honda, Y.; Ushigome, F.; Koyabu, N.; Morimoto, S.; Shoyama, Y.; Uchiumi, T.; Kuwano, M.; Ohtani, H.; Sawada, Y. Effects of grapefruit juice and orange juice components on P-glycoprotein- and MRP2-mediated drug efflux. *Br J Pharmacol* 2004, *143*, 856-864, doi:10.1038/sj.bjp.0706008.

231. Scholz, I.; Liakoni, E.; Hammann, F.; Grafinger, K.E.; Duthaler, U.; Nagler, M.; Krähenbühl, S.; Haschke, M. Effects of Hypericum perforatum (St John's wort) on the pharmacokinetics and pharmacodynamics of rivaroxaban in humans. *British journal of clinical pharmacology* 2021, *87*, 1466-1474, doi:10.1111/bcp.14553.

232. Camilleri, M.; Malagelada, J.; Brown, M.; Becker, G.; Zinsmeister, A. Relation between antral motility and gastric emptying of solids and liquids in humans.

American Journal of Physiology-Gastrointestinal and Liver Physiology 1985, *249*, G580-G585.

233. Collins, P.; Houghton, L.; Read, N.; Horowitz, M.; Chatterton, B.; Heddle, R.; Dent, J. Role of the proximal and distal stomach in mixed solid and liquid meal emptying. *Gut* 1991, *32*, 615-619.

234. Schiebinger, L.; Klinge, I.; Sánchez de Madariaga, I.; Paik, H.Y.; Schraudner, M.; Stefanick, M. Gendered innovations in science, health & medicine, engineering, and environment. Available online: (accessed on

235. Dou, L.; Mai, Y.; Madla, C.M.; Orlu, M.; Basit, A.W. P-glycoprotein expression in the gastrointestinal tract of male and female rats is influenced differently by food. *European Journal of Pharmaceutical Sciences* 2018, *123*, 569-575, doi:10.1016/j.ejps.2018.08.014.

236. Gill, S.K.; Rossi, M.; Bajka, B.; Whelan, K. Dietary fibre in gastrointestinal health and disease. *Nature Reviews Gastroenterology & Hepatology* 2021, *18*, 101-116, doi:10.1038/s41575-020-00375-4.

237. Domínguez-Avila, J.A.; Wall-Medrano, A.; Velderrain-Rodríguez, G.R.; Chen, C.O.; Salazar-López, N.J.; Robles-Sánchez, M.; González-Aguilar, G.A. Gastrointestinal interactions, absorption, splanchnic metabolism and pharmacokinetics of orally ingested phenolic compounds. *Food & Function* 2017, *8*, 15-38, doi:10.1039/c6fo01475e.

238. Xie, Q.-s.; Zhang, J.-x.; Liu, M.; Liu, P.-h.; Wang, Z.-j.; Zhu, L.; Jiang, L.; Jin, M.-m.; Liu, X.-n.; Liu, L.; et al. Short-chain fatty acids exert opposite effects on the expression and function of p-glycoprotein and breast cancer resistance protein in rat intestine. *Acta Pharmacologica Sinica* 2021, *42*, 470-481, doi:10.1038/s41401-020-0402-x.

239. Yano, K.; Shimizu, S.; Tomono, T.; Ogihara, T. Gastrointestinal Hormone Cholecystokinin Increases P-Glycoprotein Membrane Localization and Transport Activity in Caco-2 Cells. *Journal of Pharmaceutical Sciences* 2017, *106*, 2650-2656, doi:10.1016/j.xphs.2017.04.003.

240. Wessler, J.D.; Grip, L.T.; Mendell, J.; Giugliano, R.P. The P-Glycoprotein Transport System and Cardiovascular Drugs. *Journal of the American College of Cardiology* 2013, *61*, 2495-2502, doi:10.1016/j.jacc.2013.02.058.

241. Kanado, Y.; Tsurudome, Y.; Omata, Y.; Yasukochi, S.; Kusunose, N.; Akamine, T.; Matsunaga, N.; Koyanagi, S.; Ohdo, S. Estradiol regulation of P-glycoprotein expression in mouse kidney and human tubular epithelial cells, implication for renal clearance of drugs. *Biochemical and Biophysical Research Communications* 2019, *519*, 613-619, doi:10.1016/j.bbrc.2019.09.021.

242. Mai, Y.; Gavins, F.K.H.; Dou, L.; Liu, J.; Taherali, F.; Alkahtani, M.E.; Murdan, S.; Basit, A.W.; Orlu, M. A Non-Nutritive Feeding Intervention Alters the Expression of Efflux Transporters in the Gastrointestinal Tract. *Pharmaceutics* 2021, *13*, 1789.

243. Madla, C.M.; Gavins, F.K.H.; Trenfield, S.J.; Basit, A.W. Special Populations. In *Biopharmaceutics*; 2022; pp. 205-237.

244. Clarke, L.L. A guide to Ussing chamber studies of mouse intestine. *American journal of physiology-gastrointestinal and liver physiology* 2009, *296*, G1151-1166, doi:10.1152/ajpgi.90649.2008.

245. Waskom, M.L. Seaborn: statistical data visualization. *Journal of Open Source Software* 2021, *6*, 3021.

246. Mudie, D.M.; Amidon, G.L.; Amidon, G.E. Physiological Parameters for Oral Delivery and in Vitro Testing. *Molecular Pharmaceutics* 2010, *7*, 1388-1405, doi:10.1021/mp100149j.

247. Dressman, J.B.; Berardi, R.R.; Dermentzoglou, L.C.; Russell, T.L.; Schmaltz, S.P.; Barnett, J.L.; Jarvenpaa, K.M. Upper Gastrointestinal (GI) pH in Young, Healthy Men and Women. *Pharmaceutical Research* **1990**, *7*, 756-761, doi:10.1023/A:1015827908309.

248. Weinstein, D.H.; deRijke, S.; Chow, C.C.; Foruraghi, L.; Zhao, X.; Wright, E.C.; Whatley, M.; Maass-Moreno, R.; Chen, C.C.; Wank, S.A. A new method for determining gastric acid output using a wireless pH-sensing capsule. *Alimentary pharmacology & therapeutics* **2013**, *37*, 1198-1209.

249. Koziolek, M.; Grimm, M.; Becker, D.; Iordanov, V.; Zou, H.; Shimizu, J.; Wanke, C.; Garbacz, G.; Weitschies, W. Investigation of pH and Temperature Profiles in the GI Tract of Fasted Human Subjects Using the Intellicap® System. *Journal of Pharmaceutical Sciences* **2015**, *104*, 2855-2863, doi:10.1002/jps.24274.

250. Fagerholm, U.; Nilsson, D.; Knutson, L.; Lennernäs, H. Jejunal permeability in humans in vivo and rats in situ: investigation of molecular size selectivity and solvent drag. *Acta physiologica scandinavica* **1999**, *165*, 315-324.

251. Merchant, H.A.; Rabbie, S.C.; Varum, F.J.O.; Afonso-Pereira, F.; Basit, A.W. Influence of ageing on the gastrointestinal environment of the rat and its implications for drug delivery. *European Journal of Pharmaceutical Sciences* **2014**, *62*, 76-85, doi:https://doi.org/10.1016/j.ejps.2014.05.004.

252. Afonso-Pereira, F.; Dou, L.; Trenfield, S.J.; Madla, C.M.; Murdan, S.; Sousa, J.; Veiga, F.; Basit, A.W. Sex differences in the gastrointestinal tract of rats and the implications for oral drug delivery. *European Journal of Pharmaceutical Sciences* **2018**, *115*, 339-344, doi:https://doi.org/10.1016/j.ejps.2018.01.043.

253. Hörter, D.; Dressman, J.B. Influence of physicochemical properties on dissolution of drugs in the gastrointestinal tract1PII of original article: S0169-409X(96)00487-5. The article was originally published in Advanced Drug Delivery

Reviews 25 (1997) 3–14.1. *Advanced Drug Delivery Reviews* 2001, *46*, 75-87, doi:https://doi.org/10.1016/S0169-409X(00)00130-7.

254. Oldham-Ott, C.K.; Gilloteaux, J. Comparative morphology of the gallbladder and biliary tract in vertebrates: Variation in structure, homology in function and gallstones. *Microscopy Research and Technique* 1997, *38*, 571-597, doi:10.1002/(sici)1097-0029(19970915)38:6<571::Aid-jemt3>3.0.Co;2-i.

255. Dressman, J.; Yamada, K. Animal models for oral drug absorption. *Drugs and the pharmaceutical sciences* 1991, *48*, 235-266.

256. Kararli, T. Gastrointestinal absorption of drugs. *Critical Reviews in Therapeutic Drug Carrier Systems* 1989, *6*, 39-86.

257. Merchant, H.A.; Afonso-Pereira, F.; Rabbie, S.C.; Youssef, S.A.; Basit, A.W. Gastrointestinal characterisation and drug solubility determination in animals. *Journal of Pharmacy and Pharmacology* 2015, *67*, 630-639, doi:10.1111/jphp.12361.

258. Buettner, R.; Schölmerich, J.; Bollheimer, L.C. High-fat diets: modeling the metabolic disorders of human obesity in rodents. *Obesity* 2007, *15*, 798-808.

259. Homma, H.; Hoy, E.; Xu, D.-Z.; Lu, Q.; Feinman, R.; Deitch, E.A. The female intestine is more resistant than the male intestine to gut injury and inflammation when subjected to conditions associated with shock states. *American Journal of Physiology-Gastrointestinal and Liver Physiology* 2005, *288*, G466-G472.

260. Evseenko, D.A.; Paxton, J.W.; Keelan, J.A. Independent regulation of apical and basolateral drug transporter expression and function in placental trophoblasts by cytokines, steroids, and growth factors. *Drug Metabolism and Disposition* 2007, *35*, 595-601.

261. Mutoh, K.; Tsukahara, S.; Mitsuhashi, J.; Katayama, K.; Sugimoto, Y. Estrogen-mediated post transcriptional down-regulation of P-glycoprotein in MDR1-transduced human breast cancer cells. *Cancer science* 2006, *97*, 1198-1204.

262. Wang, H.; Zhou, L.; Gupta, A.; Vethanayagam, R.R.; Zhang, Y.; Unadkat, J.D.; Mao, Q. Regulation of BCRP/ABCG2 expression by progesterone and 17β-estradiol in human placental BeWo cells. *American Journal of Physiology-Endocrinology and Metabolism* 2006, *290*, E798-E807.

263. Coles, L.D.; Lee, I.J.; Voulalas, P.J.; Eddington, N.D. Estradiol and progesterone-mediated regulation of P-gp in P-gp overexpressing cells (NCI-ADR-RES) and placental cells (JAR). *Molecular pharmaceutics* 2009, *6*, 1816-1825.

264. Järvinen, E.; Deng, F.; Kidron, H.; Finel, M. Efflux transport of estrogen glucuronides by human MRP2, MRP3, MRP4 and BCRP. *The Journal of Steroid Biochemistry and Molecular Biology* 2018, *178*, 99-107.

265. Stephens, R.H.; O'Neill, C.A.; Warhurst, A.; Carlson, G.L.; Rowland, M.; Warhurst, G. Kinetic profiling of P-glycoprotein-mediated drug efflux in rat and human intestinal epithelia. *Journal of Pharmacology and Experimental Therapeutics* 2001, *296*, 584-591.

266. Haller, S.; Schuler, F.; Lazic, S.E.; Bachir-Cherif, D.; Krämer, S.D.; Parrott, N.J.; Steiner, G.; Belli, S. Expression profiles of metabolic enzymes and drug transporters in the liver and along the intestine of beagle dogs. *Drug Metabolism and Disposition* 2012, *40*, 1603-1611.

267. Vine, D.F.; Charman, S.A.; Gibson, P.R.; Sinclair, A.J.; Porter, C.J. Effect of dietary fatty acids on the intestinal permeability of marker drug compounds in excised rat jejunum. *Journal of pharmacy and pharmacology* 2002, *54*, 809-819, doi:10.1211/0022357021779159.

268. Ikemura, K.; Yamamoto, M.; Miyazaki, S.; Mizutani, H.; Iwamoto, T.; Okuda, M. MicroRNA-145 post-transcriptionally regulates the expression and function of P-glycoprotein in intestinal epithelial cells. *Molecular Pharmacology* 2013, *83*, 399-405, doi:10.1124/mol.112.081844.

269. Tarallo, S.; Ferrero, G.; De Filippis, F.; Francavilla, A.; Pasolli, E.; Panero, V.; Cordero, F.; Segata, N.; Grioni, S.; Pensa, R.G.; et al. Stool microRNA profiles reflect different dietary and gut microbiome patterns in healthy individuals. *Gut* 2022, *71*, 1302, doi:10.1136/gutjnl-2021-325168.

270. Kocic, H.; Damiani, G.; Stamenkovic, B.; Tirant, M.; Jovic, A.; Tiodorovic, D.; Peris, K. Dietary compounds as potential modulators of microRNA expression in psoriasis. *Ther Adv Chronic Dis* 2019, *10*, 2040622319864805-2040622319864805, doi:10.1177/2040622319864805.

271. Ferrero, G.; Carpi, S.; Polini, B.; Pardini, B.; Nieri, P.; Impeduglia, A.; Grioni, S.; Tarallo, S.; Naccarati, A. Intake of Natural Compounds and Circulating microRNA Expression Levels: Their Relationship Investigated in Healthy Subjects With Different Dietary Habits. *Frontiers in pharmacology* 2021, *11*, 619200-619200, doi:10.3389/fphar.2020.619200.

272. Schinkel, A.H.; Jonker, J.W. Mammalian drug efflux transporters of the ATP binding cassette (ABC) family: an overview. *Advanced Drug Delivery Reviews* 2003, *55*, 3-29, doi:10.1016/S0169-409X(02)00169-2.

273. Nguyen, T.-T.-L.; Duong, V.-A.; Maeng, H.-J. Pharmaceutical Formulations with P-Glycoprotein Inhibitory Effect as Promising Approaches for Enhancing Oral Drug Absorption and Bioavailability. *Pharmaceutics* 2021, *13*, 1103.

274. Al-Shawi, M.K.; Omote, H. The remarkable transport mechanism of P-glycoprotein: a multidrug transporter. *J Bioenerg Biomembr* 2005, *37*, 489-496, doi:10.1007/s10863-005-9497-5.

275. Lemos, C.; Jansen, G.; Peters, G.J. Drug transporters: recent advances concerning BCRP and tyrosine kinase inhibitors. *British journal of cancer* 2008, *98*, 857-862, doi:10.1038/sj.bjc.6604213.

276. Bozkurt, A.; Deniz, M.; Yegen, B.C. Cefaclor, a cephalosporin antibiotic, delays gastric emptying rate by a CCK-A receptor-mediated mechanism in the rat. *Br J Pharmacol* 2000, *131*, 399-404, doi:10.1038/sj.bjp.0703585.

277. Kissileff, H.R.; Carretta, J.C.; Geliebter, A.; Pi-Sunyer, F.X. Cholecystokinin and stomach distension combine to reduce food intake in humans. *American Journal of Physiology-Regulatory, Integrative and Comparative Physiology* 2003, *285*, R992-R998, doi:10.1152/ajpregu.00272.2003.

278. Karhunen, L.J.; Juvonen, K.R.; Huotari, A.; Purhonen, A.K.; Herzig, K.H. Effect of protein, fat, carbohydrate and fibre on gastrointestinal peptide release in humans. *Regulatory peptides* 2008, *149*, 70-78, doi:10.1016/j.regpep.2007.10.008.

279. Arias, A.; Rigalli, J.P.; Villanueva, S.S.; Ruiz, M.L.; Luquita, M.G.; Perdomo, V.G.; Vore, M.; Catania, V.A.; Mottino, A.D. Regulation of expression and activity of multidrug resistance proteins MRP2 and MDR1 by estrogenic compounds in Caco-2 cells. Role in prevention of xenobiotic-induced cytotoxicity. *Toxicology* 2014, *320*, 46-55.

280. Aykan, D.A.; Seyithanoglu, M. The effects of administration of vitamin D, infliximab, and leflunomide on testosterone concentrations in rats under atorvastatin therapy. *The Eurasian Journal of Medicine* 2019, *51*, 224.

281. Shchul'kin, A.V.; Yakusheva, E.N.; Chernykh, I.V.; Nikiforov, A.A.; Popova, N.P. Effects of Testosterone on the Functional Activity of P-Glycoprotein. *Pharmaceutical Chemistry Journal* 2017, *51*, 743-747, doi:10.1007/s11094-017-1685-1.

282. Janssen, S.; Depoortere, I. Nutrient sensing in the gut: new roads to therapeutics? *Trends in Endocrinology & Metabolism* 2013, *24*, 92-100, doi:10.1016/j.tem.2012.11.006.

283. Ee, P.L.R.; Kamalakaran, S.; Tonetti, D.; He, X.; Ross, D.D.; Beck, W.T. Identification of a novel estrogen response element in the breast cancer resistance protein (ABCG2) gene. *Cancer research* 2004, *64*, 1247-1251.

284. Amidon, G.L.; Lennernäs, H.; Shah, V.P.; Crison, J.R. A Theoretical Basis for a Biopharmaceutic Drug Classification: The Correlation of in Vitro Drug Product Dissolution and in Vivo Bioavailability. *Pharmaceutical Research* 1995, *12*, 413-420, doi:10.1023/A:1016212804288.

285. Wu, C.-Y.; Benet, L.Z. Predicting Drug Disposition via Application of BCS: Transport/Absorption/Elimination Interplay and Development of a Biopharmaceutics DrugDisposition Classification System. *Pharmaceutical Research* 2005, *22*, 11-23, doi:10.1007/s11095-004-9004-4.

286. Darwich, A.S.; Pade, D.; Rowland-Yeo, K.; Jamei, M.; Asberg, A.; Christensen, H.; Ashcroft, D.M.; Rostami-Hodjegan, A. Evaluation of an In Silico PBPK Post-Bariatric Surgery Model through Simulating Oral Drug Bioavailability of Atorvastatin and Cyclosporine. *CPT: pharmacometrics & systems pharmacology* 2013, *2*, e47, doi:10.1038/psp.2013.23.

287. Gao, H.; Wang, W.; Dong, J.; Ye, Z.; Ouyang, D. An integrated computational methodology with data-driven machine learning, molecular modeling and PBPK modeling to accelerate solid dispersion formulation design. *European Journal of Pharmaceutics and Biopharmaceutics* 2021, *158*, 336-346, doi:10.1016/j.ejpb.2020.12.001.

288. Jogiraju, V.K.; Avvari, S.; Gollen, R.; Taft, D.R. Application of physiologically based pharmacokinetic modeling to predict drug disposition in pregnant populations.

Biopharmaceutics & Drug Disposition 2017, *38*, 426-438, doi:https://doi.org/10.1002/bdd.2081.

289. Jones, H.M.; Gardner, I.B.; Watson, K.J. Modelling and PBPK simulation in drug discovery. *The AAPS journal* 2009, *11*, 155-166.

290. Kohlmann, P.; Stillhart, C.; Kuentz, M.; Parrott, N. Investigating Oral Absorption of Carbamazepine in Pediatric Populations. *The AAPS Journal* 2017, *19*, 1864-1877, doi:10.1208/s12248-017-0149-6.

291. Wagner, C.; Kesisoglou, F.; Pepin, X.J.H.; Parrott, N.; Emami Riedmaier, A. Use of Physiologically Based Pharmacokinetic Modeling for Predicting Drug–Food Interactions: Recommendations for Improving Predictive Performance of Low Confidence Food Effect Models. *The AAPS Journal* 2021, *23*, 85, doi:10.1208/s12248-021-00601-0.

292. Paul, D.; Sanap, G.; Shenoy, S.; Kalyane, D.; Kalia, K.; Tekade, R.K. Artificial intelligence in drug discovery and development. *Drug discovery today* 2021, *26*, 80-93, doi:10.1016/j.drudis.2020.10.010.

293. Rodriguez-Perez, R.; Vogt, M.; Bajorath, J.r. Support vector machine classification and regression prioritize different structural features for binary compound activity and potency value prediction. *ACS omega* 2017, *2*, 6371-6379.

294. Drucker, H. Improving regressors using boosting techniques. In Proceedings of the ICML, 1997; pp. 107-115.

295. Friedman, J.H. Greedy function approximation: a gradient boosting machine. *Annals of statistics* 2001, 1189-1232.

296. James, G.; Witten, D.; Hastie, T.; Tibshirani, R. *An introduction to statistical learning*; Springer: 2013; Volume 112.

297. Lombardo, F.; Berellini, G.; Obach, R.S. Trend Analysis of a Database of Intravenous Pharmacokinetic Parameters in Humans for 1352 Drug Compounds. *Drug Metabolism and Disposition* 2018, *46*, 1466-1477, doi:10.1124/dmd.118.082966.

298. Landrum, G. RDKit: Open-source cheminformatics. Available online: http://www.rdkit.org (accessed on 01/03/2021).

299. Zhang, S.; Shang, X.; Wang, W.; Huang, X. Optimizing the classification accuracy of imbalanced dataset based on SVM. In Proceedings of the 2010 International Conference on Computer Application and System Modeling (ICCASM 2010), 22-24 Oct. 2010, 2010; pp. V4-338-V334-341.

300. Núñez, H.; Gonzalez-Abril, L.; Angulo, C. Improving SVM Classification on Imbalanced Datasets by Introducing a New Bias. *Journal of Classification* 2017, *34*, 427-443, doi:10.1007/s00357-017-9242-x.

301. Wang, S.; Liu, W.; Wu, J.; Cao, L.; Meng, Q.; Kennedy, P.J. Training deep neural networks on imbalanced data sets. In Proceedings of the 2016 International Joint Conference on Neural Networks (IJCNN), 24-29 July 2016, 2016; pp. 4368-4374.

302. Waskom, M.; Botvinnik, O.; O'Kane, D.; Hobson , P.; Lukauskas, S.; Gemperline, D.C.; Augspurger, T.; Halchenko, Y.; Cole, J.B.; Warmenhoven, J.; et al. mwaskom/seaborn: v0.8.1. Available online: https://doi.org/10.5281/zenodo.883859. (accessed on 10/01/2021).

303. Tharwat, A. Classification assessment methods. *Applied Computing and Informatics* 2021, *17*, 168-192, doi:10.1016/j.aci.2018.08.003.

304. Belgiu, M.; Drăguţ, L. Random forest in remote sensing: A review of applications and future directions. *ISPRS Journal of Photogrammetry and Remote Sensing* 2016, *114*, 24-31, doi:https://doi.org/10.1016/j.isprsjprs.2016.01.011.

305. Morgan, H.L. The Generation of a Unique Machine Description for Chemical Structures-A Technique Developed at Chemical Abstracts Service. *Journal of Chemical Documentation* 1965, *5*, 107-113, doi:10.1021/c160017a018.

306. Pilnenskiy, N.; Smetannikov, I. Modern Implementations of Feature Selection Algorithms and Their Perspectives. In Proceedings of the 2019 25th Conference of Open Innovations Association (FRUCT), 5-8 Nov. 2019, 2019; pp. 250-256.

307. Pasupa, K.; Sunhem, W. A comparison between shallow and deep architecture classifiers on small dataset. In Proceedings of the 2016 8th International Conference on Information Technology and Electrical Engineering (ICITEE), 5-6 Oct. 2016, 2016; pp. 1-6.

308. Han, R.; Xiong, H.; Ye, Z.; Yang, Y.; Huang, T.; Jing, Q.; Lu, J.; Pan, H.; Ren, F.; Ouyang, D. Predicting physical stability of solid dispersions by machine learning techniques. *Journal of Controlled Release* 2019, *311-312*, 16-25, doi:10.1016/j.jconrel.2019.08.030.

309. Ryu, S.; Kwon, Y.; Kim, W.Y. A Bayesian graph convolutional network for reliable prediction of molecular properties with uncertainty quantification. *Chemical science* 2019, *10*, 8438-8446.

310. Koziolek, M.; Schneider, F.; Grimm, M.; Modeβ, C.; Seekamp, A.; Roustom, T.; Siegmund, W.; Weitschies, W. Intragastric pH and pressure profiles after intake of the high-caloric, high-fat meal as used for food effect studies. *Journal of Controlled Release* 2015, *220*, 71-78, doi:https://doi.org/10.1016/j.jconrel.2015.10.022.

311. Marasanapalle, V.P.; Crison, J.R.; Ma, J.; Li, X.; Jasti, B.R. Investigation of some factors contributing to negative food effects. *Biopharmaceutics & Drug Disposition* 2009, *30*, 71-80, doi:10.1002/bdd.647.

312. Chen, E.P.; Bondi, R.W.; Michalski, P.J. Model-based Target Pharmacology Assessment (mTPA): An Approach Using PBPK/PD Modeling and Machine Learning to Design Medicinal Chemistry and DMPK Strategies in Early Drug Discovery. *Journal of Medicinal Chemistry* 2021, *64*, 3185-3196, doi:10.1021/acs.jmedchem.0c02033.

313. Willemsen, A.E.; Lubberman, F.J.; Tol, J.; Gerritsen, W.R.; van Herpen, C.M.; van Erp, N.P. Effect of food and acid-reducing agents on the absorption of oral targeted therapies in solid tumors. *Drug discovery today* 2016, *21*, 962-976.

314. Baxevanis, F.; Zarmpi, P.; Kuiper, J.; Fotaki, N. Investigation of drug partition kinetics to fat in simulated fed state gastric conditions based on drug properties. *European Journal of Pharmaceutical Sciences* 2020, *146*, 105263, doi:https://doi.org/10.1016/j.ejps.2020.105263.

315. Porter, C.J.; Pouton, C.W.; Cuine, J.F.; Charman, W.N. Enhancing intestinal drug solubilisation using lipid-based delivery systems. *Advanced drug delivery reviews* 2008, *60*, 673-691.

316. Schultz, H.B.; Meola, T.R.; Thomas, N.; Prestidge, C.A. Oral formulation strategies to improve the bioavailability and mitigate the food effect of abiraterone acetate. *International Journal of Pharmaceutics* 2020, *577*, 119069, doi:https://doi.org/10.1016/j.ijpharm.2020.119069.

317. Gu, C.-H.; Li, H.; Levons, J.; Lentz, K.; Gandhi, R.B.; Raghavan, K.; Smith, R.L. Predicting Effect of Food on Extent of Drug Absorption Based on Physicochemical Properties. *Pharmaceutical Research* 2007, *24*, 1118-1130, doi:10.1007/s11095-007-9236-1.

318. Singh, B.N. A quantitative approach to probe the dependence and correlation of food-effect with aqueous solubility, dose/solubility ratio, and partition coefficient (Log P) for orally active drugs administered as immediate-release

formulations. *Drug Development Research* 2005, *65*, 55-75, doi:https://doi.org/10.1002/ddr.20008.

319. Gatarić, B.; Parojčić, J. An Investigation into the Factors Governing Drug Absorption and Food Effect Prediction Based on Data Mining Methodology. *The AAPS Journal* 2019, *22*, 11, doi:10.1208/s12248-019-0394-y.

320. Xiao, J.; Tran, D.; Zhang, X.; Zhang, T.; Seo, S.; Zhu, H.; Zou, P. Biliary Excretion–Mediated Food Effects and Prediction. *The AAPS Journal* 2020, *22*, 124, doi:10.1208/s12248-020-00509-1.

321. Bennett-Lenane, H.; Griffin, B.T.; O'Shea, J.P. Machine Learning Methods for Prediction of Food Effects on Bioavailability: A Comparison of Support Vector Machines and Artificial Neural Networks. *European Journal of Pharmaceutical Sciences* 2021, 106018, doi:https://doi.org/10.1016/j.ejps.2021.106018.

322. Danishuddin; Kumar, V.; Faheem, M.; Woo Lee, K. A decade of machine learning-based predictive models for human pharmacokinetics: Advances and challenges. *Drug Discovery Today* 2022, *27*, 529-537, doi:https://doi.org/10.1016/j.drudis.2021.09.013.

323. Reddy, V.P.; Jones, B.C.; Colclough, N.; Srivastava, A.; Wilson, J.; Li, D. An Investigation into the Prediction of the Plasma Concentration-Time Profile and Its Interindividual Variability for a Range of Flavin-Containing Monooxygenase Substrates Using a Physiologically Based Pharmacokinetic Modeling Approach. *Drug Metabolism and Disposition* 2018, *46*, 1259-1267, doi:10.1124/dmd.118.080648.

324. Hosea, N.A.; Jones, H.M. Predicting pharmacokinetic profiles using in silico derived parameters. *Molecular Pharmaceutics* 2013, *10*, 1207-1215, doi:10.1021/mp300482w.

325. Kosugi, Y.; Hosea, N. Prediction of Oral Pharmacokinetics Using a Combination of In Silico Descriptors and In Vitro ADME Properties. *Molecular Pharmaceutics* 2021, *18*, 1071-1079, doi:10.1021/acs.molpharmaceut.0c01009.

326. Zhang, J.; Mucs, D.; Norinder, U.; Svensson, F. LightGBM: An effective and scalable algorithm for prediction of chemical toxicity–application to the Tox21 and mutagenicity data sets. *Journal of chemical information and modeling* 2019, *59*, 4150-4158.

327. Tsai, H.-H.; Lin, H.-W.; Simon Pickard, A.; Tsai, H.-Y.; Mahady, G.B. Evaluation of documented drug interactions and contraindications associated with herbs and dietary supplements: a systematic literature review. *International Journal of Clinical Practice* 2012, *66*, 1056-1078, doi:10.1111/j.1742-1241.2012.03008.x.

328. Foley, S.E.; Tuohy, C.; Dunford, M.; Grey, M.J.; De Luca, H.; Cawley, C.; Szabady, R.L.; Maldonado-Contreras, A.; Houghton, J.M.; Ward, D.V.; et al. Gut microbiota regulation of P-glycoprotein in the intestinal epithelium in maintenance of homeostasis. *Microbiome* 2021, *9*, 183, doi:10.1186/s40168-021-01137-3.

329. Chittick, G.E.; Gillotin, C.; McDowell, J.A.; Lou, Y.; Edwards, K.D.; Prince, W.T.; Stein, D.S. Abacavir: Absolute Bioavailability, Bioequivalence of Three Oral Formulations, and Effect of Food. *Pharmacotherapy: The Journal of Human Pharmacology and Drug Therapy* 1999, *19*, 932-942, doi:https://doi.org/10.1592/phco.19.11.932.31568.

330. Laube, H. Acarbose. *Clinical drug investigation* 2002, *22*, 141-156.

331. FDA. Sectral®(Acebutolol hydrochloride). Available online: https://www.accessdata.fda.gov/drugsatfda_docs/label/2007/018917s024lbl.pdf (accessed on 10/01/2021).

332. Forrest, J.A.; Clements, J.A.; Prescott, L.F. Clinical pharmacokinetics of paracetamol. *Clinical Pharmacokinetics* 1982, *7*, 93-107, doi:10.2165/00003088-198207020-00001.

333. Moore, R.A.; Derry, S.; Wiffen, P.J.; Straube, S. Effects of food on pharmacokinetics of immediate release oral formulations of aspirin, dipyrone, paracetamol and NSAIDs – a systematic review. *British Journal of Clinical Pharmacology* 2015, *80*, 381-388, doi:https://doi.org/10.1111/bcp.12628.

334. FDA. Prescribing information - Zovirax. Available online: https://www.accessdata.fda.gov/drugsatfda_docs/label/2005/018828s030%2C020089s019%2C019909s020lbl.pdf (accessed on 10/01/2021).

335. Lahner, E.; ANNIBALE, B.; DELLE FAVE, G. Systematic review: impaired drug absorption related to the co-administration of antisecretory therapy. *Alimentary Pharmacology & Therapeutics* 2009, *29*, 1219-1229, doi:10.1111/j.1365-2036.2009.03993.x.

336. Tsugawa, N. [Clinical Pharmacokinetics of Active Vitamin D3 and its derivatives, and Vitamin K2(Menatetrenone).]. *Clinical Calcium* 2016, *26*, 1547-1558.

337. emC. Alfuzosin HCl 2.5 mg film-coated tablets. Available online: https://www.medicines.org.uk/emc/product/5205 (accessed on 23/09/2021).

338. FDA. DUZALLO® (lesinurad and allopurinol) tablets. Available online: https://www.accessdata.fda.gov/drugsatfda_docs/label/2017/209203s000lbl.pdf (accessed on 10/01/2021).

339. FDA. AXERT® (almotriptan malate) tablets. Available online: https://www.accessdata.fda.gov/drugsatfda_docs/label/2009/021001s010s011lbl.pdf (accessed on 10/01/2021).

340. Palmer, J.; Noordin, N.; Andrew, P.; Corrigan, B. The effect of gender on the pharmacokinetics of alosetron. *Pharmaceutical Sciences* 1998, *1*, 465.

341. Smith, R.B.; Kroboth, P.D.; Vanderlugt, J.T.; Phillips, J.P.; Juhl, R.P. Pharmacokinetics and pharmacodynamics of alprazolam after oral and IV administration. *Psychopharmacology* 1984, *84*, 452-456, doi:10.1007/BF00431449.

342. Johnsson, G.; Regårdh, C.-G. Clinical pharmacokinetics of β-adrenoceptor blocking drugs. *Clinical pharmacokinetics* 1976, *1*, 233-263.

343. FDA. GOCOVRITM (amantadine) extended release capsules,. Available online: https://www.accessdata.fda.gov/drugsatfda_docs/label/2017/208944lbl.pdf (accessed on 10/01/2011).

344. FDA. Cordarone® (amiodarone HCl) TABLETS Available online: https://www.accessdata.fda.gov/drugsatfda_docs/label/2010/018972s042lbl.pdf (accessed on 10/01/2021).

345. Liedholm, H.; Lidén, A. Food intake and the presystemic metabolism of single doses of amitriptyline and nortriptyline. *Fundamental & clinical pharmacology* 1998, *12*, 636-642, doi:10.1111/j.1472-8206.1998.tb00998.x.

346. FDA. Amlodipine Besylate Tablets. Available online: https://www.accessdata.fda.gov/drugsatfda_docs/label/2007/019787s042lbl.pdf (accessed on 10/01/2021).

347. FDA. AMOXIL (amoxicillin) capsules,. Available online: https://www.accessdata.fda.gov/drugsatfda_docs/label/2015/50542s029,50754s019,50760s019,50761s016lbl.pdf (accessed on 10/01/2021).

348. Eshelman, F.N.; Spyker, D.A. Pharmacokinetics of amoxicillin and ampicillin: crossover study of the effect of food. *Antimicrobial agents and chemotherapy* **1978**, *14*, 539-543, doi:10.1128/aac.14.4.539.

349. FDA. EMEND (aprepitant) capsules. Available online: https://www.accessdata.fda.gov/drugsatfda_docs/label/2015/207865lbl.pdf (accessed on 10/01/2021).

350. FDA. ABILIFY (aripiprazole) Tablets Available online: https://www.accessdata.fda.gov/drugsatfda_docs/label/2005/021713s004,021436s007lbl.pdf (accessed on 10/01/2021).

351. Melander, A.; Stenberg, P.; Liedholm, H.; Scherstén, B.; Wåhlin-Boll, E. Food-induced reduction in bioavailability of atenolol. *European journal of clinical pharmacology* **1979**, *16*, 327-330, doi:10.1007/bf00605630.

352. FDA. STRATTERA® (atomoxetine HCl). Available online: https://www.accessdata.fda.gov/drugsatfda_docs/label/2007/021411s004s012s013s015s021lbl.pdf (accessed on 10/01/2021).

353. Rolan, P.E.; Mercer, A.J.; Weatherley, B.C.; Holdich, T.; Meire, H.; Peck, R.W.; Ridout, G.; Posner, J. Examination of some factors responsible for a food-induced increase in absorption of atovaquone. *British journal of clinical pharmacology* **1994**, *37*, 13-20, doi:10.1111/j.1365-2125.1994.tb04232.x.

354. FDA. ZITHROMAX®. Available online: https://www.accessdata.fda.gov/drugsatfda_docs/label/2013/050710s039,050711s036,050784s023lbl.pdf (accessed on 10/01/2021).

355. Nyberg, L.; Rosenborg, J.; Weibull, E.; Jönsson, S.; Kennedy, B.M.; Nilsson, M. Pharmacokinetics of bambuterol in healthy subjects. *British journal of clinical pharmacology* **1998**, *45*, 471-478.

356. FDA. Kerlone® betaxolol hydrochloride tablets Available online: https://www.accessdata.fda.gov/drugsatfda_docs/label/2009/019507s007lbl.pdf (accessed on 10/01/2021).

357. Toothaker, R.D.; Randinitis, E.J.; Nelson, C.; Kinkel, A.W.; Goulet, J.R. The influence of food on the oral absorption of bevantolol. *The Journal of Clinical Pharmacology* 1987, *27*, 297-299, doi:10.1002/j.1552-4604.1987.tb03017.x.

358. FDA. TRACLEER® (bosentan) tablets. Available online: https://www.accessdata.fda.gov/drugsatfda_docs/label/2017/209279s000lbl.pdf (accessed on 10/01/2021).

359. FDA. ENTOCORT® EC (budesonide) capsules. Available online: https://www.accessdata.fda.gov/drugsatfda_docs/label/2011/021324s009lbl.pdf (accessed on 10/01/2021).

360. McCrindle, J.L.; Li Kam Wa, T.C.; Barron, W.; Prescott, L.F. Effect of food on the absorption of frusemide and bumetanide in man. *British journal of clinical pharmacology* 1996, *42*, 743-746, doi:10.1046/j.1365-2125.1996.00494.x.

361. Hoffmann-La_Roche. Rocaltrol Product Monograph. 2016.

362. FDA. ATACAND (candesartan cilexetil) TABLETS Available online: https://www.accessdata.fda.gov/drugsatfda_docs/label/2006/020838s026lbl.pdf (accessed on 10/01/2021).

363. FDA. CAPOTEN® (Captopril Tablets, USP). Available online: https://www.accessdata.fda.gov/drugsatfda_docs/label/2014/018343s085lbl.pdf (accessed on 10/01/2021).

364. Levison, M.E.; Levison, J.H. Pharmacokinetics and pharmacodynamics of antibacterial agents. *Infect Dis Clin North Am* 2009, *23*, 791-vii, doi:10.1016/j.idc.2009.06.008.

365. FDA. PRESCRIBING INFORMATION COREG® (carvedilol) Tablets. Available online: https://www.accessdata.fda.gov/drugsatfda_docs/label/2005/020297s013lbl.pdf (accessed on 02/09/2021).

366. Wise, R. The pharmacokinetics of the oral cephalosporins--a review. *Journal of Antimicrobial Chemotherapy* 1990, *26 Suppl E*, 13-20, doi:10.1093/jac/26.suppl_e.13.

367. FDA. SUPRAX® (cefixime) tablets. Available online: https://www.accessdata.fda.gov/drugsatfda_docs/label/2017/202091s005,203195s006lbl.pdf (accessed on

368. FDA. Cefzil® (CEFPROZIL) Tablets. Available online: https://www.accessdata.fda.gov/drugsatfda_docs/label/2007/050664s024,050665s024lbl.pdf (accessed on 10/01/2021).

369. FDA. CEFTIN ® Tablets (cefuroxime axetil tablets). Available online: https://www.accessdata.fda.gov/drugsatfda_docs/label/2004/50605slr039,50672slr025_ceftin_lbl.pdf (accessed on

370. Gower, P.E.; Dash, C.H. Cephalexin: human studies of absorption and excretion of a new cephalosporin antibiotic. *British Journal of Pharmacology* 1969, *37*, 738-747, doi:10.1111/j.1476-5381.1969.tb08513.x.

371. Tulpule, A.; Krishnaswamy, K. Effect of food on bioavailability of chloroquine. *European Journal of Clinical Pharmacology* 1982, *23*, 271-273, doi:10.1007/bf00547567.

372. FDA. Advil Allergy Sinus Available online: https://www.accessdata.fda.gov/drugsatfda_docs/nda/2004/21-587_Advil_biopharmr.pdf (accessed on 10/01/2021).

373. Dahl, S.G.; Strandjord, R.E. Pharmacokinetics of chlorpromazine after single and chronic dosage. *Clinical Pharmacology & Therapeutics* 1977, *21*, 437-448.

374. Dudkowski, C.; Karim, A.; Munsaka, M. Effects of Food Intake on the Pharmacokinetics of Azilsartan Medoxomil and Chlorthalidone Alone and in Fixed-Dose Combination in Healthy Adults. *Clinical Pharmacology in Drug Development* 2016, *5*, 393-398, doi:10.1002/cpdd.249.

375. Desmond, P.V.; Harman, P.J.; Gannoulis, N.; Kamm, M.; Mashford, M.L. The effect of an antacid and food on the absorption of cimetidine and ranitidine. *Journal of pharmacy and pharmacology* 1990, *42*, 352-354, doi:10.1111/j.2042-7158.1990.tb05425.x.

376. FDA. Sensipar® (cinacalcet) Tablets Available online: https://www.accessdata.fda.gov/drugsatfda_docs/label/2009/021688s013lbl.pdf (accessed on 10/01/2021).

377. FDA. CIPRO® (ciprofloxacin hydrochloride) tablet. Available online: https://www.accessdata.fda.gov/drugsatfda_docs/label/2016/019537s086lbl.pdf (accessed on 10/01/2021).

378. Bezchlibnyk-Butler, K.; Aleksic, I.; Kennedy, S.H. Citalopram--a review of pharmacological and clinical effects. *Journal of Psychiatry and Neuroscience* 2000, *25*, 241-254.

379. Rodvold, K.A. Clinical pharmacokinetics of clarithromycin. *Clinical Pharmacokinetics* 1999, *37*, 385-398, doi:10.2165/00003088-199937050-00003.

380. Laitinen, K.; Patronen, A.; Harju, P.; Löyttyniemi, E.; Pylkkänen, L.; Kleimola, T.; Perttunen, K. Timing of food intake has a marked effect on the bioavailability of clodronate. *Bone* 2000, *27*, 293-296, doi:10.1016/s8756-3282(00)00321-5.

381. Hvidberg, E.F.; Dam, M. Clinical pharmacokinetics of anticonvulsants. *Clinical pharmacokinetics* 1976, *1*, 161-188.

382. FDA. KAPVAY (clonidine hydrochloride) extended-release tablets. Available online: https://www.accessdata.fda.gov/drugsatfda_docs/label/2010/022331s001s002lbl.pdf (accessed on 10/01/2021).

383. FDA. CLOZARIL® (clozapine) Tablets Available online: https://www.accessdata.fda.gov/drugsatfda_docs/label/2010/019758s062lbl.pdf (accessed on 10/01/2021).

384. FDA. Codeine sulfate tablets. Available online: https://www.accessdata.fda.gov/drugsatfda_docs/label/2009/022402s000lbl.pdf (accessed on 10/01/2021).

385. Vella, S.; Buetow, L.; Royle, P.; Livingstone, S.; Colhoun, H.M.; Petrie, J.R. The use of metformin in type 1 diabetes: a systematic review of efficacy. *Diabetologia* 2010, *53*, 809-820, doi:10.1007/s00125-009-1636-9.

386. Singh, B.N.; Malhotra, B.K. Effects of food on the clinical pharmacokinetics of anticancer agents. *Clinical pharmacokinetics* 2004, *43*, 1127-1156.

387. FDA. PRADAXA® (dabigatran etexilate mesylate) capsules. Available online: https://www.accessdata.fda.gov/drugsatfda_docs/label/2011/022512s007lbl.pdf (accessed on 10/01/2021).

388. Wuis, E.W. *Pharmacokinetics of antispastic drugs: a study on baclofen and dantrolene*; 1991.

389. Zuidema, J.; Hilbers-Modderman, E.S.M.; Merkus, F.W.H.M. Clinical Pharmacokinetics of Dapsone. *Clinical Pharmacokinetics* 1986, *11*, 299-315, doi:10.2165/00003088-198611040-00003.

390. FDA. ENABLEX ® (darifenacin) extended-release tablet. Available online: https://www.accessdata.fda.gov/drugsatfda_docs/label/2011/021513s007lbl.pdf (accessed on

391. Kakuda, T.N.; Brochot, A.; Tomaka, F.L.; Vangeneugden, T.; Van De Casteele, T.; Hoetelmans, R.M. Pharmacokinetics and pharmacodynamics of boosted once-daily darunavir. *Journal of Antimicrobial Chemotherapy* 2014, *69*, 2591-2605, doi:10.1093/jac/dku193.

392. Ciraulo, D.A.; Barnhill, J.G.; Jaffe, J.H. Clinical pharmacokinetics of imipramine and desipramine in alcoholics and normal volunteers. *Clinical Pharmacology & Therapeutics* 1988, *43*, 509-518.

393. FDA. HIGHLIGHTS OF PRESCRIBING INFORMATION HEMADY (dexamethasone tablets). Available online: https://www.accessdata.fda.gov/drugsatfda_docs/label/2019/211379s000lbl.pdf (accessed on 10/01/2021).

394. FDA. Focalin® dexmethylphenidate hydrochloride tablets Available online: https://www.accessdata.fda.gov/drugsatfda_docs/label/2010/021278s013lbl.pdf (accessed on 10/01/2021).

395. Greenblatt, D.J.; Allen, M.D.; MacLaughlin, D.S.; Harmatz, J.S.; Shader, R.I. Diazepam absorption: Effect of antacids and food. *Clinical Pharmacology & Therapeutics* 1978, *24*, 600-609, doi:https://doi.org/10.1002/cpt1978245600.

396. Pearson, R.M. Pharmacokinetics and response to diazoxide in renal failure. *Clinical pharmacokinetics* 1977, *2*, 198-204.

397. FDA. Voltaren® (diclofenac sodium enteric-coated tablets) Available online: https://www.accessdata.fda.gov/drugsatfda_docs/label/2009/019201s038lbl.pdf (accessed on 10/01/2021).

398. Brayfield, A. *Martindale: The Complete Drug Reference (Ed)* 2014/09/05 ed.; 2014; Volume 22, p. 12.

399. FDA. VIDEX® (didanosine) Available online: https://www.accessdata.fda.gov/drugsatfda_docs/label/2006/020154s50,20155s39,20156s40,21183s16lbl.pdf (accessed on 10/01/2021).

400. Tempero, K.F.; Cirillo, V.J.; Steelman, S.L. Diflunisal: a review of pharmacokinetic and pharmacodynamic properties, drug interactions, and special tolerability studies in humans. *British journal of clinical pharmacology* **1977**, *4 Suppl 1*, 31s-36s, doi:10.1111/j.1365-2125.1977.tb04511.x.

401. FDA. Digoxin Bioequivalence Review. Available online: https://www.accessdata.fda.gov/drugsatfda_docs/anda/2002/76268_Digoxin_Bioeqr.pdf (accessed on 10/01/2021).

402. Kramer, W.G.; Perentesis, G.; Affrime, M.B.; Patrick, J.E. Pharmacokinetics of dilevalol in normotensive and hypertensive volunteers. *The American journal of cardiology* **1989**, *63*, I7-I11.

403. FDA. CARDIZEM® LA (diltiazem Hydrochloride). Available online: https://www.accessdata.fda.gov/drugsatfda_docs/label/2010/021392s014lbl.pdf (accessed on 10/01/2021).

404. Nimmo, W. Drugs, diseases and altered gastric emptying. *Clinical pharmacokinetics* **1976**, *1*, 189-203.

405. FDA. AGGRENOX (aspirin/extended-release dipyridamole). Available online: https://www.accessdata.fda.gov/drugsatfda_docs/label/2001/20884s1lbl.pdf (accessed on

406. Cook, C.S.; Zhang, L.; Osis, J.; Schoenhard, G.L.; Karim, A. Mechanism of compound- and species-specific food effects of structurally related

antiarrhythmic drugs, disopyramide and bidisomide. *Pharmaceutical research* **1998**, *15*, 429-433, doi:10.1023/a:1011976331738.

407. FDA. TIKOSYN ® (dofetilide) Capsules Available online: https://www.accessdata.fda.gov/drugsatfda_docs/label/2013/020931s007lbl.pdf (accessed on 10/01/2021).

408. FDA. ANZEMET ® Tablets (dolasetron mesylate) Available online: https://www.accessdata.fda.gov/drugsatfda_docs/label/2013/020623s010lbl.pdf,020624s023lbl.pdf (accessed on 10/01/2021).

409. emc. Domperidone 10mg Tablets. Available online: (accessed on 11/01/2021).

410. FDA. Biopharmaceutics Review Silenor (doxepin HCl). Available online: https://www.accessdata.fda.gov/drugsatfda_docs/nda/2010/022036Orig1s000ClinPharmR.pdf (accessed on 10/01/2021).

411. Welling, P.G.; Koch, P.A.; Lau, C.C.; Craig, W.A. Bioavailability of tetracycline and doxycycline in fasted and nonfasted subjects. *Antimicrobial agents and chemotherapy* **1977**, *11*, 462-469, doi:10.1128/aac.11.3.462.

412. FDA. CYMBALTA® (duloxetine hydrochloride) Available online: https://www.accessdata.fda.gov/drugsatfda_docs/label/2007/021427s009s011s013lbl.pdf (accessed on 10/01/2021).

413. FDA. RELPAX® (eletriptan hydrobromide) tablets. Available online: https://www.accessdata.fda.gov/drugsatfda_docs/label/2013/021016s021s023s024s027lbl.pdf (accessed on 10/01/2021).

414. Somogyi, A.A.; Bochner, F.; Keal, J.A.; Rolan, P.E.; Smith, M. Effect of food on enoxacin absorption. *Antimicrobial agents and chemotherapy* **1987**, *31*, 638-639, doi:10.1128/aac.31.4.638.

415. FDA. COMTAN® (entacapone) Tablets. Available online: https://www.accessdata.fda.gov/drugsatfda_docs/label/2010/020796s15lbl.pdf (accessed on 10/01/2021).

416. Rizea-Savu, S.; Duna, S.N.; Ghita, A.; Iordachescu, A.; Chirila, M. The Effect of Food on the Single-Dose Bioavailability and Tolerability of the Highest Marketed Strength of Duloxetine. *Clinical Pharmacology in Drug Development* 2020, *9*, 797-804, doi:10.1002/cpdd.759.

417. FDA. TARCEVA® (erlotinib) tablets. Available online: https://www.accessdata.fda.gov/drugsatfda_docs/label/2010/021743s14s16lbl.pdf (accessed on 10/01/2021).

418. Malmborg, A.S. Effect of food on absorption of erythromycin. A study of two derivatives, the stearate and the base. *Journal of Antimicrobial Chemotherapy* 1979, *5*, 591-599, doi:10.1093/jac/5.5.591.

419. FDA. Esomeprazole Summary Review. Available online: https://www.accessdata.fda.gov/drugsatfda_docs/nda/2015/207920Orig1s000SumR.pdf (accessed on 10/01/2021).

420. FDA. ORIAHNN (elagolix, estradiol, and norethindrone acetate capsules; elagolix capsules). Available online: https://www.accessdata.fda.gov/drugsatfda_docs/label/2020/213388s000lbl.pdf (accessed on 10/01/2021).

421. FDA. MYAMBUTOL (ethambutol hcl) tablets Available online: https://www.accessdata.fda.gov/drugsatfda_docs/label/2008/016320s063lbl.pdf (accessed on 10/01/2021).

422. Harvey, V.J.; Slevin, M.L.; Joel, S.P.; Johnston, A.; Wrigley, P.F. The effect of food and concurrent chemotherapy on the bioavailability of oral etoposide. *British journal of cancer* 1985, *52*, 363-367, doi:10.1038/bjc.1985.202.

423. FDA. PEPCID® (FAMOTIDINE) TABLETS Available online: https://www.accessdata.fda.gov/drugsatfda_docs/label/2011/019462s037lbl.pdf (accessed on 10/01/2021).

424. FDA. PLENDIL® (felodipine) EXTENDED-RELEASE TABLETS Available online: https://www.accessdata.fda.gov/drugsatfda_docs/label/2012/019834s025lbl.pdf (accessed on 30/08/2021).

425. FDA. PROSCAR® (FINASTERIDE) TABLETS Available online: https://www.accessdata.fda.gov/drugsatfda_docs/label/2010/020180s037lbl.pdf (accessed on 10/01/2021).

426. Tjandra-Maga, T.; Verbesselt, R.; Hecken, A.v.; Mullie, A.; Schepper, P.d. Flecainide: single and multiple oral dose kinetics, absolute bioavailability and effect of food and antacid in man. *British journal of clinical pharmacology* 1986, *22 3*, 309-316.

427. FDA. DIFLUCAN® (Fluconazole Tablets) Available online: https://www.accessdata.fda.gov/drugsatfda_docs/label/2011/019949s051lbl.pdf (accessed on 10/01/2021).

428. Kunka, M.E.; Cady, E.A.; Woo, H.C.; Thompson Bastin, M.L. Flucytosine Pharmacokinetics in a Critically Ill Patient Receiving Continuous Renal Replacement Therapy. *Case Rep Crit Care* 2015, *2015*, 927496-927496, doi:10.1155/2015/927496.

429. Busto, U.; Bendayan, R.; Sellers, E. Clinical pharmacokinetics of non-opiate abused drugs. *Clinical pharmacokinetics* 1989, *16*, 1-26.

430. Luer, M.S.; Penzak, S.R. Pharmacokinetic Properties. In *Applied Clinical Pharmacokinetics and Pharmacodynamics of Psychopharmacological Agents*; Springer: 2016; pp. 3-27.

431. FDA. HIGHLIGHTS OF PRESCRIBING INFORMATION Lescol® (fluvastatin sodium). Available online: https://www.accessdata.fda.gov/drugsatfda_docs/label/2012/021192s019lbl.pdf (accessed on 10/01/2021).

432. FDA. Fluvoxamine Maleate Tablets. Available online: https://www.accessdata.fda.gov/drugsatfda_docs/label/2012/021519s003lbl.pdf (accessed on 10/01/2021).

433. FDA. MONUROL Available online: accessdata.fda.gov/drugsatfda_docs/label/2008/050717s005lbl.pdf (accessed on 10/01/2021).

434. FDA. FROVA® (frovatriptan succinate) Tablets. Available online: https://www.accessdata.fda.gov/drugsatfda_docs/label/2009/021006s006s009s010lbl.pdf (accessed on 10/01/2021).

435. Bockbrader, H.N.; Wesche, D.; Miller, R.; Chapel, S.; Janiczek, N.; Burger, P. A comparison of the pharmacokinetics and pharmacodynamics of pregabalin and gabapentin. *Clinical Pharmacokinetics* 2010, *49*, 661-669, doi:10.2165/11536200-000000000-00000.

436. Lavelle, J.; Follansbee, S.; Trapnell, C.B.; Buhles, W.C.; Griffy, K.G.; Jung, D.; Dorr, A.; Connor, J. Effect of food on the relative bioavailability of oral ganciclovir. *The Journal of Clinical Pharmacology* 1996, *36*, 238-241, doi:10.1002/j.1552-4604.1996.tb04193.x.

437. Swaisland, H.C.; Smith, R.P.; Laight, A.; Kerr, D.J.; Ranson, M.; Wilder-Smith, C.H.; Duvauchelle, T. Single-dose clinical pharmacokinetic studies of gefitinib. *Clinical Pharmacokinetics* 2005, *44*, 1165-1177, doi:10.2165/00003088-200544110-00004.

438. Pop, D.; Gheldiu, A.-M.; Oroian, M.; Marcovici, A.; Bhardwaj, S.; Khuroo, A.; Kochhar, R.; Vlase, L. Effect of Food on the Pharmacokinetics of Gliclazide 60 mg Modified Release Tablet in Healthy Caucasian Volunteers. *Acta Marisiensis - Seria Medica* 2018, *64*, 161-168, doi:doi:10.2478/amma-2018-0022.

439. FDA. AMARYL (glimepiride) tablets. Available online: https://www.accessdata.fda.gov/drugsatfda_docs/label/2013/020496s027lbl.pdf (accessed on 10/01/2021).

440. FDA. GLUCOTROL XL® (glipizide) extended release tablets. Available online: https://www.accessdata.fda.gov/drugsatfda_docs/label/2015/020329s029lbl.pdf (accessed on 10/01/2021).

441. Marathe, P.H.; Arnold, M.E.; Meeker, J.; Greene, D.S.; Barbhaiya, R.H. Pharmacokinetics and bioavailability of a metformin/glyburide tablet administered alone and with food. *The Journal of Clinical Pharmacology* 2000, *40*, 1494-1502.

442. emc. Granisetron 1 mg film-coated tablets. Available online: (accessed on 10/01/2021).

443. FDA. INTUNIV® (guanfacine) extended-release tablets. Available online: https://www.accessdata.fda.gov/drugsatfda_docs/label/2013/022037s009lbl.pdf (accessed on 10/01/2021).

444. Mauri, M.C.; Paletta, S.; Di Pace, C.; Reggiori, A.; Cirnigliaro, G.; Valli, I.; Altamura, A.C. Clinical pharmacokinetics of atypical antipsychotics: an update. *Clinical pharmacokinetics* 2018, *57*, 1493-1528.

445. Breimer, D.D. Clinical pharmacokinetics of hypnotics. *Clinical pharmacokinetics* 1977, *2*, 93-109, doi:10.2165/00003088-197702020-00002.

446. FDA. DILAUDID® TABLETS (hydromorphone hydrochloride). Available online: https://www.accessdata.fda.gov/drugsatfda_docs/label/2009/019034s018lbl.pdf (accessed on 10/01/2021).

447. Tett, S.E. Clinical pharmacokinetics of slow-acting antirheumatic drugs. *Clinical pharmacokinetics* **1993**, *25*, 392-407.

448. FDA. BONIVA (ibandronate sodium) Tablets Available online: https://www.accessdata.fda.gov/drugsatfda_docs/label/2015/021455s019lbl.pdf (accessed on 10/01/2021).

449. FDA. Motrin® Ibuprofen Tablets, USP. Available online: https://www.accessdata.fda.gov/drugsatfda_docs/label/2007/017463s105lbl.pdf (accessed on 10/01/2021).

450. Goswami, D.; Gurule, S.; Lahiry, A.; Anand, A.; Khuroo, A.; Monif, T. Clinical development of imatinib: an anticancer drug. *Future Sci OA* **2016**, *2*, FSO92-FSO92, doi:10.4155/fso.15.92.

451. Abernethy, D.R.; Divoll, M.; Greenblatt, D.J.; Harmatz, J.S.; Shader, R.I. Absolute bioavailability of imipramine: Influence of food. *Psychopharmacology* **1984**, *84*, 146-146, doi:10.1007/BF00432048.

452. Aoyagi, N.; Kaniwa, N.; Ogata, H. Effects of Food on Bioavailability of Two Indomethacin Capsules Containing Different Sizes of Particles. *Chemical and pharmaceutical bulletin* **1990**, *38*, 1338-1340, doi:10.1248/cpb.38.1338.

453. Jáuregui-Garrido, B.; Jáuregui-Lobera, I. Interactions between antihypertensive drugs and food. *Nutrición hospitalaria* **2012**, *27*, 1866-1875.

454. FDA. AVAPRO (irbesartan) tablets. Available online: https://www.accessdata.fda.gov/drugsatfda_docs/label/2016/020757s059s067lbl.pdf (accessed on 10/01/2021).

455. FDA. monoket® tablets (isosorbide mononitrate). Available online: https://www.accessdata.fda.gov/drugsatfda_docs/label/2014/020215s024lbl.pdf (accessed on 10/01/2021).

456. Schran, H.F.; Jaffe, J.M.; Gonasun, L.M. Clinical pharmacokinetics of isradipine. *The American Journal of Medicine* 1988, *84*, 80-89.

457. Zimmermann, T.; Yeates, R.A.; Laufen, H.; Pfaff, G.; Wildfeuer, A. Influence of concomitant food intake on the oral absorption of two triazole antifungal agents, itraconazole and fluconazole. *European journal of clinical pharmacology* 1994, *46*, 147-150, doi:10.1007/bf00199879.

458. FDA. CORLANOR® (ivabradine) tablets. Available online: https://www.accessdata.fda.gov/drugsatfda_docs/label/2019/209964lbl.pdf (accessed on 10/01/2021).

459. Persson, B.; Heykants, J.; Hedner, T. Clinical pharmacokinetics of ketanserin. *Clinical Pharmacokinetics* 1991, *20*, 263-279, doi:10.2165/00003088-199120040-00002.

460. FDA. Orudis (ketoprofen) Capsule. Available online: https://www.accessdata.fda.gov/drugsatfda_docs/label/2007/019816s011lbl.pdf (accessed on 10/01/2021).

461. FDA. TORADOL ORAL (ketorolac tromethamine tablets). Available online: https://www.accessdata.fda.gov/drugsatfda_docs/label/2013/019645s019lbl.pdf (accessed on 10/01/2021).

462. FDA. TRANDATE® (labetalol hydrochloride) Tablets. Available online: https://www.accessdata.fda.gov/drugsatfda_docs/label/2010/018716s026lbl.pdf (accessed on 10/01/2021).

463. FDA. VIMPAT® (lacosamide) film coated tablet. Available online: https://www.accessdata.fda.gov/drugsatfda_docs/label/2018/022253s042lbl.pdf (accessed on

464. FDA. EPIVIR (lamivudine) tablets for oral use. Available online: https://www.accessdata.fda.gov/drugsatfda_docs/label/2017/020564s37_020596s036lbl.pdf (accessed on 10/01/2021).

465. FDA. Femara® (letrozole tablets) Available online: https://www.accessdata.fda.gov/drugsatfda_docs/label/2007/020726s014lbl.pdf (accessed on 10/01/2021).

466. FDA. KEPPRA® (levetiracetam). Available online: https://www.accessdata.fda.gov/drugsatfda_docs/label/2009/021035s078s080,021505s021s024lbl.pdf (accessed on 10/01/2021).

467. Crevoisier, C.; Zerr, P.; Calvi-Gries, F.; Nilsen, T. Effects of food on the pharmacokinetics of levodopa in a dual-release formulation. *Journal of pharmacy and pharmacology* 2003, *55*, 71-76, doi:10.1016/s0939-6411(02)00124-8.

468. FDA. LEVAQUIN® (levofloxacin) Tablets Available online: https://www.fda.gov/files/drugs/published/Levaquin-Label.pdf (accessed on 10/01/2021).

469. FDA. ZYVOX ® (linezolid) tablets. Available online: https://www.accessdata.fda.gov/drugsatfda_docs/label/2008/021130s016,021131s013,021132s014lbl.pdf (accessed on 10/01/2021).

470. FDA. ZESTRIL (Lisinopril). Available online: https://www.accessdata.fda.gov/drugsatfda_docs/label/2009/019777s054lbl.pdf (accessed on 10/01/2021).

471. Hooper, W.D.; Dickinson, R.G.; Eadie, M.J. Effect of food on absorption of lomefloxacin. *Antimicrobial agents and chemotherapy* 1990, *34*, 1797-1799, doi:10.1128/AAC.34.9.1797.

472. Klotz, U.; Müller-Seydlitz, P.; Heimburg, P. Pharmacokinetics of Lorcainide in Man: A New Antiarrhythmic Agent. *Clinical Pharmacokinetics* 1978, *3*, 407-418, doi:10.2165/00003088-197803050-00006.

473. FDA. COZAAR® (LOSARTAN POTASSIUM TABLETS) Available online: https://www.accessdata.fda.gov/drugsatfda_docs/label/2009/020386s049lbl.pdf (accessed on 10/01/2021).

474. Schachter, M. Chemical, pharmacokinetic and pharmacodynamic properties of statins: an update. *Fundamental & Clinical Pharmacology* 2005, *19*, 117-125, doi:https://doi.org/10.1111/j.1472-8206.2004.00299.x.

475. Bauer, L.A. *Applied clinical pharmacokinetics*; McGraw-Hill Companies, Inc.: 2008.

476. FDA. SELZENTRY (maraviroc) tablets Available online: https://www.accessdata.fda.gov/drugsatfda_docs/label/2007/022128lbl.pdf (accessed on 10/01/2021).

477. FDA. Mobic® (meloxicam) tablets. Available online: https://www.accessdata.fda.gov/drugsatfda_docs/label/2012/020938s022lbl.pdf (accessed on 10/01/2021).

478. Reece, P.A.; Kotasek, D.; Morris, R.G.; Dale, B.M.; Sage, R.E. The effect of food on oral melphalan absorption. *Cancer chemotherapy and pharmacology* 1986, *16*, 194-197, doi:10.1007/bf00256176.

479. Mather, L.E.; Meffin, P.J. Clinical pharmacokinetics of pethidine. *Clinical Pharmacokinetics* 1978, *3*, 352-368, doi:10.2165/00003088-197803050-00002.

480. FDA. PURINETHOL® (mercaptopurine) tablets, for oral use. Available online: https://www.accessdata.fda.gov/drugsatfda_docs/label/2020/009053s040lbl.pdf (accessed on 10/01/2021).

481. Sambol, N.C.; Brookes, L.G.; Chiang, J.; Goodman, A.M.; Lin, E.T.; Liu, C.Y.; Benet, L.Z. Food intake and dosage level, but not tablet vs solution dosage form, affect the absorption of metformin HCl in man. *British journal of clinical pharmacology* 1996, *42*, 510-512, doi:10.1111/j.1365-2125.1996.tb00017.x.

482. Lugo, R.A.; Kern, S.E. Clinical pharmacokinetics of morphine. *Journal of pain & palliative care pharmacotherapy* 2002, *16*, 5-18.

483. FDA. METHOTREXATE TABLETS, USP. Available online: https://www.accessdata.fda.gov/drugsatfda_docs/label/2016/008085s066lbl.pdf (accessed on 10/01/2021).

484. FDA. ALDOMET® (METHYLDOPA). Available online: https://www.accessdata.fda.gov/drugsatfda_docs/label/2004/13400s086lbl.pdf (accessed on 10/01/2021).

485. Czock, D.; Keller, F.; Rasche, F.M.; Häussler, U. Pharmacokinetics and pharmacodynamics of systemically administered glucocorticoids. *Clinical Pharmacokinetics* 2005, *44*, 61-98, doi:10.2165/00003088-200544010-00003.

486. Vergin, H.; Fisch, U.; Mahr, G.; Winterhalter, B. Analysis of formulation and food effect on the absorption of metoclopramide. *Int J Clin Pharmacol Ther* 2002, *40*, 169-174, doi:10.5414/cpp40169.

487. FDA. METOPROLOL SUCCINATE EXTENDED-RELEASE TABLETS. Available online: https://www.accessdata.fda.gov/drugsatfda_docs/label/2006/019962s032lbl.pdf (accessed on 10/01/2021).

488. FDA. FLAGYL® (metronidazole) capsules. Available online: https://www.accessdata.fda.gov/drugsatfda_docs/label/2013/020334s008lbl.pdf (accessed on 10/01/2021).

489. Shami, M.; Elliott, H.L.; Kelman, A.W.; Whiting, B. The pharmacokinetics of mianserin. *British journal of clinical pharmacology* **1983**, *15*, 313S-322S.

490. FDA. Savella® (milnacipran HCl) Tablets Available online: https://www.accessdata.fda.gov/drugsatfda_docs/label/2016/022256s022lbl.pdf (accessed on 10/01/2021).

491. FDA. MINOCIN® (minocycline hydrochloride) Available online: https://www.accessdata.fda.gov/drugsatfda_docs/label/2010/050649023lbl.pdf (accessed on 10/01/2021).

492. Gottlieb, T.B.; Thomas, R.C.; Chidsey, C.A. Pharmacokinetic studies of minoxidil. *Clinical Pharmacology & Therapeutics* **1972**, *13*, 436-441.

493. FDA. REMERON® (mirtazapine) tablets, for oral use Available online: https://www.accessdata.fda.gov/drugsatfda_docs/label/2020/020415s029,%20021208s019lbl.pdf (accessed on 10/01/2021).

494. Mesnil, F.; Mentré, F.; Dubruc, C.; Thénot, J.-P.; Mallet, A. Population pharmacokinetic analysis of mizolastine and validation from sparse data on patients using the nonparametric maximum likelihood method. *Journal of Pharmacokinetics and Biopharmaceutics* **1998**, *26*, 133-161.

495. FDA. SINGULAIR®(MONTELUKAST SODIUM) Available online: https://www.accessdata.fda.gov/drugsatfda_docs/label/2009/020829s051_020830s052_021409s028lbl.pdf (accessed on 10/01/2021).

496. DrugBank. Morphine. Available online: https://go.drugbank.com/drugs/DB00295 (accessed on 10/01/2021).

497. FDA. AVELOX (moxifloxacin hydrochloride) tablets. Available online: https://www.accessdata.fda.gov/drugsatfda_docs/label/2016/021085s063lbl.pdf (accessed on 10/01/2021).

498. Buice, R.G.; Subramanian, V.S.; Duchin, K.L.; Uko-Nne, S. Bioequivalence of a highly variable drug: an experience with nadolol. *Pharmaceutical research* 1996, *13*, 1109-1115, doi:10.1023/a:1016031313065.

499. Berkowitz, B.A. The relationship of pharmacokinetics to pharmacological activity: morphine, methadone and naloxone. *Clinical pharmacokinetics* 1976, *1*, 219-188.

500. DrugBank. Naltrexone. Available online: https://go.drugbank.com/drugs/DB00704 (accessed on 10/01/2021).

501. FDA. NAPRELAN® (naproxen sodium) CONTROLLED-RELEASE TABLETS Available online: https://www.accessdata.fda.gov/drugsatfda_docs/label/2011/020353s028lbl.pdf (accessed on 10/01/2021).

502. FDA. AMERGE® (naratriptan hydrochloride) tablets. Available online: https://www.accessdata.fda.gov/drugsatfda_docs/label/2016/020763s011lbl.pdf (accessed on 10/01/2021).

503. FDA. STARLIX® (nateglinide) tablets. Available online: https://www.accessdata.fda.gov/drugsatfda_docs/label/2017/021204s015lbl.pdf (accessed on 10/01/2021).

504. Greene, D.S.; Barbhaiya, R.H. Clinical pharmacokinetics of nefazodone. *Clinical Pharmacokinetics* 1997, *33*, 260-275, doi:10.2165/00003088-199733040-00002.

505. Ahmad, M.; Yaqoob, M.; Murtaza, G. Study of pharmacokinetics and comparative bioavailability of nefopam 30 mg tablets in twelve fasting healthy Pakistani male

young subjects: single-dose, randomized, two-period, two-treatment and two-way cross-over design. *Medical Principles and Practice* 2012, *21*, 271-276.

506. Delchier, J.C.; Guerret, M.; Vidon, N.; Dubray, C.; Lavene, D. Influence of digestive secretions and food on intestinal absorption of nicardipine. *European journal of clinical pharmacology* 1988, *34*, 165-171, doi:10.1007/bf00614554.

507. APPS. AUSTRALIAN PRODUCT INFORMATION – IKOREL® (NICORANDIL). Available online: https://apps.medicines.org.au/files/swpikore.pdf (accessed on 10/01/2021).

508. Schug, B.S.; Brendel, E.; Wonnemann, M.; Wolf, D.; Wargenau, M.; Dingler, A.; Blume, H.H. Dosage form-related food interaction observed in a marketed once-daily nifedipine formulation after a high-fat American breakfast. *European journal of clinical pharmacology* 2002, *58*, 119-125, doi:10.1007/s00228-002-0444-7.

509. FDA. NYMALIZE (nimodipine). Available online: https://www.accessdata.fda.gov/drugsatfda_docs/label/2013/203340lbl.pdf (accessed on 10/01/2021).

510. Yamazaki, A.; Kumagai, Y.; Fujita, T.; Hasunuma, T.; Yokota, S.; Maeda, M.; Otani, Y.; Majima, M. Different effects of light food on pharmacokinetics and pharmacodynamics of three benzodiazepines, quazepam, nitrazepam and diazepam. *Journal of Clinical Pharmacy and Therapeutics* 2007, *32*, 31-39, doi:https://doi.org/10.1111/j.1365-2710.2007.00795.x.

511. Walter-Sack, I.; Klotz, U. Influence of Diet and Nutritional Status on Drug Metabolism. *Clinical Pharmacokinetics* 1996, *31*, 47-64, doi:10.2165/00003088-199631010-00004.

512. FDA. MACROBID - nitrofurantoin monohydrate and nitrofurantoin, macrocrystalline capsule. Available online:

https://www.accessdata.fda.gov/drugsatfda_docs/label/2009/020064s019lbl.pdf (accessed on 10/01/2021).

513. FDA. Axid® (nizatidine). Available online: https://www.accessdata.fda.gov/drugsatfda_docs/label/2005/21494s001lbl.pdf (accessed on 10/01/2021).

514. Alestig, K. The pharmacokinetics of oral quinolones (norfloxacin, ciprofloxacin, ofloxacin). *Scandinavian Journal of Infectious Diseases, Supplement* 1990, *68*, 19-22.

515. FDA. OFLOXACIN TABLETS. Available online: https://www.accessdata.fda.gov/drugsatfda_docs/label/2014/076182Orig1s014lbl.pdf (accessed on 10/01/2021).

516. FDA. Benicar (olmesartan medoxomil) tablets Available online: https://www.accessdata.fda.gov/drugsatfda_docs/label/2011/021286s020lbl.pdf (accessed on 10/01/2021).

517. FDA. Omeprazole. Available online: https://www.accessdata.fda.gov/drugsatfda_docs/nda/2017/209400Orig1s000ClinPharmR.pdf (accessed on 10/01/2021).

518. FDA. HIGHLIGHTS OF PRESCRIBING INFORMATION ZOFRAN (ondansetron hydrochloride). Available online: https://www.accessdata.fda.gov/drugsatfda_docs/label/2016/020103s035_020605s019_020781s019lbl.pdf (accessed on

519. FDA. HIGHLIGHTS OF PRESCRIBING INFORMATION TAMIFLU® (oseltamivir phosphate) Available online: https://www.accessdata.fda.gov/drugsatfda_docs/label/2011/021087s057lbl.pdf (accessed on 10/01/2021).

520. John, V.A.; Smith, S.E. Influence of food intake on plasma oxprenolol concentrations following oral administration of conventional and Oros preparations. *British Journal of Clinical Pharmacology* 1985, *19 Suppl 2*, 191s-195s, doi:10.1111/j.1365-2125.1985.tb02761.x.

521. FDA. DITROPAN® (oxybutynin chloride) Tablets and Syrup Available online: https://www.accessdata.fda.gov/drugsatfda_docs/label/2008/017577s034,018211s017,020897s018lbl.pdf (accessed on 10/01/2021).

522. FDA. PACKAGE INSERT OXYCONTIN® (OXYCODONE HCl CONTROLLED-RELEASE) TABLETS Available online: https://www.accessdata.fda.gov/drugsatfda_docs/label/2009/020553s060lbl.pdf (accessed on

523. FDA. INVEGA® (paliperidone) Extended-Release Tablets. Available online: https://www.accessdata.fda.gov/drugsatfda_docs/label/2019/021999s036lbl.pdf (accessed on 12/01/2021).

524. FDA. PROTONIX (pantoprazole sodium). Available online: https://www.accessdata.fda.gov/drugsatfda_docs/label/2012/020987s045lbl.pdf (accessed on 10/01/2021).

525. FDA. ZEMPLAR® (paricalcitol) Capsules. Available online: https://www.accessdata.fda.gov/drugsatfda_docs/label/2009/021606s004lbl.pdf (accessed on

526. FDA. PRESCRIBING INFORMATION PAXIL® (paroxetine hydrochloride) Tablets and Oral Suspension Available online: https://www.accessdata.fda.gov/drugsatfda_docs/label/2008/020031s060,020936s037,020710s024lbl.pdf (accessed on 10/01/2021).

527. Bressolle, F.; Gonçalves, F.; Gouby, A.; Galtier, M. Pefloxacin Clinical Pharmacokinetics. *Clinical Pharmacokinetics* **1994**, *27*, 418-446, doi:10.2165/00003088-199427060-00003.

528. Yeh, S.Y.; Todd, G.D.; Johnson, R.E.; Gorodetzky, C.W.; Lange, W.R. The pharmacokinetics of pentazocine and tripelennamine. *Clinical Pharmacology & Therapeutics* **1986**, *39*, 669-676, doi:10.1038/clpt.1986.117.

529. FDA. Trental Tablets (Pentoxifylline). Available online: https://www.accessdata.fda.gov/drugsatfda_docs/nda/97/018631_s030ap.pdf (accessed on 10/01/2021).

530. Murphy, J.E. *Clinical pharmacokinetics*; ASHP: 2011.

531. Kong, S.T.; Lim, S.-H.; Lee, W.B.; Kumar, P.K.; Wang, H.Y.S.; Ng, Y.L.S.; Wong, P.S.; Ho, P.C. Clinical Validation and Implications of Dried Blood Spot Sampling of Carbamazepine, Valproic Acid and Phenytoin in Patients with Epilepsy. *PLOS ONE* **2014**, *9*, e108190, doi:10.1371/journal.pone.0108190.

532. FDA. Visken®. Available online: https://www.accessdata.fda.gov/drugsatfda_docs/label/2007/018285s034lbl.pdf (accessed on 10/01/2021).

533. FDA. Mirapex® (pramipexole dihydrochloride) Available online: https://www.accessdata.fda.gov/drugsatfda_docs/label/2008/020667s014s017s018lbl.pdf (accessed on 10/01/2021).

534. Mäntylä, R.; Männistö, P.; Nykänen, S.; Koponen, A.; Lamminsivu, U. Pharmacokinetic interactions of timolol with vasodilating drugs, food and phenobarbitone in healthy human volunteers. *European Journal of Clinical Pharmacology* **1983**, *24*, 227-230, doi:10.1007/BF00613822.

535. Frey, B.M.; Frey, F.J. Clinical pharmacokinetics of prednisone and prednisolone. *Clinical Pharmacokinetics* 1990, *19*, 126-146, doi:10.2165/00003088-199019020-00003.

536. FDA. RAYOS (prednisone) delayed-release tablets 1 mg, 2 mg, 5 mg Available online: https://www.accessdata.fda.gov/drugsatfda_docs/label/2012/202020s000lbl.pdf (accessed on

537. Cuong, B.T.; Binh, V.Q.; Dai, B.; Duy, D.N.; Lovell, C.M.; Rieckmann, K.H.; Edstein, M.D. Does gender, food or grapefruit juice alter the pharmacokinetics of primaquine in healthy subjects? *British Journal of Clinical Pharmacology* 2006, *61*, 682-689, doi:https://doi.org/10.1111/j.1365-2125.2006.02601.x.

538. Selen, A.; Amidon, G.; Wellingx, P. Pharmacokinetics of probenecid following oral doses to human volunteers. *Journal of pharmaceutical sciences* 1982, *71*, 1238-1242.

539. FDA. PRESCRIBING INFORMATION COMPAZINE® brand of prochlorperazine Available online: https://www.accessdata.fda.gov/drugsatfda_docs/label/2005/010571s096lbl.pdf (accessed on 10/01/2021).

540. Hu, O.Y.-P.; Tang, H.-S.; Sheeng, T.-Y.; Chen, S.-C.; Lee, S.-K.; Chung, P.-H. Pharmacokinetics of promazine: I disposition in patients with acute viral hepatitis B. *Biopharmaceutics & Drug Disposition* 1990, *11*, 557-568, doi:https://doi.org/10.1002/bdd.2510110702.

541. Taylor, G.; Houston, J.B.; Shaffer, J.; Mawer, G. Pharmacokinetics of promethazine and its sulphoxide metabolite after intravenous and oral administration to man. *British journal of clinical pharmacology* 1983, *15*, 287-293, doi:10.1111/j.1365-2125.1983.tb01501.x.

542. Axelson, J.E.; Chan, G.L.; Kirsten, E.B.; Mason, W.D.; Lanman, R.C.; Kerr, C.R. Food increases the bioavailability of propafenone. *British journal of clinical pharmacology* 1987, *23*, 735-741, doi:10.1111/j.1365-2125.1987.tb03109.x.

543. Liedholm, H.; Melander, A. Concomitant food intake can increase the bioavailability of propranolol by transient inhibition of its presystemic primary conjugation. *Clinical Pharmacology & Therapeutics* 1986, *40*, 29-36, doi:10.1038/clpt.1986.135.

544. Aquilonius, S.M.; Eckernäs, S.A.; Hartvig, P.; Lindström, B.; Osterman, P.O. Pharmacokinetics and oral bioavailability of pyridostigmine in man. *European journal of clinical pharmacology* 1980, *18*, 423-428, doi:10.1007/bf00636797.

545. emc. Accupro Tablets 40mg. Available online: https://www.medicines.org.uk/emc/product/1965/smpc#gref (accessed on 10/01/2021).

546. FDA. QUALAQUIN® (quinine sulfate) Available online: https://www.accessdata.fda.gov/drugsatfda_docs/label/2013/021799s023lbl.pdf (accessed on 10/01/2021).

547. FDA. ACIPHEX®(rabeprazole sodium) delayed-release tablets, for oral use Available online: https://www.accessdata.fda.gov/drugsatfda_docs/label/2020/020973s041lbl.pdf (accessed on

548. FDA. EVISTA (raloxifene hydrochloride) Tablet for Oral Use Available online: https://www.accessdata.fda.gov/drugsatfda_docs/label/2007/022042lbl.pdf (accessed on 10/01/2021).

549. FDA. ROZEREM (ramelteon) tablets Available online: https://www.accessdata.fda.gov/drugsatfda_docs/label/2010/021782s011lbl.pdf (accessed on 10/01/2021).

550. Roberts, C.J. Clinical pharmacokinetics of ranitidine. *Clinical Pharmacokinetics* **1984**, *9*, 211-221, doi:10.2165/00003088-198409030-00003.

551. FDA. RANEXA® (ranolazine) extended-release tablets. Available online: https://www.accessdata.fda.gov/drugsatfda_docs/label/2015/021526s028lbl.pdf (accessed on

552. MedSafe. EDRONAX (reboxetine) 2 mg, 4 mg Tablet. Available online: https://www.medsafe.govt.nz/profs/Datasheet/e/Edronaxtab.pdf (accessed on

553. FDA. PRANDIN® (repaglinide) Tablets. Available online: https://www.accessdata.fda.gov/drugsatfda_docs/label/2012/020741s040lbl.pdf (accessed on 10/01/2021).

554. FDA. COPEGUS® (ribavirin) Tablets. Available online: https://www.accessdata.fda.gov/drugsatfda_docs/label/2011/021511s023lbl.pdf (accessed on

555. FDA. rifabutin capsules, USP. Available online: https://www.accessdata.fda.gov/drugsatfda_docs/label/2008/050689s016lbl.pdf (accessed on

556. FDA. RIFADIN ® (rifampin capsules USP) Available online: https://www.accessdata.fda.gov/drugsatfda_docs/label/2010/050420s073,050627s012lbl.pdf (accessed on 10/01/2021).

557. FDA. RILUTEK® (riluzole) Tablets. Available online: https://www.accessdata.fda.gov/drugsatfda_docs/label/2009/020599s013lbl.pdf (accessed on 10/01/2021).

558. FDA. ACTONEL® (risedronate sodium) tablets. Available online: https://www.accessdata.fda.gov/drugsatfda_docs/label/2009/020835s035lbl.pdf (accessed on 10/01/2021).

559. FDA. HIGHLIGHTS OF PRESCRIBING INFORMATION RISPERDAL® (risperidone) tablets. Available online: https://www.accessdata.fda.gov/drugsatfda_docs/label/2010/020588s046lbl.pdf (accessed on 10/01/2021).

560. FDA. Exelon® (rivastigmine tartrate) Capsules. Available online: https://www.accessdata.fda.gov/drugsatfda_docs/label/2006/020823s016,021025s008lbl.pdf (accessed on 10/01/2021).

561. FDA. MAXALT® (RIZATRIPTAN BENZOATE) TABLETS Available online: https://www.accessdata.fda.gov/drugsatfda_docs/label/2010/020864s013lbl.pdf (accessed on 10/01/2021).

562. FDA. VIOXX®. Available online: https://www.accessdata.fda.gov/drugsatfda_docs/label/2016/021042s033,021052s024lbl.pdf (accessed on 10/01/2021).

563. FDA. REQUIP® (ropinirole hydrochloride) Tablets Available online: https://www.accessdata.fda.gov/drugsatfda_docs/label/2008/020658s018s020s021lbl.pdf (accessed on

564. FDA. AVANDIA (rosiglitazone maleate) Tablets. Available online: https://www.accessdata.fda.gov/drugsatfda_docs/label/2007/021071s031lbl.pdf (accessed on 11/01/2021).

565. FDA. CRESTOR (rosuvastatin calcium) tablets Available online: https://www.accessdata.fda.gov/drugsatfda_docs/label/2010/021366s016lbl.pdf (accessed on 10/01/2021).

566. FDA. Label - INVIRASE®. Available online: https://www.accessdata.fda.gov/drugsatfda_docs/label/2010/020628s032,021785s009lbl.pdf (accessed on 11/01/2021).

567. FDA. ONGLYZA (saxagliptin) tablets, for oral use. Available online: https://www.accessdata.fda.gov/drugsatfda_docs/label/2015/022350s016lbl.pdf (accessed on 10/01/2021).

568. Renner, U.D.; Oertel, R.; Kirch, W. Pharmacokinetics and pharmacodynamics in clinical use of scopolamine. *Therapeutic drug monitoring* 2005, *27*, 655-665, doi:10.1097/01.ftd.0000168293.48226.57.

569. FDA. ZELAPAR® (selegiline hydrochloride). Available online: https://www.accessdata.fda.gov/drugsatfda_docs/label/2008/021479s003s004lbl.pdf (accessed on 10/01/2021).

570. Nicolson, T.J.; Mellor, H.R.; Roberts, R.R.A. Gender differences in drug toxicity. *Trends in Pharmacological Sciences* 2010, *31*, 108-114, doi:https://doi.org/10.1016/j.tips.2009.12.001.

571. Nakashima, M.; Uematsu, T.; Kosuge, K.; Umemura, K.; Hakusui, H.; Tanaka, M. Pharmacokinetics and tolerance of DU-6859a, a new fluoroquinolone, after single and multiple oral doses in healthy volunteers. *Antimicrobial Agents and Chemotherapy* 1995, *39*, 170-174, doi:10.1128/aac.39.1.170.

572. FDA. JANUVIA® (sitagliptin) Tablets. Available online: https://www.accessdata.fda.gov/drugsatfda_docs/label/2012/021995s019lbl.pdf (accessed on 11/01/2021).

573. FDA. OFFICE OF CLINICAL PHARMACOLOGY REVIEW Vesicare LS. Available online: https://www.fda.gov/media/107507/download (accessed on 01/09/2021).

574. Kahela, P.; Anttila, M.; Tikkanen, R.; Sundquist, H. Effect of food, food constituents and fluid volume on the bioavailability of sotalol. *Acta Pharmacologica et Toxicologica* 1979, *44*, 7-12, doi:10.1111/j.1600-0773.1979.tb02288.x.

575. FDA. Zagam® (sparfloxacin) tablets. Available online: https://www.accessdata.fda.gov/drugsatfda_docs/label/2003/020677s006lbl.pdf (accessed on 10/01/2021).

576. FDA. ZERIT(stavudine). Available online: https://www.accessdata.fda.gov/drugsatfda_docs/label/2002/20412S017.pdf (accessed on 10/01/2021).

577. Hoppu, K.; Tuomisto, J.; Koskimies, O.; Simell, O. Food and guar decrease absorption of trimethoprim. *European Journal of Clinical Pharmacology* 1987, *32*, 427-429, doi:10.1007/BF00543981.

578. Das, K.M.; Dubin, R. Clinical pharmacokinetics of sulphasalazine. *Clinical Pharmacokinetics* 1976, *1*, 406-425.

579. Thornton, C.; Mason, J.C. Chapter 16 - Drugs for inflammation and joint disease. In *Clinical Pharmacology (Eleventh Edition)*, Bennett, P.N., Brown, M.J., Sharma, P., Eds.; Churchill Livingstone: Oxford, 2012; pp. 240-259.

580. FDA. IMITREX (sumatriptan succinate) Tablets. Available online: https://www.accessdata.fda.gov/drugsatfda_docs/label/2013/020132s028,020626s025lbl.pdf (accessed on 10/01/2021).

581. Welty, D.F.; Siedlik, P.H.; Posvar, E.L.; Selen, A.; Sedman, A.J. The Temporal Effect of Food on Tacrine Bioavailability. *The Journal of Clinical Pharmacology* 1994, *34*, 985-988, doi:https://doi.org/10.1002/j.1552-4604.1994.tb01970.x.

582. FDA. PROGRAF® (tacrolimus) capsule. Available online: https://www.accessdata.fda.gov/drugsatfda_docs/label/2012/050709s031lbl.pdf (accessed on 10/01/2021).

583. FDA. Flomax® (tamsulosin hydrochloride) Capsules, 0.4 mg Available online: https://www.accessdata.fda.gov/drugsatfda_docs/label/2009/020579s026lbl.pdf (accessed on 10/01/2021).

584. FDA. ZELNORM™ (tegaserod) tablets. Available online: https://www.accessdata.fda.gov/drugsatfda_docs/label/2019/021200Orig1s015lbl.pdf (accessed on 10/01/2021).

585. FDA. KETEK® (telithromycin) Tablets Available online: https://www.accessdata.fda.gov/drugsatfda_docs/label/2010/021144s014lbl.pdf (accessed on 10/01/2021).

586. FDA. MICARDIS® (telmisartan) Tablets. Available online: https://www.accessdata.fda.gov/drugsatfda_docs/label/2011/020850s032lbl.pdf (accessed on 10/01/2021).

587. FDA. TEMODAR® (temozolomide) Capsules. Available online: https://www.accessdata.fda.gov/drugsatfda_docs/label/2016/021029s031lbl.pdf (accessed on 10/01/2021).

588. FDA. VIREAD® (tenofovir disoproxil fumarate) tablets. Available online: https://www.accessdata.fda.gov/drugsatfda_docs/label/2012/022577lbl.pdf (accessed on 10/01/2021).

589. Day, R.O.; Lam, S.; Paull, P.; Wade, D. Effect of food and various antacids on the absorption of tenoxicam. *British journal of clinical pharmacology* 1987, *24*, 323-328, doi:10.1111/j.1365-2125.1987.tb03176.x.

590. FDA. HYTRIN - terazosin hydrochloride tablet Available online: https://www.accessdata.fda.gov/drugsatfda_docs/label/2009/019057s022lbl.pdf (accessed on 10/01/2021).

591. Agwuh, K.N.; MacGowan, A. Pharmacokinetics and pharmacodynamics of the tetracyclines including glycylcyclines. *Journal of Antimicrobial Chemotherapy* 2006, *58*, 256-265, doi:10.1093/jac/dkl224.

592. Su, Y.M.; Cheng, T.P.; Wen, C.Y. Study on the effect of food on the absorption of theophylline. *JOURNAL-CHINESE MEDICAL ASSOCIATION* 2003, *66*, 715-721.

593. Lancaster, D.L.; Patel, N.; Lennard, L.; Lilleyman, J.S. 6-Thioguanine in children with acute lymphoblastic leukaemia: influence of food on parent drug pharmacokinetics and 6-thioguanine nucleotide concentrations. *British Journal of Clinical Pharmacology* 2001, *51*, 531-539, doi:https://doi.org/10.1046/j.0306-5251.2001.01391.x.

594. Hosie, J.; Hosie, G.A.C. The pharmacokinetics of single and multiple doses of tiaprofenic acid in elderly patients with arthritis. *European Journal of Clinical Pharmacology* 1987, *32*, 93-95, doi:10.1007/BF00609965.

595. FDA. Tindamax (tinidazole) Clinical Pharmacology and Biopharmaceutics Review. Available online: https://www.accessdata.fda.gov/drugsatfda_docs/nda/2004/21-618_Tindamax_BioPharmr.pdf (accessed on 10/01/2021).

596. FDA. TOLBUTAMIDE- tolbutamide tablet Available online: https://dailymed.nlm.nih.gov/dailymed/fda/fdaDrugXsl.cfm?setid=3995eed8-39ec-ce5e-8cc2-062f93445c8d&type=display (accessed on

597. FDA. TASMAR® (tolcapone) tablets. Available online: https://www.accessdata.fda.gov/drugsatfda_docs/label/2013/020697s004lbl.pdf (accessed on 10/01/2021).

598. Verbeeck, R.K.; Blackburn, J.L.; Loewen, G.R. Clinical pharmacokinetics of non-steroidal anti-inflammatory drugs. *Clinical Pharmacokinetics* 1983, *8*, 297-331, doi:10.2165/00003088-198308040-00003.

599. Olsson, B.; Brynne, N.; Johansson, C.; Arnberg, H. Food increases the bioavailability of tolterodine but not effective exposure. *The Journal of Clinical Pharmacology* 2001, *41*, 298-304, doi:10.1177/00912700122010113.

600. FDA. TOPAMAX (topiramate) TABLETS. Available online: https://www.accessdata.fda.gov/drugsatfda_docs/label/2012/020844s041lbl.pdf (accessed on 10/01/2021).

601. FDA. HYCAMTIN® (topotecan) capsules, for oral use. Available online: https://www.accessdata.fda.gov/drugsatfda_docs/label/2018/020981s008lbl.pdf (accessed on 10/01/2021).

602. Kramer, W.G. Effect of Food on the Pharmacokinetics and Pharmacodynamics of Torsemide. *American journal of therapeutics* 1995, *2*, 499-503, doi:10.1097/00045391-199506000-00010.

603. FDA. ULTRAM® (tramadol hydrochloride) Tablets Available online: https://www.accessdata.fda.gov/drugsatfda_docs/label/2009/020281s032s033lbl.pdf (accessed on 10/01/2021).

604. FDA. Oleptro® (Trazodone). Available online: https://www.accessdata.fda.gov/drugsatfda_docs/nda/2010/022411s000ClinPharmR.pdf (accessed on 10/01/2021).

605. Williams, R.L.; Mordenti, J.; Upton, R.A.; Lin, E.T.; Gee, W.L.; Blume, C.D.; Benet, L.Z. Effects of formulation and food on the absorption of hydrochlorothiazide and triamterene or amiloride from combination diuretic products. *Pharmaceutical research* 1987, *4*, 348-352, doi:10.1023/a:1016409606936.

606. Abernethy, D.R.; Greenblatt, D.J.; Divoll, M.; Smith, R.B.; Shader, R.I. The Influence of Obesity on the Pharmacokinetics of Oral Alprazolam and Triazolam. *Clinical Pharmacokinetics* 1984, *9*, 177-183, doi:10.2165/00003088-198409020-00005.

607. Simpson, K.; Spencer, C.M.; McClellan, K.J. Tropisetron. *Drugs* 2000, *59*, 1297-1315, doi:10.2165/00003495-200059060-00008.

608. FDA. SANCTURA® (trospium chloride) tablets. Available online: https://www.accessdata.fda.gov/drugsatfda_docs/label/2012/021595s009lbl.pdf (accessed on 10/01/2021).

609. Gugler, R.; von Unruh, G.E. Clinical Pharmacokinetics of Valproic Acid. *Clinical Pharmacokinetics* 1980, *5*, 67-83, doi:10.2165/00003088-198005010-00002.

610. de Gasparo, M.; Unger, T.; Schölkens, B. AT1 Receptor Antagonists: Pharmacology. 2004; pp. 417-451.

611. Gupta, M.; Kovar, A.; Meibohm, B. The clinical pharmacokinetics of phosphodiesterase-5 inhibitors for erectile dysfunction. *The Journal of Clinical Pharmacology* 2005, *45*, 987-1003, doi:10.1177/0091270005276847.

612. Troy, S.M.; Parker, V.P.; Hicks, D.R.; Pollack, G.M.; Chiang, S.T. Pharmacokinetics and effect of food on the bioavailability of orally administered venlafaxine. *The Journal of Clinical Pharmacology* 1997, *37*, 954-961, doi:10.1002/j.1552-4604.1997.tb04270.x.

613. Conway, E.L.; Phillips, P.A.; Drummer, O.H.; Louis, W.J. Influence of food on the bioavailability of a sustained-release verapamil preparation. *Journal of pharmaceutical sciences* 1990, *79*, 228-231, doi:10.1002/jps.2600790310.

614. FDA. VFEND® Tablets (voriconazole) Available online: https://www.accessdata.fda.gov/drugsatfda_docs/label/2010/021266s032lbl.pdf (accessed on 10/01/2021).

615. FDA. MEDICATION GUIDE WARFARIN. Available online: https://www.accessdata.fda.gov/drugsatfda_docs/label/2007/040415s003lbl.pdf (accessed on 10/01/2021).

616. Devineni, D.; Gallo, J.M. Zalcitabine. *Clinical Pharmacokinetics* 1995, *28*, 351-360, doi:10.2165/00003088-199528050-00002.

617. Moore, K.H.P.; Shaw, S.; Laurent, A.L.; Lloyd, P.; Duncan, B.; Morris, D.M.; O'Mara, M.J.; Pakes, G.E. Lamivudine/Zidovudine as a Combined Formulation Tablet: Bioequivalence Compared with Lamivudine and Zidovudine Administered Concurrently and the Effect of Food on Absorption. *The Journal of Clinical Pharmacology* 1999, *39*, 593-605, doi:https://doi.org/10.1177/00912709922008209.

618. Miceli, J.J.; Glue, P.; Alderman, J.; Wilner, K. The effect of food on the absorption of oral ziprasidone. *Psychopharmacology Bulletin* 2007, *40*, 58-68.

619. Seaber, E.J.; Peck, R.W.; Smith, D.A.; Allanson, J.; Hefting, N.R.; Van Lier, J.J.; Sollie, F.A.E.; Wemer, J.; Jonkman, J.H.G. The absolute bioavailability and effect of food on the pharmacokinetics of zolmitriptan in healthy volunteers. *British Journal of Clinical Pharmacology* 1998, *46*, 433-439, doi:https://doi.org/10.1046/j.1365-2125.1998.00809.x.

620. Andreas, C.J.; Pepin, X.; Markopoulos, C.; Vertzoni, M.; Reppas, C.; Dressman, J.B. Mechanistic investigation of the negative food effect of modified release zolpidem. *European Journal of Pharmaceutical Sciences* 2017, *102*, 284-298, doi:https://doi.org/10.1016/j.ejps.2017.03.011.

621. emc. Zopiclone 3.75 mg Tablets. Available online: https://www.medicines.org.uk/emc/product/11210/smpc#gref (accessed on 10/01/2021).